GeoMod 2021

September 19-23, Utrecht, The Netherlands

Abstract volume

Evening lecture, Monday September 20, 20:30-21:15

Climate modelling with national and global impact

Wilco Hazeleger (1*)
(1) Faculty of Geosciences, Utrecht University
* Contact: w.hazeleger@uu.nl

Abstract

Last summer the 6th Assessment Report of the Intergovernmental Panel on Climate Change (IPCC) was released. It made headline news and confirmed again that Earth's climate is changing fast, and human activities are an important driver of those changes. If emissions continue to grow, substantial further changes are anticipated in regional climate and extremes, and this will have a large impact on society. Previous IPCC reports have provided a scientific basis for major policy responses worldwide such as the well-known Paris Agreement that aims to restrict global temperature rise to 1.5 degrees C compared to preindustrial levels.

Many findings rely on climate models. That is, numerical simulations of the climate system based on knowledge of the atmosphere, oceans, ice and land surface. Over time climate models increased in complexity. Originally representing merely atmospheric physics, now they include the biosphere and many chemical processes. Another development, aided by increased computational capabilities, is the increased spatial resolution which allows a much more detailed view on climate change. A climate model can have a spatial resolution of 10 km now, while a few decades ago it was hundreds of kms. This has led to more robust findings on changes in extreme events, such as tropical storms, and regional effects of global change, but it is still fairly crude. Nested models are used to simulate further detailed climate effects up to the level of streets. The outcome of such models is used to develop climate adaptation strategies, for instance on water management and urban developments. All these developments are driven by and have driven development in supercomputing capabilities, making climate models one of the most important applications of large digital infrastructures.

A different class of models, called Integrated Assessment Models, couple the physical climate to the biosphere and to different socio-economic sectors, such as industry and agriculture. These models produce on the one hand emission scenarios of greenhouse gasses and aerosol precursors that feed the models of the climate system and on the other hand provide policy makers guidance on future emission strategies. They are less detailed because of the many processes involved and are less accurate but tend to be more policy-relevant.

I will take you along in this world of climate models and show that they have a major impact on policies on global and national levels. I will also explore new paradigms of climate modelling that can have large impact on science and policy. Digital Twin concepts are developed that aim to provide a detailed replicate of the climate system, consisting of simulators constrained by observational data, and capabilities to directly interact with the virtual climate system and allow testing scientific hypothesis as well as providing insight in the impact of various policies.

Evening lecture, Tuesday September 21, 20:30-21:15

Induced Seismicity of the Groningen Gas Field: the importance of physics-based models

Jan-Diederik van Wees (1,2*)
(1) TNO – Dutch geological society, (2) Utrecht University
*Jan_Diederik.vanWees@tno.nl

The Groningen gas field is a very large gas field located onshore in the Netherlands. Gas production from the Groningen field started in 1963. Induced seismicity of the field first was recorded in 1991 (M_L 2.4). During the subsequent 10 yr, induced seismicity stayed at a rate of about five events ($M_L \geq 1.5$) per year, increasing afterwards. In 2012, the largest socalled Huizinge event (M_L 3.6) occurred, which caused the most damage to date. The induced seismicity resulted in many research studies on the Groningen Gas Field, and the government decision in 2018 to halt in production in 2022, eight years earlier than initially planned.

In the years before the Huizinge event, Induced seismicity was considered a managed issue, as forecasted future event-rates were assuming a rather stationary behavior and were marked by a relatively low maximum magnitude prognosis (<< M=4). However, in the close aftermath of the Huizinge event a number of studies pointed out that both these assumptions were incorrect and could lead to more and significantly higher magnitude events than earlier anticipated. Extensive research programmes, including the NWO funded DeepNL programme, have focused since on in-depth understanding of induced seismicity in the Groningen Field.

This paper is focused on recent physics-based model studies on the Groningen field, and aims to highlight the importance of geomechanical models for forecasting of stress and frictional (rupture) responses in conjunction with in-depth understanding of the structural complexity of the field, its depletion history, and spatial-temporal variability of the seismic response. Key is the assessment of two factors: (1) the stress development on the Groningen faults, and (2) the frictional (rupture) response of the faults to induced stresses. Both factors have large uncertainties that must be honored and then reduced thanks to observational constraints. In addition physics-based models can assist in providing more robust estimates for the maximum earthquake magnitude (Mmax), which is strongly affecting seismic hazard and which is at present largely based on statistics and expert judgement approaches.

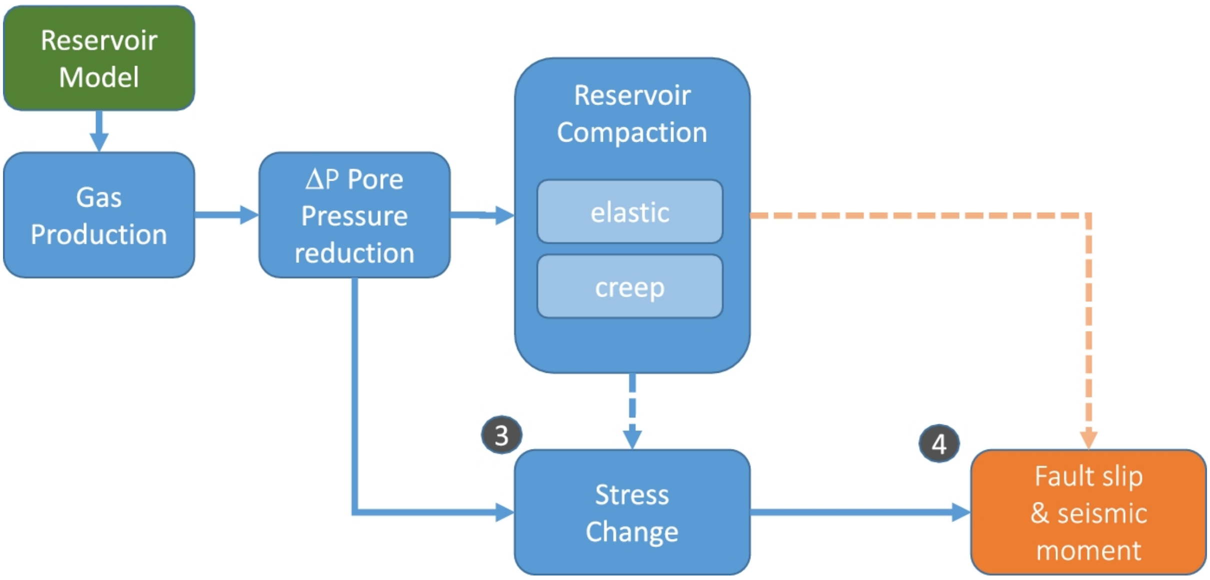

Session 0

State-of-the-art in modeling: methods and techniques

- Mariano Arnaiz-Rodríguez. *MantleMod1D: an interactive 1D code to forward model the thermal, compositional, and mechanical structure of the Earth's mantle*
- Nestor Cardozo. *cdem: A unique software suite for discrete element modelling of tectonic structures*
- Michele Cooke. *Prediction of Off-Fault Deformation from Experimental Strike-slip Fault Structures using the Convolutional Neural Networks*
- Stephane Dominguez. *Searching for a suitable analogue material to investigate geomorphic processes in active tectonic settings: success, limitations, improvements, and hopes*
- Jan Oliver Eisermann. *Long-term isostatic crustal relaxation of large terrestrial meteorite impact structures: insights from scaled analogue experiments*
- Clément Garcia-Estève. *Tectonic/erosion/sedimentation processes – comparison between analog and numerical modelling*
- Paraskevi Io Ioannidi. *Coupling Discrete Element and Lattice Boltzmann methods to simulate grain comminution in "wet" ring shear experiments*
- Boris Kaus. *Developing the next generation geodynamics codes using Julia*
- Emilie Macherel. *GPU-based pseudo-transient finite difference solution for 3-D gravity- and shear-driven power-law viscous flow*
- Nicolás Molnar. *Challenges, limitations, and lessons learned from analogue models of thick-skinned tectonics focused on basement fault reactivation*
- Ronald Pijnenburg. *Free access to research facilities and data: EPOS-NL, the Dutch research infrastructure for solid Earth sciences*
- Michael Rudolf. *Time dependent properties of granular media – The GeoMod Benchmark 2021*
- Stefan Schmalholz. *Thermo-Hydro-Mechanical-Chemical modelling: applications to dehydration vein formation and reactive melt migration*
- Thorben Schöfisch. *Strain distribution across modelled thrust imbricates described by magnetic fabric*
- Eh Tan. *GPU Acceleration on Geodynamic Simulation via OpenACC*

MantleMod1D: an interactive 1D code to forward model the thermal, compositional, and mechanical structure of the Earth's mantle

Mariano S. Arnaiz-Rodríguez (1*), Javier Fullea (1)
(1) Universidad Complutense de Madrid Facultad de Ciencias Físicas* Contact: mararnai@ucm.es

Abstract

We present MantleMod1D an interactive 1-D computer program designed to forward model the structure of the Earth's crust and mantle from 1D geophysical observations with petrological constrains. Developed in Julia Language (Bezanson et al. 2014), the code is intended to be a fast, easy-to-use, flexible and open-source platform to investigate the Earth's thermochemical structure from the surface to the core-mantle boundary (CMB). Furthermore, MantleMod1D is designed to exploit the large repertoire of 1D seismological data available, namely: surface wave dispersion curves (of fundamental and higher modes of Rayleigh and Love waves) and receiver functions (of P, S and SKS waves), as well as surface elevation (isostasy) and heat-flow data.. Following a similar scheme as its predecessors, LitMod and WINTERC (Afonso et al., 2008; Fullea et al., 2009; 2021), the code derives all relevant physical properties to solve the forward problems as a function of temperature, pressure and composition.

The usage of MantleMod1D is very straight forward. The user inputs the composition of each layer:

(a) The composition of the sediments is given as a triad of percentages corresponding to the abundance of Quartz, Carbonates, and Shales (a simplification of the Schwab et al., 2018 diagram) in each sedimentary layer. Porosity is also provided for each layer.

(b) The composition of crustal igneous rocks is provided as anther triad of percentages corresponding to Quartz, Alkali feldspar, Plagioclase (similar to the QAP diagram; Streckeisen, 1974 and 1978). Note that Feldespatoids are left out to keep the input as simple as possible.

(c) The Mantle is separated into four sections: the lithospheric mantle, the asthenospheric mantle, the transition zone and the lower mantle. Each is assumed to have a homogeneous composition that is specified in %wt of AL_2O_3 and FeO, with the other relevant major oxides computed accordingly based on statistical correlations from global petrological data bases.

The layer thickness for each sedimentary and igneous layer is provided by the user (the basement and Moho depths), as well as the Lithosphere-Asthenosphere Boundary (LAB) depth. Phase changes in the mantle are automatically using as a function of pressure and composition.

Afterwards, the temperature at the surface, the LAB (usually 1300 ℃) and the CMB are provided, as well as the adiabatic gradient for the mantle. The temperature at each depth is then computed by solving the heat equation twice, once for the lithosphere and one for the mantle as heat transfer is different in both systems and the LAB marks this change. Both include the radiogenic heat generation term, and the mantle one includes the adiabatic term (e.g. Gerya, 2007). Additional thermal anomalies can be introduced at any depths.

The code uses the composition, temperature and pressure to compute compressional and shear wave velocities (Vp and Vs), as well as density and Qs. This is achieved via several linear interpolation from a lookup table that samples the compositional space as well as T and P. This tables are loaded into Julia functions and were created with the MinVel program (Hacker and Abers, 2004, Abers and Hacker 2016) for the sediments and crust, and with Perple_X for the mantle (Connolly, 2005). The properties are updated three times to achieve convergence between pressure and the geophysical properties (and pressure and density are dependent variables). Finally, MantleMod1D uses these values to compute dispersion curves via FEM method (Haney and Tsai, 2017 and 2019) and receiver functions with an updated version of the propagator algorithm (Jacobsen and Svenningsen, 2008) for the generated geophysical model. These can be compared to real data to check the validity of the modelling and modify the parameters accordingly.

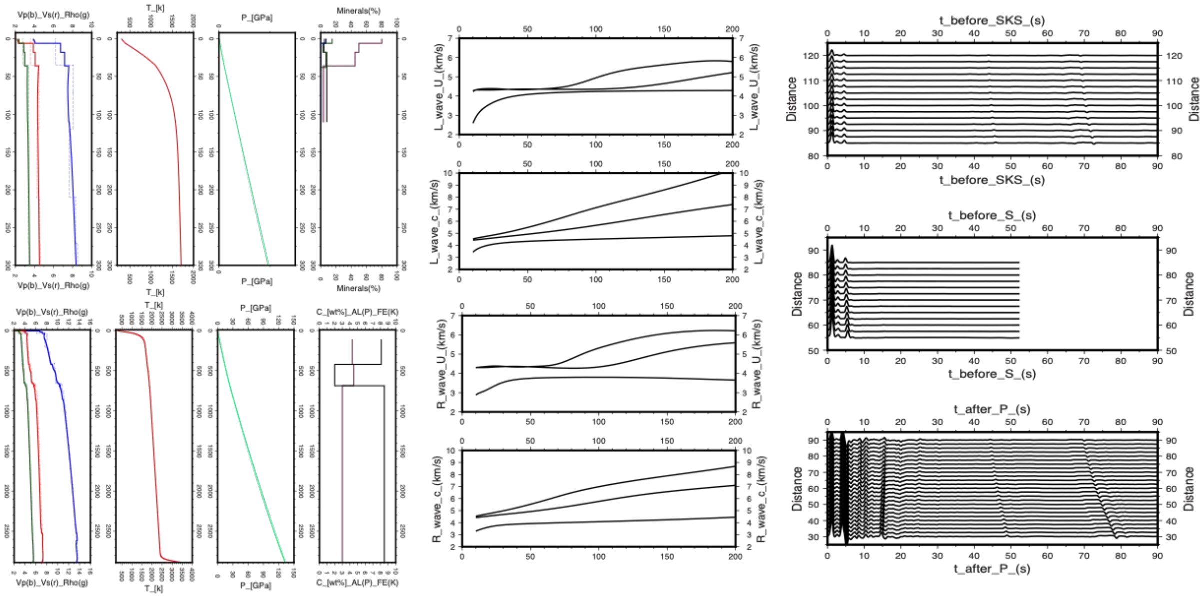

Figure 1: Standard outputs from the MantleMod1D code

References

Abers, G.A., and Hacker, B.R., 2016, A MATLAB toolbox and Excel workbook for calculating the densities, seismic wave speeds, and major element composition of minerals and rocks at pressure and temperature: Geochem. Geophys. Geosys., v. 16, p. 616–624.

Connolly, J. A. D. (2005), Computation of phase equilibria by linear programming: A tool for geodynamic modeling and its application to subduction zone decarbonation, Earth Planet. Sci. Lett., 236, 524–541, doi:10.1016/j.epsl.2005.04.033.

Bezanson, J., Karpinski, S., Shah, V.B., Edelman, A., 2012. Julia: a Fast Dynamic Language for Technical Computing. arXiv:1209.5145v1.

Fullea, J., Afonso, J. C., Connolly, J. A. D., Fernàndez, M., García-Castellanos, D., & Zeyen, H. (2009). LitMod3D: Geochemistry, Geophysics, Geosystems, 10(8), n/a–n/a. doi:10.1029/2009gc002391

J Fullea, S Lebedev, Z Martinec, N L Celli, WINTERC-G: …satellite data, Geophysical Journal International, Volume 226, Issue 1, July 2021, Pages 146–191, https://doi.org/10.1093/gji/ggab094

Hacker, B.R., and Abers, G.A., 2004, Subduction Factory 3: An Excel worksheet and macro for calculating the densities, seismic wave speeds, and H2O contents of minerals and rocks at pressure and temperature: Geochem. Geophys. Geosys., v. 5, no. Q01005.

Jacobsen, B. H., & Svenningsen, L. (2008). Enhanced Uniqueness and Linearity of Receiver Function Inversion. Bulletin of the Seismological Society of America, 98(4), 1756–1767. doi:10.1785/0120070180

Schwab, Frederick L., Folk, Robert Louis, Beck, Kevin Charles et al. 2018. Sedimentary rock. Encyclopædia Britannica. https://www.britannica.com/science/sedimentary-rock.

Shim, S.H. and Catalli, K. (2009) Compositional dependence of structural transition pressures in amorphous phases with mantle-related compositions. Earth and Planetary Science Letters 283, 174-180

Sowers, T., and Boyd, O.S., 2019, Petrologic and mineral physics database for use with the U.S. Geological Survey National Crustal Model: U.S. Geological Survey Open-File Report 2019–1035, 17 p., https://doi.org/10.3133/ofr20191035.

Streckeisen, A. (1974). "Classification and Nomenclature of Plutonic Rocks: Recommendations of the IUGS Subcommission on the Systematics of Igneous Rocks". Geologische Rundschau. 63 (2): 773–786. Bibcode:1974GeoRu..63..773S. doi:10.1007/BF01820841.

Streckeisen, A. L., 1978. IUGS Subcommission on the Systematics of Igneous Rocks. Classification and Nomenclature of Volcanic Rocks, Lamprophyres, Carbonatites and Melilite Rocks. Recommendations and Suggestions. Neues Jahrbuch für Mineralogie, Abhandlungen, Vol. 141, 1–14.

cdem: A unique software suite for discrete element modelling of tectonic structures

Nestor Cardozo (1*), Stuart Hardy (2)
(1) Department of Energy Resources, University of Stavanger, Norway (2) ICREA and Facultat de Geologia, Universitat de Barcelona, Spain.
* Contact: nestor.cardozo@uis.no

Abstract

Since the pioneering work of Cundall and Strack (1979), the discrete element method (DEM) has been used extensively to model tectonic structures. In comparison to continuum methods such as the finite element method (FEM), the DEM handles naturally large deformations and localisation (faulting), although model calibration to realistic rock behaviour is more complicated. Commercial and open-source DEM codes exist, and even codes that combine FEM and DEM. However, these codes involve a steep learning curve, they often work as a black box and are not necessarily tailored to geological problems. We present a software suite for realistic and friendly modelling of tectonic structures. It consists of a document-based macOS DEM program, cdem, and a more powerful platform-independent DEM code, cdem2D. Both programs are based on the same DEM engine that simulates rocks as frictional-cohesive materials, they are designed to target all the machine cores (although using different technologies) and allow different boundary conditions including normal and reverse faulting, caldera and detachment faults, collapse simulations, and biaxial tests. cdem is more friendly and has a user interface (UI) for pre-processing, processing, and visualisation. cdem2D does not have a UI (it is command based), but it has functionalities not present in cdem such as growth strata and salt deformation. However, we have made possible for cdem to import simulations from cdem2D, thus bringing together the best of these two worlds. We illustrate this technology first using biaxial and collapse tests in cdem at different unit scaling, element radii, and spring and damping constants, which highlight the complexity of the assembly calibration. We then use the calibrated assemblies to model in cdem single faults, and a fold and thrust belt. Finally, we show the integration of the two programs via a cdem2D simulation of tectonic inversion with growth strata (Figure 1).

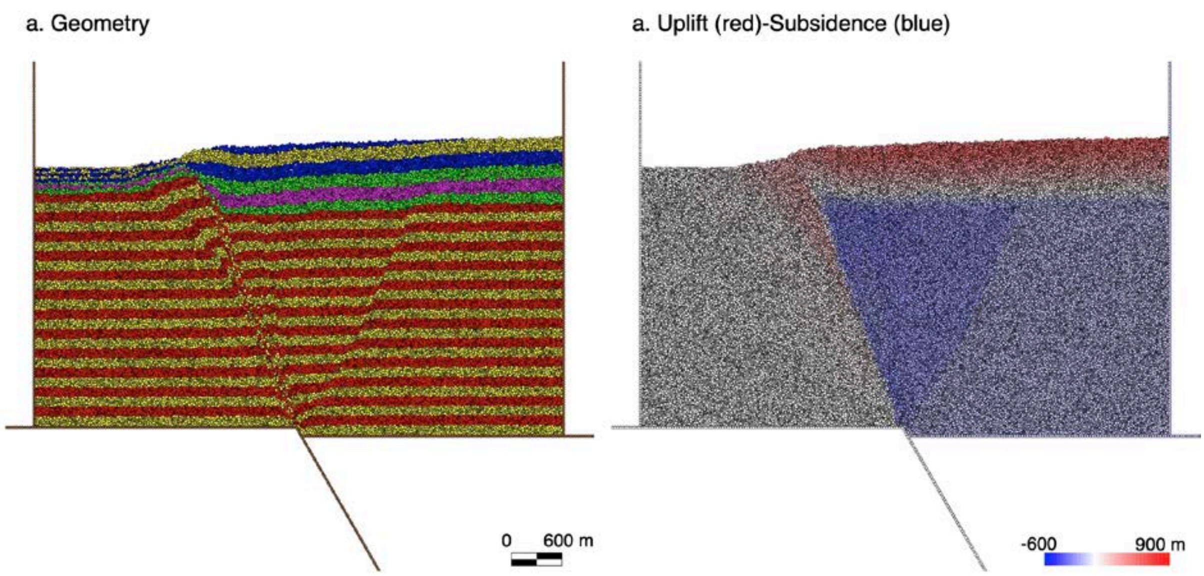

Figure 1: cdem2D model of tectonic inversion with growth strata, imported and visualized in cdem. (a) is geometry, and (b) is the total uplift (red)-subsidence (blue).

References

Cundall,P.A. and Strack,O.D.L. 1979. A discrete numerical model for granular assemblies. Géotechnique 29, 47-65.

Prediction of Off-Fault Deformation from Experimental Strike-slip Fault Structures using the Convolutional Neural Networks

L. Chaipornkaew (1), H. Elston (2), M. Cooke (2*), T. Mukerji (1), S. Graham (1)
(1) Stanford University, (2) University of Massachusetts Amherst
* Contact: cooke@umass.edu

Abstract

Crustal deformation occurs both as localized slip along faults and distributed deformation off faults; however, we have few robust estimates of off-fault deformation. Scaled physical experiments simulate crustal strike-slip faulting and allow direct measurement of the ratio of fault slip to regional deformation, quantified as Kinematic Efficiency (KE). The hypothesis that smoother faults produce greater slip is strongly supported by scaled physical experiments of strike-slip fault evolution that directly document that as faults mature and become smoother, the % of fault slip quantified as kinematic efficiency (KE = 1 - % off fault deformation) increases. Studies of the coseismic deformation fields and experiments show correlations of amount of fault slip with strike-slip fault trace roughness/complexity (Hatem et al., 2017; Milliner et al., 2016). While fractal dimension can quantify the degree of fault roughness of a continuous fault trace (e.g., Brown, 1987), this metric cannot reliably capture the roughness of segmented faults where connectivity controls fault slip. Because any single metric will overlook aspects that may relate strike-slip fault architecture and KE, we need an alternative approach.

In this study, we harness a machine learning algorithm on an experimental time series of fault maps to estimate kinematic efficiency. (KE). Experiments that are scaled to simulate crustal strike-slip fault development allow direct detailed observation of the evolution of both active fault network and KE under a range of loading rates and boundary conditions. Machine learning has been used to predict the timing and size of lab quakes (Corbi et al., 2019; Rouet-Leduc et al., 2017). We use Convolutional Neural Networks (CNNs), which have proved successful for a wide range of computer vision tasks (e.g., LeCun et al., 2010) because they can relate relevant parameters in higher dimensions to specific prediction tasks. With experimental strike-slip fault dataset, our CNNs associate the complexity of the active fault network with the degree of off-fault deformation.

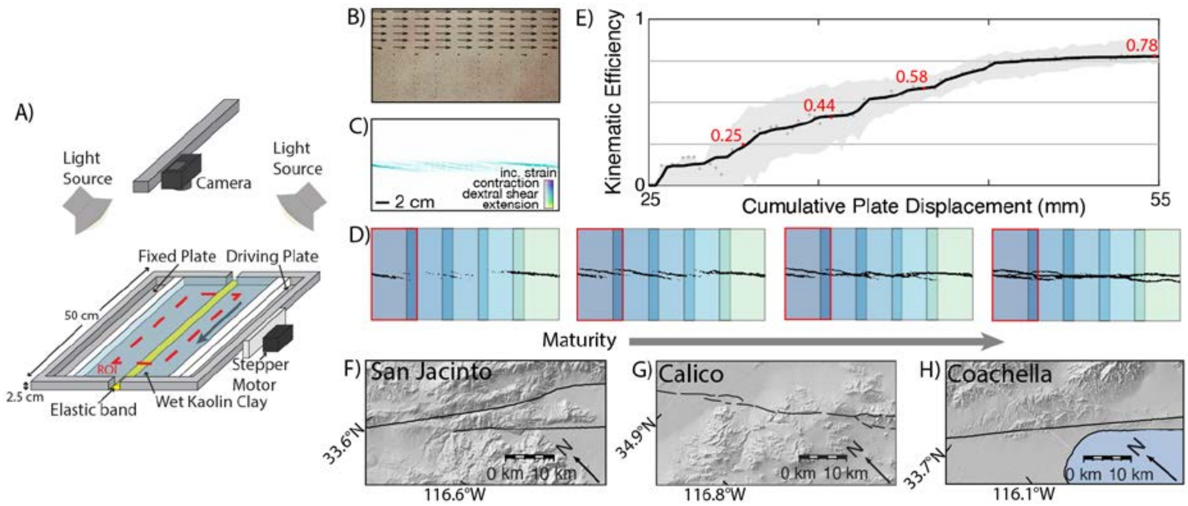

Figure 1: A) Schematic of the distributed basal shear experiment loaded in strike-slip. B) The incremental displacement vectors at a snapshot of the fault evolution (overlain on photo of the experiment) inform C) the incremental shear strain maps. D) Example experiment fault maps (1.5 mm/min distributed basal shear). Color shading delineates individual windows and their overlap. E) KE for the experiment increases with strike-slip fault maturity. The grey band indicates the range of KE within individual windows along the experimental fault. The red numbers report KE for specific example windows outlined in red in D). F) Strike slip fault traces from Southern California show how complexity changes with increasing fault maturity along the B) San Jacinto fault (map center at 33.45°N 116.45°W), C) Calico fault (map center at 34.65°N 166.6°W), and D) Coachella

segment of the San Andreas fault near Mecca Hills (map center at 33.58°N 116.95°W).

We offer an approach for kinematic efficiency (KE) prediction using a 2D Convolutional Neural Network (CNN) trained directly on images of fault maps produced by physical experiments. A suite of strike-slip experiments of wet kaolin with different loading rate and basal boundary conditions, contribute over 13,000 fault maps throughout strike-slip fault evolution (Figure 1). Strain maps allow us to directly calculate KE and its uncertainty, utilized in the loss function and performance metric.

To ensure that the trained CNN can generalize to unseen data, we use the minimum loss of the evaluation dataset to guide tuning of the hyperparameters. We use a custom loss function and custom accuracy, which fully utilize both the KE labels and their standard deviation. Our best model illustrates a good fit, and the CNN model stops improving after approximately 50 training epochs, where we impose an early stopping of the training process. Additionally, we confirm the repeatability of the models' performance by reproducing mini-batch accuracy over 90% on all training using the same set of hyperparameters while varying the randomized initialization. The CNN's prediction on an unseen test dataset yields satisfactory performance of 90.9% accuracy (Figure 2).

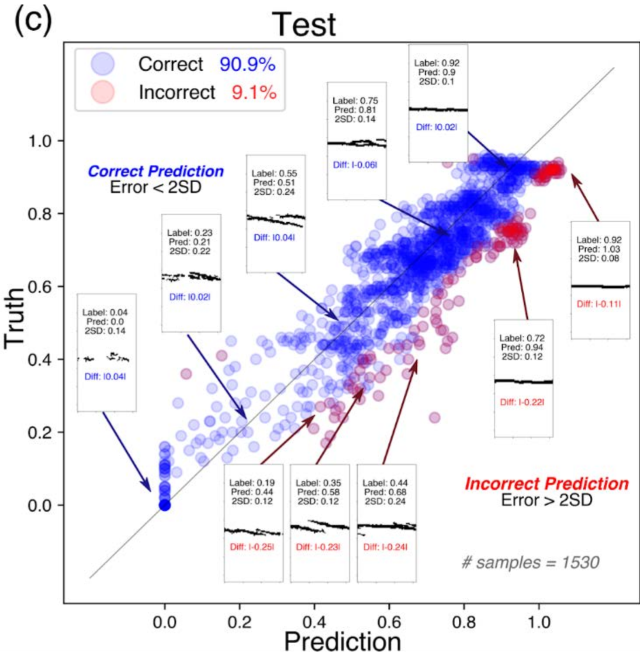

Figure 2: Trained CNN can predict KE of an unseen test dataset with 91% accuracy. On the upper left, we display selected fault maps from all KE ranges. These examples represent datasets that can be accurately predicted by CNN. On the lower right, we display examples of a few outliers that cannot be predicted correctly by the trained CNN.

Although we have few geologic estimates of off-fault deformation in the crust, we may be able to use the CNN trained on experimental faults that are scaled to simulate the crust to predict KE of crustal faults. Here, we compare the off-fault deformation estimates from three geologic studies to CNN predicted KE that use the active fault maps of those studies. These studies use evidence of off-fault deformation accumulated across different time spans. The match of the CNN to crustal fault maps with off-fault deformation estimates shows the potential for applying experimentally trained CNNs to crustal faults.

References

Brown, S. R. (1987). A note on the description of surface roughness using fractal dimension. G*RL*, *14*(11), 1095–1098.

Corbi, F., Sandri, L., Bedford, J., Funiciello, F., Brizzi, S., Rosenau, M., & Lallemand, S. (2019). Machine Learning Can Predict the Timing and Size of Analog Earthquakes. *GRL*, *46*(3), 1303–1311. https://doi.org/10.1029/2018GL081251

Hatem, A. E., Cooke, M. L., & Toeneboehn, K. (2017). Strain localization and evolving kinematic efficiency of initiating strike-slip faults within wet kaolin experiments. *JSG*, *101*, 96–108. https://doi.org/10.1016/j.jsg.2017.06.011

LeCun, Y., Kavukcuoglu, K., & Farabet, C. (2010). Convolutional networks and applications in vision. In *Proceedings of 2010 IEEE international symposium on circuits and systems* (pp. 253–256). IEEE.

Milliner, C. W. D., Sammis, C., Allam, A. A., Dolan, J. F., Hollingsworth, J., Leprince, S., & Ayoub, F. (2016). Resolving Fine-Scale Heterogeneity of Co-seismic Slip and the Relation to Fault Structure. *Scientific Reports*, *6*(June), 1–9. https://doi.org/10.1038/srep27201

Rouet-Leduc, B., Hulbert, C., Lubbers, N., Barros, K., Humphreys, C. J., & Johnson, P. A. (2017). Machine learning predicts laboratory earthquakes. *GRL*, *44*(18), 9276–9282.

Searching for a suitable analogue material to investigate geomorphic processes in active tectonic settings: success, limitations, improvements, and hopes

Stephane Dominguez(1*), Romain Sylvain (1), Clément Garcia-Estève (1), Rodolphe Cattin (1), Fabien Graveleau (2)
(1) Géosciences Montpellier Laboratory, University of Montpellier, France (2) University of Lille, Laboratoire d'océanologie et de Géosciences, France
* Contact: stephane.dominguez@umontpellier.fr

Abstract
Investigating experimentally the interactions between tectonics and surface processes is a challenging task imposing the development of an analogue material capable to simulate jointly geomorphic processes and geological deformation mechanisms. Under external forcings, typically surface water run-off induced by a rainfall system and deviatoric stresses imposed by a mechanical device, the analogue material must be able to develop a wide variety of morphological and tectonic markers such as watersheds, channels networks, alluvial fans, fluvial terraces, folds, faults scarps, etc.

The physical and mechanical processes, behind the formation and evolution of tectonically controlled morphologies, act over a wide range of time and space scales and affect both the model surface and its internal structure. Rigorous model scaling can become, then, a serious issue. Laboratory constraints and the time and space characteristics of natural geological processes lead to typical length and temporal scalings in the ranges of 1 cm = 10-1000 meters, and 1 s = 1-1000 years, respectively. Based on these imposed parameters, more or less well-established scaling rules are used to determine the suitable properties of the analog material. In practice, they are probably not sufficient (see Paola et al., 2009 for a review).

In the framework of the ANR Topo-Extreme project, we recently put some efforts to improve the morphological properties of the MATIV analog material used by our group to investigate Tectonics-Erosion-Sedimentation couplings in different geological contexts (see Graveleau et al., 2015 for a review). We completed the first step by correcting some limitations of the MATIV material such as its relatively low erodibility and drainage density. Adding pumice powder, capable to store water at a microscopic scale while preserving the very low permeability of the material, clearly boosted model surface erosion. By decreasing the granulometry of the coarser MATV components, we also significantly improved the level of detail exhibited by the experimental landforms.

Figure 1: Perpective view of a 3D analog experiment using the new MATV material to investigate mountain foreland landscape evolution under various tectonics and climates forcings.

Results (figure 1) show that if we succeed in improving qualitatively and quantitatively model topography without degrading the simulation of tectonic processes, some of its morphological characteristics are still unsatisfactory. For instance, as shown by the length/width ratios, channel vertical incision appears not vigorous enough compare to channel lateral erosion. This could be partly corrected by increasing the material cohesion but it would strongly decrease material erodibility and generate also out-of-scale deformation processes. This recurrent issue can be limited by performing rainfall cycles, alternating dry and wet periods of a few seconds. By doing this, it becomes possible to modify the balance between channel erosion and slope diffusion processes. Indeed, as soon as the wet stage ends, slope processes are inhibited while water and sediments continue to be transported in the drainage network for a few more seconds until the complete cessation of water flows. During this period, vertical channel incision is more efficient because channel transport capacity is enhanced. However, using rainfall cycles does not solve totally the problem. What we suspect is that the use of dense silica particles, in both the MATIV and MATV mixtures causes two undesirable effects. First, it decreases the transport distance of the eroded particles, and, as shown by the erosion/sedimentation maps, part of these eroded materials are found stored in the lower part of the watersheds instead of being evacuated into the foreland basin. Second, the critical slope angle from which the analog material starts to erode is up to a few degrees while in nature this value is much lower (< 1°).

To improve model scaling procedure and address the issues described above, we initiate a second step by including a numerical modeling approach. Our objective is to clone numerically the analog model using its morphometric characteristics to calibrate the numerical model. The latter is then used to analyze quantitatively model morphology and identify potential scaling discrepancies. First results are encouraging and provide new investigational pathways to further improve the MATV.

References

Paola, C., Straub, K., Mohrig, D., Reinhardt, L., (2009).The “unreasonable effectiveness” of strati-graphic and geomorphic experiments. Earth Sci. Rev. 97 (1–4), 1–43. https://doi.org/10.1016/j.earscirev.2009.05.003

Graveleau, F., V. Strak, S. Dominguez, J. Malavieille, M. Chatton, I. Manighetti, C. Petit, (2015). Experimental modelling of tectonics–erosion–sedimentation interactions in compressional, extensional, and strike–slip settings, Geomorphology, Volume 244, Pages 146-168, ISSN 0169-555X, https://dx.doi.org/10.1016/j.geomorph.2015.02.011

Strzerzynski, P., Dominguez, S., Boudiaf, A., Déverchère, J., (2021). Tectonic inversion and geomorphic evolution of the Algerian margin since Messinian times: Insights from new onshore/offshore analog modeling experiments, Tectonics, 40, e2020TC006369. https://doi.org/10.1029/2020TC006369

Long-term isostatic crustal relaxation of large terrestrial meteorite impact structures: insights from scaled analogue experiments

Jan Oliver Eisermann (1*) & Ulrich Riller (1)
(1) Institut für Geologie, Universität Hamburg, Germany
* Jan.Oliver.eisermann@uni-hamburg.de

Abstract

Meteorite impacts are recognized as a fundamental geological process of the solar system. Although mechanisms of large hypervelocity impact cratering have been studied intensely, mostly by numerical modelling, an outstanding problem concerns long-term crater modification, which operates on time scales of tens of thousands of years after impact. Localized deformation in the form of radial and concentric floor fractures (FFCs) are known from large craters on all terrestrial planets. On Earth we can observe the occurrence of radial and concentric impact melt rock dikes in eroded large impact structures, such as Sudbury (Canada) and Vredefort (South Africa). Two mechanisms were proposed in the past to explain the formation of FFCs: the intrusion of igneous bodies directly below the crater floor and/or long-term isostatic relaxation of target rocks (Jozwiak et al., 2012). Using two-layer analogue experiments scaled to physical conditions on Earth, we explore to what extent isostatic re-equilibration of crust may account for the observed dike patterns of FFCs.

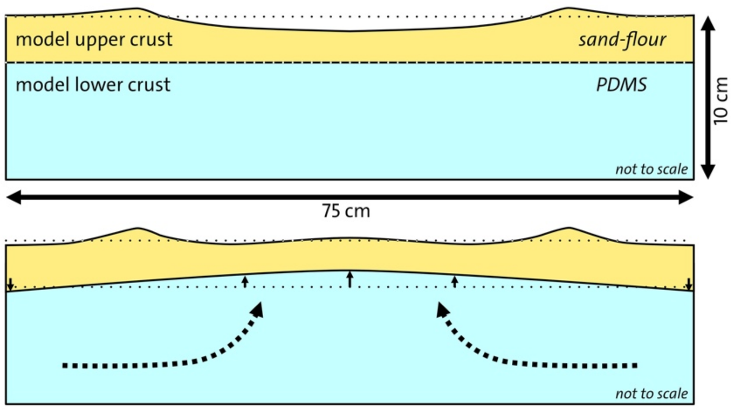

Figure 1: Sketches illustrating model crustal layering of craters before (top) and after (bottom) isostatic relaxation.

The structural evolution of model upper crust was examined for a variety of initial depths and diameters of crater floors. The crater diameter to depth ratio was scaled according to numerical models for average continental crust (Collins et al., 2005). Specifically, a tank was filled with PDMS, representing the viscous middle and lower crust and granular material, simulating the brittle upper crust. In particular, we developed a new method, which allows us to generate any shapes of peak- and multi-ring impact craters. This is achieved by a plastic beam, the base of which has the shape of an inverse radial topographic crater profile. The curved beam is attached to a rotating metal rod. While rotating, the plastic beam is gently lowered into the top part of the 2:1 flour-quartz sand mixture, thereby excavating a specific crater profile with centro-symmetric morphology in the granular material. Added value of this procedure is the fact that during excavation, ejected material is evenly distributed around the model crater, akin to the distribution of natural ejecta deposits.

The experiment surfaces were monitored with a 3D digital image correlation system allowing us to quantify key parameters, such as surface motion as well as the distribution and evolution of surface strain. The results of our scale models enable us to quantify the duration, geometry and distribution of brittle deformation of upper crust. Most importantly, the analogue experiments provide, for the first time, a quantitative relationship between diameter, depth and fracture geometry of crater floors.

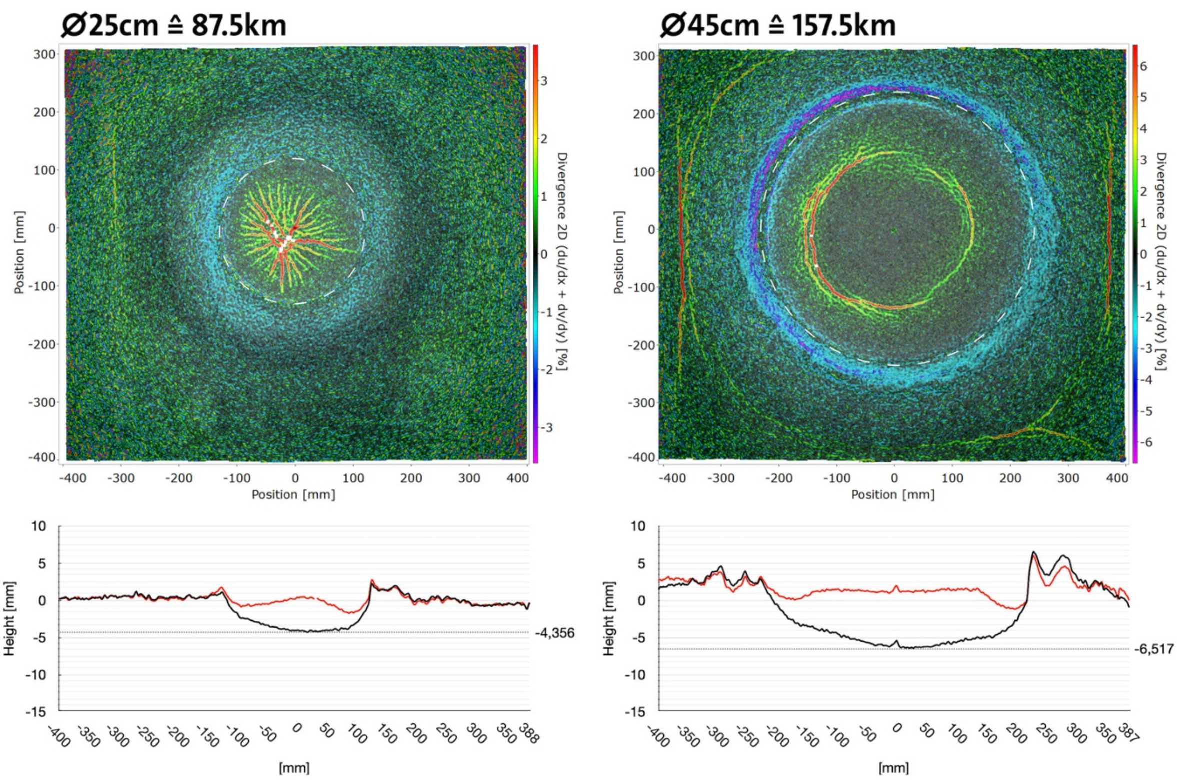

Figure 2: Images and cross sections showing radial (25 cm) and concentric (45cm) dilatational fracture patterns developing after 198 minutes. The cross sections represent the radial topography of the initial crater floors (black lines) and the final crater floors.

Overall, we conclude that FFCs are caused by long-term uplift of the crater floor, compensated by dilation of material below the crater floor. The resulting dilation fractures are ideal sites for the emplacement of impact melt. This process is accompanied by subsidence of the crater periphery. Our experimental results indicate, therefore, that long-term isostatic re-equilibration of crust underlying large impact craters is most important for the formation of FFCs. Development of radial and concentric fractures depends on crater diameter and crater depth and, hence, is controlled by isostacy and crater floor strength. In terms of geometry and distribution of fractures, the resulting model craters are strikingly similar to impact melt rock dikes at Sudbury and Vredefort, known respectively as Offset dikes and Granpphyre dikes. Comparison of model structural patterns with remotely sensed ones from other celestial bodies holds important information for understanding the importance of isostacy and crustal rheology on other planets and moons such as the Moon, Mars, Enceladus, Ceres, Venus and Mercury.

References

Collins, G. S., Melosh, H. J., & Marcus, R. A. (2005). Earth impact effects program: A web - based computer program for calculating the regional environmental consequences of a meteoroid impact on Earth. *Meteoritics & planetary science, 40*(6), 817-840.

Jozwiak, L. M., Head, J. W., Zuber, M. T., Smith, D. E., & Neumann, G. A. (2012). Lunar floor-fractured craters: Classification, distribution, origin and implications for magmatism and shallow crustal structure. *Journal of Geophysical Research: Planets, 117*(E11),

Tectonic/erosion/sedimentation processes - comparison between analog and numerical modelling

Clément Garcia-Estève (1*), R. Cattin (1), S. Dominguez (1), Y. Caniven (2)

(1) Géosciences Montpellier Laboratory, University of Montpellier, France, , (2) Rice University, USA
* Contact: estevecle@gmail.com

Abstract

Surface topography results from complex couplings and feedbacks between tectonics and surface processes. We combine analog and numerical models, sharing similar geometry and boundary conditions, to assess the morphologic evolution of an alluvial fan crossed by an active thrust fault. This joint approach allows the calibration of parameters constraining the river deposition-incision laws, such as the settling velocity of suspended sediments, the bed-rock erodibility, or the slope exponent.

Comparing analog and numerical models reveals a slope-dependent threshold process, where a critical slope of ca. 0.08 controls the temporal evolution of the drainage network. We only evidence minor topographic differences between stable and stick-slip fault behavior, localized along the fault scarp. Although this topographic signature may increase with the slip rate and the return time of slip events, it remains slight compared to the cumulated displacement along the scarp.

Our results demonstrate that the study of morphology cannot be used alone to study the slip mode of active faults but can be a valuable tool complementing stratigraphic and geodetic observations. In contrast, we underline the significant signature of the distance between the fault and the sediment source, which controls the channels incision degree and the density of the drainage network.

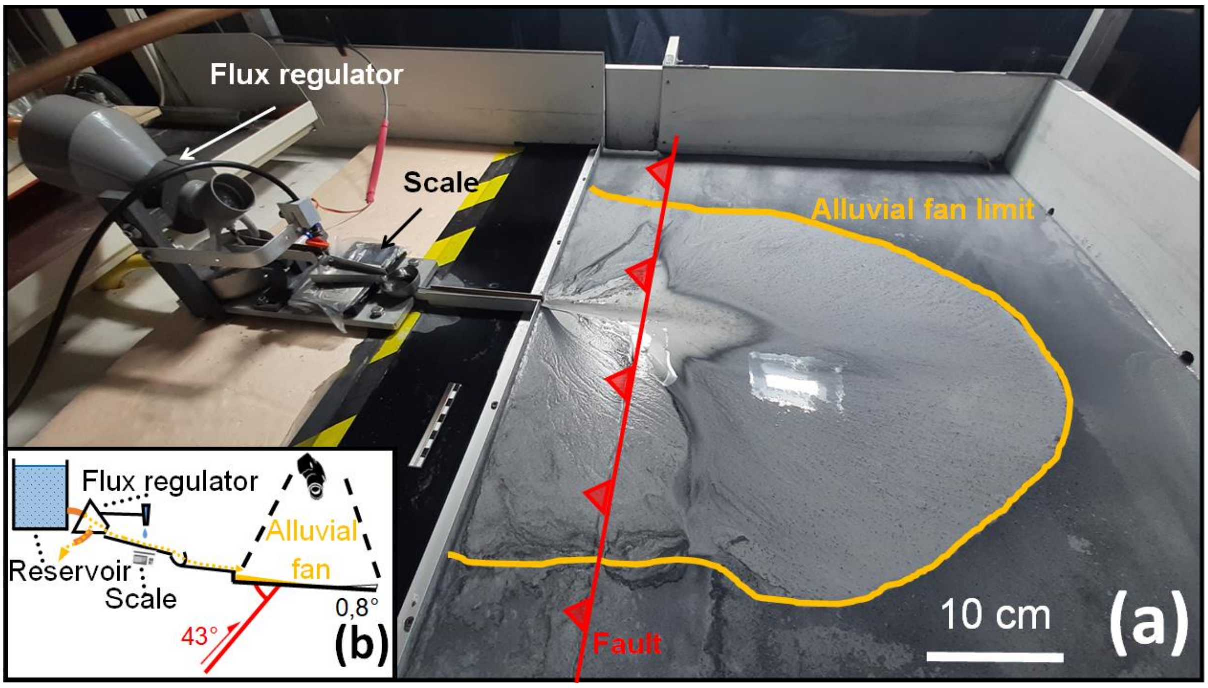

Figure 1: Experimental device used to perform the analog models. (a) General picture of the setup. On the left, the sediments go through a regulator flux then it is weighed on the scale. On the right, the alluvial fan is deposed on an area of 60 x 60 cm. The alluvial fan boundary is outlined by an orange line, and the reverse fault by a red line. (b) Schematic diagram of the experimental setup showing the circulation of sedimentary flux. The depositional area has a slight slope of 0.8° and the fault dips 43° toward the left.

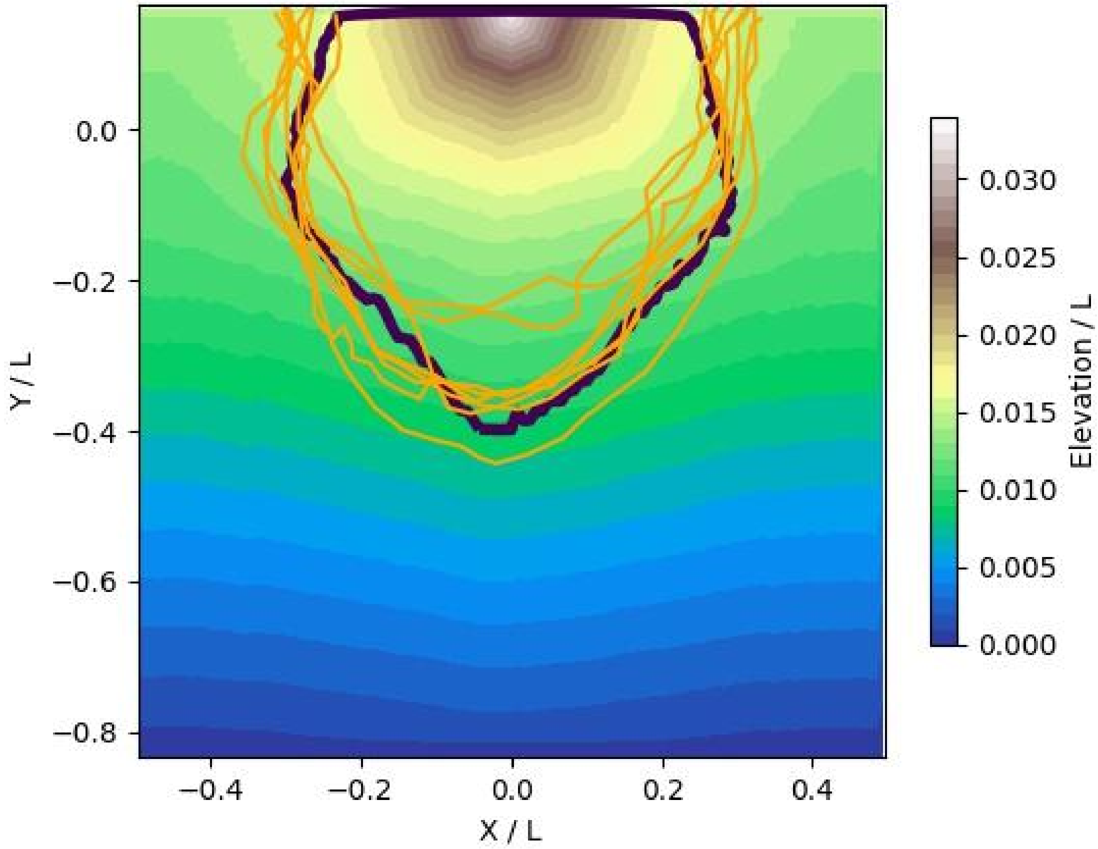

Figure 2: Alluvial fan geometry obtained experimentally after one hour of fan building without tectonics. The color scale gives the calculated topography of the best-fitting numerical model calculated using the Landlab software with the following parameters:

$k_{river} = 10^{-5}$, $v_S = 1$ m. yr^{-1}, $k_{hill} = 8.\ 10^{-4}$ m. yr^{-1}and n = 2.5.

Orange lines show the location of the alluvial fan boundaries obtained in the analog experiments. The thick black line is the fan boundary obtained from the numerical approach. Distance and elevation are normalized by the model size ?, which is equal to 60 cm and 6 km in analog and numerical models, respectively. In the analog experiments, the fan apex height $h_?$ is 1.85 cm, which corresponds to an Elevation/L ratio of 0.031.

References

Barnhart, K. R., Hutton, E. W. H., Tucker, G. E., Gasparini, N. M., Istanbulluoglu, E., Hobley, D. E. J., Lyons, N. J., Mouchene, M., Nudurupati, S. S., Adams, J. M., and Bandaragoda, C., (2020). Short communication: Landlab v2.0: a software package for Earth surface dynamics, Earth Surf. Dynam., 8, 379–397, https://doi.org/10.5194/esurf-8-379-2020.

Hobley, D. E. J., Adams, J. M., Nudurupati, S. S., Hutton, E. W. H., Gasparini, N. M., Istanbulluoglu, E., and Tucker, G. E., (2017). Creative computing with Landlab: an open-source toolkit for building, coupling, and exploring two-dimensional numerical models of Earth-surface dynamics, Earth Surf. Dynam., 5, 21–46, https://doi.org/10.5194/esurf-5-21-2017.

Coupling Discrete Element and Lattice Boltzmann methods to simulate grain comminution in "wet" ring shear experiments

Paraskevi Io Ioannidi (1*), Gabriele Morra (2), Jacqueline E. Reber (1)

(1) Department of Geological and Atmospheric Sciences, Iowa State University, Ames, IA, USA, (2) Department of Physics and School of Geosciences, University of Louisiana at Lafayette, Lafayette, LA, USA
* Contact: ioannidi@iastate.edu

Abstract

Field observations of fossil shear zones have revealed the co-existence of heterogenous materials, comprising a strong, rigid phase embedded within a weaker viscous one. Concurrently, field data and analog experiments suggest that there are two end-members of slip in shear zones, namely episodic stick-slip behavior and steady creep, as well as a range of deformation modes between these end members. Deformation of heterogeneous material might lead to flow of stronger grains or blocks within a less competent matrix. The amount of stronger grains/blocks and the rheology of the flowing matrix can affect the type of slip: high concentration of grains/blocks may result in jamming and subsequent rearangement and breakage of grains, which leads to stick-slip behavior. On the other hand, a matrix-rich setup favors distributed viscous deformation of the shear zone, resulting in continuous slip in the form of creep. In between these two deformation end-members, a range of mixed deformation types might exist. Depending on the amount of grains/blocks in the system (shear zones), these may either break or flow, hence leading to a distinct signature in the slip dynamics of said system.

Laboratory experiments have tackled the problem of grain comminution both in dry granular and in mixed granular-fluid systems. The former have focused on the breaking of the grains and the corresponding changes in force. The latter experiments have shown that the viscosity of fluid has a significant impact on the deformation dynamics, such as the duration of a slip event and the strain localization (e.g., Reber et al., 2014). Our group at ISU has performed analog ring shear experiments both with "dry" and "wet" granular media, with different concentrations of grains, aimed at understanding the effect of grain comminution on the slip dynamics during shearing. Our current, ongoing study aims at benchmarking numerical models relative to the experiments, using the material parameters from the experiments first, and, at a later stage, using parameters of rocks to extrapolate experimental findings to natural conditions. Therefore, we will be presenting preliminary results of the coupling between two fundamentally different codes and discussing our findings.

Few numerical studies have modeled the breaking of "dry" particles under conditions similar to ring shear experiments, using Discrete Element Methods (DEM, Cundall and Strack 1979). Concurrently, the bulk deformation of grains or blocks within an encompassing fluid (matrix) has been investigated using continuum models, such as Finite Element or Finite Difference Methods. The latter methods, however, cannot explicitly model the breaking of particles, and most DEM codes do not include a viscous phase.

In our current models, we simulate granular deformation using the Discrete Element Code EsyS-Particle (Wang and Mora, 2009; https://launchpad.net/esys-particle). Each grain is represented as an assembly of spherical particles, each of which may interact with neighbouring particles or the domain/model walls. The numerical solution is obtained by computing the net force acting on each particle at a given time, then updating particle velocities and positions via an explicit finite difference integration scheme. In our case, the use of the DE method has several advantages over continuum methods, such as Finite Element or Finite Difference methods: DEM can explicitly compute fracturing related to tensile forces as broken bonds, which form and coalesce into macroscopic fractures, does not require incompressibility or even the Boussinesq approximation like most Eulerian codes. Preliminary results of our "dry" DEM models show that EsyS-Particle can effectively model the breaking of spherical grains under simple shear experiments.

The existence of a viscous phase in analog experiments plays an important role in the transfer of forces between grains and their subsequent comminution and slip dynamics of the system. To study the effect of the surrounding fluid on the breaking of the grains, we will use a scalable parallel implementation of the Lattice Boltzmann Method (Mora et al., 2019). The Lattice Boltzmann Method (LBM) involves simulating the Boltzmann Equations on a discrete lattice, rather than solving the Navier– Stokes Equations, since in the

macroscopic limit the two solutions coincide. In addition, LBM is a matrix-free method that guarantees better scaling on large supercomputers. Its simplicity to code and its easy parallelization and running on accelarators such as GPU(s) made it gain popularity in Geosciences. So far, only few studies have focused on coupling the DE and LB methods (e.g., Xue et al., 2015) because there is no established framework to do so, for instance on how the codes should exchange position/momentum/force. We present here preliminary tests of the stability and correctness of LB-DE coupling by 1. imposing moving boundary conditions for a curved shape; 2. transfering momentum between the solid particles and the fluid; and 3. transfering force from the fluid to the solid particles.

By combining DE and LB methods, we aim to model the dynamic deformation of known analog materials numerically. This will help us extrapolate experimental observations to natural conditions and gain insight into the slip dynamics of complex/heterogeneous shear zones.

References

Cundall, P. A., Strack, O. D. L. (1979). A discrete numerical model for granular assemblies, Géotechnique, 29 (1), Pages 47–65, https://doi:10.1680/geot.1979.29.1.47.

Mora, P., Morra, G., Yuen, D. A. (2019). A concise Python implementation of the Lattice Boltzmann Method on HPC for geo-fluid flow, Geophysical Journal International, Volume 220, Issue 1, Pages 682–702, https://doi.org/10.1093/gji/ggz423.

Reber, J. E., Hayman, N. W., Lavier, L. L. (2014). Stick-slip and creep behavior in lubricated granular material: Insights into the brittle-ductile transition. Geophysical Research Letters, 41(10), 3471–3477. https://doi.org/10.1002/2014GL059832.

Wang, Y.C. & Mora, P. (2009). ESyS-Particle: A new 3-D discrete element model with single particle rotation. Advances in Geocomputing, Springer, ed. HL Xing, 183-228.

Xue, S., Yuan, L., Wang, J., Wang, Y., Xie, J. (2015). A coupled DEM and LBM model for simulation of outbursts of coal and gas, Int. J. Coal Sci. Technol., 2, pp. 22-29.

Developing the next generation geodynamics codes using Julia

Boris Kaus (1*), Nicolas Berlie (1), Arne Spang (1), Mara Arts (1), Daniel Kiss (1), Marcel Thielmann (2), Patrick Sanan (3), Ludovic Raess (3)

(1) Johannes-Gutenberg University, Mainz, Germany
(2) Bayerisches GeoInstitut Bayreuth, University of Bayreuth, Germany
(3) ETH Zurich
* Contact: kaus@uni-mainz.de

Abstract

Most geodynamicists have learned how to write codes in numerical modelling classes in which typically high-level languages such as MATLAB or Python were used to explain how to discretize the governing Stokes equations and solve them. That is useful as it is easy to create setups, solve the equations, and plot the results in such languages. Yet, going from a Stokes solver to a full production code, with which we can do lithospheric-scale simulations, often requires quite a bit of additional work including non-dimensionalization, adding (nonlinear) creep laws, and advection schemes (e.g., marker and cell advection). To not loose time with this, many MSc and PhD students use one of the available open-source codes to perform such simulations. MATLAB-based codes that have been widely used are MVEP2 or SiStER. This works fine in 2D, but MATLAB has the disadvantage that it does not scale well in parallel (particularly not on MPI-parallel machines) and that it is commercial. As a result, most 3D codes are written in low-level languages such as C,C++ or Fortran, and many of them rely on PETSc or Trilinos in the background to solve the governing equations on massively-parallel MPI-machines (examples are Underworld, ASPECT, LaMEM or pTatin).

The advantage of such compiled codes is that they run fast and in parallel. The disadvantage is that it is significantly more difficult and time-consuming to develop and debug the code, or to create plots. This issue, which is also known as the two-language problem, also often frequently introduces bugs while translating which makes developer loose time. Overall, in low-level codes, many of the advantages of MATLAB/Python are gone and, as a result, very few PhD students are able to develop a fully new, scalable, 3D code during the time of their PhD. This is a pity as many of the future computational challenges in geodynamics likely involve multiphysics problems, which will require the development of new solvers. Changing the solver in one of the existing codes is possible but certainly a non-trivial task, particularly for new students or postdocs. A related issue is that PETSc works well on CPU-based machines, but many of the next generation high-performance computers rely on GPU's for which PETSc is currently less-well suited. For these cases, pseudo-transient solver approaches appear to be an interesting alternative, which requires a quite different solver strategy altogether.

The Julia programming language is an extremely powerful alternative that combines the easiness of writing codes (as in MATLAB) with the speed of C or fortran. It is a high-level language, fully open source, has a very easy way to develop, share, test and document packages and works on both MPI-based supercomputers and on GPU-machines. As the language itself has many useful features, the resulting lines of code the user needs to write to achieve a certain task is significantly smaller than the equivalent in C/C++ or Fortran. Moreover, many packages already exist that can be easily integrated into your own work.

Here we will discuss our efforts in making Julia a development platform for geodynamic applications that significantly simplifies the process of going from a working solver to a production code. We are working on several packages that simplify certain steps that many geodynamics codes have in common:

- GeoParams.jl is a package in which you can specify constitutive relationships (such as various creeplaws) for your model setup. It automatically handles the (non-)dimensionalization of all input parameters and includes computational routines that can directly be integrated in your solvers. It also includes pre-defined creep laws (e.g., dislocation and diffusion creep laws) and a mechanism to automatically construct data tables from the input, which minimizes the chance of making mistakes while writing papers. By integrating this into your code you can also ensure that the implemented rheologies are consistent with that of other codes.
- PETSc.jl is the main interface from Julia to PETSc. We have recently extended the package to include an interface to DMSTAG, such that you create a staggered finite difference grid and

assemble the stiffness matrix in a simple way in Julia. You can use automatic differentiation tools in Julia to create the Jacobians for nonlinear equations, which again minimizes the required lines of code (compared to their C counterparts). At the same time, it works on MPI-parallel machines, and the full range of (nonlinear) PETSc solvers is available. This is thus very well suited to write implicit solvers.

- ParallelStencil.jl and ImplicitGlobalGrid.jl are packages that are devoted to solving stencils in a very efficient manner on (parallel) GPU or CPU machines, which scales to very large GPU-based high-performance computers. It is particularly efficient in combination with pseudo-transient iterative solvers.
- GeophysicalModelGenerator.jl is a package that gives you a simple way to collect geophysical/geological data of a certain region and combine that to construct an input model geometry.

Ongoing efforts include the development of a grid generation and a marker and cell advection package that work seamlessly with both ParallelStencil.jl and PETSc.jl. This will allow developers to apply both direct-iterative and pseudo-transient implicit solvers to the same problem, while only having to make minimal changes to the model setup.
Combined, these packages will make the step from developing a new (nonlinear) solver to having an efficient production code much easier. We believe that, on the long term, creating a new parallel 3D code is therefore no longer out of scope for a PhD student.

As much of this work is in progress, we will give an overview of the status of our development effort and show several examples on how this can be utilized. Some of the newly developed packages are collected here:
https://github.com/JuliaGeodynamics

GPU-based pseudo-transient finite difference solution for 3-D gravity- and shear-driven power-law viscous flow

Emilie Macherel (1*), Yuri Podladchikov (1), Ludovic Räss (2,3), Stefan M. Schmalholz (1),
(1) University of Lausanne, ISTE, Lausanne, Switzerland, (2) Laboratory of Hydraulics, Hydrology and Glaciology (VAW), ETH Zurich, Switzerland, (3) Swiss Federal Institute for Forest, Snow and Landscape Research (WSL), Birmensdorf, Switzerland
* Contact: emilie.macherel@unil.ch

Abstract

Power-law viscous flow accurately describes the first-order features of long-term lithosphere deformation. Stresses resulting from a deforming lithosphere control processes such as metamorphic reactions, decompression melting, subduction initiation or earthquakes. Calculating these stresses in a three-dimensional (3-D), geometrically and mechanically heterogeneous lithosphere requires high-resolution and high-performance computing.

The pseudo-transient finite difference (PTFD) method enables efficient simulations of high-resolution 3-D deformation processes, implementing an iterative implicit solution strategy of the governing equations for power-law viscous flow driven by buoyancy forces and/or external shear forces. Main challenges for the PTFD method are to guarantee convergence, minimize the required iteration count and speed-up the iterations.

Here, we present PTFD simulations of mechanically heterogeneous (weak spherical inclusion) incompressible 3-D power-law viscous flow in cartesian coordinates. The viscous flow is described by a linear combination of a linear viscous flow law, representing diffusion creep, and a power-law viscous flow law, representing dislocation creep. The iterative solution strategy builds upon pseudo-viscoelastic behavior or flow law to minimize iteration count by exploiting the fundamental characteristics of viscoelastic wave propagation. We performed systematic numerical simulations to investigate the impact of (i) buoyancy versus shear forces and (ii) linear versus power-law viscous flow on the vertical velocity of a weak spherical inclusion. We report the systematic results using the controlling dimensionless numbers and compare the numerical results with analytical predictions for buoyancy-driven flow of inclusions in a power-law matrix. We also aim to unveil preliminary results for 3-D spherical configurations.

We implemented the PTFD algorithm using the Julia language (julialang.org) to enable optimal parallel execution on multiple CPUs and GPUs using the ParallelStencil.jl module (https://github.com/omlins/ParallelStencil.jl). ParallelStencil.jl enables execution on multi-threaded CPU and Nvidia GPUs using a single switch.

Challenges, limitations, and lessons learned from analogue models of thick-skinned tectonics focused on basement fault reactivation

Nicolás Molnar (1*), Susanne Buiter (1)
(1) Tectonics and Geodynamics, RWTH Aachen University, 52064 Aachen, Germany
* Contact: nicolas.molnar@tag.rwth-aachen.de

Abstract

Tectonic styles of deformation in fold-and-thrust belts are generally classified based on the degree of basement involved in the shortening. Thin-skinned (little-to-no basement involvement) and thick-skinned (substantial basement involvement) styles represent end members within this classification. Thin-skinned experimental studies of fold-and-thrust belts have confirmed critical taper theory and have significantly contributed to a better understanding of fundamental aspects of tectonic modelling, such as the interaction of faulting and folding and surface processes. However, only few previous models have investigated thick-skinned tectonics.

While this may be supported by the fact that examples with little basement involvement are more common in nature, recent studies point towards a different direction. Interpretations taking into account new geological data, better resolution subsurface imaging, and thermochronological data, suggest that most orogens show evidences of both thin-skinned and thick-skinned components (Pfiffner, 2017). These different shortening styles are often related to changes in space and time within the orogenic system. Therefore, experimental studies of fold-and-thrust belts investigating basement deformation represent an appropriate method for elucidating their complex spatio-temporal structural evolution.

An additional explanation of why analogue models of thick-skinned fold-and-thrust belts are less common may lie in the practical challenges involved in deforming thick layers of brittle granular materials. Here we discuss the main limitations that we encountered during the planning, setup and running stages of our most recent series of analogue models. Technical challenges range from time-consuming and inefficient methods of sieving thick sand layers to mechanical issues related to deforming very large volumes of granular materials at constant, slow speeds.

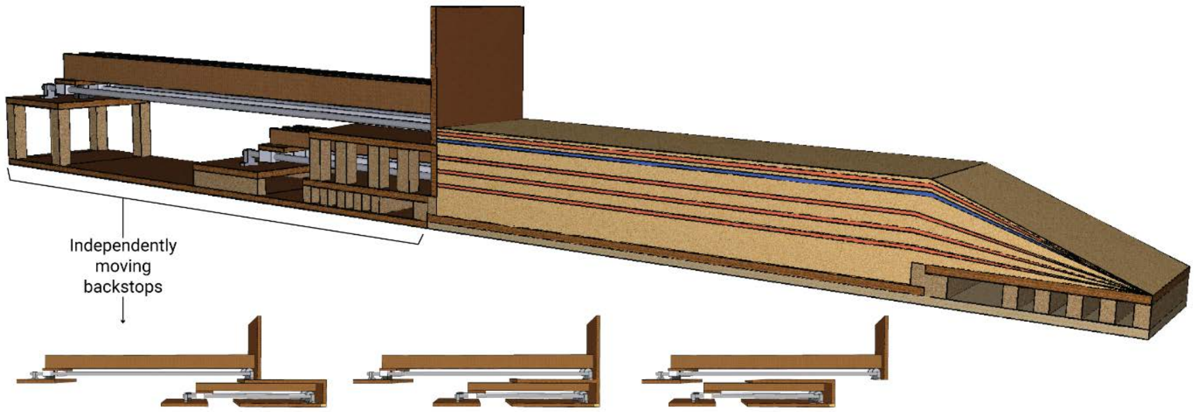

Figure 1: Simplified sketch of the experimental apparatus. After Gottron (2018, MSc Thesis)

Our experimental approach is based on a push-type apparatus containing two independently moving backstops, allowing to impose shortening in both thick- and thin-skinned style, and vary between them over time. The first series of experiments employing this apparatus was carried out with the objective of understanding how pre-existing structures within the basement, such as thrusts or shear zones, control later structural evolution. For this, we initially impose thick-skinned shortening to create deep-rooted thrust systems, which are later affected by a second phase of either thin- or thick-skinned deformation. We use quartz sand to simulate crustal materials and microbeads for weaker, detachment layers. Surface and lateral strain, as well as topography, is quantified using a high-resolution particle imaging velocimetry and digital photogrammetry monitoring system.

Our overarching aim is to create analogue models of thick-skinned fold-and-thrust belts, with a focus on better understanding the role of pre-existing conditions in the basement. Here we present a summary of the main practical challenges we have identified to date, together with possible solutions and potential ways of overcoming them. We hope for an exchange of ideas and experiences with members of the modelling community, not only to make progress towards our main objective, but also to put forward a series of best practices for future experimental setups of thick-skinned tectonics.

References

Pfiffner, A. O., (2017). Thick-skinned and Thin-skinned Tectonics: A Global Perspective. Geosciences 71. doi:10.3390/geosciences7030071

Free access to research facilities and data: EPOS-NL, the Dutch research infrastructure for solid Earth sciences

Ronald Pijnenburg (1)*, Susanne Laumann (2), Richard Wessels (1), Geertje ter Maat (1), Lora Armstrong (2), Jarek Bieńkowski (3), Otto Lange (1), Reinoud Sleeman (3), Philip Vardon (2), David Bruhn (2), Auke Barnhoorn (2), André Niemeijer (1), Oliver Plümper (1), Ernst Willingshofer (1), Kees Wapenaar (2), Jeannot Trampert (1) and Martyn Drury (1)

(1) Utrecht University, Faculty of Geosciences
(2) Technical University of Delft, Faculty of Civil Engineering and Geosciences
(3) Royal Netherlands Meteorological Institute (KNMI)
* Corresponding author: r.p.j.pijnenburg@uu.nl

Abstract
Current Earth scientific research frequently requires access to top research facilities, data and models. Dutch universities and knowledge institutions operate advanced laboratory facilities and produce and maintain unique research data and models. However, these facilities, data and models are often less than optimally accessible for external users. EPOS-NL (European Plate Observing System- Netherlands) aims to overcome this limited accessibility by (further) developing facilities and by providing international, free of charge access to these facilities and derived data.

EPOS-NL facilities include: 1) The Earth Simulation Lab at Utrecht University, including the Tectonic Modelling Lab and the High Pressure and Temperature Lab; 2) The Delft Petrophysics Lab; 3) The Groningen gas field seismological network and the ORFEUS Data Center at the Royal Netherlands Meteorological Institute, 4) The deep geothermal doublet (DAPwell), to be installed on the Delft University campus, 5) A facility for multi-scale imaging and tomography (MINT), shared between the Utrecht and Delft universities.

EPOS-NL provides the financial, technical and scientific support needed for free of charge, open access to its research facilities, data and models. To get facility access, any researcher can apply to a bi-annual call on our website (see below). EPOS-NL further provides central access to essential data and models (e.g. pertaining to the seismogenic Groningen gas field) within the framework of the European infrastructure EPOS. In that way, EPOS-NL contributes to cost-effective and multi-disciplinary research into geo-societal challenges of our densely populated planet.

Interested? Have a look on our website: www.EPOS-NL.nl.

Time dependent properties of granular media – The GeoMod Benchmark 2021

Michael Rudolf (1*), Matthias Rosenau (1), Onno Oncken (1)
(1) Helmholtz Centre Potsdam GFZ German Research Centre for Geosciences
* Contact: michael.rudolf@gfz-potsdam.de

Abstract

Deformation of mountain belts is localized along zones of weakness that are usually inherited from previous tectonic events. This effect leads to the inversion of extensional structures by reactivation of older fault zones which is energetically more favourable than creating new faults. In natural systems several mechanisms of structural weakening are evident. Some act on a short term, such as fluid over pressure or shear heating, others are long term effects of continuous deformation, e.g. mineral reactions or cataclasis over many cycles (Ruh, 2019, and references therein). The processes that lead to weakening can be strain, strain-rate dependent or both. Constitutive equations for deformation can show a grain-size dependence (diffusion creep) which means that with decreasing grain size due to increasing strain, the material becomes increasingly weaker (Bürgmann et al., 2008). Other deformation mechanisms, such as dislocation glide, are grain size independent. Below seismogenic zones the crust is additionally weakened by cyclic stressing through large earthquakes which leads to structural weakening. Furthermore, friction along seismogenic zones is characterized by strong strain rate weakening which facilitates the nucleation and propagation of earthquakes (Scholz, 1998).

In analogue modelling the strain and strain-rate dependent weakening of granular materials is exploited to create models of basin inversion. Some materials such as sand and glass beads show a strain dependent weakening when sheared that leads to localization phenomena. When re-sheared, the reactivation strength is typically lower than the initial peak strength. This may lead to the reactivation of pre-existing faults during inversion instead of the formation of new faults. The reactivation strength is not only influenced by the amount of strain weakening during localization but also by time dependent healing during the inactive phase which might last from seconds during stick-slip cycles in seismotectonic analogue models, to minutes or hours in models on basin inversion which run at loading rates of a few cm per hour. Furthermore, strain rate dependent weakening can influence the localization of faults during extension (Ruh, 2019) although this effect does not play a major role in most basin inversion models because they are run at very low strain rates ($< 10^{-6}$ s^{-1}).

In our study we constrain the time dependent healing effect of the materials which are in use at the Helmholtz Laboratory for Tectonical Modeling. For example, we show that fused glass microbeads exhibit healing which follows a power-law relation of $\Delta\mu_p \propto b \ln t_h$ with b=0.005 which means that for an e-fold increase in hold time the strength required to reactivate the given fault increases by 0.5% (Figure 1 a, c + d). Consequently, if a fault is inactive for a longer period of time, it is slightly stronger in comparison with a fault with less inactivity. Additionally, granular fault zones show a strain rate weakening which scales similarly and leads to a reduction of dynamic friction with increasing sliding rate. The amount of strain rate weaking (b-a) is 8.7% per e-fold increase in sliding velocity which can lead to substantial reductions in dynamic strength for seismotectonic analogue models (Figure 1 e).

To further improve the material characterisation, we want to test more samples that are used by the community, complement and re-evaluate previous measurements to estimate the amount of weakening and the strain range for which strain weakening occurs (e.g. Ritter et al. 2016). We plan to do slide-hold-slide tests and velocity stepping tests on many of the materials we received for testing in previous years and to supplement the Geomod 2008 Benchmark (Klinkmüller et al. 2016) with friction parameters relevant for re-activation and rate dependency. Finally, we invite everyone to send us new samples or mixtures of materials that are in use for their experiments.

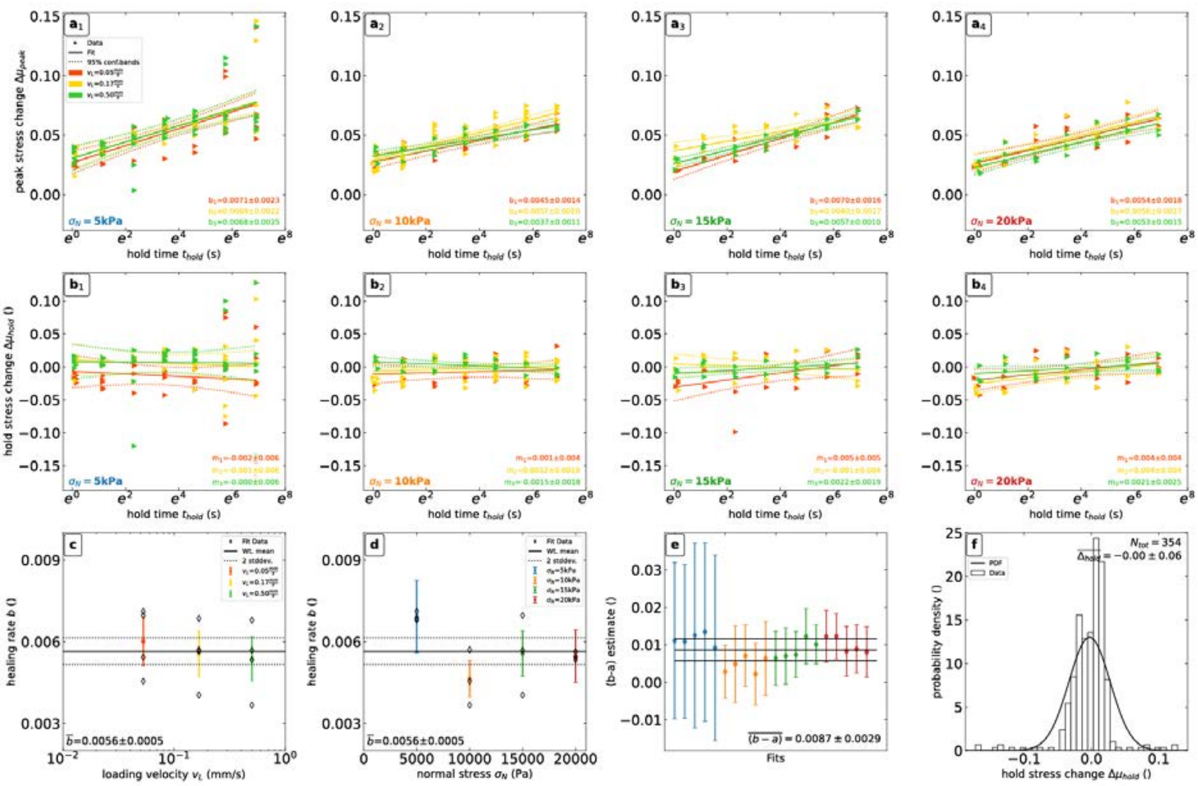

Figure 1. Various time-dependent changes in frictional strength of glass beads. a) Change in peak reloading stress with hold time. Higher hold times lead to a log-linear increase in reactivation strength. b) Transient stress change during the hold phase. Indicates ongoing creep after holding due to relaxation. c) Average healing rate (log-linear slope in a)) with increasing reloading velocity. d) Healing rate with respect to normal stress. e) Estimates for strain rate dependency, denoted by the difference of rate-and-state parameters b (healing rate) and a (direct effect). If (b-a) > 0 the material is strain rate weakening and if (b-a) < 0 the material is strain rate strengthening. f) Hold stress change in all experiments as a histogram to estimate the effect of post-hold creep on stress changes in the granular materials. Figure from Rudolf et al. (in rev).

References

R. Bürgmann and G. Dresen, “Rheology of the lower crust and upper mantle: evidence from rock mechanics, geodesy, and field observations,” Annual Review of Earth and Planetary Sciences, vol. 36, no. 1, Art. no. 1, 2008, doi: 10.1146/annurev.earth.36.031207.124326.

M. Klinkmüller, G. Schreurs, M. Rosenau, and H. Kemnitz, “Properties of granular analogue model materials: A community wide survey,” Tectonophysics, vol. 684, pp. 23–38, 2016

M. C. Ritter, K. Leever, M. Rosenau, and O. Oncken, “Scaling the Sand Box - Mechanical (Dis-) Similarities of Granular Materials and Brittle Rock,” J. Geophys. Res. Solid Earth, 2016, doi: 10.1002/2016jb012915.

M. Rudolf, M. Rosenau, and O. Oncken, “The spectrum of slip behaviours of a granular fault gouge analogue governed by rate and state friction.,” Geochemistry, Geophysics, Geosystems. (in revision)

J. B. Ruh, “Effects of fault-weakening processes on oblique intracontinental rifting and subsequent tectonic inversion,” American Journal of Science, vol. 319, no. 4, Art. no. 4, 2019.

C. H. Scholz, “Earthquakes and friction laws,” Nature, vol. 391, no. 6662, Art. no. 6662, 1998, doi: 10.1038/34097.

Thermo-Hydro-Mechanical-Chemical modelling: applications to dehydration vein formation and reactive melt migration

Stefan Markus Schmalholz (1*)
(1) Institute of Earth Sciences, Géopolis, University of Lausanne, 1015 Lausanne, Switzerland
* Contact: stefan.schmalholz@unil.ch

Abstract

Many geodynamic processes, such as subduction or magmatism, involve the coupling of thermal (e.g. heat conduction), hydrological (e.g. porous flow), mechanical (e.g. viscous shearing) and chemical (e.g. dehydration reaction) processes. However, our knowledge of these coupled processes is still limited, and the quantification of such coupled processes remains challenging. One possibility to study such coupled processes is the application of mathematical models and their corresponding numerical solutions. Such mathematical models for the coupled processes mentioned above are frequently termed Thermo-Hydro-Mechanical-Chemical (THMC) models. We present the fundamentals of a particular type of THMC models and show two applications of this model: (1) A two-dimensional (2D) HMC model for the formation of dehydration veins in viscously deforming serpentinite and (2) 1D and 2D THMC models for melt migration and chemical differentiation by reactive porosity waves. The HMC model is applied to olivine veins in meta-serpentinites, observed in the Erro-Tobbio unit (Ligurian Alps, Italy). We discuss the different characteristic time scales controlling dehydration vein formation and quantify the impact of deformation and kinetic rates on the growth velocity of the dehydration veins. The THMC model is applied to melt migration around the lithosphere-asthenosphere boundary to better understand the formation of so-called petit-spot volcanoes, which are observed on the subducting Pacific plate east of Japan. These models show that chemical differentiation, particularly the variation of silica content, affects melt migration since it changes the densities of solid and melt. Both HMC and THMC models are numerically solved with the pseudo-transient finite difference method, for which we explain the main features. We will also briefly discuss the numerical solutions for CPU and GPU computer architectures.

Strain distribution across modelled thrust imbricates described by magnetic fabric

Thorben Schöfisch (1*), Hemin Koyi (1), Bjarne Almqvist (1)
(1) Hans Ramberg Tectonic Laboratory, Department of Earth Sciences, Uppsala University, Villavägen 16, 752 36 Uppsala, Sweden
* Contact: thorben.schofisch@geo.uu.se

Abstract

Introduction and Method

The anisotropy of magnetic susceptibility (AMS) is a useful indicator for penetrative strain in structural geology (e.g., review by Parés, 2015). Recently, Almqvist and Koyi (2018) highlighted the potential of combining analogue modelling with AMS to reveal links between magnetic fabric and strain in compressional tectonic settings. In this study, we apply AMS on three sandbox models (Model A: 16%, Model B: 24.5%, and Model C: 34% bulk shortening) to look into the intensity and distribution of magnetic fabric across a thrust imbricate and at different stages of its evolution. Samples are taken throughout the wetted models for AMS analysis with a MFK1-FA Kappabridge (Agico Inc.). The magnetic fabric is described by the principal axes of susceptibility ($k_{max} \geq k_{int} \geq k_{min}$), that outline the bulk orientation of magnetite grains in a sample, and by the degree of anisotropy and the shape of the resulting ellipsoid.

Results and Interpretation

During shortening, all three models initially developed a main boxfold bounded by backthrust(s) and forekink zone(s). With further shortening, several forethrusts developed in front of the main boxfold in the models. AMS analysis of the samples from different parts of the model describe characteristic sets of magnetic fabric, which are summarized in Figure 1 using Model B as a representative model. Away from thrusts and kinkzones, the magnetic fabric is oblate and magnetic foliation (k_{max}-k_{int} girdle distribution) is parallel to bedding. Nevertheless, the principal axis orientation of k_{max} and k_{int} scatter around the primitive circle in the areas away from thrusts and kinkzones, that indicate penetrative strain. However, the principal axes inclination changes and the degree of anisotropy decreases towards a thrust or kinkzone. In the vicinity of a thrust or kinkzone, prolate fabric are observed. These changes in magnetic fabric as a function of distance to a thrust or kinkzone highlight a change in the nature of strain associated with different structures. Similar observations in magnetic fabric change reported here are made in natural analogies, such as in the Hikurangi accretionary prism (e.g., Greve et al., 2020).

Thrusts developed a magnetic fabric that has a magnetic foliation parallel to the thrust surface, which can be interpreted as thrust-induced fabric (Schöfisch et al., 2021). Additionally, the degree of anisotropy decreases downdip along the thrusts. This trend is independent of the amount of displacement on a thrust, since all thrusts developed similar degree of anisotropy. Despite the structural variation along a thrust, e.g., thrust splay or intersection with other thrusts, the trend in degree of anisotropy with depth can be related to the development of a thrust. Compaction and folding precedes thrusting and we interpret that the fabric related to compaction and folding is inherited in the finite “thrust-induced” fabric in the models, especially at depth.

In the forekink zones, the magnetic fabric consists of broad girdles and scattered clusters of the principal axis. The AMS data reflects the complex interaction between thrusting (magnetic foliation parallel to minor thrusts within the kinkzone) and folding (magnetic lineation parallel to fold axes). Therefore, AMS analysis of samples from these kinkzones represent different contributions to strain forming of a complex magnetic fabric.

Conclusion

This study illustrates strain development via AMS across modelled thrust imbricates in detail and provides information about deformation processes. At the beginning of model shortening, the initial magnetic fabric in the models is modified by penetrative strain and folding. With further bulk shortening of the models, further folding and thrusting overprint the magnetic fabric locally, producing a magnetic fabric associated with the structure. AMS signals created prior to thrusting can be inherited within the finite “thrust-induced” fabric. Towards the developed thrusts and kinkzones a gradient in strain can be identified by changes in the magnetic

fabric. Overall, different deformation processes competing in overprinting the magnetic fabric during evolution of a thrust imbricate, but strain can be revealed by AMS analyses.

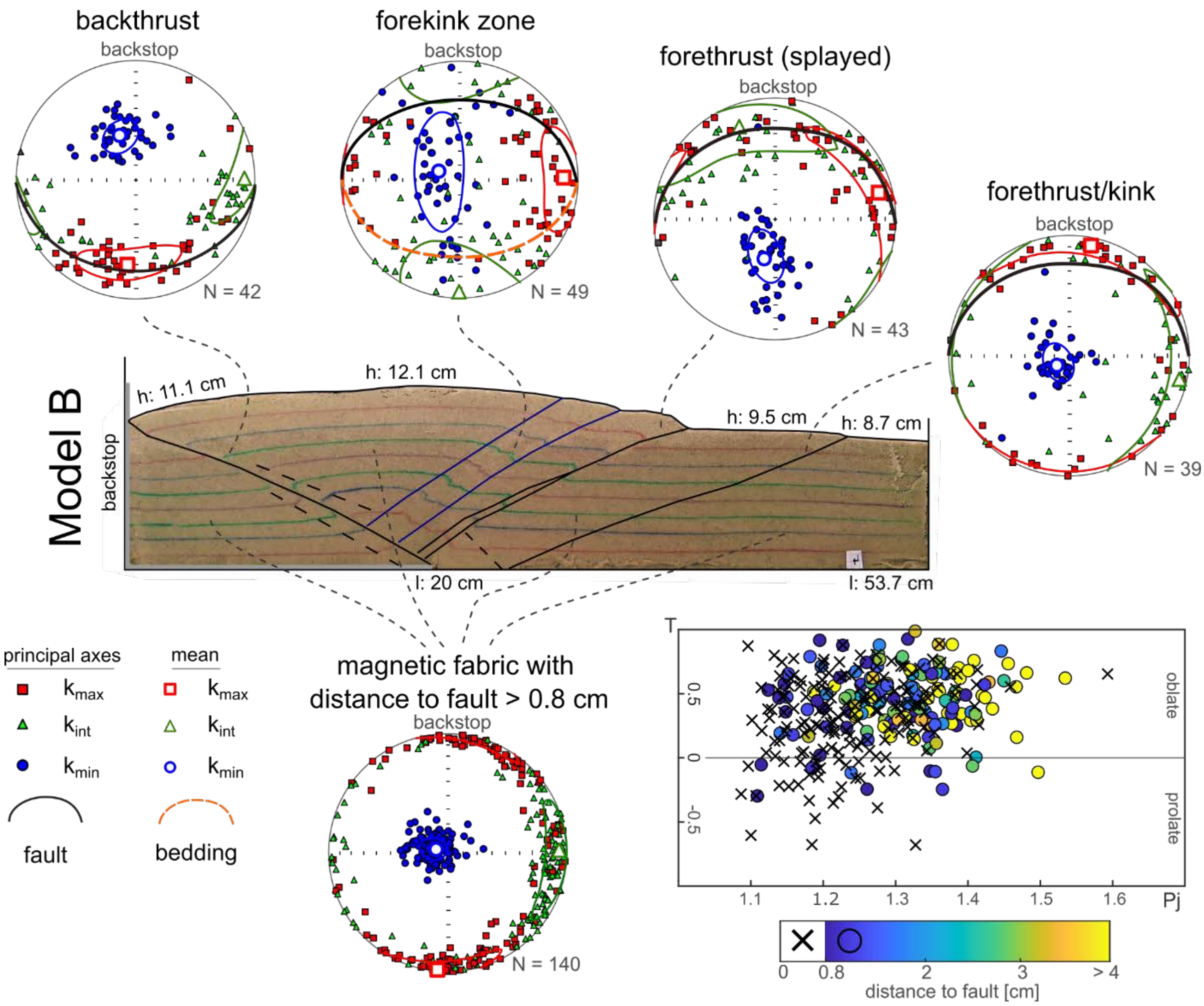

Figure 1: Representative profile of Model B (24.5 % bulk shortening) showing a boxfold bounded by a backthrust and a forekink zone with two forethrusts in front of the boxfold. The principal axis distribution ($k_{max} \geq k_{int} \geq k_{min}$), with means and confidence ellipses, is plotted on a stereographic lower hemisphere projection for each structure/area with backstop defined as north. The degree of anisotropy (Pj) is plotted against the shape of anisotropy (T) as a Jelinek plot.

References

Almqvist, B. S. G., & Koyi, H. (2018). Bulk strain in orogenic wedges based on insights from magnetic fabrics in sandbox models. *Geology*, *46*(6), 483–486. https://doi.org/10.1130/G39998.1

Greve, A., Kars, M., Zerbst, L., Stipp, M., & Hashimoto, Y. (2020). Strain partitioning across a subduction thrust fault near the deformation front of the Hikurangi subduction margin, New Zealand: A magnetic fabric study on IODP Expedition 375 Site U1518. *Earth and Planetary Science Letters*, *542*, 116322. https://doi.org/10.1016/j.epsl.2020.116322

Parés, J. M. (2015). Sixty years of anisotropy of magnetic susceptibility in deformed sedimentary rocks. *Frontiers in Earth Science*, *3*, 4. https://doi.org/10.3389/feart.2015.00004

Schöfisch, T., Koyi, H., & Almqvist, B. (2021). Influence of décollement friction on anisotropy of magnetic susceptibility in a fold-and-thrust belt model. *Journal of Structural Geology*, *144*(September 2020). https://doi.org/10.1016/j.jsg.2020.104274

Keywords: Analogue Modelling; Anisotropy of Magnetic Susceptibility; Thrust Imbricate; Boxfold; Strain distribution;

GPU Acceleration on Geodynamic Simulation via OpenACC

Eh Tan (1*), Chase C.H. Shyu (1,2), Fang-Yi Lee (3), Chi-Chin Lee (1)
(1) Institute of Earth Sciences, Academia Sinica, (2) Taiwan International Graduate Program - Earth System Science Program, Academia Sinica and National Central University, (3) Institute of Oceanography, National Taiwan Unversity
* Contact: tan2@earth.sinica.edu.tw

Abstract

Numerical simulation on geodynamic processes is computationally expensive. Pursuit of higher resolution and more accurate physical simulation requires more and more computation power. The speed improvement of CPUs has stalled in recent years. Moreover, the speed of memory access has improved only slowly in decades, which further reduces the performance of the simulation. The advance of GPGPU (General Purpose computing on GPU) can help to solve the performance problem. GPU provides quick memory access and fast context switch to hide memory access latency while keeps the computation units busy. Traditionally, the GPU and CPU have separated memory space. Programmers have to transfer data between GPU and CPU manually before and after the computation. The newer generation of Nvidia GPU provides unified memory space to avoid manual data transfers. Additionally, we can port the CPU codes to GPUs using a few lines of OpenACC directives. In the end, we completely ported our explicit geodynamic simulation code to GPU and achieved a 40x speed-up, compared to a single CPU performance. We will detail the porting strategy and compare the similarity of OpenACC to OpenMP.

Session 1

Surface processes, landscapes, sediment fluxes and depositional systems

- Todd Ehlers. *How Plants Shape Mountains* ***(keynote)***
- Òscar Gratacós. *Constraining environmental parameters using forward numerical modelling. Application to an Aptian carbonate system (E. Iberia)*
- Hanneke Heida. *Flexural-isostatic modelling of the vertical motions and paleotopography of the Alboran Sea since the Messinian Salinity Crisis*
- Maarten Kleinhans. *Living landscapes in the lab: bio-morphodynamics of rivers, estuaries and tidal systems* ***(keynote)***
- Paul Perron. *Constraining the mantle contribution to thermal history of sedimentary basins by driving kinematically 2D thermomechanical simulations of passive margins*
- Magdalena Scheck-Wenderoth. *Closing the gap between data and models: from static 3D data-based configurations to process simulations* ***(keynote)***

How Plants Shape Mountains

Todd A. Ehlers (1*) *(keynote)*
(1) Department of Geosciences, University of Tübingen, Germany
* Contact: todd.ehlers@uni-tuebingen.de

Abstract

Earth surface processes are modulated by fascinating interactions between climate, tectonics, and biota. These interactions are manifested over diverse temporal and spatial scales ranging from seconds to millions of years, and microns to thousands of kilometers, respectively. Investigations into Earth surface shaping by biota have gained growing attention over the last decades and are a research frontier. Examples of the scales of biotic interactions with surface processes range from microbial and fungal consumption of mineral surfaces over short temporal and small spatial scales, to vegetation interactions with climate, sedimentation and erosion over temporal scales of hours (individual storms) to millennia (global climate change), and spatial scales of centi- to kilometers (encompassing individual plants to catchment scale biomes). Finally, mountain building and Milankovitch cycle-driven climate change produce ecologic, climate, and erosional gradients across temporal scales of millennia to millions of years and large spatial scales.

In this lecture, I present an integration of new observational and numerical modeling research on the influence of vegetation cover on catchment denudation and topographic evolution. I do this through an investigation of millennial timescale catchment denudation rates measured along the extreme climate and ecologic gradient of the western margin of South America from Peru to central Chile (6 to 36 Degrees S latitude). Results identify different zones of behavior between vegetation and catchment denudation that are separated by two distinct thresholds, where the effects of vegetation cover on denudation exhibit either an increasing or decreasing correlation with denudation rates. Additional insights into the observed latitudinal variations, and non-linear behavior in vegetation and denudation rates are provided with coupled dynamic vegetation and paleoclimate models, and a landscape evolution model that accounts for vegetation cover effects on hillslope and fluvial erosion. The modeling approach provides insights into a physical explanation for precipitation and vegetation controls on denudation along the western South American margin.

References

Mutz, S. G., & Ehlers, T. A. (2019). Detection and explanation of spatiotemporal patterns in Late Cenozoic palaeoclimate change relevant to Earth surface processes. *Earth Surface Dynamics*, *7*(3), 663–679. https://doi.org/10.5194/esurf-7-663-2019

Schmid, M., Ehlers, T. A., Werner, C., Hickler, T., & Fuentes-Espoz, J.-P. (2018). Effect of changing vegetation and precipitation on denudation – Part 2: Predicted landscape response to transient climate and vegetation cover over millennial to million-year timescales. *Earth Surface Dynamics*, *6*(4), 859–881. https://doi.org/10.5194/esurf-6-859-2018

Starke, J., Ehlers, T. A., & Schaller, M. (2020). Latitudinal effect of vegetation on erosion rates identified along western South America. *Science*, *367*(6484), 1358–1361. https://doi.org/10.1126/science.aaz0840

Werner, C., Schmid, M., Ehlers, T. A., Fuentes-Espoz, J. P., Steinkamp, J., Forrest, M., et al. (2018). Effect of changing vegetation and precipitation on denudation – Part 1: Predicted vegetation composition and cover over the last 21 thousand years along the Coastal Cordillera of Chile. *Earth Surface Dynamics*, *6*(4), 829–858. https://doi.org/10.5194/esurf-6-829-2018

Constraining environmental parameters using forward numerical modelling. Application to an Aptian carbonate system (E Iberia).

Òscar Gratacós (1*)(3), Telm Bover-Arnal (2)(3), Roger Clavera-Gispert (4), Ana Carmona (4), David García-Sellés (1)(3)

(1) Departament de Dinàmica de la Terra i de l'Oceà, Facultat de Ciències de la Terra, University of Barcelona, Martí i Franqués, s/n, 08028 Barcelona, Spain.
(2) Departament de Mineralogia, Petrologia i Geologia Aplicada, Facultat de Ciències de la Terra, Universitat de Barcelona, Martí i Franquès s/n, 08028 Barcelona, Spain.
(3) Institut de Recerca Geomodels, Facultat de Ciències de la Terra, Universitat de Barcelona, Martí i Franqués, s/n, 08028 Barcelona, Spain.
(4) External Consultant, Institut de Recerca Geomodels, Facultat de Ciències de la Terra, Universitat de Barcelona, Martí i Franqués, s/n, 08028 Barcelona, Spain.

* Contact: ogratacos@ub.edu

Abstract

The facies distribution in time and space of sedimentary successions is controlled by a complex interplay between physical, chemical and biological processes, which are nowadays difficult to construe from the geological record. Numerical models constitute a valuable tool to identify and quantify such controlling factors permitting a reliable 3D extrapolation and prediction of stratigraphic and facies architectures beyond outcropping rock strata.

This study assesses the roles of three controlling parameters being carbonate production rate, relative sea-level changes and siliciclastic supply, on the evolution of an Aptian carbonate system (Bover-Arnal et al., 2009). The SIMSAFADIM-CLASTIC, a 3D process-based sedimentary-stratigraphic forward model, was used for this evaluation (Gratacós et al., 2009, Clavera-Gispert et al., 2017). The carbonate succession modelled crops out in the western Maestrat Basin (E Iberia), and corresponded to a platform-to-basin transition comprising three depositional environment-related facies assemblages: platform top, slope and basin.

Testing of geological parameters in forward modelling results in a wide range of possible 3D geological scenarios. The documented distribution of facies and sequence-stratigraphic framework combined with a virtual outcrop model were used as a reference to perform geometric (quantitative) and architectural and stacking pattern (qualitative) research by model-data comparison. The time interval modelled spans 1450 ky. The best-fit simulation run (Figure 1) characterizes and quantifies (1) relative sea-level fluctuations recording five different genetic types of deposit (systems tracts) belonging to two depositional sequences as expected from field-data analysis, (2) a rate of terrigenous clastic sediment input ranging between 0.5 and 2.5 gr/s, and (3) a mean autochthonous carbonate production maximum rate of 0.08 m/ky.

Furthermore, the quantitative and qualitative sensitivity tests carried out highlight that the fluctuation of relative sea level exerted the main control on the resulting stratigraphic and facies architectures, whereas the effect of inflowing terrigenous clastic sediment is less pronounced. Facies assemblages show different sensitivities to each parameter, being the slope carbonates more sensitive than the platform top facies to inflowing fine terrigenous sediments. On slope depositional settings, siliciclastic input also controls stratal stacking patterns and the dimensions of the carbonate bodies formed. The final 3D model allows to spot architectural features such as stacking patterns that can be misinterpreted by looking at the resulting record in the outcrop or by using other 2D approaches, and facilitates the comprehension of reservoir connectivity highlighting the occurrence of initial disconnected regressive platforms, which were later connected during a transgressive stage. Thus, the resulting simulations and quantifications of the environmental parameters obtained could be of relevance to better constrain the growth, architecture and facies heterogeneities of coeval carbonate platforms from other basins worldwide including giant subsurface hydrocarbon reservoirs such as the Shu'aiba Formation in the Middle East.

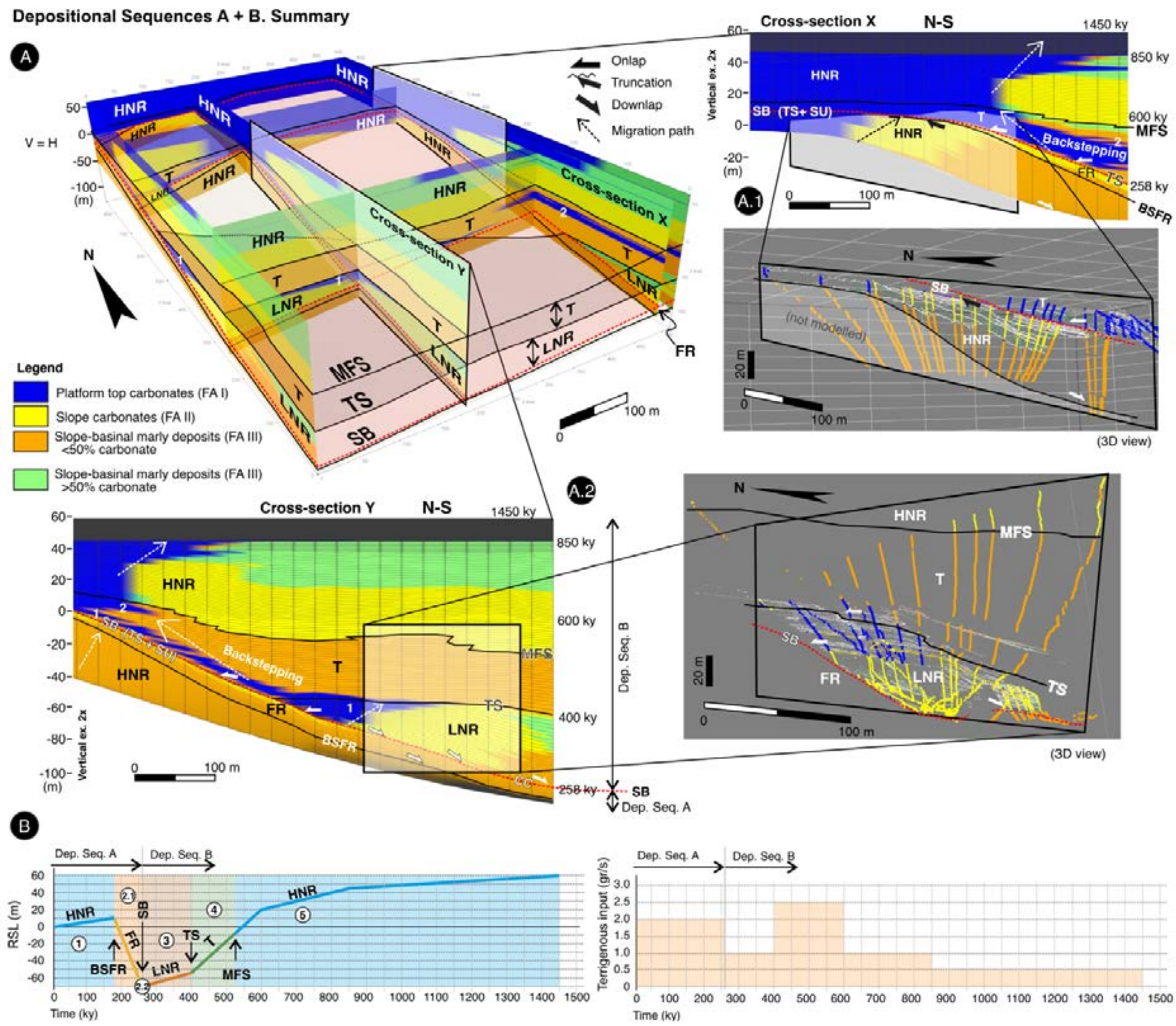

Figure 1: Summary of the final best-fit simulation for depositional sequences A and B belonging to the Aptian carbonate system (Las Mingachas). A) Fence diagram displaying the facies distribution and the sequence-stratigraphic interpretation. Two close-up views (A.1 and A.2) for the cross-sections X and Y have been also included (note the vertical exaggeration 2x). Time lines allow identifying the stacking patterns of the distinct sedimentary bodies generated. Parts of both views are compared with the facies identified in the field through the DOM (see enlarged images). B) Rates versus time of RSL changes and terrigenous input used to obtain the final model.

References

Bover-Arnal, T., Salas, R., Moreno-Bedmar, J.A., Bitzer, K., 2009. Sequence stratigraphy and architecture of a late Early-Middle Aptian carbonate platform succession from the western Maestrat Basin (Iberian Chain, Spain). Sedimentary Geology 219, 280–301.

Clavera-Gispert, R., Gratacós, O., Carmona, A., Tolosana-Delgado, R., 2017. Process-based forward numerical ecological modeling for carbonate sedimentary basins. Computational Geosciences 21, 373–391. doi: 10.1007/s10596-017-9617-4

Gratacós, O., Bitzer, K., Cabrera, L., Roca, E., 2009. SIMSAFADIM-CLASTIC: a new approach to mathematical 3D forward simulation modelling for clastic and carbonate sedimentation. Geologica Acta 7, 311–322.

Flexural-isostatic modelling of the vertical motions and paleotopography of the Alboran Sea since the Messinian Salinity Crisis

Hanneke Heida(1*), Daniel García-Castellanos(1), Ivone Jiménez-Munt(1), Ferran Estrada(2), Gemma Ercilla(2), Sophie Coulson(3), Jerry X. Mitrovica(3), Damien Do Couto(4), Abdellah Ammar(5)

(1) Geosciences Barcelona (GEO3BCN) Consejo Superior de Investigaciones Científicas (CSIC), Barcelona, Spain
(2) Instituto de Ciencias del Mar, CSIC, CMG, Passeig Marítim de la Barceloneta 37-49, 08003 Barcelona, Spain.
(3) Department of Earth and Planetary Sciences, Harvard University, Cambridge MA, United States
(4)Sorbonne Université, Paris 06, ISTEP, and CNRS, UMR 7193, F-75005, Paris, France
(5)U. Mohammed V-Agdal, Rabat, Morocco

* Contact: hheida@geo3bcn.csic.es

Abstract

The Messinian Salinity Crisis (MSC) is the last giant salt accumulation formed on Earth and was caused by changes in the Atlantic-Mediterranean connectivity in the western end of the Alboran Basin (Figure 1), a complex tectonic area affected by the Iberia-Africa collision and the retreat of a subducted lithospheric slab beneath the Betic-Rif orogen. The depth of the various Alboran subbasins and volcanic regions at the time of the MSC is controversial and has led to the proposal of two gateway locations, one at Gibraltar implying a desiccated West Alboran Basin (e.g, Garcia-Castellanos et al., 2020), and another one further to the East, north of the Alboran Ridge with the West Alboran Basin functioning as a marine refuge for Mediterranean species during the MSC (Booth-Rea et al., 2018).

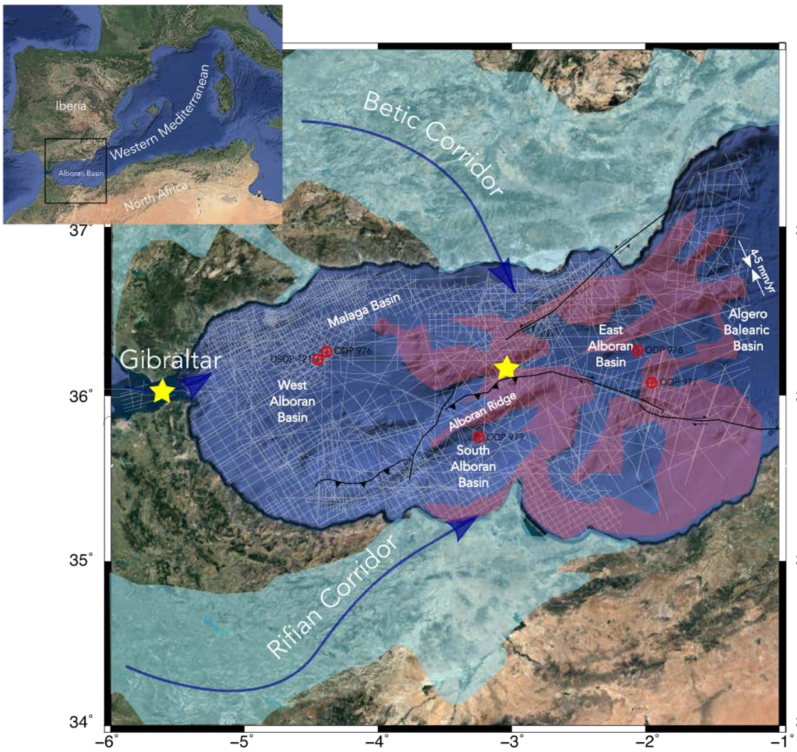

Figure 1: Bathymetric map of the study area including the seismic dataset used in this study, the main tectonic features from Gómez de la Peña et al. (2021), and locations of DSDP/ODP boreholes. Light blue: Late Miocene Atlantic-Mediterranean gateways from Krijgsman et al. (2018). Red: East Alboran Miocene Volcanic arc from Booth-Rea et al. (2018) Stars: gateway locations proposed to have ended the MSC.

Isostatic, tectonic and erosional effects on surface topography work on different spatial and temporal scales, and their relative contributions to the changes in connectivity and subsequent evaporite deposition and sea-level lowering are difficult to constrain.

We perform a 2D-planform flexural isostatic reconstruction of the Messinian Erosion Surface (MES) imaged in the Alboran Basin to reconstruct the topography and vertical motions of this region since the end of the MSC. The model accounts for sediment compaction and post-Messinian tectonic deformation and thermal subsidence. The results constrain the original depth of the Messinian erosional features and MSC-related deposits and provide an important test for various models for Mediterranean sea-level changes during the MSC. They also provide novel insight in the development of basin topography in this tectonically complex area. We find that a shallow (<1000 m) reconstructed Messinian bathymetry in the western and central parts of the Alboran Basin can explain the absence of in-situ evaporites in this region, and implies complete exposure of the basin during the lowstand stage of the MSC. Our preliminary results show that it is unlikely that the topography of the Miocene volcanic arc in the Eastern Alboran could have been shallow enough to function as a marine gateway during the MSC, suggesting that the Mediterranean sill was located, as today, further to the west in the Gibraltar Strait area.

Features identified as erosional terraces occur at a wide range of reconstructed depths, from 100-200 m (Bay of Oran, Alboran Ridge) to >1000 m in the central WAB close to the Zanclean flooding channel. This suggests that these features may have formed in response to different processes not just during the exposure of the basin but perhaps also during its reflooding. These results agree with seismic studies (e.g., Estrada et al., 2011) suggesting that the Alboran MES represents a polygenetic surface recording a number of important changes during the MSC.

References

Booth-Rea, G., R. Ranero, C., Grevemeyer, I., 2018. The Alboran volcanic-arc modulated the Messinian faunal exchange and salinity crisis. Sci. Rep. 8, 13015–13015. https://doi.org/10.1038/s41598-018-31307-7

Estrada, F., Ercilla, G., Gorini, C., Alonso, B., Vázquez, J. T., García-Castellanos, D., Juan, C., Maldonado, A., Ammar, A., & Elabbassi, M. (2011). Impact of pulsed Atlantic water inflow into the Alboran Basin at the time of the Zanclean flooding. *Geo-Marine Letters*, *31*(5–6), 361–376. https://doi.org/10.1007/s00367-011-0249-8

Garcia-Castellanos, D., Micallef, A., Estrada, F., Camerlenghi, A., Ercilla, G., Periáñez, R., Abril, J.M., 2020. The Zanclean megaflood of the Mediterranean – Searching for independent evidence. Earth-Sci. Rev. 201, 103061–103061. https://doi.org/10.1016/j.earscirev.2019.103061

Gómez de la Peña, L., R. Ranero, C., Gràcia, E., Booth-Rea, G., 2021. The evolution of the westernmost Mediterranean basins. Earth-Sci. Rev. 214, 103445. https://doi.org/10.1016/j.earscirev.2020.103445

Krijgsman, W., Capella, W., Simon, D., Hilgen, F.J., Kouwenhoven, T.J., Meijer, P.Th., Sierro, F.J., Tulbure, M.A., van den Berg, B.C.J., van der Schee, M., Flecker, R., 2018. The Gibraltar Corridor: Watergate of the Messinian Salinity Crisis. Mar. Geol. 403, 238–246. https://doi.org/10.1016/j.margeo.2018.06.008

Living landscapes in the lab: bio-morphodynamics of rivers, estuaries and tidal systems

Maarten G. Kleinhans (1*) *(keynote)*
(1) Utrecht University
* m.g.kleinhans@uu.nl

Abstract

Rivers, deltas, distributive fluvial systems, estuaries and tidal basins are ubiquitous depositional systems on Earth and Mars. Their morphological and stratigraphic patterns are complex as as result of changeable boundary conditions, setting and the physical, chemical and biological mechanisms. Analogue models of these systems in small-scale laboratory experiments offer control over the conditions and mechanisms that form the complex landscapes, but their scaling poses challenges. Here I present a synthesis of recent advances in landscape experiments that formed patterns hitherto thought intractible in the lab. Finally I discuss possibilities for experiments combining tectonics, erosion and sedimentation in large-scale facilities.

Select scaling conditions must be met to form landscapes by flowing water and sediment transport, (Kleinhans et al. 2014). The most important is the mobility of the sediment (Shields similarity), which is determined by the bed shear stress of the flow and the submerged weight of the sediment particles. Furthermore, while laminar flow conditions and supercritical flow have been used, engineering scale models require similarity of Froude number (flow velocity normalised by shallow water wave celerity) and Reynolds number (momentum divided by viscous force). It turns out that a broad range of phenomena is well represented experimentally under more relaxed conditions of subcritical flow (Froude number <1) and turbulent flow (Reynolds number >2000 and a rough bed boundary (particle size >0.5 mm). The median particle size must be >0.5 mm, which, at an experimental scale of 1:1000 to 1:100,000 would suggest a prototype particle of 0.5 to 50 m. But this size scale does not matter; what matters are spatial gradients in the sediment volume flux as these form the morphological patterns. The mobility can also be increased by lower particle density (plastics, coal and walnut shell). These conditions have produced similarity of dynamics, morphology and stratigraphy of simple alluvial fans, fan deltas and braided rivers.

Creating tidal systems in the lab has been shown impossible since the first analogue models of Reynolds for the port of London. The main reason is that the steep downward slopes (>0.005 m/m) required for sediment motion by rivers inhibit the motion of sediment during the flooding phase of the tide, while this was in reality important in forming coastal plains such as the Netherlands (de Haas et al. 2019). This issue has been resolved by driving the flow not by tidal seawater level fluctuations, but by periodic tilting (40 s) of the entire experimental facility (Figure 1, middle) at slopes of about 0.005 m/m. This produces tidally driven sediment dynamics of sufficient similarity to natural estuaries to produce geometrically and geomorphically correct tidal bars (Kleinhans et al. 2017).

Figure 1: Left: floodplain-dominated distributive fluvial system. Middle: the Metronome tidal flume (www.uu.nl/metronome, width 3 m and length 20 m) with a self-formed estuary. Right: a vegetated tidal bar (Weisscher et al. submitted). Water is dyed blue for visibility

The more complex landscapes have only recently been formed by careful composition of sediment mixtures. One could argue that the greatest degree of control over the experimental dynamics is obtained with the cleanest sediments, i.e. composed of only one particle size. This notion has long impeded progress. The groundwater percolation in course sand is much too strong and destabilises channel banks. Well-sorted course sand is cohesionless but floodplain formation with (apparent) cohesion is a necessary condition for meandering and for isolating channel belts in finer sediment as found in large sedimentary basins. Furthermore, levee and floodplain formation in shallow flows requires a range of fine sediments. All these experimental scaling issues are largely resolved by broad sediment mixtures, of which permeability, shear strength and the range of sediment mobilities can be controlled. Our broad sediment mixtures have produced the first dynamic meandering laboratory rivers with pointbars and cutoffs through floodplain (Kleinhans et al. 2014) and floodplain-dominated distributive fluvial systems with channel avulsion dynamics (Figure 1 left, Terwisscha et al. 2020).

Most complex natural landscapes since the Precambrium are partially shaped by vegetation (Figure 1 right). Plants resist flow, cause apparent cohesion, capture fine sediment and create conditions for further colonisation of vegetation. Seedlings of small plant species have been used successfully to create living landscapes with floodplain in experiments for two decades. Again, size does not matter, but the effects do. Seed density and mobility and plant sensitivity to inundation determine the water depths of colonisation, stem density determines hydraulic resistance and rooting depth and density determine apparent cohesion of channel banks. Collectively, these effects stabilised channel banks, differentiated floodplain from channel and cause fundamentally different equilibrium morphologies of living landscapes than without vegetation.

Recent advances in alluvial and tectonic experiments allow for a fusion of experiments that build mountains and form basins and continental margins, and experiments that erode mountains, fill basins and form deltas. The scaling of analogue models for alluvial and for tectonic systems are similar conceptually (balancing of forces) and in part thematically (strength and rheology of materials). Moreover, they model different parts of the same continental systems, and the shorter timescale of morphodynamics begins to overlap with the large timescale of tectonics. We can now begin to test experiments, for example, of subsiding basins depending on sediment weight, and of mountain uplift balanced by erosion. This opens up possibilities to explore feedbacks between global tectonics, global climate and life and infer testable hypotheses for effects on morphology and stratigraphy to be tested in the field.

References

Broerse, T., B. Norder, R. Govers, D. Sokoutis, E. Willingshofer and S.J. Picken (2019), New analogue materials for nonlinear lithosphere rheology, with an application to slab break-off, Tectonophysics 756, 73–96, https://doi.org/10.1016/j.tecto.2018.12.007

de Haas, T., L. van der Valk, K.M. Cohen, H.J. Pierik, S.A.H. Weisscher, M.P. Hijma, A.J.F. van der Spek and M.G. Kleinhans (2019), Long-term evolution of the Old Rhine estuary: Unravelling effects of changing boundary conditions and inherited landscape. The Depositional Record 5, 84-108, https://doi.org/10.1002/dep2.56

Kleinhans, M.G., M. van der Vegt, J. Leuven, L. Braat, H. Markies, A. Simmelink, C. Roosendaal, A. van Eijk, P. Vrijbergen and M. van Maarseveen (2017). Turning the tide: comparison of tidal flow by periodic sealevel fluctuation and by periodic bed tilting in scaled landscape experiments of estuaries, Earth Surf. Dynam. 5, 731-756, https://www.earth-surf-dynam.net/5/731/2017/

Kleinhans, M.G., W.M. van Dijk, W.I. van de Lageweg, D.C.J.D. Hoyal, H. Markies, M. van Maarseveen, C. Roosendaal, W. van Weesep, D. van Breemen, R. Hoendervoogt and N. Cheshier (2014), Quantifiable effectiveness of experimental scaling of river- and delta morphodynamics and stratigraphy, Earth-Science Reviews 133, 43-61, http://dx.doi.org/10.1016/j.earscirev.2014.03.001

Leuven, J.R.F.W., Pierik, H.J., Vegt, M.v.d., T. Bouma and M.G. Kleinhans (2019), Sea-level-rise-induced threats depend on the size of tide-influenced estuaries worldwide. Nat. Clim. Chang. 4 nov, https://doi.org/10.1038/s41558-019-0608-4, https://www.researchgate.net/publication/337016595_Sea-level-rise-induced_threats_depend_on_the_size_of_tide-influenced_estuaries_worldwide

Terwisscha van Scheltinga, R.C., McMahon W.J., van Dijk W.M., Eggenhuisen J.T., and M.G. Kleinhans (2020), Experimental distributive fluvial systems: Bridging the gap between river and rock record. Depositional Rec. 2020;6:670–684. https://doi.org/10.1002/dep2.124

Weisscher, S.A.H., K. van den Hoven, H.J. Pierik and M.G. Kleinhans (submitted). Building and raising land: mud and vegetation effects in infilling estuaries. Submitted to JGR Earth Surface

Constraining the mantle contribution to thermal history of sedimentary basins by driving kinematically 2D thermomechanical simulations of passive margins

Paul Perron (1*), Laetitia Le Pourhiet (1), Anthony Jourdon (2), Tristan Cornu (2), Claude Gout (2)
(1) Sorbonne Université, ISTeP, Paris, France ; (2) TotalEnergies, CSTJF, Pau, France
* Contact: paul.perron@upmc.fr

Abstract

For a long time, the complexity of the lithosphere was ignored by numerical modelling because the inherited structural and compositional complexity of the “real” lithosphere is indeed mainly unknown to geologists so modeler preferred to understand first order parameters such as rate of extension, lithospheric thickness, mechanical coupling or decoupling at the Moho. These models were not representative of any particular region but they were helpful. As a wider community of geologist became interested in numerical modelling, a growing number of numerical models have attempted to account for a major player in structural geology: inheritance. However, the complexity of “real” Earth has been simplified and “idealized” where inherited “anomalies” (e.g., fault, pluton, craton) or a combination of them has been added without really knowing the exact initial conditions which are the unknown of the problem (e.g. Manatschal et al., 2015). Yet another approach has been to add a lot of them in a more or less random mater or to replace them by initial noise in the parameters. None of these approaches actually fulfil the need for end-users community to have predictive models.

Realizing that structural inheritance is some kind of kinematic forcing in the solution of the models but also that it is not possible to anticipate and identify all the geological structures that can be inherited in rifted margin lithospheres, we have developed a new approach, through the integration of a new kinematic module to pTatin2D thermomechanical code, permitting to understand the kinematics of deformation of the continental lithosphere and asthenosphere through time leading to the establishment of passive margins. A star/stop loop method is settled and validated by fitting the architecture (i.e., basement, Moho, LAB, Tmax) and by solving the kinematics of a random unknow 2D cross section extracted from 3D thermomechanical rifted margin model (Figure 1).

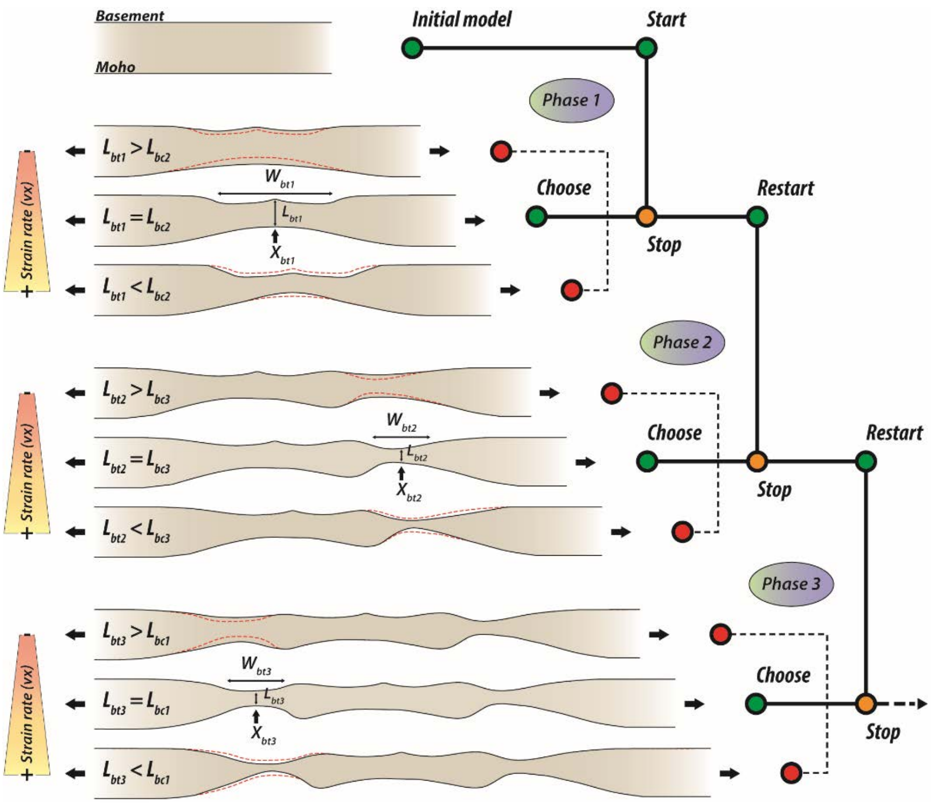

Figure 1: Illustration of the loop of star and stop reconstruction of a rifted margin where W is the width of the basins/sub-basins, X is the center of the basin depocenter and L the crustal thickness at depocenter.

This new tool aims to help geologists to better constrain the thermal state in the different basins and sub-basins of passive margins (i.e. temperature isotherms, heat flux…). For the illustration, it is applied on the classical natural case of the Iberia-Newfoundland conjugate rifted margins (Figure 2).

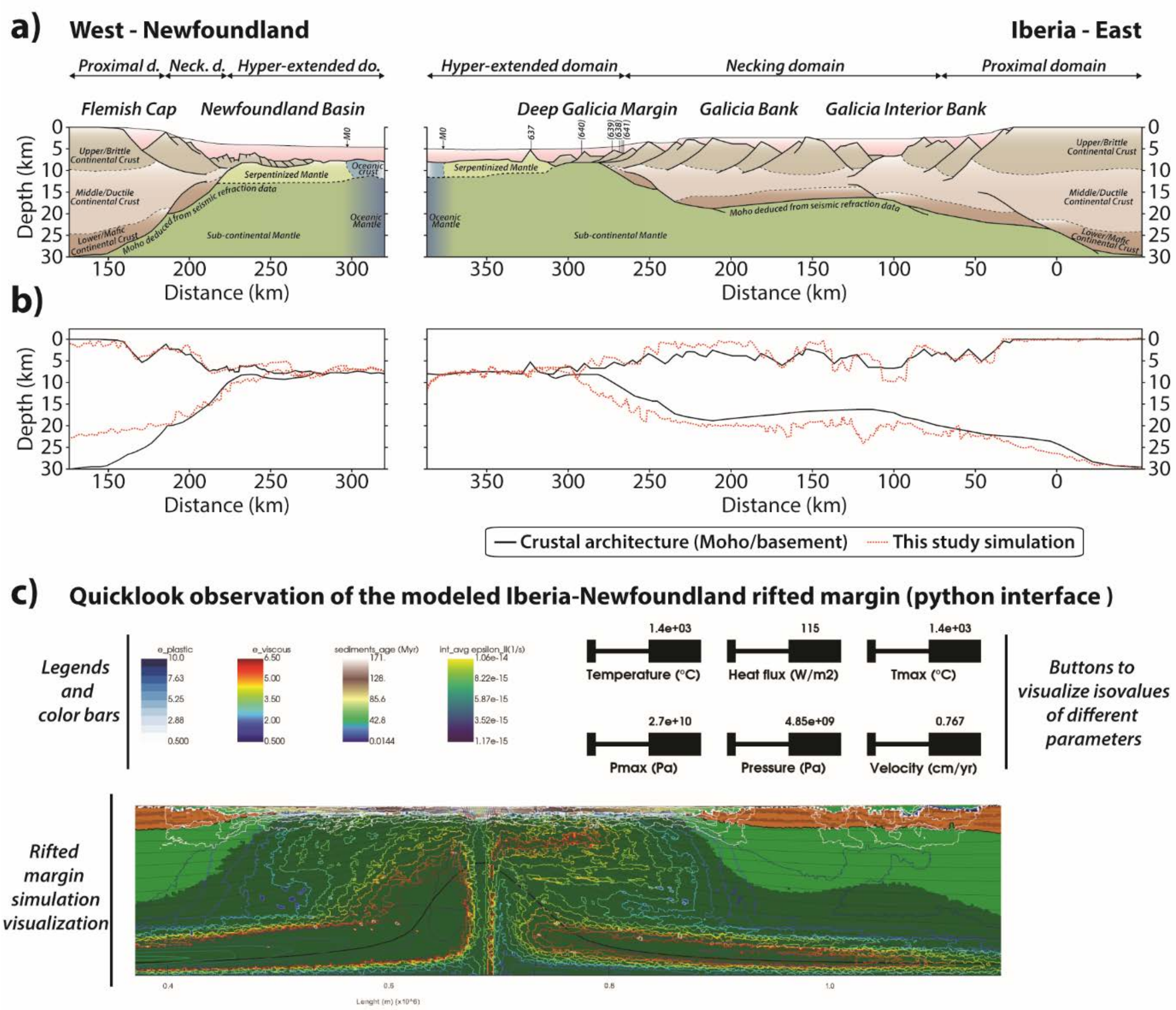

Figure 2: a) Seismic reflection/refraction interpreted profile of North Iberia-Newfoundland conjugate rifted margins modified from Sutra et al., (2013). b) Calibration of the architecture of rifted margins (Moho and basement positions) between the best fit simulation and data extracted from a). c) Interface of the quicklook python code developped to compare and observe the different parameters (temperature isotherms, heat flux, Tmax, Pmax...) of passive margins (here is presented the case of Iberia-Newfoundland).

References

Manatschal, G., Lavier, L., and Chenin, P.: The role of inheritance in structuring hyperextended rift systems: Some considerations based on observations and numerical modeling, Gondwana Research, 27, 140–164, https://doi.org/10.1016/j.gr.2014.08.006, 2015.

Sutra, E., Manatschal, G., Mohn, G., and Unternehr, P.: Quantification and restoration of extensional deformation along the Western Iberia and Newfoundland rifted margins, 14, 2575–2597, 2013.

Closing the gap between data and models: from static 3D data-based configurations to process simulations

Magdalena Scheck-Wenderoth (1*), Mauro Cacace, Denis Anikiev, Judith Bott, Ershad Gholamrezaie, Cameron Spooner, Maximilian Frick, Hans Jürgen Götze, Ajay Kumar, Boris Kaus *(keynote)*

(1) GFZ Potsdam

* magdalena.scheck-wenderoth@gfz-potsdam.de

Abstract
Integrating observations on the physical configuration of the lithosphere into data-based 3D structural models resolving the first order variations in physical properties is still a major challenge in geosciences. Nevertheless, such integration yields 3D representations of subsurface heterogeneities that improve with the amount and variety of data integrated. We use 3D models that integrate surface geology, well information, seismic and seismological observations as well as gravity and heat flow observations to resolve the first order characteristics of the present-day physical state of the sedimentary domain, the crystalline crust and the uppermost mantle in different tectonic settings. We then use these 3D geological models as a basis to calculate the thermal and rheological configuration that together describe the present-day background natural thermomechanical stability of a certain setting. Cross validations with an additional independent type observation such as the distribution of seismicity or observed surface deformation already points to causal relationships between configuration and processes. Recent developments allow utilizing such static models as initial conditions for transient process simulations of coupled heat and fluid transport or even coupled thermohydraulic-mechanical processes. We present first examples of simulations based on regional data-constrained configurations such as the intracontinental Central European Basin System, the rift setting of the Rhine Graben, the orogen-foreland system of the Alps and the transform setting of the Marmara Sea.

Session 2

Magmatic systems from plumes to dikes

- Séverine Furst. *Dynamic propagation of magma intrusions, a new 2D numerical approach constrained by analogue modeling*
- Richard Katz. *Magma dynamics at rifts: from the viscous mantle to the brittle lithosphere* ***(keynote)***
- Dániel Kiss. *2D thermo-mechanical-chemical coupled numerical models of interactions between a cooling magma chamber and a visco-elasto-plastic host rock*
- Mingqi Liu. *Surplus melt induces the dynamic LAB near the mid-ocean ridge*
- Aurélie Louis-Napoléon. *Volume-of-fluid simulations of gravitational instabilities in the Earth's crust, application to the migmatite domes of Naxos (Greece)*
- Valentina Magni. *Magmatism from the onset to the end of a subduction zone* ***(keynote)***
- Sam Poppe. *Laboratory experiments support a paradigm shift in numerical modelling of complex magma-induced deformation* ***(keynote)***
- Adina Pusok. *Buoyancy-driven flow beneath mid-ocean ridges: the role of chemical heterogeneity*

Dynamic propagation of magma intrusions, a new 2D numerical approach constrained by analogue modeling

Séverine Furst (1*), Francesco Maccaferri (2), Virginie Pinel (1)
(1) Université Savoie Mont Blanc
(2) National Institute of Geophysics and Volcanology / Vesuvius Observatory
* Contact: severine.furst@univ-smb.fr

Abstract

The tortuous travel of magma through the crust may sometimes result in volcanic eruptions at the surface. In the brittle crust, magma propagation usually occurs by fracturing the rock and opening its own way through them. This process of diking is controlled by the interaction of many complex physical processes including rock fracture, flow of compressible fluids, phase transitions, heat exchange. Current models of dikes consider either a fracturing-dominated approach, that neglects the viscous flow and allow to estimate the trajectory of dike propagation or a viscous-dominated approach that neglects the fracturing at the dike tip allowing to infer the propagation velocity of the dike. Here we propose a new numerical approach aiming at modeling both the magma path and velocity.

We start from a two-dimensional Boundary Element model solving for the trajectory of a quasi-static crack in an elastic medium subjected to external stress (Maccaferri et al, 2011), and implement the effects of the viscous fluid flow assuming a Poiseuille flow. We build on the previous work by Dahm (2000) but relaxing the assumption of stationary propagation, thus allowing to take into account heterogeneous crustal stresses, complex dike paths, and dike velocity variations. The fluid flow results in a viscous pressure drop applied to the crack wall, which modifies the crack shape and contributes to the energy balance of the propagating dike. In fact, the energy dissipated by viscous flow is linearly dependent on the viscosity of the fluid and the crack propagation velocity.

It follows that the velocity can be inferred from the total energy budget by imposing that the viscous energy dissipation and the energy spent to fracture the rocks equals the strain-plus-gravitational energy release. Starting from an initial velocity guess, a first crack shape is estimated leading to a viscous dissipation energy. Then during each propagation step, we use a steepest gradient descent method to update the velocity in order to produce a crack shape whose energy budget compensates for compensate the viscous dissipation energy.

In order to validate the results from our numerical simulations, we performed analogue experiments which consisted in injecting viscous oil in a solidified gelatin block forming oil-filled propagating cracks. The crack shape (length, width and opening) is deduced from time lapse photos processed using MatLab image toolbox functions (Galetto et al, 2021), while position of the crack tip and propagation velocity are estimated using Tracker software. This analogue modelling technique is routinely used to simulate magmatic dike propagation in the crust.

We will present the comparison between experimental observations and numerical simulation results, and we will discuss the influence of various numerical and physical parameters, such as initial velocity guess, the gelatin fracture toughness, free surface effects, and the volume of the injected oil.

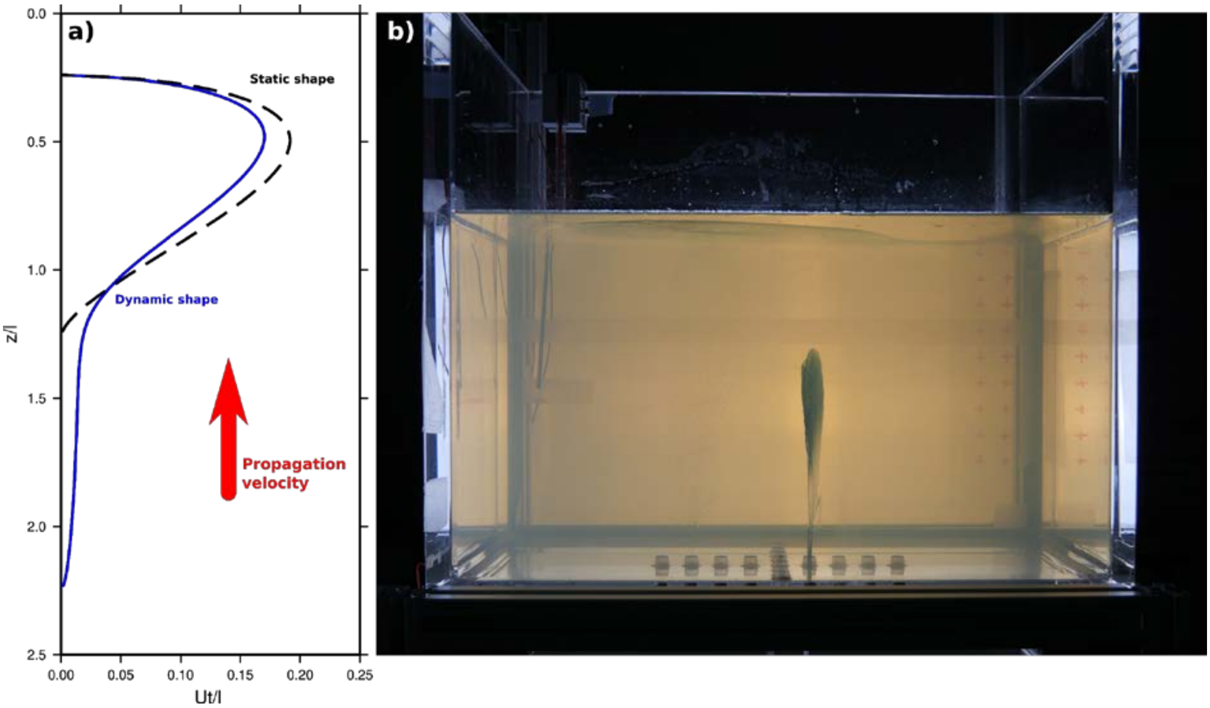

Figure 1: a) Dynamic crack shape estimated for a viscous oil propagation (blue plain line) and equivalent crack shape for a static propagation. In the numerical simulation, the propagation occurs from bottom to top (red arrow). b) Photo from an analogue experiment: injection of 30 mL of viscous oil (η=970x10^{-3} Pa.s) in a gelatin tank.

References

Dahm, T. (2000). On the shape and velocity of fluid-filled fractures in the Earth. Geophysical Journal International. v142, 181-192. https://doi.org/10.1046/j.1365-246X.2000.00148.x.

Galetto, F., Bonarccorso, A., Acocella, V. (2021) Relating dike geometry and injection rate in analogue flux driven experiments. Frontiers in Earth Science. 9:665865. https://doi.org/10.3389/feart.2021.665865.

Maccaferri, F., Smittarello, D., Pinel, V., Cayol, V. (2019) On the propagation of magma-filled dikes and hydrofractures: the competition between external stress, internal pressure and crack length. Geochemistry, Geophysics, Geosystems. V20. https://doi.org/10.1029/2018GC007915

Magma dynamics at rifts: from the viscous mantle to the brittle lithosphere

Richard F Katz (1*), Yuan Li (1), Adina Pusok (1), Dave May (2) *(keynote)*

(1) Department of Earth Sciences, University of Oxford
(2) Scripps Institution of Oceanography, Univ California San Diego

* richard.katz@earth.ox.ac.uk

Abstract

Since the discovery of plate tectonics, understanding the physics of plate boundaries has been a key scientific objective. Plate-tectonic boundaries are shaped by coupled behaviour of rock, magma, and fluids, above and below the lithosphere–asthenosphere boundary. The physical complexity of this two-phase system makes modelling and interpreting the observations a major challenge. Here we discuss this challenge, canonical theories and their shortcomings, and progress on a way forward.

The supply of magma at plate-tectonic boundaries is derived from the hot and ductile asthenosphere. Thermodynamic equilibrium at the grain scale leads to a dispersed, interconnected network of pores that allows melt to segregate from the solid residue by porous flow. Reactions between liquid and solid may cause flux channelisation, but brittle fracture of the asthenosphere is not, in general, observed or expected. The situation is different in the lithosphere, where lower temperatures lead to rigidity and impermeability, and liquid-driven fracture is the dominant means of magmatic ascent. Dynamics of the transitional regime between the asthenosphere and the lithosphere remain poorly understood. A theory for magma transport valid for both the asthenosphere and lithosphere must capture this spectrum of physical behaviour.

In this talk we review the poro-viscous theory of magmatism [McKenzie, 1984] and discuss its limitations. We then discuss extensions of the theory to complex rheological properties, accommodating viscous, elastic and plastic/brittle deformation [e.g., Keller et al., 2013]. We show that solutions in this context exhibit behaviour with a qualitative similarity to dikes and faults, and we consider whether such models can provide a quantitative, self-consistent representation of the natural system. Throughout this discussion, we review the observations that point to the importance of two-phase dynamics at plate boundaries.

References

McKenzie, D. The generation and compaction of partially molten rock. *J Petrol* 25, 713–765 (1984).
Keller, T., May, D. A. & Kaus, B. J. P. Numerical modelling of magma dynamics coupled to tectonic deformation of lithosphere and crust. *Geophysical Journal International* 195, 1406–1442 (2013).

2D thermo-mechanical-chemical coupled numerical models of interactions between a cooling magma chamber and a visco-elasto-plastic host rock

Dániel Kiss(1*), Evangelos Moulas(1), Lisa Rummel(1,2), and Boris Kaus(1)
(1) Johannes Gutenberg University Mainz, Institute of Geosciences, Mainz, Germany, (2) Federal Institute of Geosciences and Natural Resources (BGR), Hannover, Germany
* Contact: dkiss@uni-mainz.de

Abstract
A recent focus of studies in geodynamic modeling and magmatic petrology is to understand the coupled behavior between deformation and magmatic processes. Here, we present a 2D numerical model of an upper crustal magma (or mush) chamber in a visco-elastic host rock, with coupled thermal, mechanical and chemical processes, accounting for thermodynamically consistent material parameters. The magma chamber is isolated from deeper sources of magma (at least periodically) and it is cooling, and thus shrinking. We quantify the changes of pressure and stress around a cooling magma chamber and a warming host rock, using a compressible visco-elasto-plastic formulation, considering both simplified idealized and more complex and realistic geometries of the magma chamber.

We present solutions based on a self-consistent system of the conservation equations for coupled thermo-mechanical-chemical processes, under the assumptions of slow (negligible inertial forces), visco-elastic deformation and constant chemical bulk composition. The thermodynamic melting/crystallization model is based on a pelitic melting model calculated with Perple_X, assuming a granitic composition and is incorporated as a look-up table. We will discuss the numerical implementation of thermodynamic data and volumetric plasticity (including mode 1 and dilational shear plasticity) in a self consistent manner, and illustrate the effect of volume changes due to temperature changes (including the possibility of melting and crystallization) on stress and pressure evolution in magmatic systems.

Surplus melt induces the dynamic LAB near the mid-ocean ridge

Mingqi Liu (1*), Taras Gerya (1)
(1) Department of Earth Sciences, ETH Zurich
* Contact: mingqi.liu@erdw.ethz.ch

Abstract

Recently, geophysical observation through Sp receiver functions and MT imaging showed that the tectonic plate thickness undulates with age and lithosphere-asthenosphere boundary (LAB) is sharp discontinuities near the equatorial Mid-Atlantic ridge, which is not consistent with a purely thermal model. Several mechanisms have been proposed to explain the discrepancy: (1) Rayleigh wave anisotropy; (2) near solidus temperature; (3) mantle oxidation; (4) elastically accommodated grain boundary sliding; or (5) partial melt in the mantle. However, it still remains elusive. Here, we explore the formation mechanism of the sharp LAB discontinuities as well as the influence in plate tectonics through 3D self-consistent magmatic-thermomechanical numerical models. Numerical modelling results show that the sharp LAB discontinuities occur in two different configurations: (1) peeling melt is far from the mid-ocean ridge with persisting over several million years; (2) melt rises from depth and ponds beneath the plate, finally forming the new mid-ocean ridge. Both these two configurations are closely related to ridge jumps and transform faults. Ridge jumps will peel melt from the mid-ocean ridge and transform faults can induce the abnormal melt generation. In addition, localized melt leads to the small-scale convection beneath the plate and decreases the drag resistance at the base of the lithosphere.

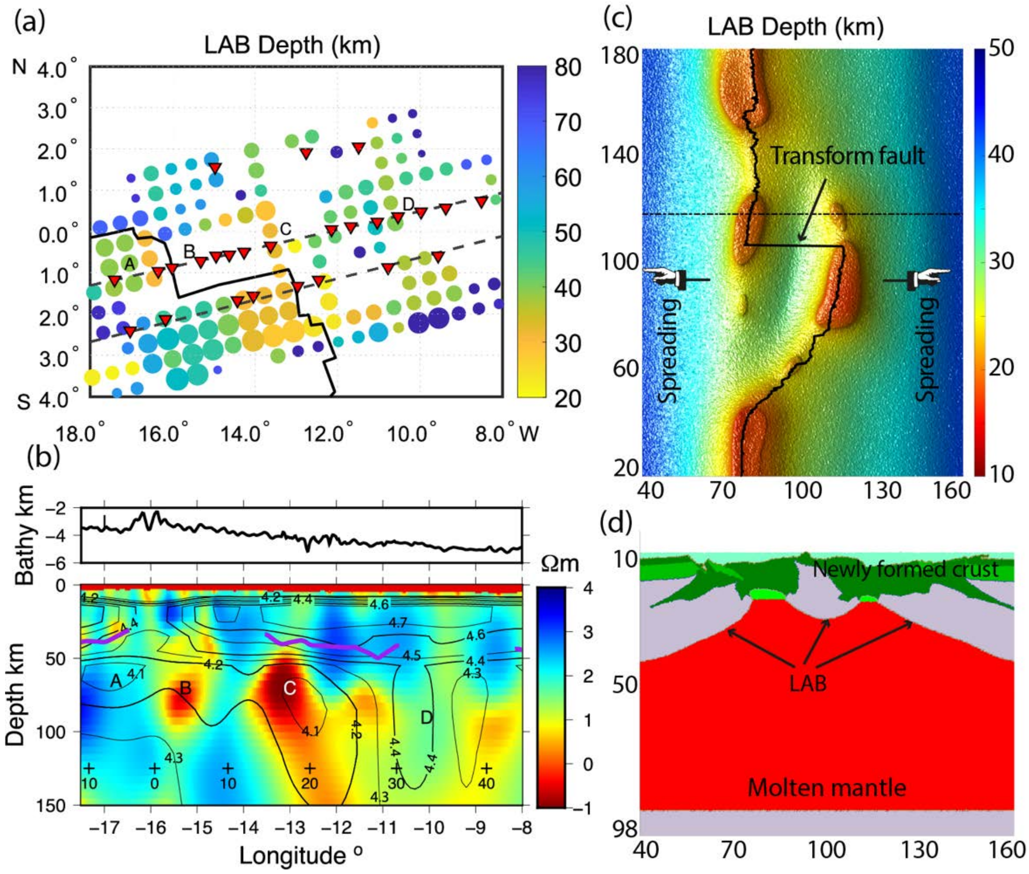

Figure 1: Comparison between observation and numerical modelling. Observation near the equatorial Mid-Atlantic Ridge (Rychert et al., 2021): (a) Map view of LAB depth from Sp receiver function; (b) Shear-wave velocity and resistivity along the dashed black line in (a). Numerical modeling: (c) Map view of LAB depth; (d) Composition along the dashed black line in (c). Thick black lines in (a, b) marks mid-ocean ridges.

References

Rychert, C. A., Tharimena, S., Harmon, N., et al. (2021). A dynamic lithosphere–asthenosphere boundary near the equatorial Mid-Atlantic Ridge. Earth and Planetary Science Letters, 566, 116949.

Volume-of-fluid simulations of gravitational instabilities in the Earth's crust, application to the migmatite domes of Naxos (Greece)

Aurélie Louis-Napoléon (1,2), Muriel Gerbault (2), Thomas Bonometti (1), Olivier Vanderhaeghe (2), Roland Martin (2)
(1) Institut de Mécanique des Fluides, Toulouse, (2) Géosciences Environnement, Toulouse, France.
* Contact: muriel.gerbault@get.omp.eu

Abstract

We apply a volume-of-fluid (VOF) method to investigate the thermo-mechanical conditions for the development of crustal scale diapirism and convection in a heterogeneous continental crust, independently from regional tectonics. As temperature increases from the base of an orogenic crust, convection is generated below an upward-propagating melting front, separating unmolten and partially molten rheologies. We take advantage of the VOF method (implemented in OpenFoam, Louis-Napoleon et al., 2020) to capture the colaescence and separation of deformable heterogeneous inclusions, which are supposed to represent sub-scale clusters of partially molten material, of several hundred meters in size, and relatively lighter and less viscous or heavier and more viscous. Modeled cases are first studied in 2D and are then extended to 3D.

A regime diagram is proposed as a function of Rayleigh numbers, which characterize the unmolten and the partially molten crustal domains. Under vigorous convection regimes (high Rayleigh numbers), the inclusions get mixed within the convective cells. At low Rayleigh numbers, the heavy inclusions segregate downwards while the light ones accumulate and float at the base of the lower crust. At a specific regime, the light inclusions may eventually form domes that accumulate at the base of the upper crust, of characteristic sizes ranging from 2 to 20 km. These domes can be maintained over time when considering additional specific assumptions, including cessation of basal heating after several My.

We discuss the key parameters responsible for such a process of segregation and dome formation, by confronting simulation results to field structures, petrological and chronological data from Naxos Island (Greece). In Naxos, ca. 2 km size domes are exposed and appear imbricated into a larger dome structure. These domes contain zircons that recorded cyclic heating over periods of about 2 My, from 24 to 16 My during the transition from compressional to tensile tectonics, suggesting convection (Vanderhaeghe et al., 2018).

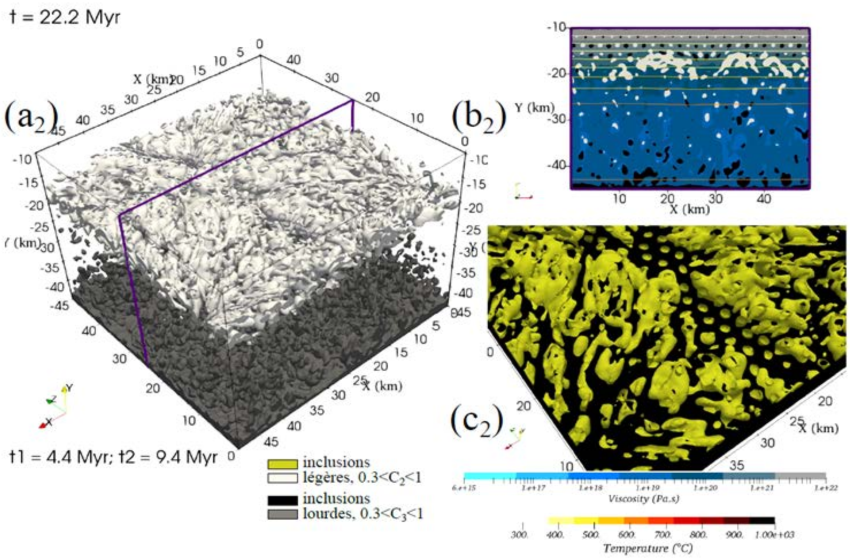

Figure 1: 3D model of the development of metamorphic domes, using OpenFoam over a 250x250x175 mesh grid (Louis- Napoélon et al., submitted). White clusters simulate heterogeneous domains of relatively light and low viscosity partially molten material, that accumulate at depth 20km and form domes.

References

Louis-Napoléon, A., et al. Geophysical Journal International, 222(1), 474-506, 2020.
Vanderhaeghe, O., et al. Tectonophysics, 746, 459-469, 2018.

Magmatism from the onset to the end of a subduction zone

Valentina Magni (1*) *(keynote)*
(1) The Centre for Earth Evolution and Dynamics (CEED), Department of Geosciences, University of Oslo
* Contact: valentina.magni@geo.uio.no

Abstract
Through the life time of a subduction zone, its dynamics usually changes many times and so does its magmatism. Magmatic products that erupt during the onset of subduction are geochemically different from those that form during the growth of an arc volcano or during the formation of new crust in a back-arc basin, and from magmas produced during and after continental collision, at the end of subduction. Here, I will explore the way magmatism evolve from the onset of a new subduction zone to its end, with a particular focus on its relationship with changes in subduction dynamics.

A good example of the link between subduction dynamics and magmatism can be observed in back-arc basins. Back-arc basins often present multiple spreading centres that form one after the other (e.g. Mariana subduction zone), propagate and rotate (e.g., Lau Basin) following trench retreat. In some cases, rift and/or ridge jumps can create continental fragments or microcontinents and exhume mantle material (e.g., Coral Sea, Central Mediterranean, Scotia Sea). Results of 3D numerical models with the finite element code CITCOM show how ridge jumps in narrow subduction zones are controlled by the ratio between the strength of the transform faults bounding the basin and that of the overriding plate. Episodic trench retreat can also affect extension in back-arc basins and result in ridge jumps and mantle exhumation. A parametric study of 2D models of continental extension with the finite element code ASPECT show that the duration of different extensional phases has a crucial role in shaping the back-arc basin and affecting the location of mantle melting. Finally, numerical models of continental collision demonstrate how the source and location of syn- and post-collisional magmatism can vary during slab break-off and crustal relamination.

Laboratory experiments support a paradigm shift in numerical modelling of complex magma-induced deformation

Sam Poppe (1*) *(keynote)*
(1) Space Research Center – Polish Academy of Sciences, Warsaw, Poland
* Contact: sam.poppe@cbk.waw.pl and sam35poppe@gmail.com

Abstract

When magma ascends through the plumbing system of active volcanoes, it deforms the surrounding host rocks. The resulting surface deformation patterns can be characterised in real-time at active volcanoes on Earth (by using Global Positioning System sensors, Interferometry Satellite Aperture Radar, photogrammetry) and have been identified on other terrestrial planetary bodies such as the Moon and Mars by radar and optical satellite systems. Seismological and geophysical monitoring techniques offer indirect means on Earth to characterize the subsurface magmatic intrusions and rock failure processes.

Analytical and numerical models then offer a path to integrating geodetic and geophysical data to estimate the intrusion characteristics - volume, depth, shape etc. – that have become essential information in volcanic eruption forecasting on Earth. Such models mostly assume that magma-induced deformation is linearly elastic, based on general similarities between field observations, elastic analytical models and laboratory experiments involving brittle-elastic gelatin (e.g. Rivalta et al., 2015). In contrast, geological observations around magmatic sheet intrusions and numerical models have documented the effects of complex, non-elastic rock failure that questions the assumption of elasticity (e.g. Bertelsen et al., 2021; Poppe et al., 2020).

Laboratory experiments are a decades-old tool to gain a deeper understanding of magma emplacement processes by using granular materials such as quartz sand as rock analogues. Technological progress has allowed to transition experimental laboratory approaches from initially qualitative reproductions of geological observations towards quantitative tools. This talk will demonstrate how laboratory experiments help addressing the question of the effect of non-elastic rock failure on observed magma-induced surface deformation patterns.

By increasing the ratio of dry quartz sand mixed with gypsum powder (plaster), a series of analogue granular materials of increasing strength can be obtained. A recent detailed characterization of such sand-plaster mixtures has shown that their mechanical behavior is similar to that of the Earth's shallow crustal rocks (Poppe et al., 2021). At plaster contents <35 wt% their mechanical behaviour is brittle, while at higher plaster contents and depth in the sand-plaster pack the rheology transitions to plastic behaviour. By controlling this mechanical strength of granular materials in magma intrusion experiments, and by using Digital Image and Volume Correlation (DIC/DVC) techniques on photographs and X-ray computed Tomography imagery, four-dimensional (3D + time) quantification of the control of these varying mechanical behaviors on fluid intrusion-induced strain fields has become possible (Sam Poppe et al., 2019). This approach has shown that low-strength sand-plaster mixtures, shear-mode deformation around dome-shaped analogue intrusions of golden syrup dominates, while in higher-strength sand-plaster mixtures, tensile-mode deformation ahead of dyke-shaped analogue intrusions dominates.

Finally, the experimentally obtained surface deformation patterns produced by analogue syrup intrusions can be used to test the performance of geodetic inversion models used on geodetic observations at natural magma intrusion events. These experimental estimates can then be compared to the geometry, depth, orientation and volume of analogue intrusions observed directly using medical X-ray Computed Tomography. Preliminary results of analytical inversions assuming an Okada-style rectangular dislocation in a linearly elastic medium have shown that, while the most optimal fit to analogue magma sheet intrusions is obtained for geometric parameters such as strike and depth of the experimental intrusion, the dip and width of the sheet intrusion is mostly underestimated, while the dislocation opening (analogue to the intrusion thickness) is largely overestimated in order to obtain magnitudes of surface uplift that are similar to those in the experiments.

By combining detailed characterisations of generally used analogue materials in laboratory experiments of magma intrusion with state-of-the-art imaging techniques such as X-ray Computed Tomography and Digital

Volume Correlation, it is now possible to gain new insights in the four-dimensional nature of magma intrusion processes. The integration of laboratory and numerical modeling techniques further allows for investigating complex, non-elastic deformation processes and the future development of improved numerical models of magma-induced deformation in the shallow crust of terrestrial planetary bodies.

References

Bertelsen, H. S., Guldstrand, F., Sigmundsson, F., Pedersen, R., Mair, K., & Galland, O. (2021). Beyond elasticity: Are Coulomb properties of the Earth’s crust important for volcano geodesy? *Journal of Volcanology and Geothermal Research*, *410*. https://doi.org/10.1016/j.jvolgeores.2020.107153

Poppe, S., Galland, O., Winter, N. J., Goderis, S., Claeys, P., Debaille, V., … Kervyn, M. (2020). Structural and geochemical interactions between magma and sedimentary host rock: the Hovedøya case, Oslo Rift, Norway. *Geochemistry, Geophysics, Geosystems*. https://doi.org/10.1029/2019GC008685

Poppe, Sam, Holohan, E. P., Galland, O., Buls, N., Van Gompel, G., Keelson, B., … Kervyn, M. (2019). An Inside Perspective on Magma Intrusion: Quantifying 3D Displacement and Strain in Laboratory Experiments by Dynamic X-Ray Computed Tomography. *Frontiers in Earth Science*, *7*, 62. https://doi.org/10.3389/feart.2019.00062

Poppe, Sam, Holohan, E. P., Rudolf, M., Rosenau, M., Galland, O., Delcamp, A., & Kervyn, M. (2021). Mechanical properties of quartz sand and gypsum powder (plaster) mixtures: Implications for laboratory model analogues for the Earth’s upper crust. *Tectonophysics*, *814*, 228976. https://doi.org/10.1016/J.TECTO.2021.228976

Rivalta, E., Taisne, B., Bunger, A. P., & Katz, R. F. (2015). A review of mechanical models of dike propagation: Schools of thought, results and future directions. *Tectonophysics*, *638*(C), 1–42. https://doi.org/10.1016/j.tecto.2014.10.003

Buoyancy-driven flow beneath mid-ocean ridges: the role of chemical heterogeneity

Adina E. Pusok (1*), Richard F. Katz (1), Dave A. May (2), Yuan Li (1)

(1) Department of Earth Sciences, University of Oxford, UK
(2) Scripps Institution of Oceanography, University of California San Diego, USA
* Contact: adina.pusok@earth.ox.ac.uk

Abstract

In the classical model, mid-ocean ridges (MOR) sit above an asthenospheric corner flow that is symmetrical about a vertical plane aligned with the ridge axis. However, geophysical observations of MORs indicate strong asymmetry in melt production and upwelling across the axis (e.g., Melt Seismic Team, 1998, Rychert et al., 2020). In order to reproduce the observed asymmetry, models of plate-driven (passive) flow require unrealistically large forcing, such as rapid asthenospheric cross-axis flow (~30 cm/yr) at high asthenospheric viscosities (~10^{21} Pa.s), or temperature anomalies of more than 100 K beneath the MELT region in the East Pacific Rise (Toomey et al, 2002).

Buoyancy-driven flows are known to produce symmetry-breaking behaviour in fluid systems. A small contribution from buoyancy-driven (active) flow promotes asymmetry of upwelling and melting beneath MORs (Katz, 2010). Previously, buoyancy has been modelled as a consequence of the retained melt fraction, but depletion of the residue (and heterogeneity) should be involved at a similar level. Here, we present new 2-D mid-ocean ridge models that incorporate density variations within the partial-melt zone due to the low density of the liquid relative to the solid (porous buoyancy), and the Fe/Mg partitioning between melt and residue (compositional buoyancy). The model is built after Katz (2010) using a new finite-difference, staggered-grid framework for solving partial differential equations (FD-PDE) for single-/two-phase flow magma dynamics (Pusok et al., 2020). The framework uses PETSc (Balay et al., 2020) and aims to separate the user input (PDE coefficients, initial and boundary conditions) from the discretisation of governing equations, thus allowing for extensible development and a robust framework for testing.

Results show that compositional buoyancy beneath the ridge is negative and can partially balance porous buoyancy. Despite this, models with both chemical and porous buoyancy are susceptible to asymmetric forcing. Asymmetrical upwelling in this context is obtained for weak forcing that is geodynamically plausible. A scaling analysis is performed to determine the relative importance of the contribution of compositional and porous buoyancy to upwelling, which is followed by predictions on the crustal thickness production and asymmetry beneath the ridge axis.

References

Balay et al. (2020), PETSc Users Manual, ANL-95/11-Revision 3.14, https://www.mcs.anl.gov/petsc

Katz (2010), Porosity-driven convection and asymmetry beneath mid-ocean ridges, G-cubed, 11(Q0AC07), 1-29, https://doi.org/10.1029/2010GC003282

Melt Seismic Team (1998), Imaging the Deep Seismic Structure Beneath a Mid-Ocean Ridge: The MELT Experiment, Science, 280(5367), 1215–1218, https://doi.org/10.1126/science.280.5367.1215

Pusok et al. (2020), Magma dynamics using FD-PDE: a new, PETSc-based, finite-difference staggered-grid framework for solving partial differential equations, EGU General Assembly 2020, EGU2020-18690 https://doi.org/10.5194/egusphere-egu2020-18690

Rychert et al. (2020), The Nature of the Lithosphere-Asthenosphere Boundary, JGR Solid Earth, 125, e2018JB016463, https://doi.org/10.1029/2018JB016463

Toomey et al. (2002), Asymmetric mantle dynamics in the MELT region of the East Pacific Rise, EPSL, 200(3-4), 287-295, https://doi.org/10.1016/S0012-821X(02)00655-6

Session 3

- Marta Adamuszek: *Long-term rheological properties of the folded impure rocksalt. A case study from the Ocnele Mari salt mine, Romania* *(keynote)*
- Anthony Adwan. *Stochastic mechanical analysis of the stress field in a thrust fold*
- Victor Alania. *Frontal zone structural geometry of retro-wedge of the Central Lesser Caucasus orogen: new insights from seismic reflection profiles data*
- Marwa Boussarsar. *Modeling the spontaneous formation of pull-apart basins: application to the El Hamma Basin, Central Tunisia*
- Onise Enukidze. *Structural model of frontal part of the eastern Achara-Trialeti fold-and-thrust belt, Georgia*
- Oriol Ferrer. *Effect of pre-salt relief on the evolution of salt-bearing passive margins: Physical models and comparison with the Santos Basin (Brazil)* *(keynote)*
- Nemanja Krstekanic. *Strain partitioning along a curved strike-slip fault system during indentation: inferences from analogue modelling*
- Sibiao Liu. *Variations in crustal thickness and faulting patterns in oceanic ridge–transform fault systems: Insights from gravity and geodynamic modelling*
- David Oakley. *Comparison of Kinematic and Elastic Dislocation Models of Fault-Propagation Folds Through Inverse Modeling*
- Leonardo Pichel. *Does rifted margins salt tectonics balance? The competition between rifting, syn-depositional flow, and gravity-driven tectonics*
- Alexandre Razmadze. *Structural model of the western Kura foreland fold-and-thrust belt using seismic reflection profiles: implication for forward kinematic modelling*
- Matthias Rosenau. *Some contributions to salt tectonics from new analogue models run at GFZ Potsdam during EPOS TNA activities: Boundary conditions, monitoring, materials*
- Emily Ross. *Relating slip behavior to off-fault deformation using physical models*
- Nedhir Sebai. *The perched synclines look-alike of central Tunisia: Examples of diapir Rise– Fall – Rise illustrated by field, geophysical, and experimental data*
- Pauline Souloumiac: *Control of geometrical and mechanical parameters on strike-slip fault segmentation: insights from sandbox experiments* *(keynote)*
- Satoshi Tonai. *Deformation and stress cycle during frontal thrust formation of sandbox Coulomb wedges*
- Sarah Visage. *Strike-slip fault in a sandbox: insight on off-fault deformation*
- Liang Wang, Daniele Maestrelli. *Investigating normal fault reactivation through analogue models of multiphase rifting: applications to the Turkana depression, East Africa*
- Michael Warsitzka. *A new analogue modelling approach integrating the effects of tectonic extension and gravity gliding on salt tectonics in rift basins*
- Frank Zwaan. *How the interaction between mantle and crustal weaknesses affects rift development: insights from a 3D experimental study*

Long-term rheological properties of folded impure rocksalt. A case study from the Ocnele Mari salt mine, Romania

Marta Adamuszek (1*), Dan M. Tămaș (2), Jessica Barabasch (3), Janos L. Urai (3) *(keynote)*

(1) Computational Geology Laboratory, Polish Geological Institute - NRI, Warszawa, Poland
(2) Department of Geology and Research Center for Integrated Geological Studies, Babeș-Bolyai University, Romania
(3) Institute for Tectonics and Geodynamics, RWTH Aachen University, Germany
* Contact: marta.adamuszek@pgi.gov.pl

Abstract

We investigate folded multilayer sequence in the Ocnele Mari salt mine in Romania to constrain the rheological properties of rock salt deforming at geologic rates. The structures can be observed on over 50 regularly spaced, clean square pillars, which allows for detailed three-dimensional analysis. Folds occur on various scales ranging from centimeters to tens of meters and represent a variety of geometries including harmonic, polyharmonic and disharmonic styles. Fold geometry and regularity of the fold pattern indicate that the sequence was mechanically stratified. The formation is composed of over 90% of halite, while distinct fine layering is caused by variation in the amount of impurities. Dark layers, compared to the light layers, contain more impurities and are characterized with less variable layer thickness variation. Consequently, they are considered as more competent.

In order to gain an insight into dominant deformation mechanisms, we carry out microstructural analysis of the rocksalt. Optical microscopy of Gamma-decorated samples shows a strong shape preferred orientation of halite grains parallel to the foliation, which is reoriented parallel to the axial plane of the folds studied. Microstructures indicate dislocation creep, together with extensive fluid-assisted recrystallization and strong evidence for solution-precipitation creep indicative for linear (Newtonian) viscous rheology during folding.

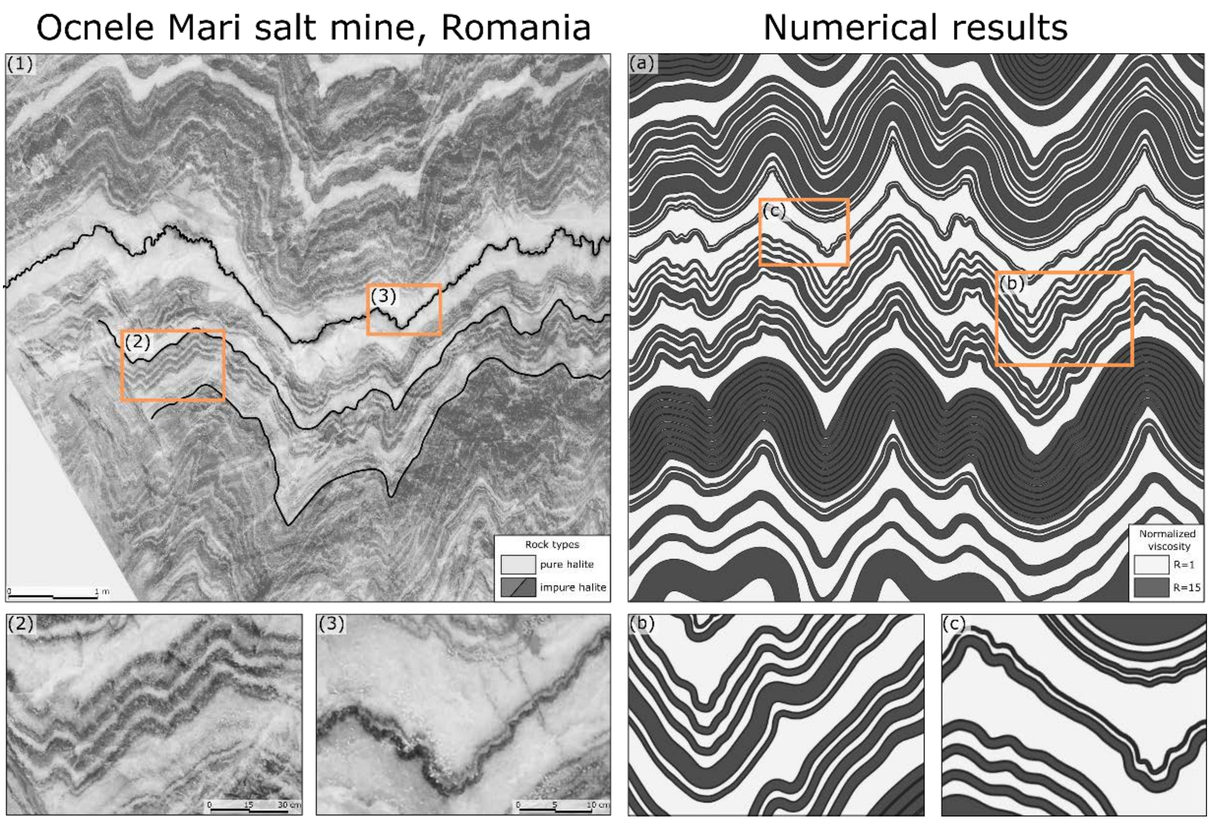

Figure 1: Comparison of the polyharmonic fold structures in the Ocnele Mari salt mine in Romania (left side) and the results of the numerical modelling of the multilayer sequence (right side).

In the project, we select an excellent exposure of the polyharmonic folds, where folds occur at three different scales (left side of Figure 1). Development of polyharmonic folds is restricted to specific sets of geometrical and mechanical parameters of the layers (e.g., Frehner and Schmalholz, 2006; Treagus and Fletcher, 2009) and for a given geometrical setup can be used to obtain mechanical characteristics of the rocks. Thus, we use field observations to constrain the geometrical parameters of the sequence, including layer thickness, and utilize characteristics of the polyharmonic folds to infer rheological parameters of the salt sequence. In the study, we employ Finite Element Method based, open-source software FOLDER that is designed to investigate evolution of the structures in the multilayer stack during layer-parallel shortening (Adamuszek et al., 2016). Our setup comprises a multilayer stack consisting of 91 layers with variable, field-constrained thicknesses, and different linear viscous rheology. In a range of numerical models, we test the role of viscosity ratio between the layers on the developing fold pattern.

Our results show that polyharmonic folds develop in models, where the viscosity ratio between the layers is below 30. Detailed comparison between the natural structures and numerically obtained results allow constraining the permissible range of layer viscosity ratio between 10 and 20. The best correspondence between the structures is obtained for R=15 (Figure 1), where we observe developing folds over three distinct orders with morphologies that can be matched with observations. Moreover, our results show that small amount of impurities (ca. 10%) can significantly change the viscosity of rocksalt and introduce anisotropy in the sequence.

References

Adamuszek, M., Dabrowski, M., Schmid, D. W., 2016, Folder: A numerical tool to simulate the development of structures in layered media, J. Struct. Geol., Vol. 84, 85–101

Dabrowski, M., Krotkiewski, M., Schmid, D. W., 2008, MILAMIN: MATLAB-based finite element method solver for large problems: MILAMIN MATLAB-BASED FEM SOLVER, Geochem. Geophys. Geosystems, 9

Frehner, M. and Schmalholz, S. M., 2006, Numerical simulations of parasitic folding in multilayers, J. Struct. Geol., 28, 1647–1657

Schmalholz, S. M. and Schmid, D. W., 2012, Folding in power-law viscous multi-layers, Philos. Trans. R. Soc. Math. Phys. Eng. Sci., 370, 1798–1826

Treagus, S. H., Fletcher, R. C., 2009, Controls of folding on different scales in multilayered rocks, J. Struct. Geol., 31, 1340–1349

Stochastic mechanical analysis of the stress field in a thrust fold.

Anthony Adwan (1*), B. Maillot, P. Souloumiac, C. Barnes, P. Leturmy.
(1) Geoscience and Environment Laboratory, CY Cergy Paris University.
*Contact: anthony.adwan@cyu.fr.

Abstract

We conduct a sensitivity analysis of the stress field with respect to rheological parameters in a kilometric scale thrust fold using a 3D numerical implementation of the theory of Limit Analysis (LA). We use the commercial software Optum G3 (2021) from the Optum CE© package. LA searches for the exact loading force at the onset of failure by adopting both a static approach and a kinematic approach (Salençon 1974 and 1983). The static approach finds a lower bound to the solution that maximizes the internal work rate over an admissible stress field with respect to a given yield condition (the Coulomb criterion in this study). The kinematic approach yields an upper bound by considering a unitary external work and finding a minimized internal work rate over a kinematically admissible velocity field. The relative difference between the upper and lower bounds is a measure of the precision of the solutions. Thus, we use this criterion as the main condition in our numerical convergence tests. Elastic parameters are not required since the resolutions of the velocity field and of the stress field are independent. We need only to define Coulomb parameters (friction angle and cohesion).

The 3D geological prototype inspired from the north-eastern Jura corresponds to the lateral termination of a partially buried fault-cored anticline. With dimensions of 15*12*4 km3, it is formed by 5 layers of Coulomb materials with various mechanical properties and two different décollement levels (Figure1-a-c). We simulate thrusting by applying a uniform compression on the back-wall of our model where we also consider a frictional interface having the same mechanical properties as the different bulk layers in contact. Based on our convergence tests, we apply an adaptive iterative tetrahedron meshing of 50.000 elements. We perform a parametric study by varying the friction angle of the bulk materials, the faults ($\emptyset_f$) as well as the friction angle on the first décollement level ($\emptyset_{d1}$). The optimal solution of the loading force is provided when the tolerance between the lower and upper bound solutions is less than 6%.

In this study, we show the convergence results obtained for a given bulk friction coefficient with décollement friction angles of 10°,20°and 30° and faults friction angle of 5°,10°,15° and 20° (Figure1-b). We then present the principal stress field obtained for two extreme cases at two different cross sections, located at A and B (Figure1-c). The aim is to consider the variation of the overall stress-field as a function of the variation of mechanical and 3D geometrical parameters. For a $\emptyset_{d1}$=10° and $\emptyset_f$=5°, we observe the activation of the first fault, closest to the back-wall. Figure1-d shows a stress concentration at the back-wall and at the root of the active fault (stress higher than 150 MPa). The rest of the bulk is shadowed by this activation and presents nearly lithostatic stress values (less than 75 MPa). Between the relief and the active fault, a small stress concentration with a magnitude varying from 37.5 MPa to 56 MPa can be observed in cross section A. Figure1-e, considers the case $\emptyset_{d1}$=10° and $\emptyset_f$=20°. Here, we have an activation of the farthest fault from the back-wall and a semi-activation of the first fault. With a magnitude higher than 110 MPa, the stress propagates throughout all the model while being mainly concentrated in the rigid material layer located directly above the first décollement. In this case, the stress also extends to the paleozoic carboniferous layer (under the first décollement level) at the base of the active fault. This can be explained by its tendency to create a back-thrust. We can also observe that the sandwiched clay layer is protected by both rigid layers and presents relatively low stresses. At the root of the first fault, the stress concentration is starting to build-up, signaling the semi-activation of this fault. The second smaller fault seems to be blocked, despite a stress build-up. Yet, we can observe the formation of a spontaneous, steeper thrust reaching the clay layer. This indicates that the pre-defined dip of 15° is too low to activate this fault. As in Figure1-d we also observe a higher stress magnitude under the relief while it is lower as we go further from it.

This is a modelling exercise to prepare for the setting up of an inverse problem using, first, synthetic stress borehole data to retrieve the fault parameters and second, real borehole lithology and stress data.

Acknowledgements: We acknowledge the financial support from Swiss topo, ENSI, and CY Cergy Paris University for the PhD project of Anthony Adwan.

References

Optum G3, (2021), https://optumce.com.

Salençon, J. (1974), Théorie de la plasticité pour les applications à la mécanique des sols, Eyrolles, Paris (1974).

Salençon, J. (1983), Calcul à la rupture et analyse limite, Presses des Ponts et Chaussées, Paris (1983).

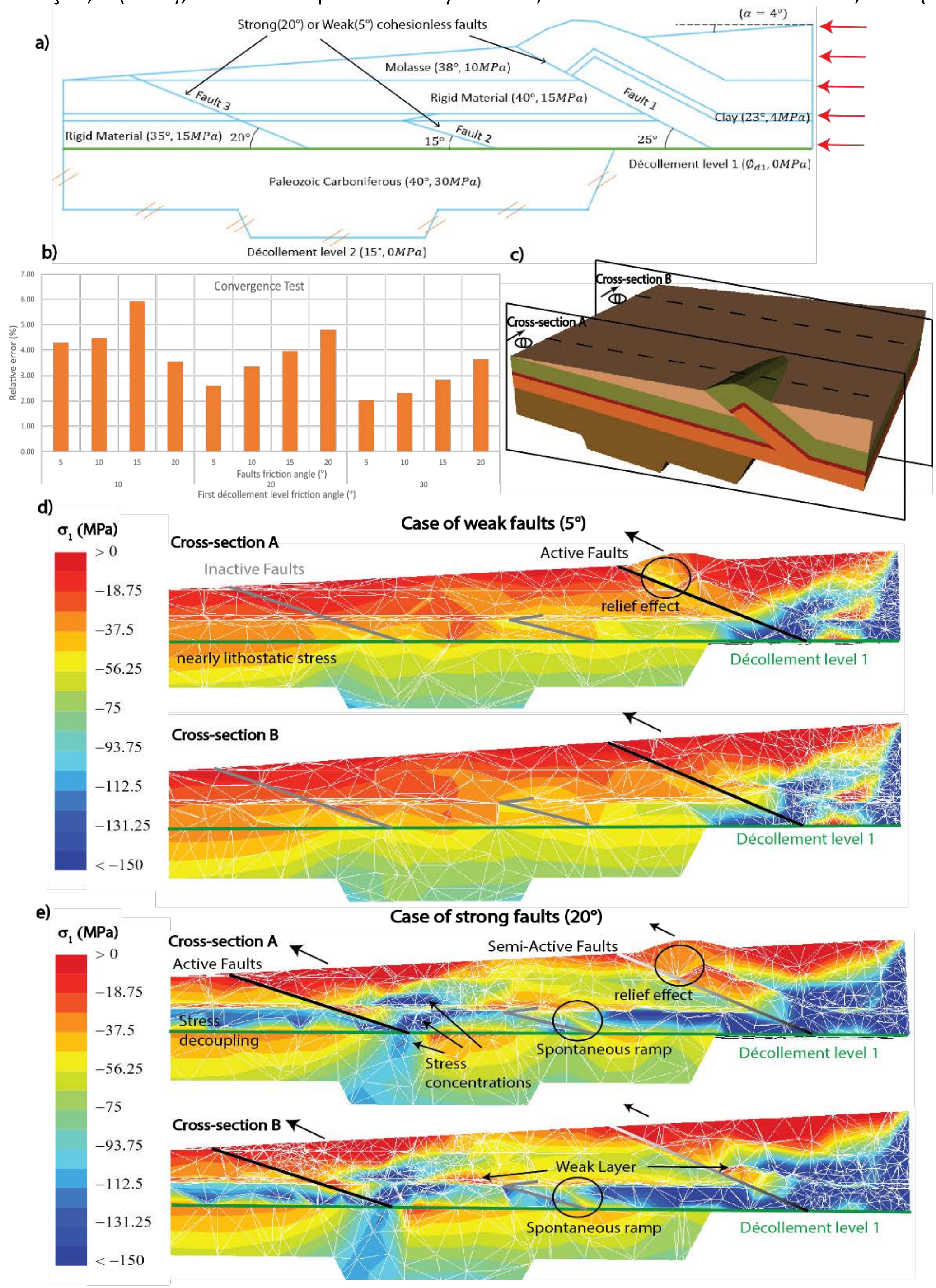

Figure 1: a) Frontal view of the 3D model, presenting the 5 different layers and the localization of the different faults and décollement levels. b) Acceptable convergence results for several parameter combinations. The relative error formula is:(Upper bound solution-Lower bound solution)/Upper bound solution*100. c) 3D representation of the model showing both cross-sections A and B. d-e) Representation of the principal stress state in both cross-sections for two distinguished cases of fault friction angle equal to 5° and 20° respectively. The first décollement is shown in green, the active faults in black, the inactive faults in gray and the semi-active faults in a gradient color varying between black and gray. The black arrows at the top of the model show the expected displacement direction. Their lengths reflect the expected displacement rate.

Frontal zone structural geometry of retro-wedge of the Central Lesser Caucasus orogen: new insights from seismic reflection profiles data

Victor Alania (1*)

(1) M. Nodia Institute of Geophysics, I. Javakhishvili Tbilisi State University, Tbilisi, Georgia
* victor.alania@tsu.ge

Abstract

The Lesser Caucasus (LC) is located in the northernmost part of the Arabia-Eurasia collision zone and is one of the best examples of collision-driven far-field deformations. Like the Greater Caucasus (GC) orogen, the LC is a double wedge orogen and forms a W-E-trending, bivergent thrust system (Alania et al., 2021). The tectonic evolution of LC and GC is the result of the Arabia-Eurasia collision during Alpine times, which led to the inversion of back-arc basins and formation of two orogens with the foreland basins (Rioni and Kura) in between (e.g., Adamia et al., 2010; Tari et al., 2018). Stratigraphy in the study area records the evolution from the extensional basins to the Kura foreland basin (KFB) of the Arabia-Eurasia collision zone. The sedimentary succession of the frontal part of the LC and KFB is commonly represented by more than 7 km thick Jurassic, Cretaceous, Paleogene and Neogene deep marine, shallow marine and thick continental strata (Adamia et al., 2010).

Seismic interpretation of the combined profiles shows north and south-vergent thrusts and fault-related folds (Fig. 1). On the basis of interpretations of combined seismic profiles from the frontal part of the central LC orogen reveal the presence of the kilometric scale tectonic wedges. Classifications of tectonic wedges within the study area are determined by the Type II triangle zone (Couzens & Wiltschko, 1996). As we now know, the type II triangle zones develop due to a mechanical layering of weak shale-rich cover sequence, competent rocks forming horses, and weak underlying detachments in shale (e.g., Couzens & Wiltschko, 1996). Formation of south-vergent thrust above the structural wedge is related to break-back thrust sequences and is represented by passive-backthrusts. The kinematic evolution of the south-vergent passive-backthrusts is related to the northward propagating of structural wedge (Fig. 2).

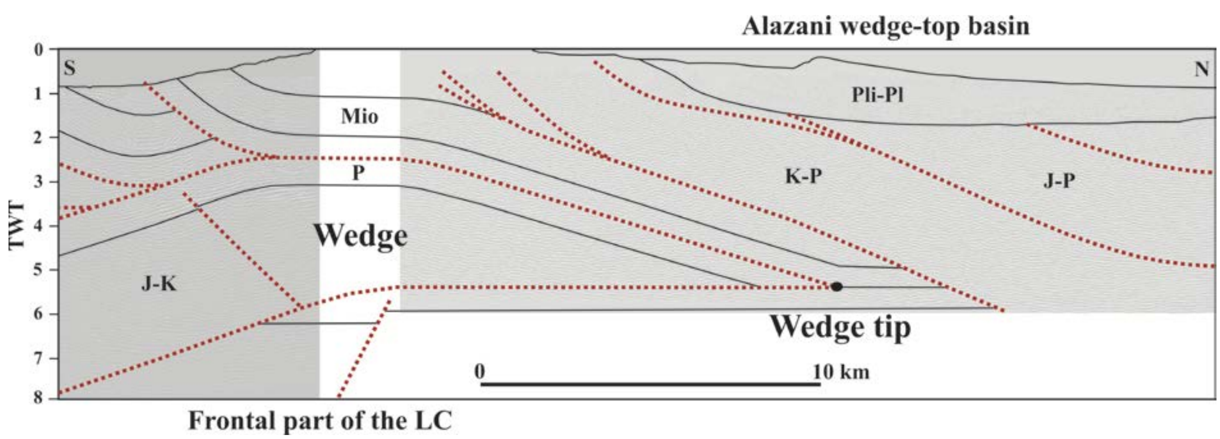

Figure 1. Interpreted combined seismic reflection profiles through central Georgia.

Based on published information about historical and recent earthquake data (e.g., Tsereteli et al. 2016), fission-track data from LC (Gusmeo et al. 2021), age of syn-tectonic units from frontal part of LC orogen and KFFTB (Alania et al. 2017), and interpreted seismic profiles, indicates that compressive deformation within LC-GC convergence zone started in the Middle-Upper Miocene and continues today. Near the LC-GC convergence zone is located Tbilisi city, where the north- and south-vergent thrusts of this collision zone represent a significant seismic hazard.

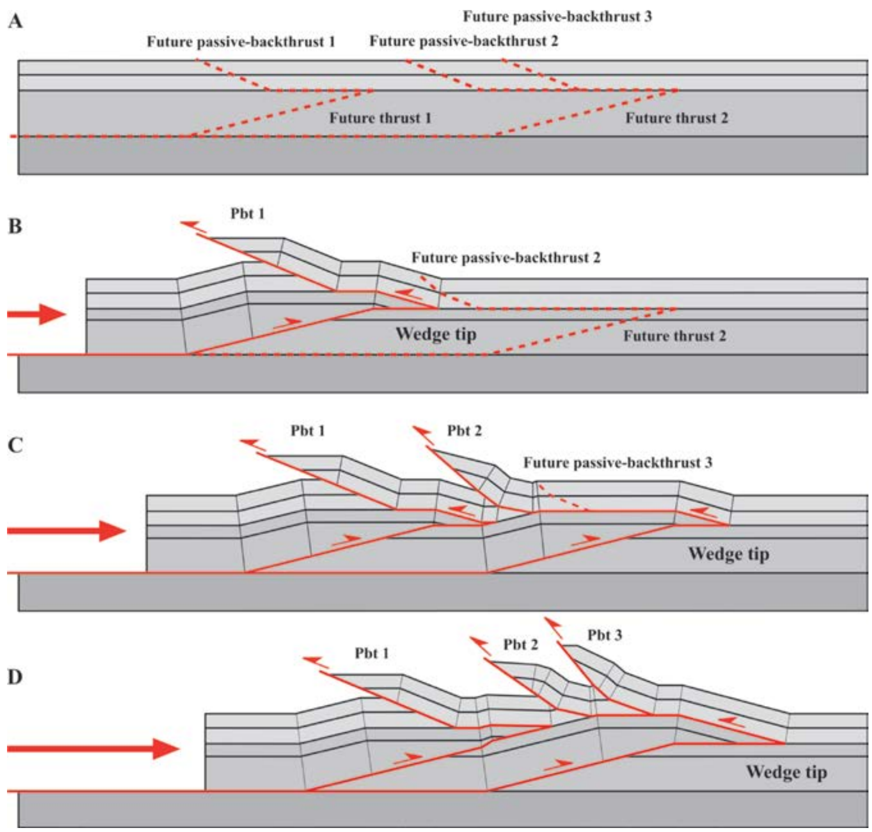

Figure 2. (A-D) Proposed kinematic model for the frontal part of the Central LC repro-wedge. The final geometry shows similarities to the frontal part of the LC.

Acknowledgments: The work was supported by Shota Rustaveli National Science Foundation of Georgia (SRNSF #YS-19-1104).

References

Adamia, Sh., et al. (2010). Evolution of the Late Cenozoic basins of Georgia (SW Caucasus): a review. Geological Society, London, Special Publication. v340, 239-259. https://doi.org/10.1144/SP340.11

Alania, V., et al. (2021). The Geometry of the Two Orogens Convergence and Collision Zones in Central Georgia: New Data from Seismic Reflection Profiles. In: Bonali, F.L., et al. (Eds.), Building Knowledge for Geohazard Assessment and Management in the Caucasus and other Orogenic Regions, NATO Science for Peace and Security Series C: Environmental Security, 73-88.

Alania, V., et al. (2017). Growth structures, piggy-back basins and growth strata of Georgian part of Kura foreland fold and thrust belt: implication for Late Alpine kinematic evolution. Geological Society, London, Special Publications. v428, 171-185. https://doi.org /10.1144/SP428.5

Couzens, B. A., & Wiltschko, D. V. (1996). The control of mechanical stratigraphy on the formation of triangle zones, Bull. Can. Pet. Geol. v44, 165-179.

Gusmeo, T., et al. (2021). Structural inversion of back-arc basins-The Neogene Adjara-Trialeti fold-and-thrust belt (SW Georgia) as a far-field effect of the Arabia-Eurasia collision. Tectonophysics. v803, 228702. https://doi.org/10.1016/j.tecto.2020.228702

Tari, G., et al. (2018). Stratigraphy, structure and petroleum exploration play types of the Rioni Basin, Georgia. Geological Society, London, Special Publication. v464, 403-438. https://doi.org/10.1144/SP464.14

Modeling the spontaneous formation of pull-apart basins: application to the El Hamma Basin, Central Tunisia

Marwa Boussarsar (1-2*), Bruno C. Vendeville (2), Chedly Abbes (1) and Mouna Hassine (1)
(1) Univ. Sfax, Fac. Sciences de Sfax, Laboratoire GéoModèle - LR16ES17, BP 1171, Sfax 3000, Tunisie
(2) Univ. Lille, CNRS, Univ. Littoral Côte d'Opale, UMR 8187, LOG, Laboratoire d'Océanologie et de Géosciences, Lille 59000, France

*marwa.boussarsar.etud@fss.usf.tn, Bruno.Vendeville@univ-lille.fr, chedly.abbes@fss.usf.tn, mouna.hassine.etud@fss.usf.tn

Abstract

Most (if not all) analogue experiments on the formation of pull-apart basins have been conducted using basal discontinuities that transmitted from the bottom up strike-slip motion into the overlying sedimentary cover.
Here, we present a totally new design, in which the mechanical discontinuities are located within the cover itself. This set up provides more freedom for the pull-apart basin to form and evolve.
We based our work on a field area, the El Hamma Basin located in central Tunisia (West of Gabes), where the extent of viscous, Triassic evaporites is still debated. The basin of El Hamma is a pull apart located at the northern edge of the mole of Matmata. This is an area of non-deposition during the whole period of the Triassic-Lower Cretaceous (Mello and Bouaziz, 1987; Bouaziz, 1995; Bouaziz et al., 2002). On the southern margin of this mole, the Upper Triassic is lacunar and was deposited with an evaporitic facies only in the Tataouine basin, whose northern edge corresponds to the Zemlet El Ghar fault. North of this mole, at the northern edge of El Hamma pull-apart (in an area named (Jebel El Melah), the evaporitic Triassic rocks crop out, . Moreover, Hassin (2019) demonstrated on the basis of gravimetric and seismic data that the evaporitic sedimentation of the Upper Triassic, well characterized in the basins of Tataouine in the South and Central Tunisia in the North, were not present in the region corresponding to the pull-apart basin of El Hamma-Gabes. Hence, the paleo-limit of the evaporitic Triassic remains unknown.
Here, we present results from three selected experiments in which we tested cases where the entire basin was underlain by mobile evaporites, or if only its Northern part was, whereas its southern part was underlain by a mechanically weak but denser (i.e., shale) acted as a *decollement*.
Results show a great similarity with seismic data from the area. The basin comprised two grabens separated by a central horst. Some experiments led to the formation of a salt diapir that rose and reached the surface, as we can observe in the field (El-Melah diapir).

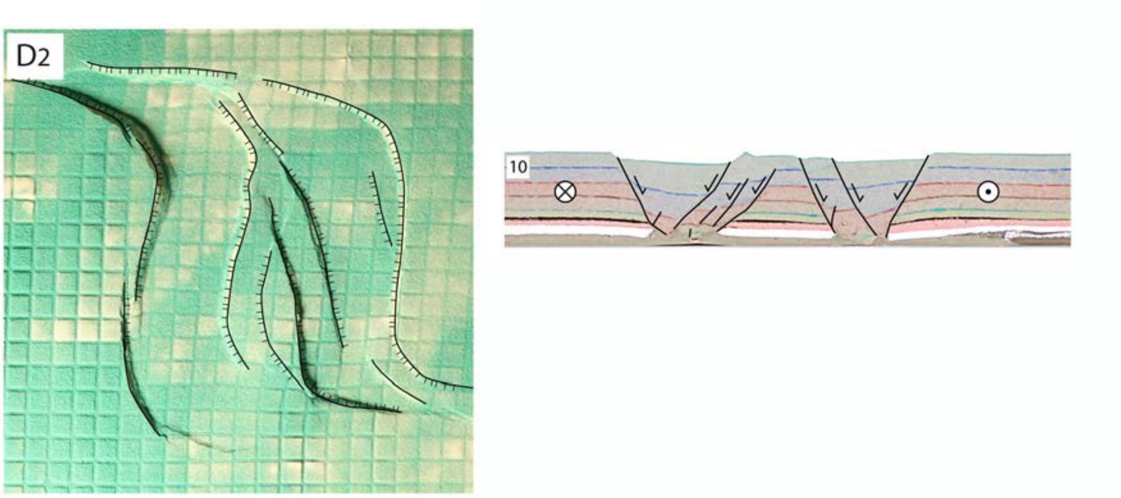

Figure 1: Overhead view and one cross section of the model assuming that not evaporates were present beneath the El Hamma pull-apart basin.

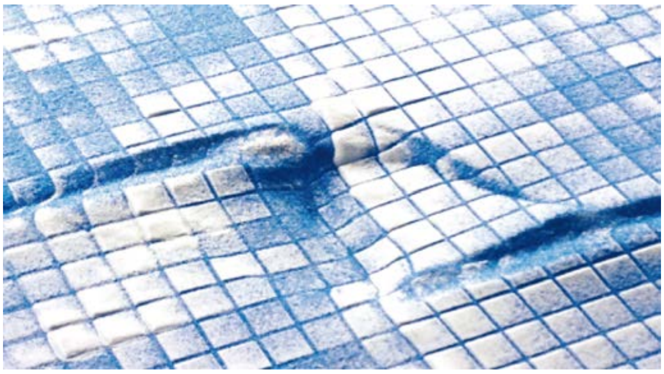

Figure 2: Side view of one model showing the piercing diapir located along the North strike-slip zone, analogue to the El-Melah diapir

Bouaziz, S.,Mello, M. (1987). Mise en évidence de la discordance de Sidi Stout dans la province centrale du sud tunisien et de son terme transgressif, les dolomies de messaoudi. Notes serv. Géol. Tunisie, 54, 41-54.

Bouaziz, S.(1995). Etude de la tectonique cassante dans la plate-forme et l'Atlas saharien (Tunisie méridionale): Evolution des paléo-champs de contraintes et implications géodynamiques. Thèse de Doctorat d'Etat. Univ. Tunis II.

Bouaziz, S., Barrier, E., Soussi, M., Turki, M.M., Zouari, H. (2002). Tectonic evolution of the northern African margin in Tunisia from Pleostress data and sedimentary record. Tectonophysics 357, 227–253.

Hassine, M. (2019). Le bassin d'El Hamma-Gabes: structuration en pull-apart et évolution depuis le Jurassique à partir des données sismiques, gravimétriques et de forages. Thèse de doctorat. Univ. Sfax

Structural model of frontal part of the eastern Achara-Trialeti fold-and-thrust belt, Georgia

Onise Enukidze (1*)

(1) Tbilisi State University, M. Nodia Institute of Geophysics
*onise.enukidze@tsu.ge

Abstract

The Achara-Trialeti fold-and-thrust belt (ATFTB) is located in the frontal part of the Lesser Caucasus orogen was formed since the late Miocene by the ongoing continental collision of the Arabia-Eurasia plates (e.g. Alania et al., 2021). Our study area includes the frontal part of the eastern ATFTB and the southern part of the western Kura foreland fold-and-thrust belt (KFFTB). The sedimentary succession of the frontal part of the eastern ATFTB and southern part of KFFTB is represented by commonly more than 7 km thick Jurassic, Cretaceous, Paleogene and Neogene deep marine, shallow marine and thick continental strata. During the Cretaceous and Paleogene, the Achara-Trialeti extensional basin was filled with approximately 3500-4000m thick sediments. Syn-orogenic sediments are represented by 1500-2000m thick Middle-Upper Miocene shallow marine and thick continental deposits (Alania et al., 2017; Enukidze et al., 2019).

The seismic reflection profiles and constructed structural cross-section (Fig. 1) reveal the presence of upper and lower structural complexes. The upper structural complex is represented by a shallow triangle zone which includes a north-vergent Armazi fault-propagation fold, north-vergent duplex, and south-vergent passive- backthrust at the mountain front. The interpreted seismic profile and structural cross-section have revealed that Armazi anticline is a breakthrough fault-propagation fold developed above the thrust sheet. The imbricated structure below the Armazi anticline is characterized by break-backward thrusting. Pre-existing fault-bend folds were cut by the younger thrust ramp. Finally, the Armazi breakthrough fault-propagation fold was developed along the second new ramp.

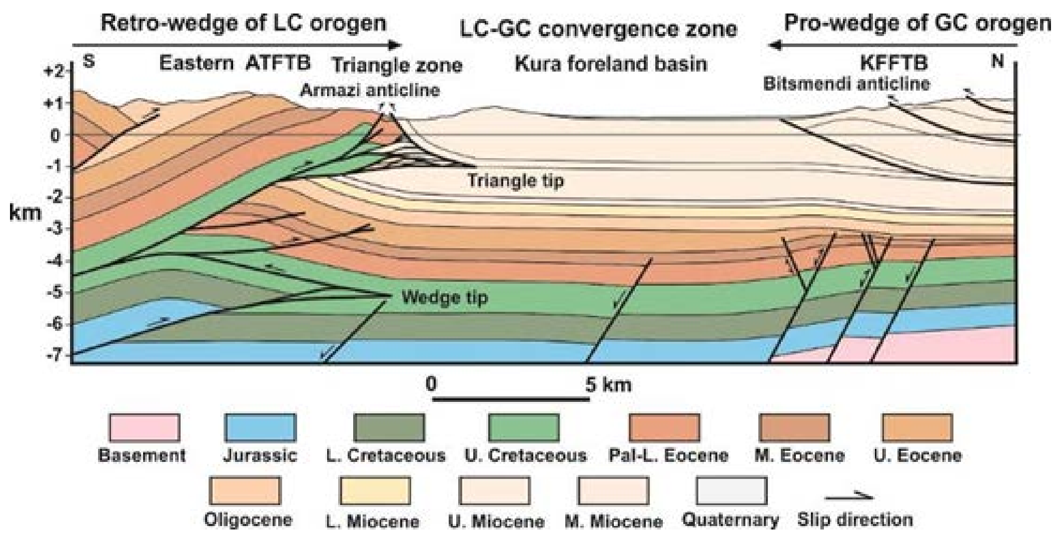

Figure 1. Structural cross-section I-J. Abbreviations: LC-Lesser Caucasus; GC-Greater Caucasus; ATFTB-Achara-Trialeti fold-and-thrust belt; KFFTB-Kura foreland fold-and-thrust belt.

The lower structural complex is represented by a structural wedge and is made up of Lower Cretaceous-Jurassic strata. Within the triangle zone, the duplex sequence comprises Cretaceous-Neogene strata that have been formed due to passive-roof duplex style of deformation. The southern part of the Kura foreland basin is represented by Miocene strata that were deformed and uplifted by passive-backthrust at the triangle zone. The kinematic evolution of the south-vergent backthrust is related to the northward propagating duplex and triangle tip is located in middle Miocene.

Acknowledgements: This work was supported by Shota Rustaveli National Science Foundation (SRNSF- #PHDF-18-1967: 2-3D structural models of frontal part of Eastern Achara- Trialeti: implication for oil-gas exploration).

References

Alania, V., Beridze, T., Enukidze, O., Maqadze, D., Lebanidze, Z., Razmadze, A., Sadradze, N., Tevzadze, N. (2021). The geometry of the two orogens convergence and collision zones in central Georgia: New data from seismic reflection profiles. In: Building Knowledge of Geohazard Assessment and Management in the Caucasus and other Orogenic Regions, Springer, https://doi.org/10.1007/978-94-024-2046-3

Alania V., Chabukiani A., Chagelishvili R., Enukidze 0., Gogrichiani K., Razmadze A., Tsereteli N. (2017). Growth structures, piggyback basins and growth strata of Georgian part of Kura foreland fold and thrust belt: implication for Late Alpine kinematic evolution. Geological Society, London, Special Publications, v428, 171-185.

Enukidze, O., Alania, V., Bluashvili, D., Chabukiani, A. (2019). Structure of frontal part (Dzegvi-Kavtiskhevi area) of the eastern Achara-Trialeti fold-and-thrust belt, Georgia. Geophysical Research Abstracts 21, EGU2019-7598-2.

Effect of pre-salt relief on the evolution of salt-bearing passive margins: Physical models and comparison with the Santos Basin (Brazil)

Oriol Ferrer (1*), Leonardo M. Pichel (2), Eugeni Benaiges (1), Christopher A-L. Jackson (2), Eduard Roca (1)
(keynote)
(1) Geomodels Research Institute, Dept. Earth & Ocean Dynamics, University of Barcelona, SPAIN
(2) Basin Research Group, Department of Earth Science and Engineering, Imperial College London, South Bennington Campus, SW7 2BP, UK

* Contact: joferrer@ub.edu

Abstract

The Santos Basin is the largest and most prolific salt basin in the South Atlantic. It presents a remarkably complex and controversial structural evolution and distribution of salt-related structural domains. One of its most striking and enigmatic features is the Albian Gap, a c. 450 km long and up to 60 km wide feature located in the transition between the updip extensional and intermediate translational domains (Fig. 1). This gap is characterized by an equally large counter-regional rollover of Upper Cretaceous age overlying depleted Aptian salt and in which the Albian section is absent (Fig. 1c). Two main different hypotheses have been proposed to explain its origin and kinematics. The first, the thin-skinned extension model, argues that the Albian Gap formed due to post-Albian gravity-driven extension along a 40-60 km wide landward-dipping listric fault, the Cabo Frio Fault (CFF) (Demercian et al., 1993; Guerra and Underhill, 2012; Rowan and Ratliff, 2012). In contrast, the second model, the salt expulsion model, proposes that the Albian Gap was already formed during the Albian, and post-Albian deformation was driven primarily by progradational loading and salt expulsion without significant lateral extension (Krezseck et a., 2007; Jackson et al., 2015b). A more recent model proposes a hybrid evolution, arguing that post-Albian extension and salt expulsion, both of which driven by progradational loading, were equally important (Pichel et al., 2019c; Pichel and Jackson, 2020b).

Another prominent feature in this portion of the basin is the Merluza Graben, a large rift-related depocentre that underlies the southern portion of the Albian Gap and creates significant (up to 3.5-4 km) of base-salt relief influencing its salt-related kinematics, trend and architecture. Further downdip, another remarkable and controversial province, the São Paulo Plateau (SPP), is defined by a large pre-salt structural high with significant base-salt topography and overlain by ~2.5 km thick salt (Pichel et al., 2018;)(Fig. 1c). Salt tectonics in this region is kinematically linked to the Albian Gap and is interpreted to have been driven by either shortening in response to updip extension within the Albian Gap (cf. Guerra and Underhill, 2012; Fiduk and Rowan, 2012) or by salt inflation with limited overburden translation and lateral salt tectonics (Krezseck et a., 2007; Jackson et al., 2015a-b).

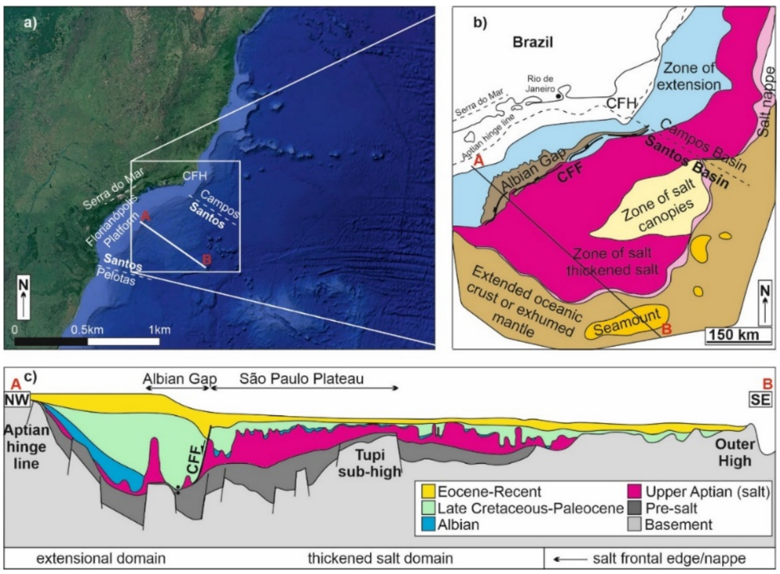

Figure 1: a) Santos Basin; b) Structural domains of the Santos Basin; c) Cross-section along the Santos Basin (see location in Fig. 1b) with the main structural domains and the related deformation (Pichel et al. 2018).

Using an experimental approach based on scaled 3D physical models, the aim to this work is to understand the interplay between laterally-variable base-salt relief, gravity-gliding and spreading on salt flow and overburden deformation in salt-bearing passive margins, with special focus on the highly complex and controversial Santos Basin. Different parameters as salt thickness, base-salt relief geometry, and pre-salt fault displacement were tested. Models were carried out at the Geomodels Analogue Modelling Laboratory, in the 3D modelling rig that allows a progressive tilting of the 140 cm length and 70 cm width base plate of the deformation box. Overhead time-lapse pictures were used to analyse the evolution of the model. At the end, each experiment was preserved and sectioned in 3 mm thick sections that were also recorded with photographs. These pictures were used to build 3D voxel images and 3D pseudo-seismic that were used to analyse the evolution of the structures along strike as well as the thickness of the different units at the end of the experiment. Digital Image Correlation techniques were also applied to the overhead pictures.

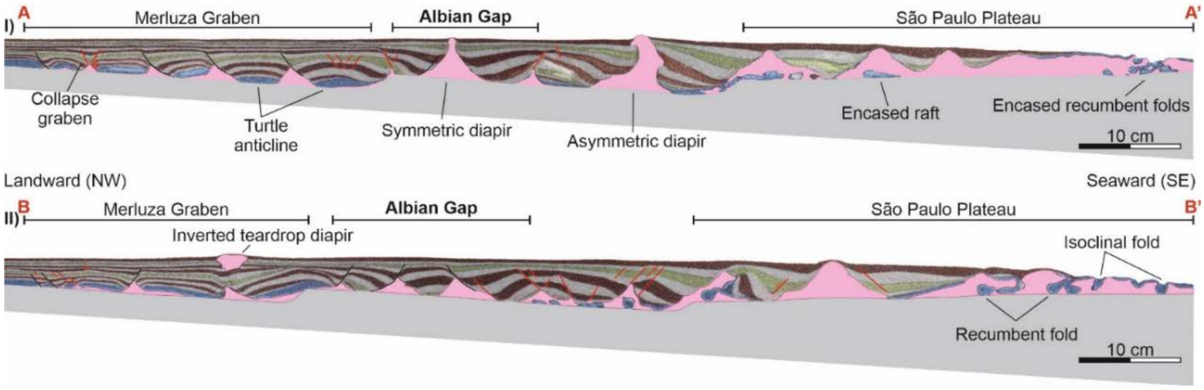

Figure 2: Final cross-sections at the eastern i) and western ii) part of model 2 with the equivalence of the structural domains of the natural analogue.

Our experimental results produce similar evolution and architecture of salt and post-salt deformation the Santos Basin, and improve understanding on the interaction and distribution of salt-related gravity-driven processes. The structural processes and salt-related geometries resulting from the modelling are also comparable and relevant to many other salt-bearing rifted margins (i.e., Gulf of Mexico, West Africa, Campos-Espirito Santo, Morocco and Nova Scotia).

References

Demercian, S., Szatmari, P., & Cobbold, P. R. (1993). Style and pattern of salt diapirs due to thin-skinned gravitational gliding, Campos and Santos basins, offshore Brazil. Tectonophysics, 228(3-4), 393-433.

Fiduk, J. C., & Rowan, M. G. (2012). Analysis of folding and deformation within layered evaporites in Blocks BM-S-8 &-9, Santos Basin, Brazil. Geological Society, London, Special Publications, 363(1), 471-487.

Guerra, M. C., & Underhill, J. R. (2012). Role of halokinesis in controlling structural styles and sediment dispersal in the Santos Basin, offshore Brazil. Geological Society, London, Special Publications, 363(1), 175-206.

Jackson, C. A. L., Jackson, M. P., Hudec, M. R., & Rodriguez, C. R. (2015b). Enigmatic structures within salt walls of the Santos Basin—Part 1: Geometry and kinematics from 3D seismic reflection and well data. Journal of Structural Geology, 75, 135-162.

Krézsek, C., Adam, J. & Grujic, D (2007). Mechanics of fault and expulsion rollover systems developed on passive margins detached on salt: insights from analogue modelling and optical strain monitoring. Geological Society, London, Special Publications, 292(1), pp.103-121.

Pichel, L. M., Peel, F., Jackson, C. A. & Huuse, M. (2018). Geometry and kinematics of salt-detached ramp syncline basins. Journal of Structural Geology, v115, 208–230, doi: 10.1016/j.jsg.2018.07.016.

Pichel, L. M., Jackson, C. A. L., Peel, F., & Dooley, T. P. (2019c). Base-salt relief controls salt tectonic structural style, São Paulo Plateau, Santos Basin, Brazil. Basin Research.

Pichel, L. M., & Jackson, C. A. L. (2020b). The enigma of the Albian Gap: spatial variability and the competition between salt expulsion and extension. Journal of the Geological Society, 177, 1129-1148.

Rowan, M. G., & Ratliff, R. A. (2012). Cross-section restoration of salt-related deformation: Best practices and potential pitfalls. Journal of Structural Geology, 41, 24-37.

Strain partitioning along a curved strike-slip fault system during indentation: inferences from analogue modelling

Nemanja Krstekanic (1,2*), Ernst Willingshofer (1), Taco Broerse (1), Liviu Matenco (1), Marinko Toljić (2), Uros Stojadinovic (2)
(1) Utrecht University, Faculty of Geosciences, Utrecht, the Netherlands, (2) University of Belgrade, Faculty of Mining and Geology, Belgrade, Serbia
* Contact: n.krstekanic@uu.nl

Abstract

Large-scale continental strike-slip faults are associated with significant strain partitioning in releasing/restraining bends and often display map-view curvatures ending in horse-tail structures. Commonly, these strike-slip faults are associated with indentation, where shortening in front of rigid blocks is transferred laterally to transpression, strike-slip and the formation of transtensional and extensional basins. We investigate how these structurally distinct domains are kinematically linked by performing a series of crustal-scale analogue modelling experiments where a deformable crust is moved against a stable and rigid indenter. The modelling demonstrates that the geometry of the indenter margins is the major controlling parameter driving strain partitioning and deformation transfer from thrusting and transpression to strike-slip and transtension, whereas the rotation of the mobile plate controls the opening of triangular shaped transtensional basins. Flow of the ductile crust distributes the deformation over a wider area, facilitating strike-slip splaying into transtension/extension behind the indenter. These results (Figure 1) show a very good correlation with the Moesian indentation in the Carpatho-Balkanides orogenic system of South-Eastern Europe, where the >100 km of Cerna-Timok dextral offset is partitioned to thrusting in the frontal, Balkanides, part of the Moesian indenter and to transtension and extension in the neighboring South Carpathians, behind the Moesia. The modelling also infers that the gradual transfer of strike-slip deformation from the Cerna-Timok system to thrusting/transpression and extension/transpression explains their observed variability in offset along strike.

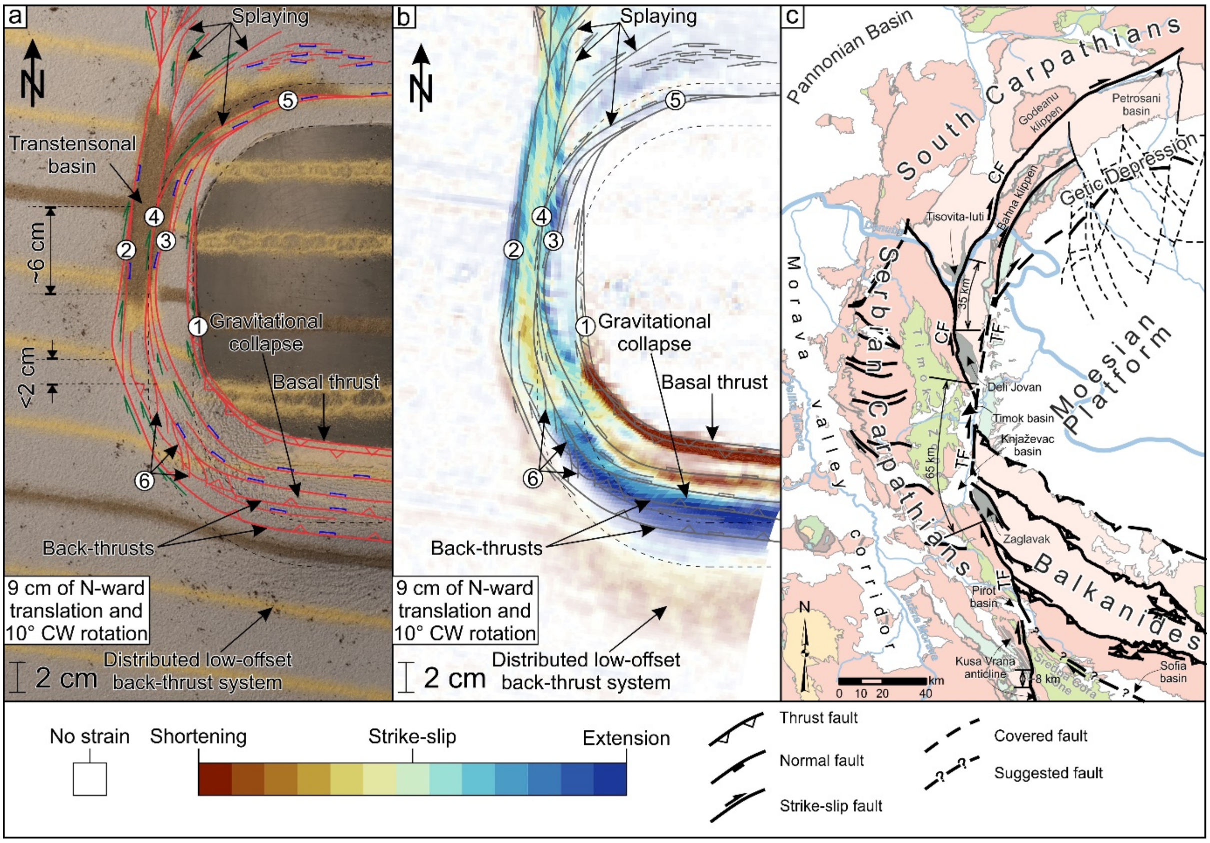

Figure 1: Best-fit model and natural example of the Cerna-Timok fault system (modified after Krstekanić et al., 2021). a) Interpreted top-view photo of the best-fit model at the end of the experiment. b) Cumulative

strain type map of the best-fit model at the end of the experiment. c) Tectonic map of the Cerna-Timok fault system in the South Carpathians-Serbian Carpathians-Balkanides orocline around the Moesian Platform.

References

Krstekanić, N., Willingshofer, E., Broerse, T., Matenco, L., Toljić, M., & Stojadinovic, U. (2021). Analogue modelling of strain partitioning along a curved strike-slip fault system during backarc-convex orocline formation: Implications for the Cerna-Timok fault system of the Carpatho-Balkanides. Journal of Structural Geology 149, 104386. https://doi.org/10.1016/j.jsg.2021.104386

Control of geometrical and mechanical parameters on strike-slip fault segmentation: insights from sandbox experiments.

Marthe Lefèvre (1), Pauline Souloumiac (2*), Nadaya Cubas (3), Bertrand Maillot (2), Yann Klinger (4) *(keynote)*
(1) Observatoire Royale de Belgique, (2) CY Cergy Paris Université, Géosciences et Environnement, France, (3) ISTeP - CNRS, Sorbonne Université, France, (4) IPGP – CNRS, Université de Paris, France.
* Contact: pauline.souloumiac@cyu.fr

Abstract

Co-seismic continental strike-slip ruptures are usually segmented, separated by geometrical complexities. This segmentation affects the dynamics of earthquakes but the physical processes governing the scale of this segmentation remains unclear. Furthermore, on field, the length of segments has been shown to vary from 18km to 25km, independently of the regional tectonic setting (Klinger, 2010). These observations led the author to suggest that the thickness of the seismogenic crust could control this structural scaling. Thus, to test this hypothesis, we use analogue modelling to investigate the structural development of strike-slip faults and the physical parameters controlling this segmentation. Theoretically, the evolution from en échelon Riedel until horizontal shear segments has been thoroughly described qualitatively by Tchalenko (1970). Here we test and quantify the effect of the sand pack thickness as well as the internal and basal frictions on the length of segments. We then compare our results to natural case to conclude on their potential relationship with the seismogenic thickness. We show that ratios between the segment length and the brittle material thickness are similar for coseismic ruptures and sandbox experiments. We show also that variations of rheological properties have a minor effect on the linearly relationship betwen the lenght of segments and the brittle material thickness. Finally this study demonstrates that the inherited complexities influence the localisation of segments and relay zones observed on strike-slip faults.

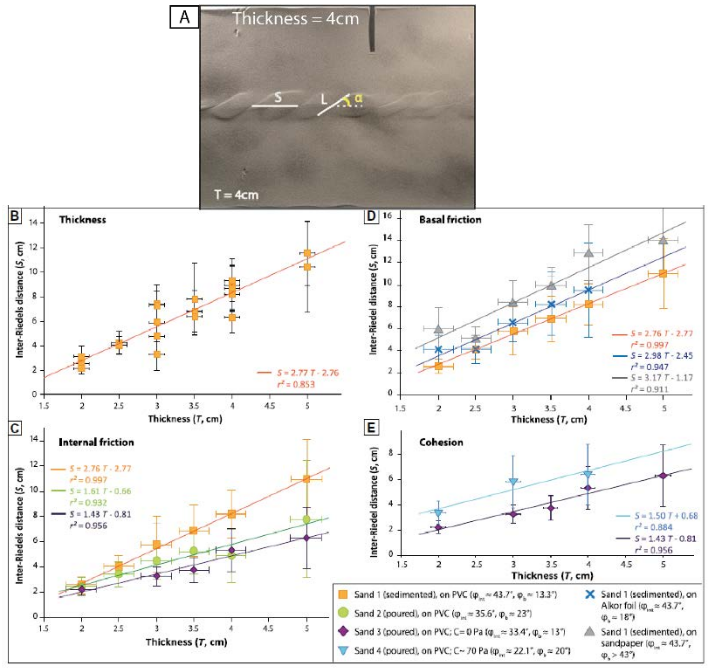

Figure 1: A – Topview of the sandbox after 11 mm of displacement highlighting the en échelon Riedel faults. [B-E] Comparison between inter-Riedel distance (*S*) and sand-pack thickness (*T*) for different frictional and cohesional properties of sand. Modified from Lefèvre et al, 2020.

Sandbox apparatus and experimental procedure

The specific sandbox for Riedel experiments is composed of two PVC plates simulating the base of the upper crust. One plate is movable and can be pushed forward to simulate a sinistral strike-slip fault at the base of the model thanks to a lead screw. The other plate is fixed. The dimensions of the box (80x210cm) are large enough to ensure that a significant part of the observations escapes boundary effects. The sand pack is flat and the edges are free. Top view photos are taken every 0.5 mm.

We test sand pack varying from 2 to 6 cm thick. To get different internal frictions, the sand is poured in two different mods: (1) sedimented with a sand distributor used to achieve a uniform sand density and a high internal friction (CV32): $\square_{int}$=43.7° and (2) by sprinkling and scraping the sand pack for a lower friction (CV32): $\square_{int}$=35.6°. A third type of sand with a different grain size range (Ga39) is also tested: $\square_{int}$= 33.4°. Two different basal frictions were tested: $\square_b$=13° (sand/PVC) and $\square_b$=18° (sand/Alkor foil®). For each experiment, three parameters are measured: the spacing between Riedels (S), the Riedels' length (L) and the angle (□) formed by the Riedel and the direction of the strike slip fault at the base of the model (Fig. 1). In order to obtain satisfactory statistical results and to provide a correlation between parameters, 45 experiments were run for this study.

Experimental results

The thickness of the sand pack has a significant influence on the Riedels spacing. The thicker the sand layer is, the greater the spacing is (and implicitly longer). The thickness and the average spacing between Riedels appear to be linearly correlated (slope ~1.5) (Fig 1).

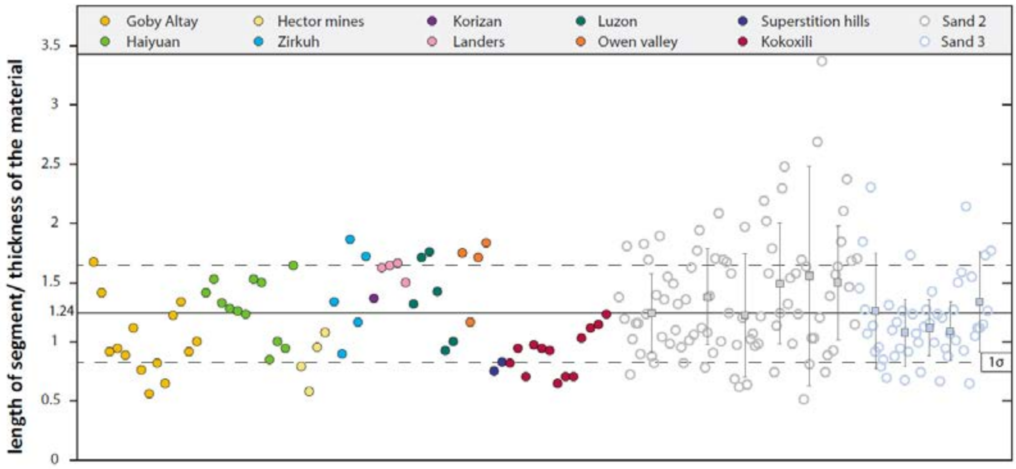

Figure 2: Normalized length of individual fault segments for several continental strike-slip earthquakes (Klinger, 2010; Lauer et al., 2018) and for individual analogue-fault segments (Sands 2 and Sand 3). From Lefèvre, 2018 (PhD Thesis).

If the sand layer thickness is constant, the larger the sand internal friction is, the longer the spacing is (Fig.1). Similarly, a linear relation relates the thickness and the average spacing between Riedels with the internal friction (slope ~1.5). Obviously, different internal frictions lead to various coefficients for this relation (slope and intercept): a frictional variation of 0.1 corresponds to a slope variation equal to 0.25. Furthermore, it seems that basal friction has no influence on the Riedels. Finally, considering a standard internal friction for the upper crust, this study shows that we are able to retrieve the same length over thickness ratio as for the natural cases (Fig.2).

References

Klinger Y. 2010. Relation between continental strike-slip earthquake segmentation and thickness of the crust, J. Geophys. Res., 115, B07306, doi:10.1029/2009JB006550.

Lefevre, M., Souloumiac, P., Cubas, N., & Klinger, Y. (2020). Experimental evidence for crustal control over seismic fault segmentation. *Geology*, *48*(8), 844-848.

Tchalenko 1970. Similarities between shear-zones of different magnitudes. *Geological Society of America Bulletin 81*, Pages 1625–1640.

Lauer, B., Grandin, R., & Klinger, Y. (2020). Fault geometry and slip distribution of the 2013 Mw 7.7 Balochistan earthquake from inversions of SAR and optical data. *Journal of Geophysical Research: Solid Earth*, 125(7), e2019JB018380.

Lefèvre, M., Souloumiac, P., Cubas, N., & Klinger, Y. (2020). Experimental evidence for crustal control over seismic fault segmentation. *Geology*, 48(8), 844-848.

Lefèvre, M. (2018) *Segmentation des grands décrochements, du cycle sismique à la déformation long terme, exemple de la faille du levant.* Thèse de doctorat. IPGP, France.

Variations in crustal thickness and faulting patterns in oceanic ridge–transform fault systems: Insights from gravity and geodynamic modelling

Sibiao Liu (1*), Lars H. Rüpke (1), Zhikui Guo (1), Ingo Grevemeyer (1), Jason P. Morgan (2), Yu Ren (1), Dietrich Lange (1), Yanan Shi (2), Colin W. Devey (1), Katharina A. U. Moreno (1)
(1) GEOMAR Helmholtz Centre for Ocean Research Kiel, Kiel, Germany, (2) Southern University of Science and Technology, Shenzhen, China
* Contact: sliu@geomar.de

Abstract

Oceanic transform faults (OTFs) are one of the major types of plate boundaries and characterize a strike-slip motion between two mid-ocean ridge segments. Conventional plate tectonics theory suggests that as the oceanic plate moves away from the ridge and gradually ages, the lithosphere or crust cools and sinks along transform fault to adjacent fracture zone. However, recent high-resolution multibeam bathymetric data show this plate-cooling argument is too simplistic; the seafloor over transform faults is systematically deeper than that of fracture zones which implies a thinner lithosphere or crust along OTFs (Grevemeyer et al., 2021). Moreover, these compelling discoveries and interpretation require further verification from other geophysical observations such as gravity signature.

Previous gravity studies have shown that crustal thickness variation between OTFs and associated ridge segments is recognized to depend on the spreading rate (Gregg et al., 2007), yet such variation between transform faults and their adjacent fracture zones is not well established. Here we calculate the residual mantle Bouguer gravity anomaly (RMBA) of 12 oceanic ridge-transform systems in the light of these bathymetric data, satellite gravity anomaly data and 3D mantle upwelling thermal models. To investigate the thermal structure in the system we first apply different rheological regimes in the thermal models. We find that the brittle rheology (i.e., plasticity in the model) plays an important role in controlling the thermal structure beneath oceanic transform-fracture zones. Then the RMBA is corrected by removing the gravimetric effect of temperature changes as estimated from the thermal models with the inclusion of nonlinear visco-plastic rheology. We show that transform faults exhibit more positive RMBA than fracture zones, which typically implies a thickening of the crust from transform faults to fracture zones across the ridge-transform intersection.

Further, dikes propagating associated with oceanic crustal accretion along the ridge axis may alter crustal thickness along the transform fault by penetrating past the transform into the adjacent old oceanic crust and curving in the direction of the transform (Gregg et al., 2007). Different patterns of crustal accretion under different magma supply can lead to the variations in faulting styles (Buck et al., 2005). Therefore, we develop thermomechanical models of crustal accretion in oceanic ridge-transform system to investigate how crustal thickness and fault patterns vary with spreading rate and crustal accretion, and whether these variations are systematical behavior for ridge-transform systems with respect to different spreading rates.

References

Buck, W. R., Lavier, L. L., & Poliakov, A. N. B. (2005). Modes of faulting at mid-ocean ridges. Nature, 434(7034), 719–723. https://doi.org/10.1038/nature03358.

Gregg, P. M., Lin, J., Behn, M. D., & Montési, L. G. J. (2007). Spreading rate dependence of gravity anomalies along oceanic transform faults. Nature, 448(7150), 183–187. https://doi.org/10.1038/nature05962.

Grevemeyer, I., Rüpke, L. H., Morgan, J. P., Iyer, K., & Devey, C. W. (2021). Extensional tectonics and two-stage crustal accretion at oceanic transform faults. Nature, 591(7850), 402–407. https://doi.org/10.1038/s41586-021-03278-9.

Comparison of Kinematic and Elastic Dislocation Models of Fault-Propagation Folds Through Inverse Modeling

David O. S. Oakley (1*), Nestor Cardozo (1), Jack P. Loveless (2)
(1) Department of Energy Resources, University of Stavanger, Stavanger, Norway
(2) Department of Geosciences, Smith College, Northampton, MA, USA
* Contact: david.o.oakley@uis.no

Abstract

Kinematic models of fault-related folding, such as trishear, are valuable and widely used tools in structural geology. These methods can be used to provide estimates of fault or fold geometry in areas where data are lacking and to infer fault slip and propagation history. Inversion methods can be used to fit kinematic models to data that describe the shape of a fold, providing not only a best-fit model, but also a range of possible solutions and estimates of model parameter uncertainty (Cardozo and Oakley, 2019).

A weakness of kinematic models is that they do not directly account for the mechanical processes of deformation. Elastic dislocation (ED) boundary element models are an alternative method to model fault-related folds in a way that considers the mechanics of deformation (Dee et al., 2007). While typically limited to purely elastic deformation in a homogeneous medium, the method can be extended to include mechanically active layering, allowing it to simulate layer-parallel slip during folding (Huang and Johnson, 2016; Johnson, 2018).

In this study, we use the simulated annealing method to fit both kinematic and ED models to synthetic and natural examples of folds formed by slip on listric, propagating thrusts. For a kinematic model, we use trishear deformation ahead of the fault tip combined with inclined shear in the hanging wall, as described by Cardozo and Brandenburg (2014). For ED models, we test unlayered, frictionless layered, and frictional layered models. Due to the irreversibility of models involving friction, we test all models by forward modeling, rather than by restoration. Figure 1 shows best-fit models to a folded bed from a Niger Delta structure, which was previously modeled kinematically by Cardozo and Brandenburg (2014) and which shows features of both fault-propagation and detachment folding (Kostenko et al., 2008).

Preliminary results provide insight into the differences between the two modeling approaches and their abilities to model different styles of deformation. We find that ED models have difficulty fitting the steep forelimbs and asymmetric shapes of trishear-style folds. Layered models come closer than unlayered models in this respect, but trishear remains the best of the methods tested at modeling the forelimb geometry in Figure 1, suggesting that trishear approximates a style of folding in which inelastic, non-layer parallel deformation is important. On the other hand, the curved backlimb can be reasonably well fit by both trishear and ED models. This result is somewhat surprising since the physical principle underlying inclined shear is different from layer-parallel slip, and it suggests that backlimb geometry (at least of a single horizon) may be insufficient to reliably determine the style of deformation. Kinematic and mechanical models also provide different results for model parameters such as the amount of slip on the detachment, which drives folding in our models. These differences constitute a form of epistemic uncertainty, deriving from the choice of model, which should be considered when using models to make inferences about fault slip or other parameters of interest. Finally, our results show that global optimization methods previously used to fit kinematic models to data can also be applied to mechanics-based models, at least for the relatively computationally efficient case of boundary element models. Combining inverse methods with mechanics-based models offers a promising path for inverse modeling beyond kinematics, but challenges remain in ensuring that complex styles of deformation, such as trishear-style deformation, can be represented in such models.

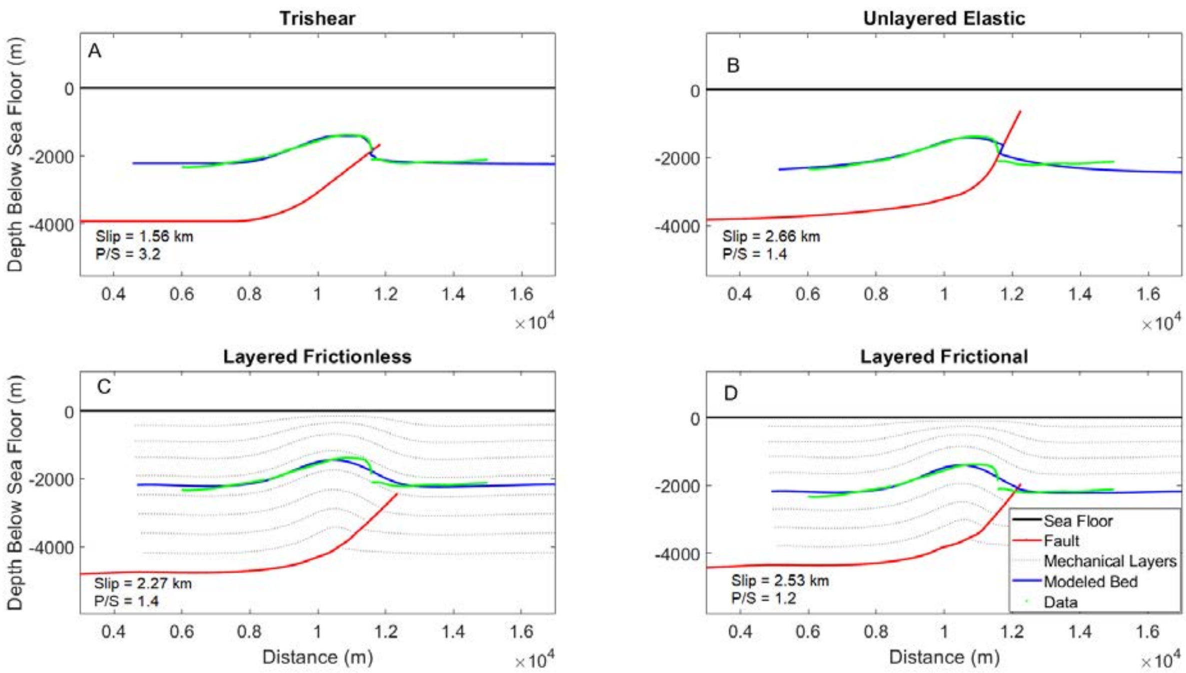

Figure 1: Comparison of best fit model results using (a) trishear and inclined shear, (b) an unlayered ED model, (c) an ED model without friction, and (d) an ED model with friction. The data (green points) are from Bed 3 of Cardozo and Brandenburg (2014), their Figure 8. Slip is the slip on the detachment. P/S is the ratio of fault propagation to fault slip. The faults in all examples begin propagating from the detachment.

References

Cardozo, N. and Brandenburg, J.P., 2014. Kinematic modeling of folding above listric propagating thrusts. Journal of Structural Geology, v. 60, 1-12. http://dx.doi.org/10.1016/j.jsg.2013.12.004

Cardozo, N. and Oakley, D., 2019. Inverse modeling for possible rather than unique solutions. Journal of Structural Geology, v. 125, 285-295. https://doi.org/10.1016/j.jsg.2018.05.026

Dee, S.J., Yielding, G., Freeman, B., Healy, D., Kusznir, N.J., Grant, N., and Ellis, P., 2007. Elastic dislocation modeling for prediction of small-scale fault and fracture network characteristics. Geological Society, London, Special Publications 270.1, 139-155. doi: 10.1144/GSL.SP.2007.270.01.10

Huang, W.-J. and Johnson, K.M., 2016. A fault-cored anticline boundary element model incorporating the combined fault slip and buckling mechanisms. Terrestrial, Atmospheric and Oceanic Sciences, v. 27(1), 73-85. doi: 10.3319/TAO.2015.06.18.01(TT)

Johnson, K.M., 2018. Growth of fault-cored anticlines by flexural slip folding: Analysis by boundary element modeling. Journal of Geophysical Research: Solid Earth, v. 123, 2426-2447. https://doi.org/10.1002/2017JB014867

Kostenko, O.V., Naruk, S.J., Hack. W., Poupon, M., Meyer, H.-J., Mora-Glukstad, M., Anowai, C., and Mordi, M., 2008. Structural evaluation of column-height controls at a toe-thrust discovery deep-water Niger Delta. AAPG Bulletin, v. 92(12), 1615-1638.

Does rifted margins salt tectonics balance? The competition between rifting, syn-depositional flow, and gravity-driven tectonics

Leonardo M. Pichel (1), Ritske S. Huismans (1), Robert Gawthorpe (1), Jan Inge Faleide (2), Thomas Theunissen (1)

(1) Department of Earth Science, University of Bergen, Bergen, Norway
(2) Department of Geosciences, University of Oslo, Oslo, Norway

* Leonardo.m.pichel@uib.no

Abstract

Rifted margins are often associated with widespread and thick evaporite (i.e., salt) deposits, and pronounced salt tectonics. The majority and largest salt basins formed during the latest stages of rifting, immediately prior to continental breakup. Salt tectonics along these margins is commonly depicted as linked domains where gravity-driven updip extension is balanced by downdip shortening in the form of buckle-folding, diapir squeezing and salt nappe thrust advance. We use 2D thermo-mechanically coupled finite-element modelling of lithospheric extension to investigate the genesis and evolution of salt tectonics along wide rifted margins and the interplay between rifting and post-rift gravity-driven deformation. The models are the first to integrate lithospheric extension with post-rift salt tectonics using a geodynamically self-consistent modelling approach where the geometries of the lithosphere and salt basins are not prescribed. The models confirm that salt-bearing wide rifted margins are characterized by gravity-driven updip extension and downdip shortening. However, the models also show that syn-depositional salt flow occurs in the distal portions of salt basins formed prior to continental breakup and this early deformation is driven by rift-related stretching. This produces lengthening of the salt basin and emplacement of an equally wide salt nappe over the newly formed oceanic crust prior to gravity-driven tectonics. Sensitivity tests using different salt viscosities, margin architecture and post-salt sedimentation rates show similar processes but with contrasting magnitudes, spatial and temporal distribution and resultant salt structural styles. Models also show that there can be excess in downdip shortening and salt inflation relative to updip extension due to pressure-driven (i.e., Poiseuille) salt flow. These aspects contradict the paradigm of balanced extension and shortening (i.e., Couette flow) along rifted margins salt basins. The results can be directly compared to examples from various salt-bearing rifted margins and improve our understanding on the enigmatic genesis and evolution of salt basins as well as on the interpretation of sub-salt crustal geometries.

Structural model of the western Kura foreland fold-and-thrust belt using seismic reflection profiles: implication for forward kinematic modelling

Alexander Razmadze (1*)

(1) Tbilisi State University, M. Nodia Institute of Geophysics

* alrazmadze@gmail.com

Abstract
The active Kura foreland thin-skinned fold and thrust belt, which is one of the best examples of the collision-driven far-field deformations is associated with Arabia-Eurasia convergency. Kura foreland fold and thrust belt which developed formerly as a foreland basin (Oligocene-Lower Miocene or Oligocene-Upper Miocene) is located between Greater Caucasus and Lesser Caucasus orogens (e.g. Alania et al., 2008, 2017; Forte et al., 2010). Neogene shallow marine and continental sediments in Kura foreland fold-and-thrust belt keep the record on the stratigraphy and structural evolution of the study area during the compressive deformation.

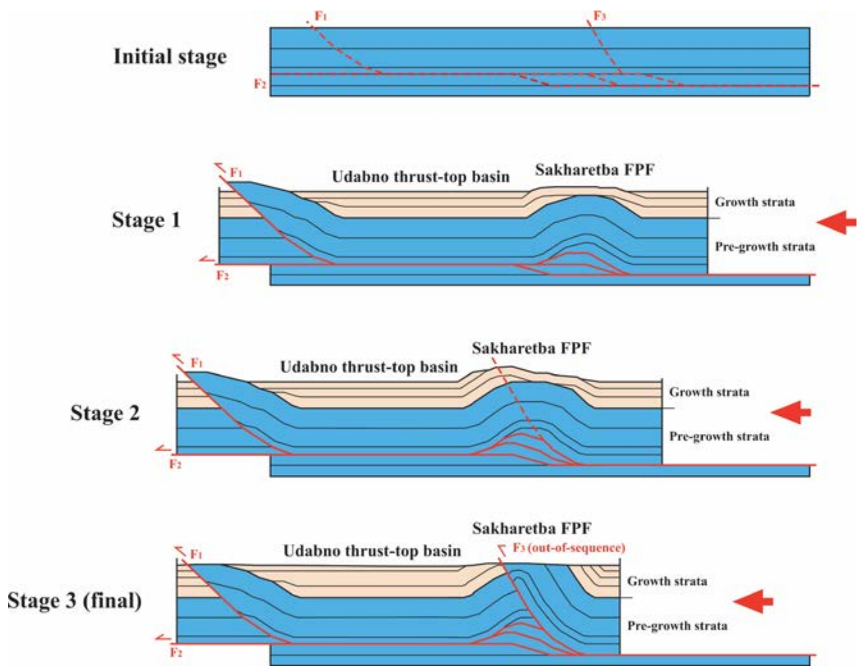

Figure 1. Forward kinematic modelling.

Fault-related folding theory were used for the interpretation of seismic reflection profiles and construction of the forward kinematic modelling (Shaw et al. 2006; Suppe and Medwedeff 1990). Identification of stratigraphic units at depth for seismic profiles was based on outcrop and deep-wells data correlations. On the basis of interpreted seismic reflection profiles, the main style of deformation within the Kura foreland fold-and-thrust belt is represented by a set of fault-related folds and their duplexes. Within the study area, a series of thrust-top basins developed. The evolution of the thrust-top basins was mainly controlled by the kinematics of competing growth fault-propagation folds. The geometry of syn-orogenic sedimentation, associated with footwall synclines and the sedimentary infill of thrust-top basins, provides information on the thrusting activity within western Kura foreland fold-and-thrust belt. Forward kinematics modelling was used to develop a tectonic model for the evolution of the western Kura foreland fold-and-thrust belt (Fig. 1).

Acknowledgements: This work was supported by Shota Rustaveli National Science Foundation (SRNSF - #PHDF-19-268).

References

Alania V., Chabukiani A., Chagelishvili R., Enukidze 0., Gogrichiani K., Razmadze A., & Tsereteli N. (2017). Growth structures, piggyback basins and growth strata of Georgian part of Kura foreland fold and thrust belt: implication for Late Alpine kinematic evolution. Geological Society, London, Special Publications, v428, 171-185.

Alania, V., Enukidze, O., Koiava, K., Razmadze, A., & Sanishvili, A. (2008). Thrust systems and time of deformation of the Gare Kakheti foothills, eastern Georgia (Georgia). Bollettino di Geofisica, teorica ed applicate, v49, 207-208.

Forte, A., Cowgill, E., Bernardin, T., Kreylos, O., & Hamann, B. (2010). Late Cenozoic deformation of Kura fold-thrust belt, southern Greater Caucasus. Geological Society of America Bulletin, v122 (3-4), 465-486.

Suppe, J., & Medwedeff, D.A. (1990). Geometry and kinematics of fault-propagation folding. Eclogae. Geol. Helv., v83, 409–454.

Shaw, J. H., Connors, C. D., & Suppe, J. (2006). Seismic interpretation of contractional fault-related folds. AAPG Studies in Geology, 156 p.

Some contributions to salt tectonics from new analogue models run at GFZ Potsdam during EPOS TNA activities: Boundary conditions, monitoring, materials

Matthias Rosenau (1*), Zhiyuan Ge (2,3), Michael Warsitzka (1,4)

(1) Helmholtz Centre Potsdam – GFZ German Research Centre for Geosciences, 14473 Potsdam, Germany
(2) State Key Laboratory of Petroleum Resources and Prospecting, China University of Petroleum (Beijing), Beijing, 102249, China
(3) College of Geosciences, China University of Petroleum (Beijing), Beijing, 102249, China
(4) Institute of Geophysics of the Czech Academy of Sciences, Boční II/1401, 141 31 Prague 4, Czech Republic

* Contact: rosen@gfz-potsdam.de

Abstract

Analogue modelling is an important scientific tool in salt tectonics because of its capability in simulating the long term and regional scale deformation in a physically self-consistent manner. In natural salt basins, kinematic and dynamic boundary conditions often vary in space and time and gravitational and tectonic forces may also interfere at different stages. Prototypes of natural salt tectonic deformation typically show non-cylindrical and time-varying deformation requiring three-dimensional modelling at high spatial and temporal resolution.

Salt tectonics has been the strength of analogue modelling because of the intrinsic three-dimensional character and space-time continuity, such that model resolution is not a limiting factor compared to numerical simulation. With the advent of DIC (digital image correlation) methods, like Particle Image Velocimetry (PIV), Particle Tracking and Structure-from-Motion, the monitoring resolution and ability to quantify deformation evolution has dramatically increased.

The rheology in salt tectonic experiments is rather straightforward yet vital: Salt is considered a rather homogenous and linear-viscous (Newtonian) material while the sedimentary cover is a Mohr-Coulomb-type brittle material. In contrast to geodynamic models, temperature, pressure and petrologic dependencies of the rheology are considered irrelevant in salt tectonic settings. However, the brittle-ductile coupling between salt and overburden results in time-dependent and rate-sensitive deformation, which needs to be considered in interpretations of the finite structure.

We here provide examples of analogue modelling studies on salt tectonics realized at GFZ Potsdam in recent years and initiated during an EPOS (European Plate Observing System) TNA (Transnational access) activity in the year 2018. We provide some new perspectives on the methodological challenges and advances in that field of research. We demonstrate for example how the classical instantaneous margin tilt scenario differs from a more realistic continuous tilt scenario in terms of the evolution and final structure of the evolving fault system and relate the variations to significantly different brittle-viscous coupling (Ge et al., 2019a, 2019c). Application of Coulomb wedge theory to salt tectonic systems shed some new lights the mechanisms of sedimentary wedge collapse and its coupling on salt flow underneath (Ge et al., 2021). All these findings are made possible by high-resolution 3D digital image correlation in quantifying experimental surface deformation (Ge et al., 2019b,d) allowing for the inversion of salt flow (Ge et al., 2021). Finally, we also discuss material properties of new low-density granular materials used in the experiments (Warsitzka et al., 2019).

In compliancy with the EPOS TNA strategy to make research results and data open access in a FAIR (Findable, Accessible, Interoperable, and Re-usable) way we published all model results open access. All underlying image correlation data as well as the material properties of the analogue materials used have been published with GFZ Data Service as open access data sets. We thank Frank Neumann and Thomas Ziegenhagen for construction of the model setup and assistance.

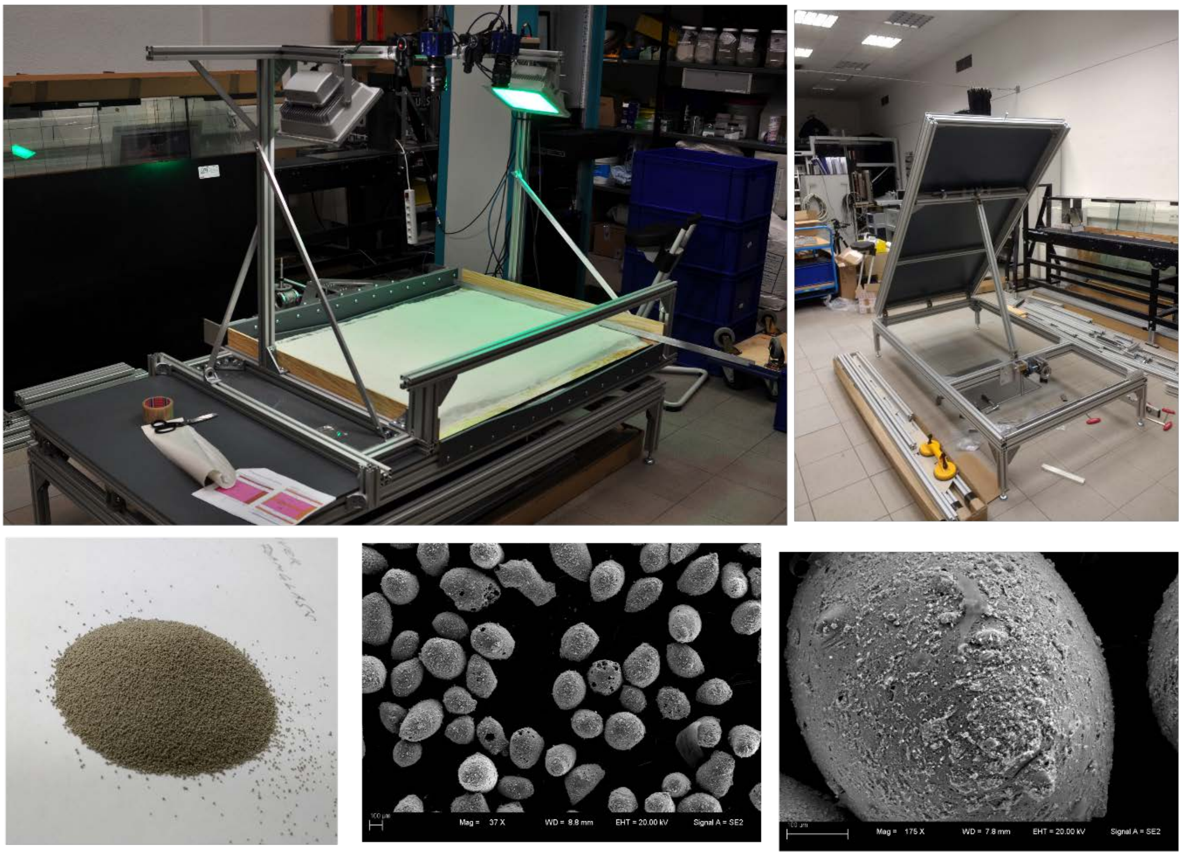

Figure 1: Lab impressions during the TNA activity: Upper panels: Typical model setup with stereoscopic high-resolution image correlation-based surface strain monitoring and the original continuous tilting mechanism. Lower panels: Low-density foam glass material (SEM images from Warsitzka et al. 2019).

References

Ge, Z., Rosenau, M., Warsitzka, M., Gawthorpe, R.L. (2019a). Overprinting translational domains in passive margin salt basins: Insights from analogue modelling, Solid Earth, 10, 1283–1300, https://doi.org/10.5194/se-10-1283-2019

Ge, Z., Rosenau, M., Warsitzka, M., Rudolf, M., Gawthorpe, R.L. (2019b). Digital image correlation data from analogue modeling experiments addressing mechanisms of overprinting translational domains in passive margin salt basins. GFZ Data Services. https://doi.org/10.5880/GFZ.4.1.2019.001.

Ge, Z., Warsitzka, M., Rosenau, M., Gawthorpe, R.L. (2019c). Progressive tilting of salt-bearing continental margins controls thin-skinned deformation. Geology, v47, 1122–1126. https://doi.org/10.1130/G46485.1.

Ge, Z., Rosenau, M., Warsitzka, M., Gawthorpe, R.L. (2019d). Digital image correlation data from analogue modeling experiments addressing controls of tilting rate on thin-skinned deformation at salt-bearing continental margins. GFZ Data Services. https://doi.org/10.5880/GFZ.4.1.2019.006.

Ge, Z., Rosenau, M., Warsitzka, M. (2021). How Topographic Slopes Control Gravity-spreading in Salt-bearing Passive Margins, ESSOAr, https://doi.org/10.1002/essoar.10506599.1.

Warsitzka, M., Ge, Z., Schönebeck, J.-M., Pohlenz, A., Kukowski, N. (2019): Ring-shear test data of foam glass beads used for analogue experiments in the Helmholtz Laboratory for Tectonic Modelling (HelTec) at the GFZ German Research Centre for Geosciences in Potsdam and the Institute of Geosciences, Friedrich Schiller University Jena. GFZ Data Services. https://doi.org/10.5880/GFZ.4.1.2019.002.

Relating slip behavior to off-fault deformation using physical models

Emily Ross (1*), Jacqueline Reber (1), Sarah Titus (2)
(1) Iowa State University, (2) Carleton College
*eoross@iastate.edu

Abstract
In strike-slip fault systems, fault geometry, slip distribution, and changes in rheology have all been hypothesized as factors controlling off-fault deformation. Variations in fault geometry are known to distribute deformation away from the fault, but off-fault deformation is also observed along well-developed, straight strike-slip faults. Present-day variations in slip rates along strike-slip faults are observed in nature using GPS velocity fields. Geologic indicators of slip rate, however, lack the precision and spatial density to resolve long-term variations in slip. Permanent off-fault deformation must be inferred indirectly from fold patterns, paleomagnetism, and field structures. It is therefore difficult to relate structures that form over millions of years to decadal scale geodetic measurements of strain. This leads to the question: Can a change in slip behavior explain observed off-fault deformation? Here we model the relationship between a change in slip behavior and off-fault deformation using physical experiments. Physical models simplify a number of the complexities presented by natural strike-slip fault systems. Variations in rock type, unknown deformation history, erosion, deposition, and low-resolution sampling all complicate the natural system and highlight the need for a simplified model isolating slip behavior as the only variable influencing deformation.
In order to model a change in slip behavior along a strike-slip fault, a 2 cm thick slab of silicone is placed on a simple shear apparatus. A discrete slip plane is cut and lubricated to model creeping slip behavior, while silicone is left intact across a distributed slip region to model locked slip behavior (Figure 1A). Silicone serves as a homogeneous, linear-viscous crustal analogue, which allows for non-elastic deformation. Progressive model deformation in 2D is documented using particle image velocimetry, and deformation in 3D is documented using photogrammetry. By photographing the experimental deformation continuously, we can generate evenly spaced, high-resolutison strain fields for comparison to the lower-resolution and unevenly spaced geologic indicators and present-day velocity fields.

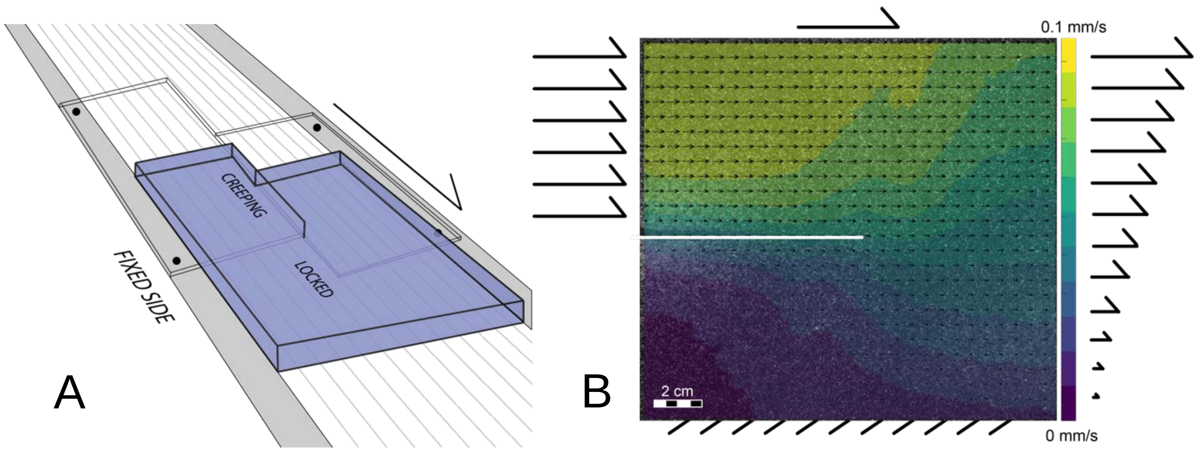

Figure 1: Experimental shear table setup (A) with deforming silicone slab (purple) and TecPIV velocity field (B) showing the transition from lubricated, discrete slip (left) to distributed slip (right).

In the experiments, regions of extension and compression develop on either side of the transition in slip behavior, with alternating zones of extension and compression extending into the creeping section (Figure 2). In the compressional region of the experiment, the elevation rises throughout the experiment while a basin develops in the extensional region. These features are offset as displacement increases over the course of the experiment.

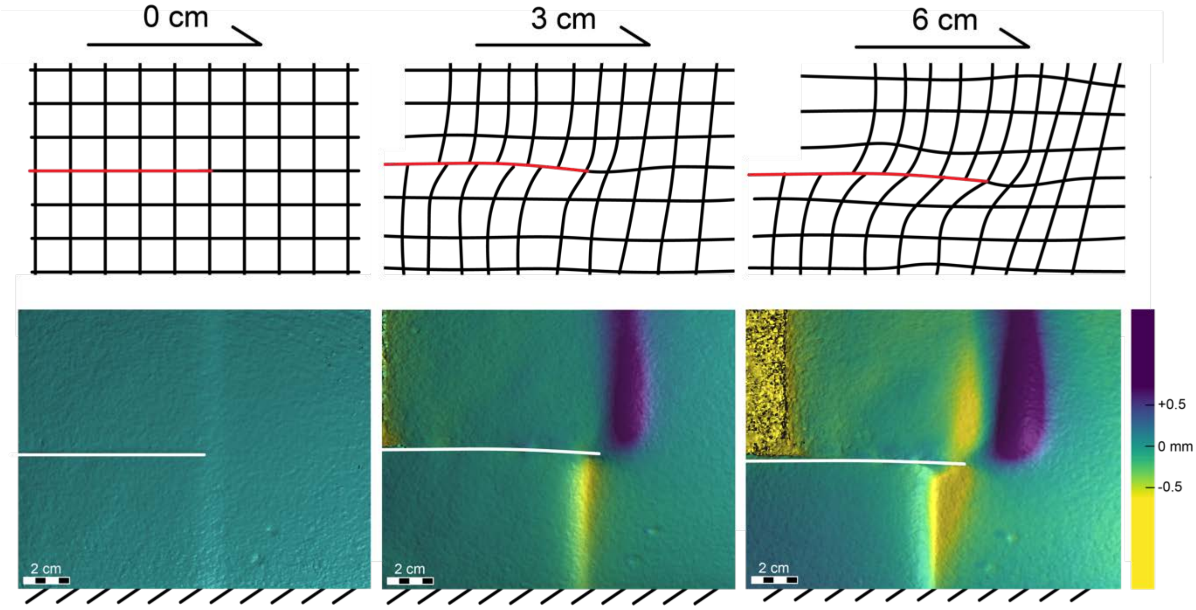

Figure 2: Top-down views of 2D grid deformation (above) traced from timelapse photographs and 3D vertical elevation change (below) generated using Agisoft Metashape after 0, 3, and 6 cm of displacement.

A well-developed and highly monitored example of a change in slip rate occurs in central California along the San Andreas fault. In the locked sections of the fault, displacement is accommodated by earthquakes, recorded seismically and as rapid changes in GPS station location. However, in the creeping section of the fault, displacement occurs aseismically and continuously (~28 mm/year). Additionally, some component of overall plate motion is accommodated by off-fault deformation, as rocks deform permanently away from the main trace of the fault. Surface velocities, measured at GPS stations, vary in magnitude and orientation along the fault, indicating regions of relative compression and extension around the transition from locked to creeping segments. Offset examples of compressional and extension structures are observed on opposite sides of the experiment, matching regions of compressional and extensional field structures in nature. This pattern matches experimental dilatation fields, suggesting that the change in slip behavior can explain observed off-fault dilatation patterns and off-fault deformation.

The perched synclines look-alike of central Tunisia: Examples of diapir Rise– Fall – Rise illustrated by field, geophysical, and experimental data

Nedhir Sebai (1*), Bruno C. Vendeville (2), Noureddine Boukadi (1), and Ferid Dhahri (1,3).

(1) LR18ES37 : Laboratoire de Recherche Géodynamique, Géo-ressources, Géo-numérique, Faculté des Sciences de Tunis, Université de Tunis El Manar, Tunisia. *nadhirsbai@gmail.com
(2) Univ. Lille, CNRS, Univ. Littoral Côte d'Opale, UMR 8187, LOG, Laboratoire d'Océanologie et de Géosciences, F 59000 Lille, France. Bruno.Vendeville@univ-lille.fr
(3) Département des Sciences de la Terre, Faculté des Sciences de Gafsa, Université de Gafsa, Campus Universitaire Sid Ahmed Zarroug, 212, Gafsa, Tunisia. feriddhahri@yahoo.fr

Abstract

Central Tunisia has been subjected to a complex series of successive regional tectonic phases, both extensional and compressional. This history is made even more complex by the presence of mobile Triassic evaporites that generated halokinetic deformation and partly decoupled the subsalt "basement" from the overburden.

At the southern end of a major regional lineament called "the North-South Axis" are some enigmatic structures cored by the Upper Eocene Jebs Formations: the Kef Ennsour and Zebbeus structures. The center of these structures is made of synform (concave-upward) strata of Upper Cretaceous to Cenozoic age resting unconformably onto the Triassic evaporites. A significant part of the stratigraphic series (i.e., Lower Cretaceous) is missing (in the perched syncline). The Cenozoic strata are particularly thick within the synclines, whereas they are thin or absent outside the synclines. In contrast, the Mesozoic series is continuous and thicker outside the synclines. These form topographic highs raised above the regional datum.

We hypothesize that these perched synclines have a halokinetic, rather that solely tectonic origin. The absence of parts of the lower stratigraphic series in the center of the structure indicates that the Triassic evaporites were rising as a passive diapir. During the Cenozoic, source-layer depletion combined with local extension forced the diapir to fall and its crest to subside, thus trapping thicker overburden strata within the syncline and bending them, resulting in a concave-upward geometry. During the latest stage a phase of regional shortening rejuvenated the fallen diapir, raising its synform roof above the regional datum.

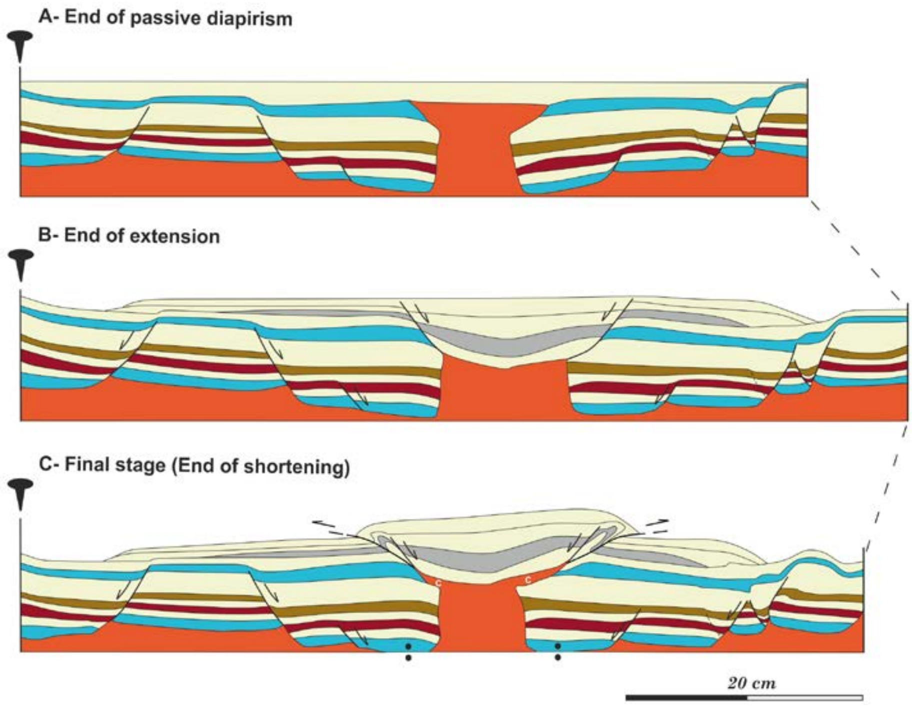

Figure 1. Schematic restored cross section in Model I at the end of the passive diapiric stage (A), at the end of the diapir fall stage (B) and at the end of the shortening stage (C).

We provide field and seismic data, as well as results from a set of analogue models of such a Rise-Fall-Rise structural history. The final geometry changes when varying the amounts and rates of passive diapir rise, sedimentation, extension, and late shortening. Results from most experiments closely match the geometries of the field examples from Central Tunisia. In addition, one model, in which the amount of diapir fall (and extrusion) was extreme, is very similar to the Tumb Diapir located offshore SW Iran.

References:

Sebai, N., Vendeville, B. C., Boukadi, N., Dhahri, N., 2021. The perched synclines look-alike of central Tunisia: examples of diapir Rise-Fall-Rise illustrated by field, geophysical, and experimental data. https://doi.org/10.1016/j.jsg.2021.104336

Deformation and stress cycle during frontal thrust formation of sandbox Coulomb wedges

Satoshi Tonai (1*), Takami Tachibana (1), Kei Kawakami (1, 2), Yasuhiro Yamada (3)
(1) Kochi University, (2) Current affiliation, Career Planning Co., Ltd., (3) Kyushu University
* Contact: s-tonai@kochi-u.ac.jp

Abstract

Coulomb wedges formed at plate subduction zones are characterized by the formation of multiple shear bands. These shear bands control the deformation styles of the wedge and its internal fluid flow, thus the mechanism of shear band formation has vital importance. Some previous studies that investigated the frontal area of the Coulomb wedges by sandbox modeling and reported dynamic deformation and kinematic nature of this area (e.g., Adam et al., 2005; Dotare et al., 2016; Ritter et al., 2018). In this study, we investigated the variation of deformation style of the sand layers by making several types of Coulomb wedges with different sand filling ways and/or different sands.

Our Coulomb wedges are made by dry sand (20 mm thickness before deformation) in an acrylic box (width 118 mm, length 693 mm, height 158 mm) with a basal sheet, that was pulled out of the box to deform the sand layers. The horizontal displacement of the sheet was 250 mm, that displaced the sand against the fixed wall to deform. We have tested four different initial states of the sand layers; (A) a single layer of sprinkled sand, (B) a single layer of poured sand, (C) two layers consist of a basal microbeads (sprinkled) and a sprinkled sand, and (D) two layers consist of a basal microbeads (poured) and a poured sand. The deformation in each experiment was recorded by sequential photographs. Some experiments were scanned with X-ray Computed Tomography (XCT) to observe the internal deformation of the wedges. In addition, the pulling force of the sheet was also recorded by using a load cell.

In the experiment A, characteristic periodicity was observed in deformation and pulling force, and each cycle can be divided into four periods of stages (I, II, III, and IV):
Stage I is immediately after the formation of a new shear band, and the load shows constant or slight increase in this stage.
Stage II begins almost at the same time when the highest point of the wedge begins to rise. The load clearly increases in this stage.
Stage III shows a rapid increase in load. At this stage, the load applied between the sand particles becomes large in the whole or part of the wedges, and consolidation may occur in some parts.
Stage IV is characterized by the load dropping. The XCT images in this stage show decrease in CT values at the front area of the wedges, décollement propagation, and the formation of new frontal thrust. The decrease in the load may be due to the strain weakening by newly formed shear band.
These results are generally consistent with the deformation and load patterns shown by the results and interpretations of previous studies.

Among the experiments B, C and D, differences were found in the shape of the Coulomb wedge and the distribution of the shear bands (Figure 1). First, the angle of the Coulomb wedge has the largest in the experiment A and decreases in the order of the experiment B, C and D. In addition, the experiments C and D showed larger undulations on the wedge surface than in the experiment A. The deformation and pulling force, when a frontal thrust was newly formed, also showed different patterns from those of the experiment A. The changes in pulling force in stages III and IV were smaller in the experiment B than that in the experiment A. In the experiment C, the increase of pulling force in the stage III was unclear. The pulling force pattern was irregular throughout in the experiment D. These results suggest that the deformation styles and the pulling forces are largely influenced by the strength structure of the wedges.

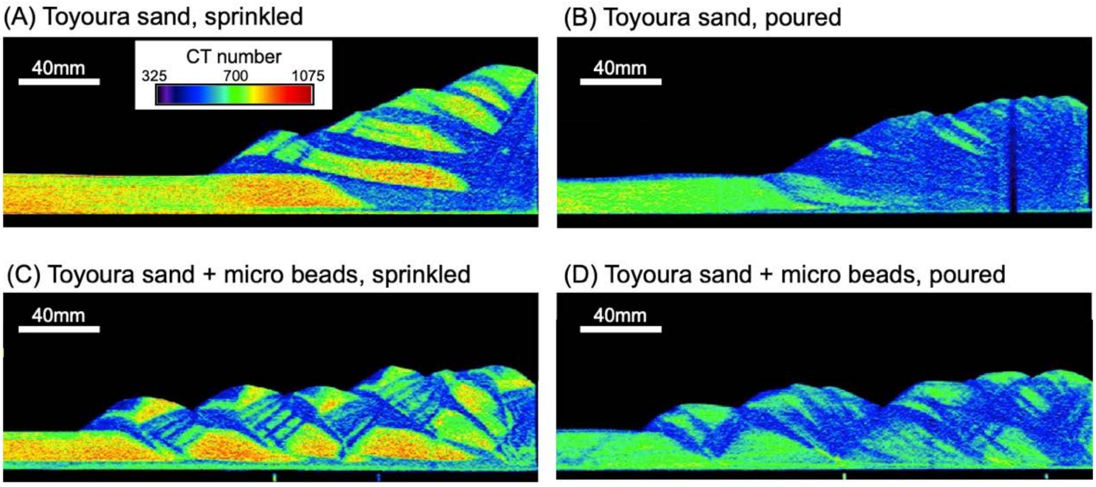

Figure 1: X-ray CT images of sand wedges with the same layer thickness (20 mm) at 250 mm of convergence. (a) Sprinkled Toyoura sand layer, (b) Poured Toyoura sand layer, (c) Sprinkled Toyoura sand and micro beads layers, and (d) Poured Toyoura sand and micro beads layers.

References

Adam, J. et al. (2005). Shear localisation and strain distribution during tectonic faulting –new insights from granular-flow experiments and high-resolution optical image correlation techniques. Journal of Structural Geology. 27, 283–301. https://doi.org/10.1016/j.jsg.2004.08.008.

Dotare, T., Yamada, Y. et al. (2016). Initiation of a thrust fault revealed by analog experiments. Tectonophysics. 684, 148–156. https://doi.org/10.1016/j.tecto.2015.12.023.

Ritter, M.C. et al. (2018). Sandbox rheometry: Co-evolution of stress and strain in Riedel– and Critical Wedge-experiments. Tectonophysics, 722, 400–409. https://doi.org/10.1016/j.tecto.2017.11.018.

Strike-slip fault in a sandbox: insight on off-fault deformation

Sarah Visage (1*), Pauline Souloumiac (1), Nadaya Cubas (2), Bertrand Maillot (1), Solène Antoine (3), Arthur Delorme (3), Yann Klinger (3).
(1) Laboratoire Géosciences et Environnement Cergy, CY Cergy Paris Université, France
(2) ISTeP, Paris-Sorbonne, France
(3) Université de Paris, Institut physique du globe de Paris, CNRS, France
* Contact: sarah.visage@cyu.fr

Abstract

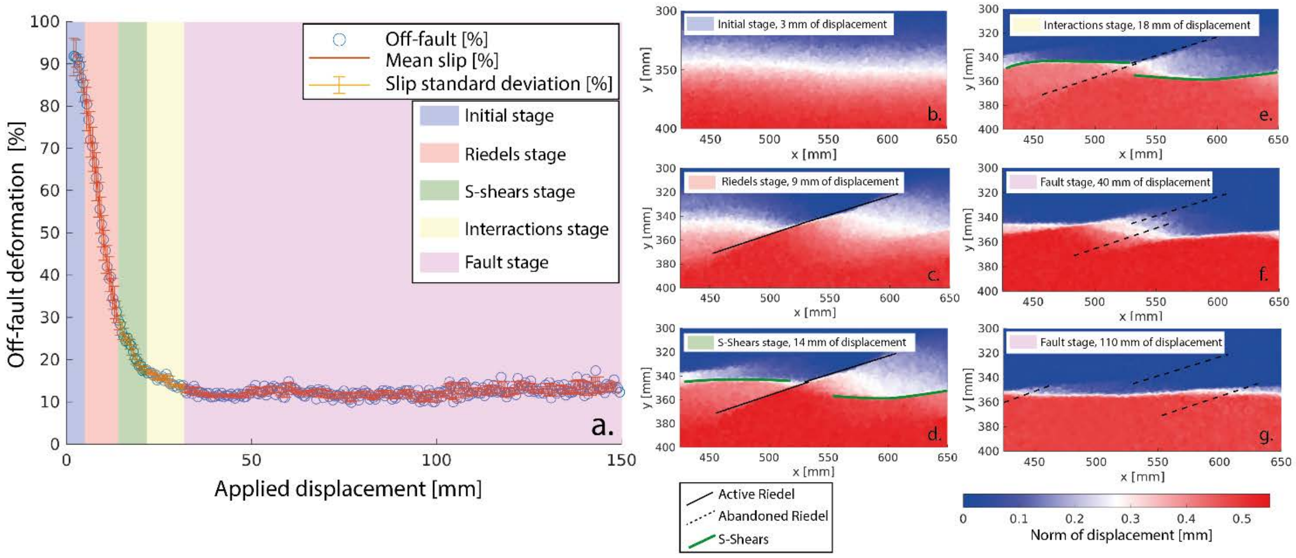

Figure 1: [a] Average off-fault deformation compared to the applied displacement, obtained for a set of 8 experiments with 4 to 8 cm sandpack thickness. [b, c, d, e, f, g] Displacement norm at different stages of experiment E481 (sandpack thickness = 6cm).

Seismic risk assessment for strike-slip faults strongly relies on the estimation of slip distribution of past earthquakes. However, during large strike-slip earthquakes, the ground surface displacement is accommodated both by on- and off-fault deformation (Antoine, et al., 2021; Hatem, et al., 2017). A significant amount of the observed surface deformation is distributed in a buffer zone of several hundred meters around the fault. The deformation distribution for a specific fault is thus a key ingredient for the assessment of seismic hazard (Baize, et al., 2019). The main goal of this project is to describe quantitatively on- and off-fault deformation from strike-slip faults in a sandbox using spatial imaging techniques (Delorme, et al., 2020; Vallage, et al., 2015) and to evaluate how it compares with natural examples.
We used a 1.50 m × 1.34 m PVC box, and study the evolution of the surface deformation of a homogeneous sand pack deposited above a straight-basal fault. Optical imagery is used at every stage of the experiment to quantify precisely on- and off-fault deformation and to describe qualitatively the 3D displacement.

We choose a criterion based on the gradient perpendicular to the fault of the the displacement Ux parallel to the fault to define the off-fault deformation $\left(0.02 \le \frac{\mathrm{dUx}}{\mathrm{dy}} \le 0.2\right)$. Regions where $\frac{\mathrm{dU_x}}{\mathrm{dy}} > 0.2$ are considered "on-fault deformation". The off-fault percentage is the ratio of the integrated gradient $\frac{\mathrm{dU_x}}{\mathrm{dy}}$ in "off-fault" regions to the applied incremental displacement. The result is further averaged over the entire length of the fault.

The figure 1a represents the evolution of the average amount of off-fault deformation along the entire length of the fault obtained for 8 experiments. The off-fault deformation decreases from 100% to 11.5% in 3 stages (Figure 1.a): (1) At the fault initiation stage, deformation is distributed along a central band (fig. 1.b), The width of this band is controlled by the thickness of the sandpack (the greater the thickness, the wider the zone) and by the internal friction of the sand. (2) Once shear bands start to form, from the Riedels to the S-shear segments, off-fault deformation strongly decreases from 100% to 11.5% (see on fig. 1.a). Off-fault is maximal in the inter-Riedels zones (fig. 1.c). (3) these structures eventually coalesce to form a fault (fig 1f and 1g), made of a succession of segments separated by geometrical complexities, or relay-zones, of variable size. Off-fault deformation remains stable (about 11.5%) (see fig.

1.a, f and g). Our modelling results also show that the relay zones are strongly controlled by inherited Riedels, and this is detailed in the poster presentation.
We finally compare our analogue results with estimates of off-fault deformation obtained for thirteen different strike-slip fault earthquakes (figure 2). Off-fault deformation induced by earthquake ruptures is significantly larger (35.2%) than the one observed in our sandbox experiments (11.5%). This difference is probably due to the unscaled high elastic stiffness of the sand, and further studies incorporating a better scaled elastic behavior should now be conducted.

Thanks to the ANR DISRUPT project and to the Initiative of Excellence of the University Paris Seine which allowed the financing of this PhD thesis.

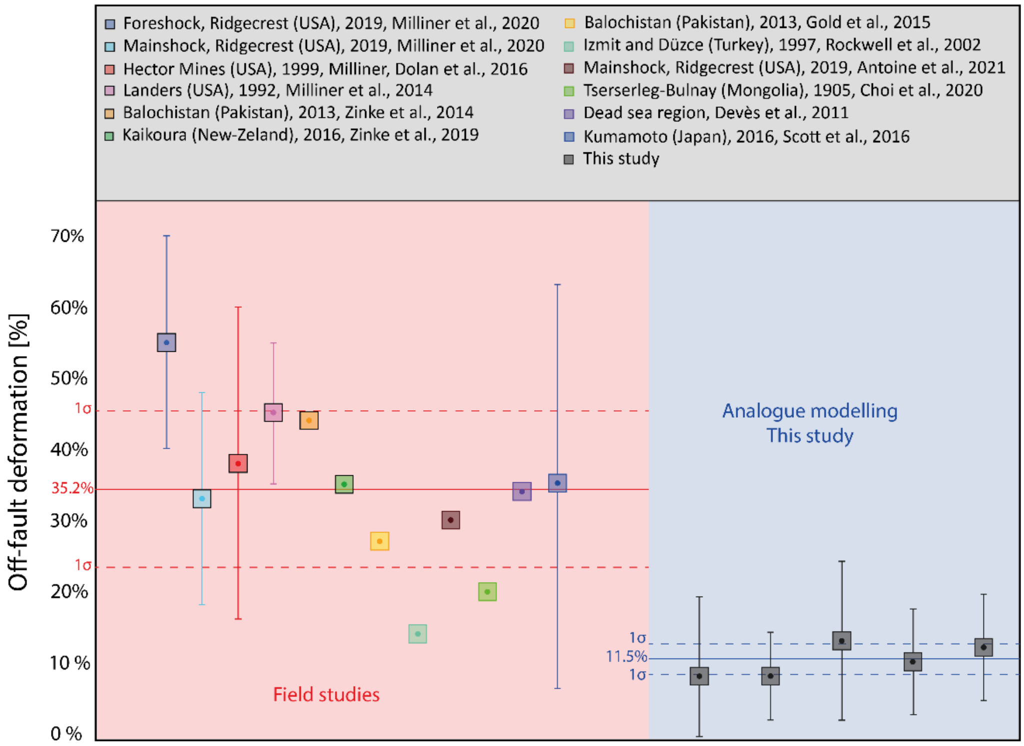

Figure 2: Percentage of off-fault deformation for different field studies and for the analogue models in this study. Averages of sandbox experiments were obtained from experiments with different sand thickness (from left to right: 4, 5, 6, 7 and 8 cm sand thickness).

References

Antoine, S. et al., 2021. Diffuse deformation and surface faulting distribution from sub-metric image correlation along the 2019 Ridgecrest ruptures (California, USA).
Baize, S. et al., 2019. A Worldwide and Unified Database of Surface Ruptures (SURE) for Fault Displacement Hazard Analyses. Seismological Research Letters, 10, Volume 91, p. 499–520.
Delorme, A. et al., 2020. Complex Deformation at Shallow Depth During the 30October 2016 Mw6.5 Norcia Earthquake: InterferenceBetween Tectonic and Gravity Processes?. Tectonics, 2.Volume 39.
Hatem, A. E., Cooke, M. L. & Toeneboehn, K., 2017. Strain localization and evolving kinematic efficiency of initiating strike-slip faults within wet kaolin experiments. Journal of Structural Geology, 8, Volume 101, p. 96–108.
Vallage, A. et al., 2015. Inelastic surface deformation during the 2013 Mw 7.7 Balochistan,Pakistan, earthquake. Geology, 10.p. G37290.1.

Investigating normal fault reactivation through analogue models of multiphase rifting: applications to the Turkana depression, East Africa

Liang Wang (1), Daniele Maestrelli (2*), Giacomo Corti (2), Yaoyao Zou (1), Chuanbo Shen (1)
(1) Key Laboratory of Tectonics and Petroleum Resources of the Ministry of Education, China University of Geosciences, Wuhan 430074, PR China (2) Consiglio Nazionale delle Ricerche, Istituto di Geoscienze e Georisorse, Via G. La Pira, 4, Firenze, Italy
* Contact: daniele.maestrelli@igg.cnr.it

Abstract

The Turkana depression (Ethiopia-Kenya) is a tectonic basin related to the Cretaceous-Early Cenozoic development of the South Sudan and the Anza grabens filled with a thick sequence of Cretaceous-Paleogene sediments reaching up to a thickness of 6–8 km. These two NW-SE trending depressions, which likely resulted from NE-SW extension, were later affected by W-E extension related to the Cenozoic East African Rift System. The influence of crustal thinning related to these NW-SE grabens on later W-E-related extension is testified by the marked change in style of deformation from the narrow rift valleys in Kenya and Ethiopia, to a distributed, basin-and-range-style faulting in the Turkana depression. Despite some local scale reactivation is visible, large scale reactivation of pre-existing NW-SE structures in the Turkana depression is not obvious, as it is extensively masked by the sedimentary and volcanic cover; consequently, contrasting hypothesis on the possible role exerted by discrete pre-existing fabrics have been proposed in the literature.

To address this controversy, we performed analogue models to investigate whether inherited structures, largely obscured by sediments in the Turkana depression, might have been reactivated during subsequent tectonic phases. We run 2-layer, brittle-ductile models deformed in two successive phases (Fig. 1): a first phase of NE-SW extension, followed by W-E extension. Different models were subjected to different amount of bulk extension during the first phase to investigate the influence of this parameter (and the importance of first-phase structures) on later reactivation. Our models indicate that the amount of deformation in the initial tectonic phase is key for structure reactivation in subsequent tectonic phases: the larger the deformation in the first phase, the higher the probability of reactivation. Comparison of the experimental results with nature (Fig. 2) suggest that, despite some local fault reactivation, large-scale structures were likely not reactivated in the Turkana depression. These outcomes represent a useful tool to decipher fault reactivation, not only in the Turkana depression but also in tectonic basins worldwide, especially where thick sedimentary covers may mask tectonic structures.

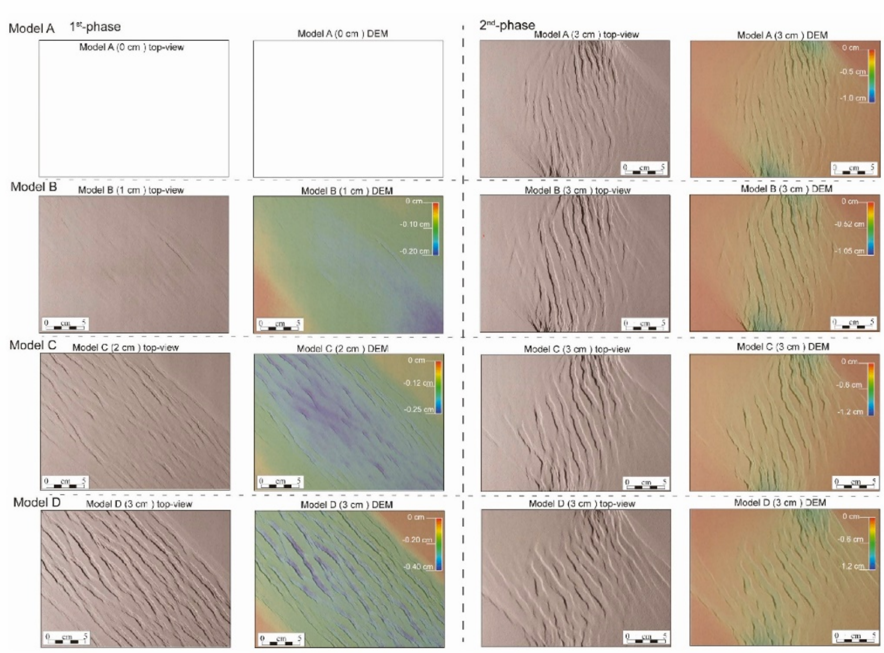

Figure 1: Overview of model results (top-view and DEM) of all the models at the end of the first-phase and 2nd-phase of deformation (modified from Wang et al., 2021).

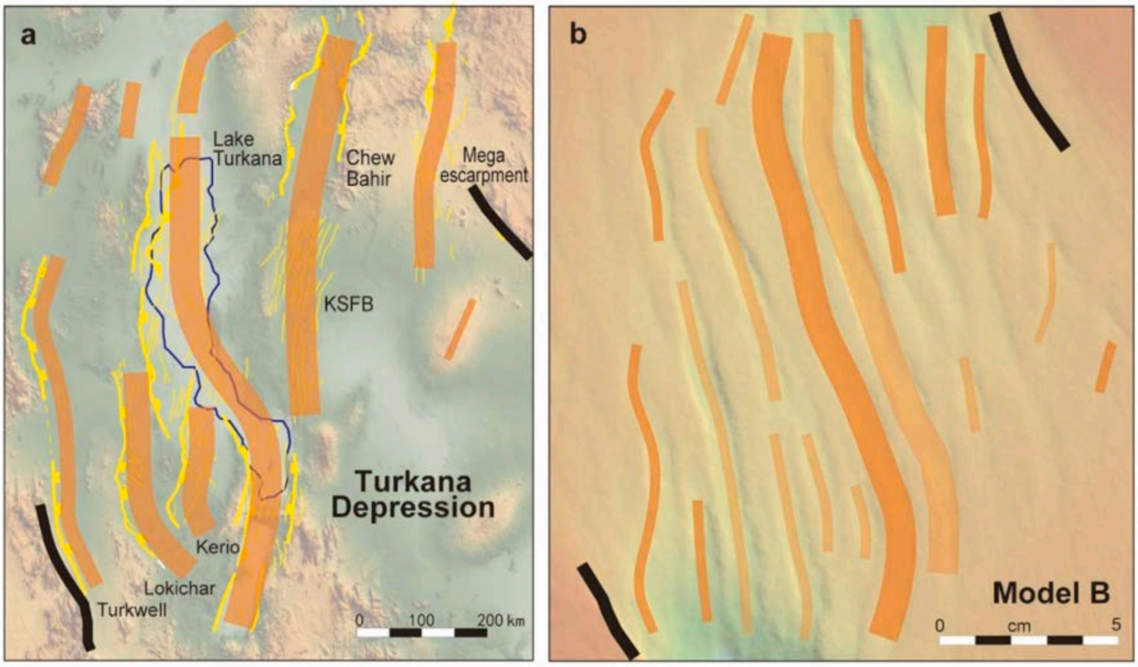

Figure 2: Comparison of the fault pattern observed in the Turkana depression (a) with the deformation pattern obtained in Models B (b). Orange lines represent the main deformation domains (modified from Wang et al., 2021).

References

Wang, L., Maestrelli, D., Corti, G., Zou, Y., & Shen, C. (2021). Normal fault reactivation during multiphase extension: Analogue models and application to the Turkana depression, East Africa. *Tectonophysics*, *811*, 228870. https://doi.org/10.1016/j.tecto.2021.228870

A new analogue modelling approach integrating the effects of tectonic extension and gravity gliding on salt tectonics in rift basins

Michael Warsitzka (1*), Prokop Závada (1), Fabian Jähne-Klingberg (2), Piotr Krzywiec (3)
(1) Institute of Geophysics of the Czech Academy of Sciences, Prague Czech Republic,
(2) Federal Institute for Geosciences and Natural Resources, Hannover, Germany,
(3) Institute of Geological Sciences, Polish Academy of Sciences, Poland
* warsitzka@ig.cas.cz

Abstract
The effects of salt tectonics on the structural evolution of sedimentary basins have been addressed in numerous analogue modelling studies. Two of the most frequently modelled deformation processes are (1) gravity gliding due to tilting of the basin floor at passive margins and (2) decoupled supra- and sub-salt extension induced by crustal stretching in rift basin. Structures and dynamics of both processes have often been investigated and simulated separately, despite the fact that both processes can act together in rift basins. The sub-salt basement in many rift basin is characterized by a significant vertical gradient, due to e.g. block rotation or widespread thermal subsidence. This might induce downward salt flow and gravity-driven deformation of the supra-salt strata in a similar manner as in passive margin basins. The essential dynamic difference between rift basins and passive margins, however, is that the sedimentary loading in rift basins is usually largest in the downslope basin centre, which promotes upward directed salt flow opposing gravity gliding. Thus, the question is, which process dominates under specific conditions or in certain phases in the evolution of a salt-bearing rift basin?
In our analogue modelling study, we investigate the overlapping effects of crustal-scale extension and gravity gliding and the opposite drivers for salt flow resulting from tilting of the basin floor and from sedimentary loading in the basin centre. We constructed a new experimental apparatus consisting of a central graben structure to mimic tectonic extension (Fig. 1a). Two bendable basal plates are attached on both sides of the graben structure, which simulate gradual tilting of the graben flanks (Fig. 1a). Using 3D digital image correlation technique, displacement and strain patterns of the experimental surface could be analysed. Here, we present results of preliminary experiment showing that downward movement of the overburden affects the entire flanks of the basin, if these are tilted simultaneously to graben extension (Fig. 1b). Consequently, extensional structures adjacent to the graben centre are overprinted and shortened (Fig. 1c), whereas thin-skinned extensional faults develop at the basin margins. This deformation patterns are similar to those occurring in salt-bearing passive margins. In an experiment in which syn-kinematic sedimentation simultaneous to extension and tilting is simulated in the basin centre, the amount of gravity gliding is significantly reduced. This indicates that gravity-driven deformation can be effectively prevented in rift basins in which sedimentation rate keeps pace with tilting rate. Our experimental apparatus allows to simulate a wide range of parameters and scenarios. In an advanced experimental series, we intend to determine specific thresholds of basin slopes, topographic gradients and overburden thickness at which gravity gliding is initiated or prevented in salt-bearing rift basins.

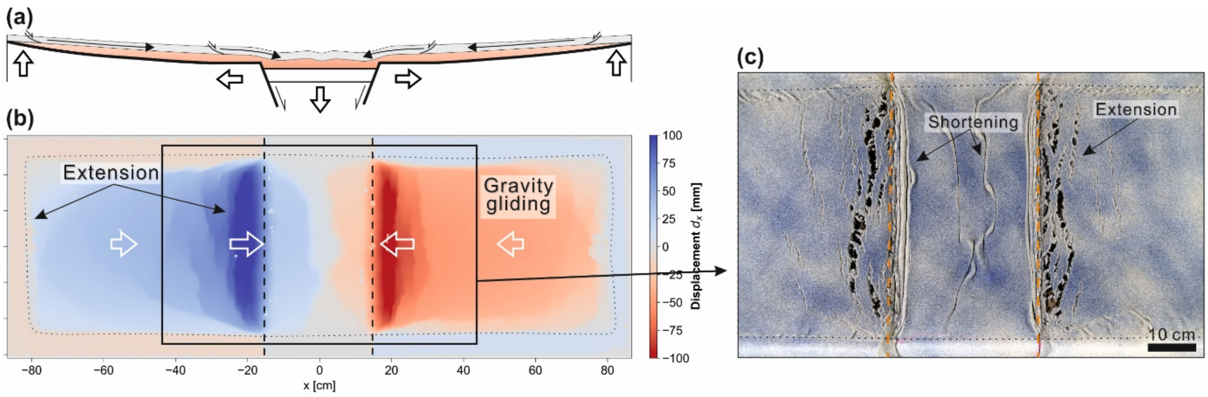

Figure 1: Analogue experiment showing the effect of gravity gliding on a salt-cover system in rift basins.

How the interaction between mantle and crustal weaknesses affects rift development: insights from a 3D experimental study

Frank Zwaan (1*), Pauline Chenin (2), Gianreto Manatschal (2), Duncan Erratt (2), Guido Schreurs (1)

(1) Universität Bern, Switzerland, (2) Université de Strasbourg, France
* Contact: frank.zwaan@geo.unibe.ch

Abstract
During extension of the continental lithosphere, deformation often localizes along weaknesses originating from previous tectonic phases. Weaknesses located in the strong upper crust or upper mantle are expected to particularly affect rift evolution. When simulating the influence of such weaknesses through analogue or numerical methods, modellers often focus on either crustal or mantle heterogeneities. By contrast, here we present results from 3D analogue models to test the combined effect and relative impact of (differently oriented) mantle and crustal weaknesses on rift systems.

Our model set-up involves a rigid base plate fixed to a mobile sidewall (Fig. 1). When this sidewall moves outward, the edge of the base plate creates a “velocity discontinuity” (VD) that acts as a fault/shear zone in the strong upper mantle. The VD is either parallel to the model axis, or 30˚ oblique. On top of this base plate, a viscous layer represents the ductile lower crust, overlain by a sand cover simulating the brittle upper crust. Crustal weaknesses were created by adding “seeds” (i.e. ridges of viscous material at the base of the sand layer), or by pre-cutting the sand. Similar to the VD, we apply different crustal weakness orientations as well.

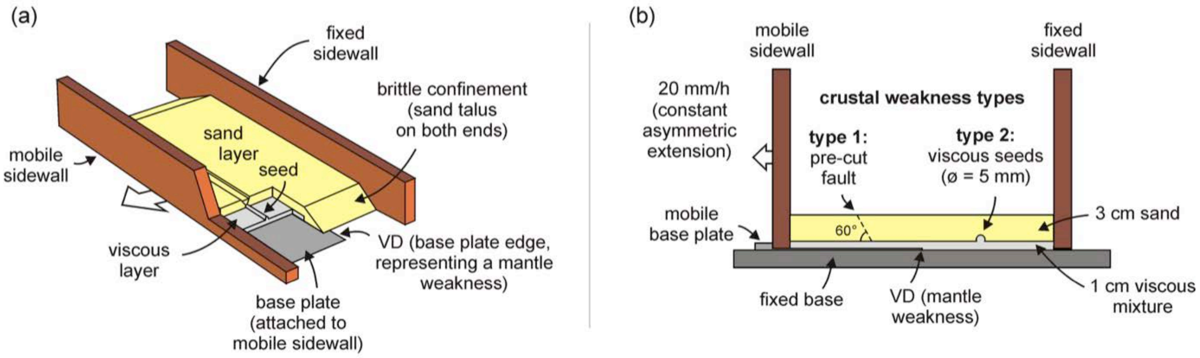

Figure 1: Model set-up. (a) 3D sketch of general set-up. VD: velocity discontinuity representing a weakness (e.g., a shear zone) in the strong upper mantle. (b) Section view depicting standard model layering and the two types of crustal weaknesses (pre-cuts and viscous seeds). Adopted from Zwaan et al. (2021)

Without weaknesses in the model crust, a model axis-parallel VD forms a rift basin above the VD (with wider spacing if the viscous layer is thicker, Fig. 2a, b), and an oblique VD creates a series of en echelon grabens (Fig. 2c). Adding different inherited crustal weaknesses strongly affects rift structures. Reactivated pre-cut faults partially overprint and segment the VD-induced rift zone (Fig. 2d, e). This overprinting and segmentation is even more pronounced in models with viscous seeds. The orientation of the weaknesses with respect to both the regional extension direction and each other has an important effect on their subsequent (re-) activation (Fig. 2d–k). Both the VD and modelled crustal weaknesses are most active when oriented orthogonally to the regional extension direction, the ideal setting for normal fault development (Fig. 2d-j). When either the VD or the crustal weaknesses are oriented obliquely to the regional extension direction, their impact is decreased. Yet when the VD and the crustal weaknesses are parallel to each other, both effectively localize deformation, even when oriented obliquely to the extension direction (Fig. 2j). Furthermore, increasing the extension velocity causes enhanced coupling between the VD and the overlying materials, overprinting the otherwise dominant control of the seeds in these models (compare Fig. 2i and Fig. 2k).

We thus find that the orientation and relative weakness of inheritances in the mantle and crust, as well as extension rates control subsequent rift structures. These structures can be complex due to the interplay of the above factors, and importantly, all develop under the same pure shear extensional boundary condition. Our results thus show that very differently oriented rift structures can form during one phase of extension without the need to invoke multiple rift phases with changing extension directions. These insights provide a strong incentive to reassess the tectonic history of various natural examples.

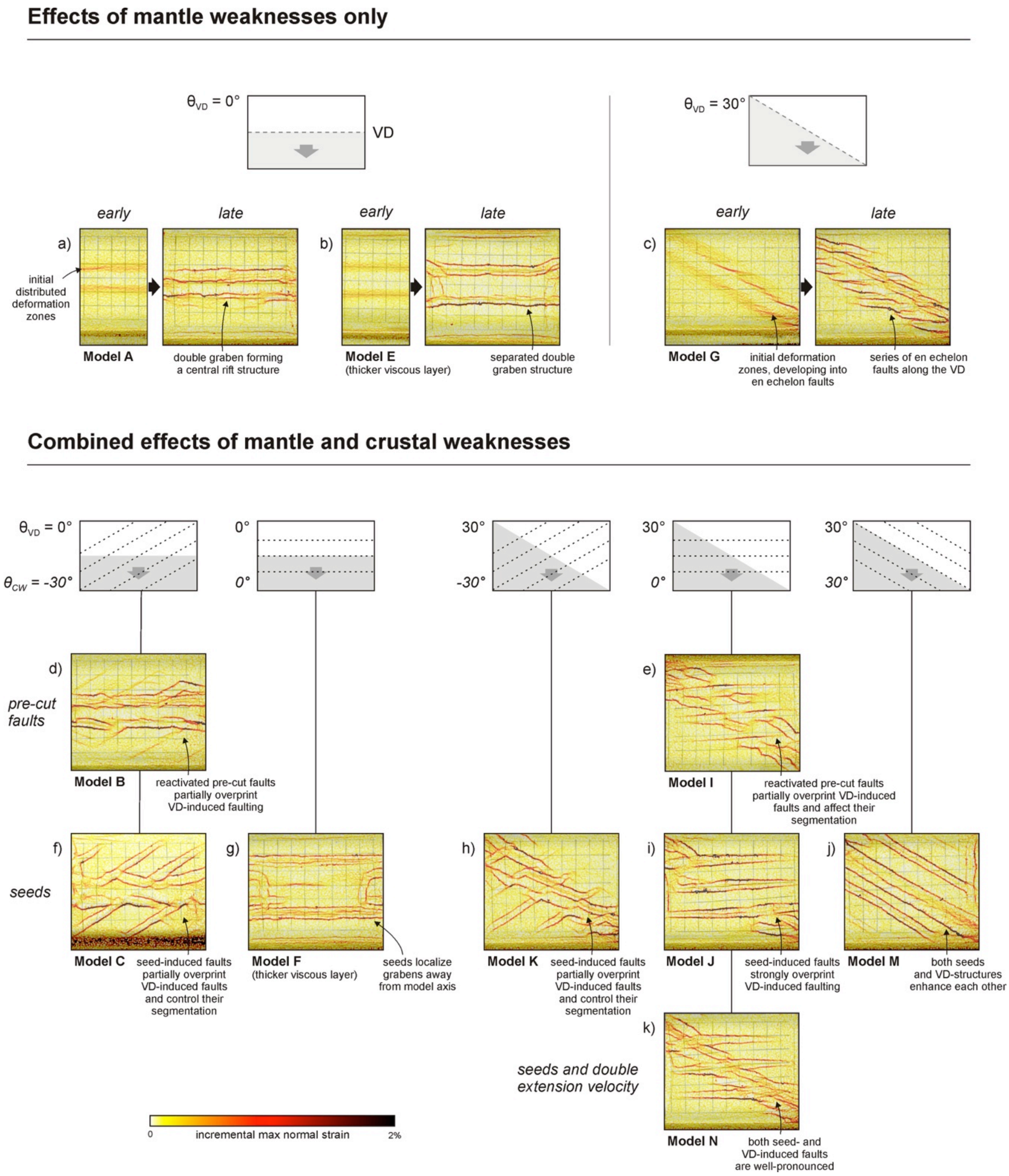

Figure 2: Summary of model results (PIV-derived incremental maximum normal strain) as a function of mantle discontinuity geometry, as well as type and geometry of crustal weakness, and extension velocity. Angle θ_{VD} indicates the orientation of the VD (velocity discontinuity, representing a mantle weakness), whereas angle θ_{CW} indicates the angle of the simulated crustal weakness. Adopted from Zwaan et al. (2021)

References

Zwaan, F., Chenin, P., Erratt, D., Manatschal, G., Zwaan, F., Chenin, P., Erratt, D., Manatschal, G., and Schreurs, G. (2021). Complex rift patterns, a result of interacting crustal and mantle weaknesses, or multiphase rifting? Insights from analogue models, Solid Earth Discuss. Preprint link: https://doi.org/10.5194/se-2020-214

Session 4

Geohazards and seismotectonics

- Jean-Phillipe Avouac. *From kinematics to dynamic modeling of slow slip events* ***(keynote)***
- Adrien Damon. *Investigating the impact of environmental forcings on fault reactivation in the Paris Basin*
- Hanna Elston. *Non-steady-state slip rates emerge along evolving restraining bends under constant loading*
- Frederic Gueydan. *Transient ductile strain localization triggered by fluid-enhanced microfracturing and sealing: a possible analogue to Episodic Tremor and Slip* ***(keynote)***
- Ehsan Kosari. *Surface deformation signals governed by mechanical-frictional interaction of the wedge and megathrust over subduction zone seismic cycles*
- Meng Li. *Deciphering earthquake nucleation in Groningen: how much slip is aseismic?*
- Valentin Marguin. *Numerical Investigation of the impact of fluid on the earthquake cycle*
- Casper Pranger. Rate-and-State frictional plasticity as a reaction-diffusion equation in a continuum model
- Matthias Rosenau. *Analogue earthquakes, seismic cycles and seismotectonic evolution: Bridging the geodetic to geologic observation gap with experimental modelling* ***(keynote)***

From kinematics to dynamic modeling of slow slip events

Jean-Philippe Avouac (1*) *(keynote)*
(1) California Institute of Technology, Pasadena, USA
*avouac@gps.caltech.edu

Abstract

Continuous geodetic recordings from GNSS stations have made it possible to document aseismic transient slip events, commonly called 'slow slip events' (SSEs), in various tectonic contexts, in particular on the sub-seismogenic portion of the subduction interface in Cascadia. The imaging of these signals using an ICA-based inversion method [Michel et al., 2019], shows that the SSEs in Cascadia are very similar to regular earthquakes, albeit in very slow motion. Like regular earthquakes they initiate as crack-like ruptures and evolve toward pulse-like ruptures. They also obey the same scaling laws as regular earthquakes. They release a moment (the integral over the slipping area of slip multiplied by the shear modulus), proportional to the cube of their duration[Michel et al., 2019 (2)]. Note worthily the M-T^3 scaling holds for pulse-like ruptures although they are no self-similar, a finding that questions the view that the M- T^3 scaling of regular earthquakes imply self-similarity. Finally, SSEs In Cascadia are found to be predictable although the prediction horizon is limited to ~15 days due to the chaotic system behavior [Gualandi et al., 2020]. The similarities between SSEs and regular earthquakes suggest that the mechanics that govern individual ruptures and their interactions might also be similar. Both types of ruptures are probably due to episodic frictional sliding, albeit SSEs require some mechanism limiting the sliding rate. It could be a transition to a rate-strengthening behavior at high slip rate [Leeman et al., 2016 & Im et al., 2020], or, if fluids are present, the effect of dilatant hardening [Segall et al., 2010]. In any case, a very low effective normal stress is required suggesting that SSE occur in fault zones with a near-lithostatic pore pressure. With such a mechanism included, dynamical simulations can yield realistic SSEs reproducing the observed scaling laws [Dal Zilio et al., 2020]. The observation and dynamic simulations of SSEs open new avenues to explore how individual seismic ruptures initiate, grow and arrest and the system dynamics that result from their interactions.

References

Michel, S., A. Gualandi, and J.P. Avouac, Interseismic Coupling and Slow Slip Events on the Cascadia Megathrust. *Pure and Applied Geophysics*, 176(9): p. 3867-3891, 2019.

Michel, S., A. Gualandi, and J.P. Avouac, Similar scaling laws for earthquakes and Cascadia slow-slip events. *Nature*, 574(7779): p. 522-+, 2019.

Gualandi, A., J.P. Avouac, S. Michel, and D. Faranda, The predictable chaos of slow earthquakes. *Science Advances*, 6(27), 2020.

Leeman, J.R., D.M. Saffer, M.M. Scuderi, and C. Marone, Laboratory observations of slow earthquakes and the spectrum of tectonic fault slip modes. *Nature Communications*, 7, 2016.

Im, K., D. Saffer, C. Marone, and J.P. Avouac, Slip-rate-dependent friction as a universal mechanism for slow slip events. *Nature Geoscience*, 13(10): p. 705-+, 2020.

Segall, P., A.M. Rubin, A.M. Bradley, and J.R. Rice, Dilatant strengthening as a mechanism for slow slip events. *Journal of Geophysical Research-Solid Earth*, 115, 2010.

Dal Zilio, L., N. Lapusta, and J.P. Avouac, Unraveling Scaling Properties of Slow-Slip Events. *Geophysical Research Letters*, 47(10), 2020.

Investigating the impact of environmental forcings on fault reactivation in the Paris Basin

Adrien Damon (1, 2*), Stéphane Mazzotti (1), Philippe Vernant (1), Frédéric Ego (2), David Baumont (3)
(1) Géosciences Montpellier, Université de Montpellier, CNRS ; Montpellier, France
(2) ANDRA, Châtenay-Malabry, France
(3) Seister, Montrouge, France
*Contact: adrien.damon@umontpellier.fr

Abstract
We investigate the impact of stress perturbations linked to environmental forcings on inherited faults in the Paris Basin. The intracontinental Paris Basin (PB) is nowadays a low seismicity region (few earthquakes with M<4), yet GNSS derived-strain rates show that there is active deformation in and around the PB (Masson et al., 2019). Active deformation potentially linked to environmental forcings observed in stable continental regions (e.g. Finland, Eastern Canada, Eastern Tennessee Seismic Zone) may lead to large earthquakes of M>6. Glacial and erosional isostasy are here investigated as environmental forcings that could be a factor of fault reactivation in the Paris Basin.

To do so, we use a numerical finite difference tool that solves plate flexure equations (gFlex; Wickert, 2015) to estimate the visco-elastic deformation of the PB lithosphere under environmental loading/unloading. Faults of interest are defined by a relationship linking fault length, potential maximum magnitude and seismic acceleration (Peak Ground Acceleration, PGA). We calculate multiple environmental deformation scenarios based on various rheological parametric study, icecap models and erosion/deposition rates. The resulting stress perturbation fields are projected onto the studied faults to estimate potential fault slip using a Mode-II slip law (Sun and Jin, 2012). Later, these fault slip estimates may allow assessing the impact on faults behavior (e.g. estimations for earthquake magnitude and PGA, seismicity recurrence rates).

Preliminary results show that, under Last Glacial Maximum (LGM) ice cap load (*see fig. 1*), stress perturbations can be as high as standard seismic stress drop (>0.1 to 1.0 MPa), indicating that the study of potential fault reactivation should be further pursued (*see fig. 2*). Furthermore, depending on the location of the faults and the lithospheric Equivalent Elastic Thickness (EET, defining the flexural rigidity), the deformation style can vary from shortening to extension (*see fig. 2*). This preliminary study with EET defined by a single value shows the very strong impact of moderate EET variations (15-32 km) on stress perturbations. Models with spatial EET variations between loading sites and the PB will also be tested. In complement to the LGM models, thicker and extended ice caps will also be tested to take into account variability on the ice models.

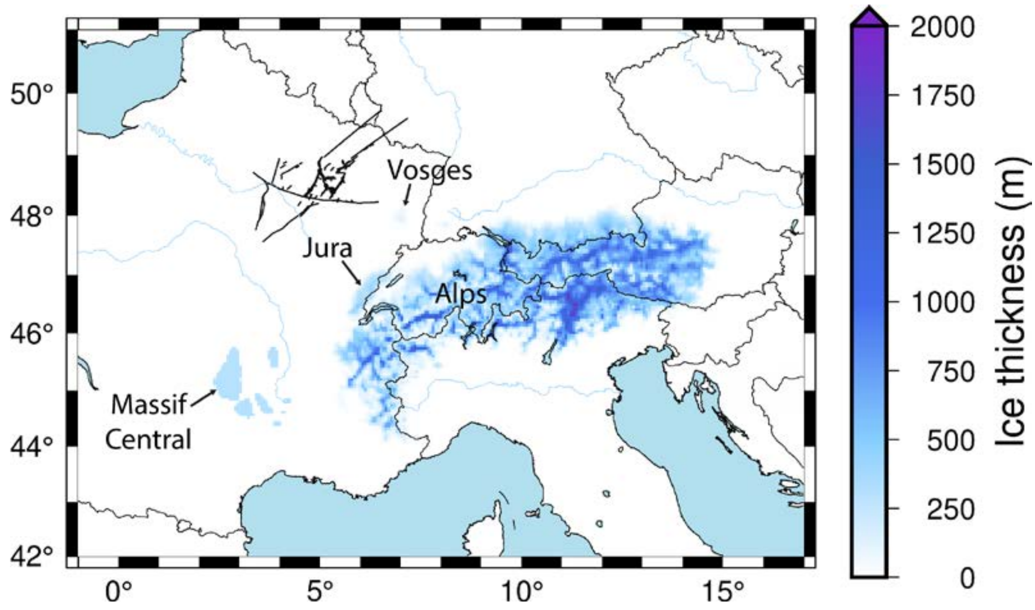

Figure 1: Modeled LGM ice thickness implemented as loads in the flexure calculation. The figure also presents selected faults in the Eastern PB.

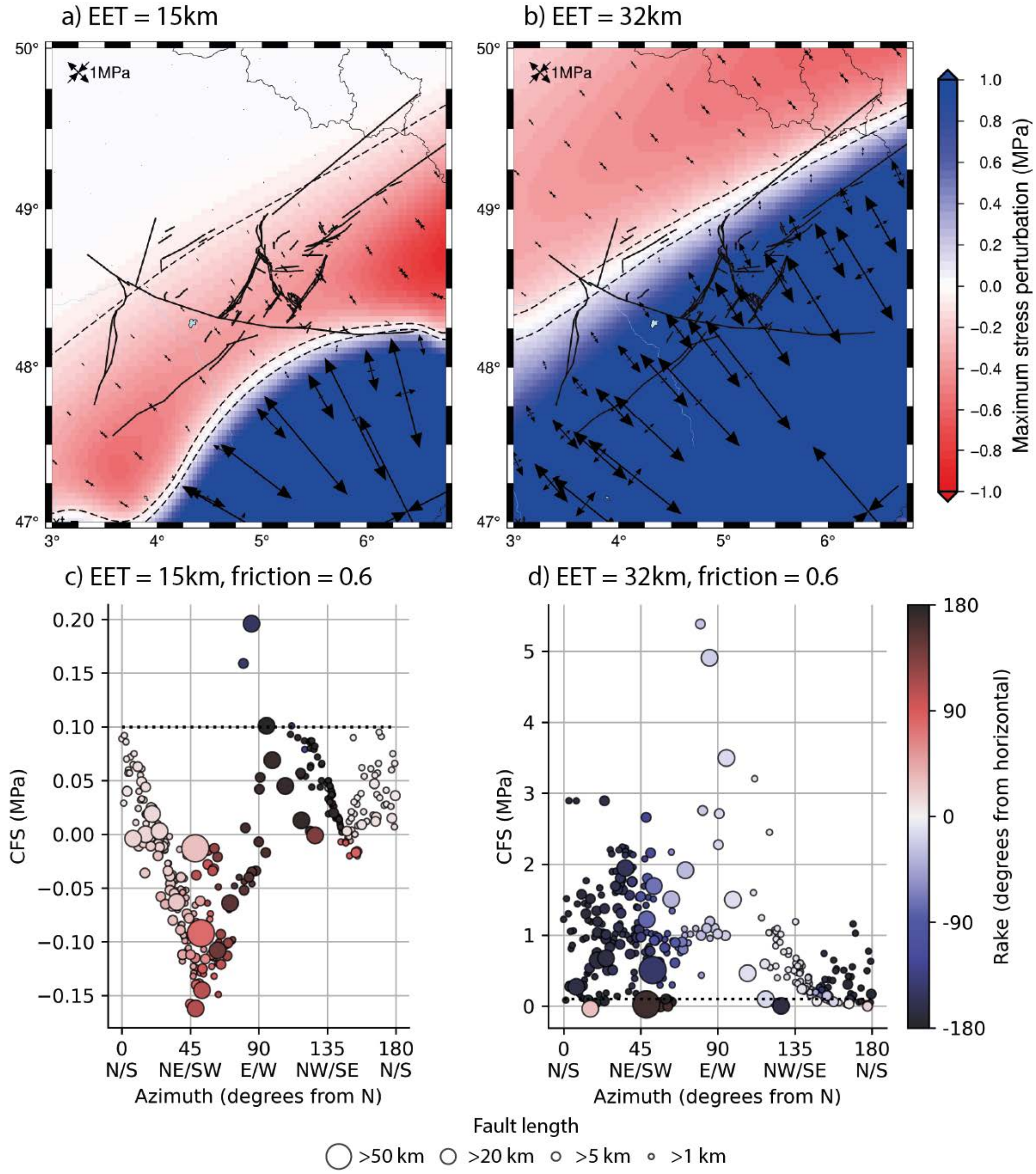

Figure 2: a), b) Modeled stress perturbations for Massif Central and Alpine LGM ice loads, for low and high PB EET values. Positive and negative stress perturbations correspond to extension and compression, respectively. Dashed lines show the ± 0.1 MPa contours. c), d) Coulomb Failure Stress (CFS) perturbations on selected faults for low and high EET, respectively. The rake corresponds to the fault slip angle (+/-90: reverse/normal fault, 0/180: left–/right–lateral fault). The dashed line corresponds to the 0.1 MPa reactivation threshold.

References

Masson, C., Mazzotti, S., Vernant, P., Doerflinger, E., 2019. Extracting small deformation beyond individual station precision from dense Global Navigation Satellite System (GNSS) networks in France and western Europe. Solid Earth 10, 1905–1920. https://doi.org/10.5194/se-10-1905-2019

Sun, C., Jin, Z.-H., 2012. Fracture Mechanics. https://doi.org/10.1016/C2009-0-63512-1

Wickert, A., 2015. Open-source modular solutions for flexural isostasy: gFlex v1.0. Geoscientific Model Development Discussions 8, 4245–4292. https://doi.org/10.5194/gmdd-8-4245-2015

Non-steady-state slip rates emerge along evolving restraining bends under constant loading

Hanna Elston (1*) and Michele Cooke (1)
(1) University of Massachusetts Amherst
* Contact: helston@geo.umass.edu

Abstract

Seismic hazard assessments assume that fault slip rates estimated from offset features 10 to 100 kyr in age will remain constant in the future However, recent studies show evidence of temporal slip rate variability over a wide range of timescales (e.g., Mouslopoulou et al., 2009; Zinke et al., 2019). Processes either internal or external to the fault system contribute to slip rate variability. External processes such as mass redistribution via glacial loading/unloading leave independent records that can be correlated with slip rate records. Internal fault system processes such as fault interaction and reorganization are difficult to track in the crust because the geologic record does not record clear evidence of these processes. While field observations alone do not provide enough evidence to distinguish how individual processes influence slip rates over time, scaled physical experiments allow us to directly observe emergent fault behavior to investigate the impacts of individual processes, such as fault interaction. Because strike-slip faults are not as susceptible as dip-slip faults to external impacts of mass redistribution and volcanism, intrinsic fault interactions likely dominate slip rate history. Furthermore, we expect that slip rates will vary around geometric complexities such as restraining bends. Here, we investigate the influence of fault reorganization (fault growth and abandonment) on fault slip rates by conducting scaled physical experiments of restraining bends along strike-slip faults using wet kaolin clay as an analog for crustal material.

We use a table-top split box apparatus filled with wet kaolin to model the evolution of a vertical precut fault that has a 15° restraining angle and a 2 cm stepover that follows the basal plate discontinuity. We scale the clay to the crust such that 1 cm of clay is equivalent to 1 – 2 km within the crust and 1 minute within the experiment is equivalent to 1.3 – 13 kyr in the crust (Cooke & Van Der Elst, 2012). Stepper motors displace one half of the box at a constant velocity that induces faulting within the overlying claypack while cameras overhead capture regularly timed images. Sand grains sieved onto the claypack surface act as tracers for digital image correlation (DIC). DIC produces incremental horizontal displacement fields that we use to calculate incremental horizontal strain maps (Figure 1) and fault slip rates throughout the experiments.

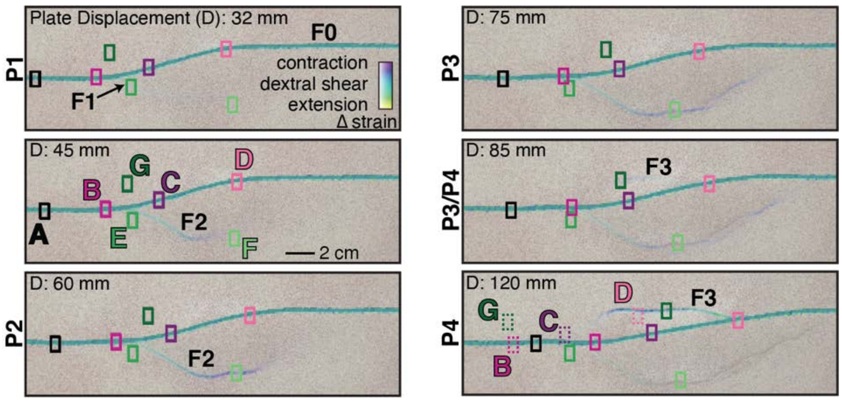

Figure 1: Incremental horizontal strain maps and the location of each site (solid rectangles) throughout the experiment. Hue indicates the sense of strain rate and saturation indicates magnitude. Dashed rectangles show the location of sites B – D and G at 0 mm plate displacement, revealing site advection. P1-P4 indicate the period in which each snapshot is taken. The timing of four periods (P1-P4) corresponding to slip rate variations is shown in Figure 2.

To assess the general distribution of strike-slip rates along the entire fault system and throughout the duration of the experiment, we plot the strike-slip rate normalized by the applied velocity for every transect along a fault. Probability density function of the strike-slip rates at all points along the faults at 30, 45, 65, 85, and 105 mm of plate displacement reveal distinct peaks indicating common values of fault slip rate for each stage of the experiment. The probability peaks guide our determination of seven distinct slip rate histories that map well onto eight fault segments. To assess the degree of slip rate variability at particular locations along the faults, we selected one site from each distinct slip rate history segment and tracked fault slip rates at each site as it advected throughout the experiment with accrued fault slip (Figure 1). This quasi-Lagrangian approach allows us to extract slip rate history such as would be revealed in a field study.

Not all sites reveal the same cumulative slip or time history of slip rate variability. The slip rate histories from the seven sites reveal strike slip rate variations (5 – 25% of the applied velocity) corresponding to fault reorganization (e.g., fault growth and abandonment) and sites migrating to new structural positions (Figure 2). Sites that advected into the restraining bend showed decreased slip rate and sites that advected out of the restraining bend showed increased slip rate. While we expect new fault growth to reduce slip rates along nearby fault segments, here we document that the growth of new oblique slip faults can increase strike-slip rates on nearby fault segments. As new oblique-slip thrust faults grew and accommodated off-fault convergence, strike-slip faults within the hanging wall of the thrust faults experienced unclamping and recorded increased slip rate. The experimental results show that even under constant loading, slip rates at sites located on stable fault segments can vary due to either reorganization elsewhere in the fault system or site advection (Figure 2). Furthermore, sites along the same fault segment can record different degrees of slip rate variability depending on their structural position.

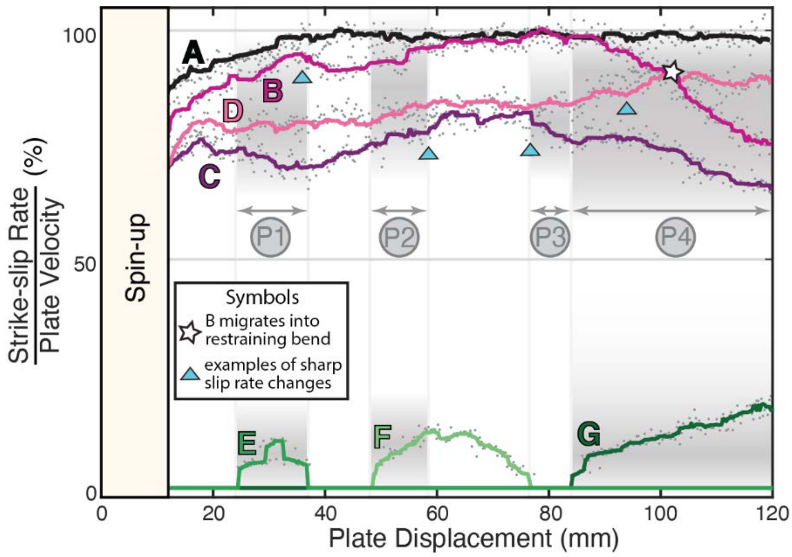

Figure 2: Strike-slip rates for sites A – G. Gray dots report raw strike-slip rates while colored lines show 11-point medians. Gray boxes bound four periods (P1-P4) when slip rates vary in response to fault reorganization.

References

Cooke, M. L., & Van Der Elst, N. J. (2012). Rheologic testing of wet kaolin reveals frictional and bi-viscous behavior typical of crustal materials. *Geophysical Research Letters*, *39*(1), 1–5. https://doi.org/10.1029/2011GL050186

Mouslopoulou, V., Walsh, J. J., & Nicol, A. (2009). Fault displacement rates on a range of timescales. *Earth and Planetary Science Letters*, *278*(3–4), 186–197. https://doi.org/10.1016/j.epsl.2008.11.031

Zinke, R., Dolan, J. F., Rhodes, E. J., Van Dissen, R., McGuire, C. P., Hatem, A. E., Brown, N. D., & Langridge, R. M. (2019). Multimillennial Incremental Slip Rate Variability of the Clarence Fault at the Tophouse Road Site, Marlborough Fault System, New Zealand. *Geophysical Research Letters*, *46*(2), 717–725. https://doi.org/10.1029/2018GL080688

Transient ductile strain localization triggered by fluid-enhanced microfracturing and sealing: a possible analogue to Episodic Tremor and Slip

Frédéric Gueydan (1*), Emilien Oliot (1), Thomas Leydier (1) and Maxime Bernaudin (1) *(keynote)*
(1) Géosciences Montpellier, Université de Montpellier, CNRS, Montpellier, France
* Contact: frederic.gueydan@umontpellier.fr

Abstract

A combination of seismic (non-volcanic tremors) and transient aseismic (slow slip events) behaviours is now commonly observed at plate interfaces in subduction zones, between locked/seismogenic zone at low depths and stable/ductile creep zone at higher depths. This association defines Episodic Tremor and Slip, systematically highlighted by over-pressurised fluids and near failure shear stress conditions. We present here a microstructural study of exhumed rocks deformed at 400°C and 35-40 km that highlights deformation mechanisms active at these PT conditions. While the rocks undergo ductile deformation, micro-fracturing of the strong phase (here K-Feldspar) is present and activated by high fluid pressure and allow fluid circulation and precipitation of new phases in the fractures (sealing, Fig. 1).

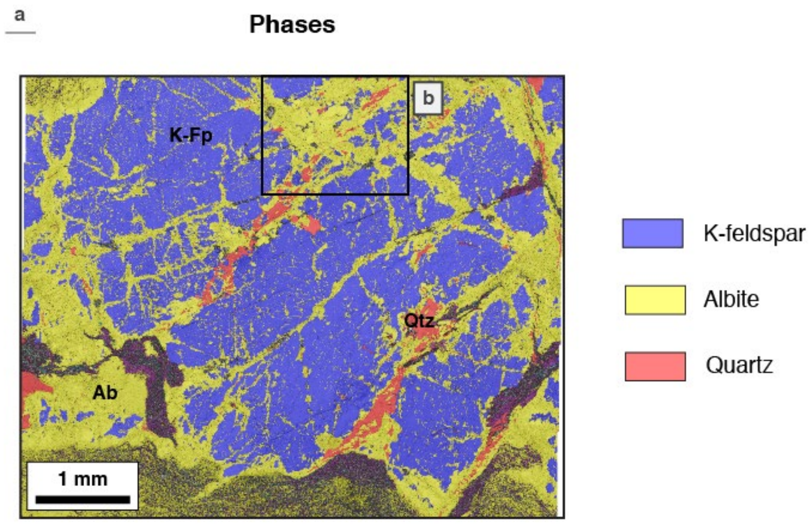

Figure 1: EBSD phase map of a microfractured K-feldspar. Colors correspond to phases

When micro-fracturing dominates over sealing, shear bands form. In contrast, when sealing dominates, a “recovery” of the large initial feldspar grain is observed. These observations allow us to propose a new ductile rheological approach that relates microstructures evolution with pore fluid pressure fluctuations. In contrast with more classical rate-and-state models, this approach is based on a ductile rheology with grain size sensitivity, fluid-driven microfracturing and sealing (e.g. grain size reduction and grain growth) and related pore fluid pressure fluctuations (Fig. 2). Our model provides a possible geological explanation of episodic tremor and slips and moreover predicts the depth and temperature ranges of their occurrence, as quantified by numerical modelling in Bernaudin and Gueydan (2018).

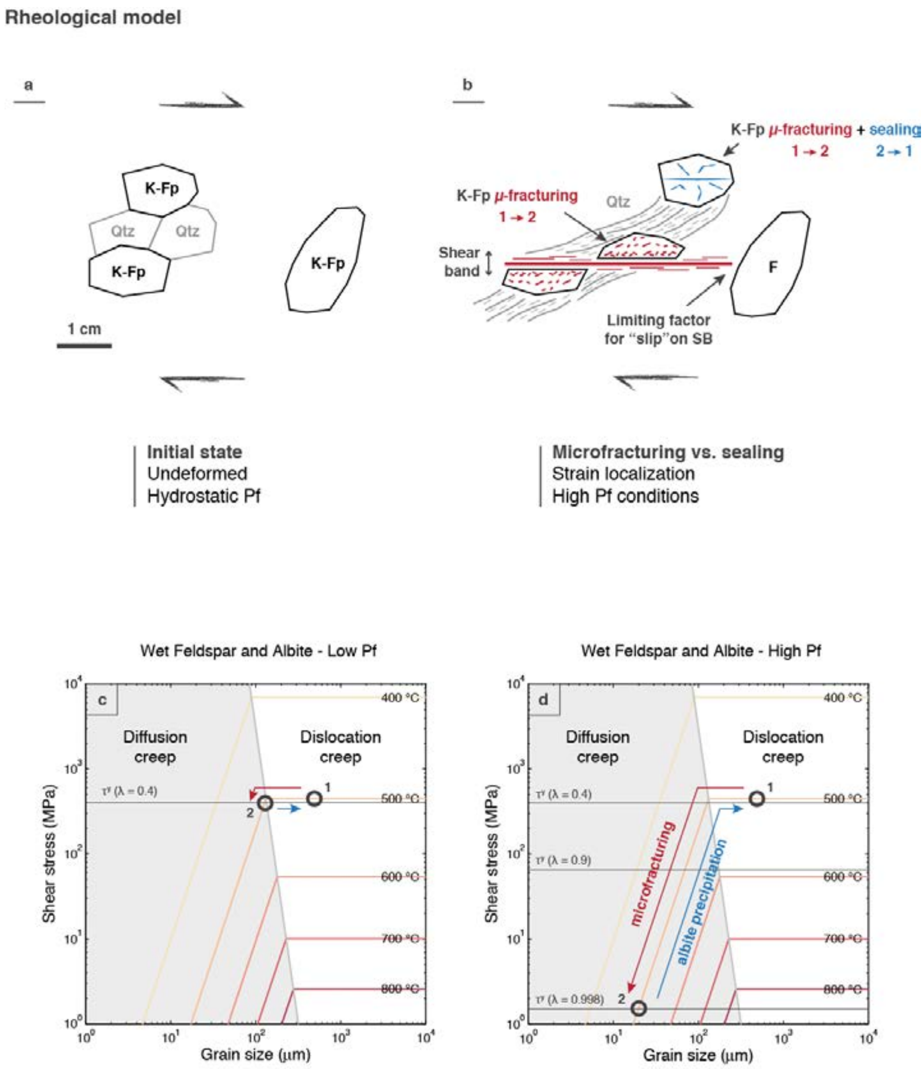

Figure 2: Rheological model proposed from our microstructural observations. **(a-b)** Schematic description of the grain size-sensitive rheological model. **(a)** Initial state: bi-phase. **(b)** Second step: microfracturing (i.e. grain size reduction) of K-feldspar with related weakening, strain localisation and fluid pumping. Third step: sealing (i.e. grain growth) of K-feldspar and subsequent strengthening of the whole rock. **(c)** Deformation mechanism map for feldspar at low fluid pressure (e.g. microfracturing is limited). Grey and white areas define domains where diffusion and dislocation creep, respectively, are dominant. Red arrow represents the effect of dynamic recrystallization on shear stress evolution. **(d)** Deformation mechanism map for wet feldspar at high fluid pressure (e.g. enhanced microfracturing). Red (microfracturing) and blue (sealing) arrows show dynamic evolution of grain size and subsequent shear stress evolution.

References

Bernaudin, M., & Gueydan, F. (2018). Episodic tremor and slip explained by fluid-enhanced microfracturing and sealing. *Geophysical Research Letters*, *45*, 3471–3480. https://doi.org/10.1029/2018GL077586

Surface deformation signals governed by mechanical-frictional interaction of the wedge and megathrust over subduction zone seismic cycles

Ehsan Kosari (1,2*), Matthias Rosenau (1), Onno Oncken (1,2)

(1) Helmholtz Centre Potsdam, GFZ German Research Centre for Geosciences, Potsdam, Germany.
(2) Department of Earth Sciences, Freie Universität Berlin, Berlin, Germany.

* Contact: ehsan.kosari@gfz-potsdam.de

Abstract

Estimating the interseismic coupling is the foremost approach to evaluate the earthquake potential of subduction megathrusts. While both up-dip and down-dip limits of megathrust ruptures are typically located offshore and near the shore, respectively, centuries-long recurrence intervals of the subduction megathrust earthquakes and insufficiently geodetically instrumented seafloors prevent us from achieving sufficient details of the shallow part of the megathrust. For instance, a weakly coupled interface had been predicted in NE Japan based on the incomplete interseismic geodetic measurements before the 2011 Tohoku-Oki megathrust event. However, the slip models derived from rare offshore geodetic data suggested a coseismic trench-breaching rupture. Besides short-term (geodetic) elastic surface deformation information, it has been suggested to explore long-term (geologic) permanent deformation signals for potential diagnostic patterns linked to megathrust behavior. Hence, for the sake of completeness of seismotectonic insights, long-term geological information should be referred to.

Elastoplastic deformation is the dominant process in the shallow portion of the subduction zones, and the mechanical properties of the wedge and megathrust govern the strain pattern in the upper plate. The strain signals could be accumulated over many seismic cycles and preserved as morphotectonic features (i.e., extensional, compressional, and shear markers), representing the mechanical state of the forearc. In an earthquake cycle, the mechanical state might be segmented in the upper plate. In other words, the rate-strengthening and rate-weakening portions of the megathrust cause time and space variable strain fields and rates over the forearc during a seismic cycle. For instance, the coastal region can be compressional in the interseismic and extensional during the coseismic stage. It is vital to understand how this leads to the topography as a persistent marker over many seismic cycles. Eventually, this may lead to incremental upper plate evolution towards its critical geometry and shape the forearc morphology. If this is the case, to what extent may we infer the seismic potential of the shallow (offshore) portion of the megathrust via onshore observations? How may a “strain switch”, i.e. from compressional/ extensional to extensional /compressional strain state, happen in the different segments of a homogeneous forearc? Is there any linkage between strain state at the positions of the coast, inner-, and outer-wedge? And finally, could permanent surface deformation be reliably used as a clue for suspecting the zones with megathrust earthquake potential?

For reaching the answers to these questions, we employ Seismotectonic Scale Modeling (Rosenau et al., 2009, 2010, 2017) to generate physically self-consistent analog megathrust earthquake ruptures and seismic cycles at the laboratory scale (Figure 1). This method has been used to study the interplay between short-term elastic (seismic) and long-term permanent deformation (Rosenau & Oncken, 2009). For mimicking the megathrust seismic cycle and its associated surface deformation, we use a zone of velocity weakening (stick-slip) and an elastoplastic wedge while the wedge is continually compressing via a basal conveyor belt (Rosenau et al., 2019; Kosari et al., 2020; Kosari et al., 2021). A stereoscopic image correlation technique has been used to monitor the surface deformation of the analog model. Generating hundreds of seismic cycles and monitoring the associated surface deformation allows us to unwrap the linkage between frictional properties at depth (velocity weakening versus velocity strengthening) and forearc strain segmentation. This shows how the strain pattern at the different portions of the upper plate (coast, inner-, and outer-wedge) may reflect the variation of the frictional properties at depth over the megathrust seismic cycles.

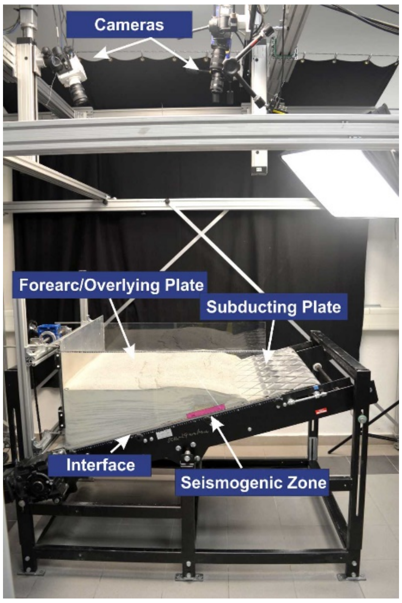

Figure 1: Seismotectonic scale model: Elastoplastic granular wedge set-up to simulate subduction megathrust seismotectonic evolution.

References

Kosari, E., Rosenau, M., Bedford, J., Rudolf, M., & Oncken, O. (2020). On the Relationship Between Offshore Geodetic Coverage and Slip Model Uncertainty: Analog Megathrust Earthquake Case Studies. Geophysical Research Letters, 47(15). https://doi.org/10.1029/2020GL088266

Kosari, E., Rosenau, M., Ziegenhagen, T., & Oncken, O. (2021). Postseismic backslip as a response to a sequential elastic rebound of upper plate and slab in subduction zones. Earth and Space Science Open Archive ESSOAr. https://doi.org/10.1002/essoar.10506467

Rosenau, M., & Oncken, O. (2009). Fore-arc deformation controls frequency-size distribution of megathrust earthquakes in subduction zones. Journal of Geophysical Research, 114, B10311. https://doi.org/10.1029/2009JB006359

Rosenau, M., Lohrmann, J., & Oncken, O. (2009). Shocks in a box: An analogue model of subduction earthquake cycles with application to seismotectonic forearc evolution. Journal of Geophysical Research, 114. https://doi.org/10.1029/2008JB005665

Rosenau, M., Nerlich, R., Brune, S., & Oncken, O. (2010). Experimental insights into the scaling and variability of local tsunamis triggered by giant subduction megathrust earthquakes. Journal of Geophysical Research, 115, B09314. https://doi.org/10.1029/2009JB007100

Rosenau, M., Corbi, F., & Dominguez, S. (2017). Analogue earthquakes and seismic cycles: Experimental modelling across timescales. Solid Earth, European Geosciences Union., 8(3), 597–635. https://doi.org/10.5194/se-8-597-2017

Rosenau, M., Horenko, I., Corbi, F., Rudolf, M., Kornhuber, R., & Oncken, O. (2019). Synchronization of great subduction megathrust earthquakes: Insights from scale model analysis. Journal of Geophysical Research: Solid Earth, 124, 3646– 3661. https://doi.org/10.1029/2018JB016597

Deciphering earthquake nucleation in Groningen: how much slip is aseismic?

Meng Li (1*), Andre Niemeijer (1), Femke Vossepoel (2) Ylona van Dinther (1)
(1) Department of Earth Sciences, Utrecht University
(2) Department of Geoscience and Engineering, Delft University of Technology
* Contact: m.li1@uu.nl

Abstract
Induced seismicity triggered by fluid injection or depletion has been studied extensively in recent years. However, simpler models focusing on the quasi-static interseismic loading and dynamic coseismic rupture may not well explain the nucleation process. Previous studies relying on Mohr-Coulomb yield criterion and/or linear slip-weakening friction law cannot quantify how much aseismic slip accumulates during nucleation, which is where rate-and-state friction law can contribute. Moreover, laboratory experiments indicate that most lithologies in the Groningen subsurface are velocity-strengthening under in-situ temperature, pressure and fluid chemistry conditions [Hunfeld et al., 2017]. This is traditionally regarded as an unfavorable property for earthquake nucleation. Therefore, it is still not understood how earthquakes in Groningen can actually nucleate under the measured frictional conditions. It is also unclear how this velocity-strengthening property affects the amount of aseismic slip accumulated. In this study, we model the normal fault setup in the Groningen field under reservoir depletion with rate-and-state friction using our newly developed code library Garnet. It is first validated by the Sequences of Earthquakes and Aseismic Slip (SEAS) benchmark BP3 (2D dipping fault setup) [Erickson et al., 2020]. We demonstrate its ability in modeling earthquake cycles under different faulting conditions (normal or thrust) and dipping angles (Figure 1). We are implementing fault loading due to fluid pressure reduction and will validate our loading stresses with analytical predictions in Janssen et al. (2019). We will provide constraints on how much aseismic slip accumulates during nucleation and how important aseismic slip is for induced seismicity in Groningen. This will be done through systematically investigating the impact of exploring the rate-and-state friction properties (a, b, c) of surrounding lithologies and their mixture using laboratory constraints. Their impact will be compared with what is due to varied fault off-set distance, fault dipping angle and off-fault rheology. Slip or strain nucleation and distribution patterns produced by our models may provide hints that can guide seismologists to identify aseismic slip from natural observations, which can in turn, support this study and constrain fault properties. The results from this study will help to better understand nucleation of induced seismicity in other locations in the Netherlands with similar lithologies and generally to understand the relevance of previous induced seismicity evaluations that ignore aseismic slip.

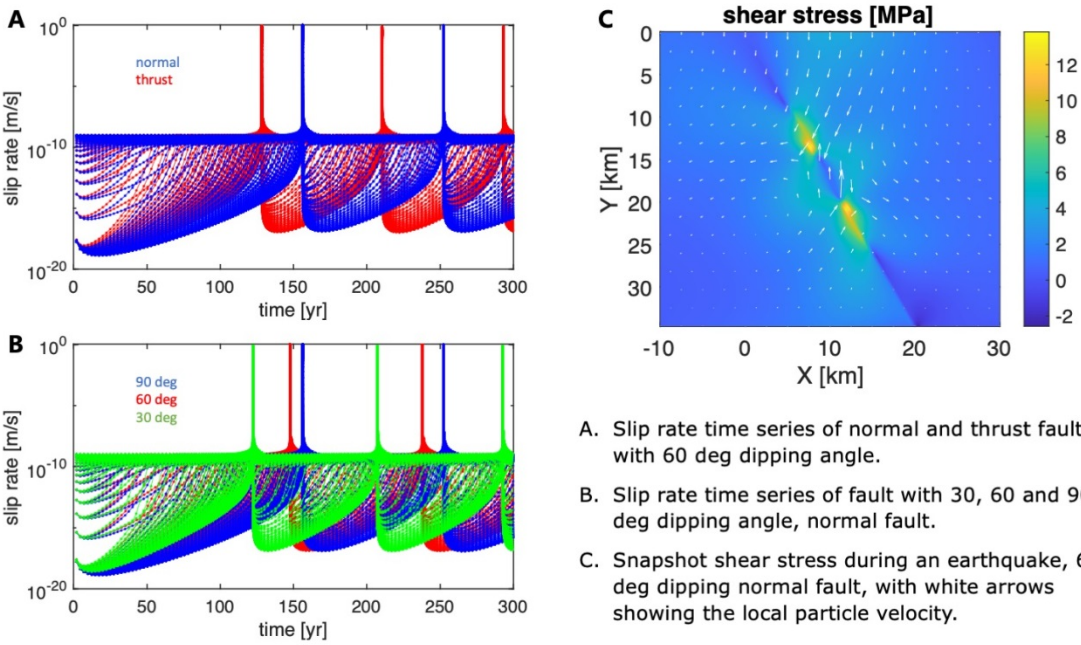

A. Slip rate time series of normal and thrust fault with 60 deg dipping angle.

B. Slip rate time series of fault with 30, 60 and 90 deg dipping angle, normal fault.

C. Snapshot shear stress during an earthquake, 60 deg dipping normal fault, with white arrows showing the local particle velocity.

Figure 1: Some representative results produced by the code library Garnet showing its ability in modeling different faulting conditions and dipping angles.

References

Hunfeld, L. B., Niemeijer, A. R., & Spiers, C. J. (2017). Frictional properties of simulated fault gouges from the seismogenic groningen gas field under in situ P-T-chemical conditions. Journal of Geophysical Research: Solid Earth, 122(11), 8969-8989.

Erickson, B. A., Jiang, J., Barall, M., Lapusta, N., Dunham, E. M., Harris, R., ... & Wei, M. (2020). The community code verification exercise for simulating sequences of earthquakes and aseismic slip (SEAS). Seismological Research Letters, 91(2A), 874-890.

Jansen, J. D., Singhal, P., & Vossepoel, F. (2019). Insights from closed-form expressions for injection- and production-induced stresses in displaced faults. Journal of Geophysical Research: Solid Earth, 124, 7193– 7212.

Numerical Investigation of the impact of fluid on the earthquake cycle

Valentin Marguin (1*), Guy Simpson (1)

(1) Department of Earth Sciences, University of Geneva, Rue des Maraîchers 13, Geneva, Switzerland.
*Contact: valentin.marguin@unige.ch

Abstract

The strength and sliding behavior of faults in the upper crust is largely controlled by friction and the effective stress, which is itself modulated by the fluid pressure (Sibson, 1990, 1992). However, while many studies have investigated the role of friction on the earthquake cycle (Marone, C.,1998), relatively little effort has gone into understanding effects linked to dynamic changes in fluid pressure (see however Zhu et al, 2020). Here, we explore coupled interactions between slow tectonic loading and fluid pressure generation during the interseismic period with rapid sliding and elastic stress transfer during earthquakes on a plane strain thrust fault in two dimensions. Our models incorporate rate- and state-dependent friction along with dramatic changes in the fault permeability during sliding. Preliminary results show that elevated fluid pressures near the base of the seismogenic layer provides a means for faults to slip at shear stress levels that are well below those required for static sliding. In these modes, earthquakes are nucleated where fluid pressures are locally high. Ruptures are then propagated as slip pulses onto stronger parts of the fault facilitated by dramatic coseismic weakening (Di Toro et al., 2004). Overall, ruptures in the presence of fluids are slow relative to ruptures in dry crust (as also found by Passelègue et al, 2020). These results might eventually enable one to distinguish 'tectonic earthquakes' from earthquakes that are driven by variations in fluid pressure.

References

Marone, C. (1998). The effect of loading rate on static friction and the rate of fault healing during the earthquake cycle. Nature, 391(6662), 69–72.

Zhu, W., Allison, K. L., Dunham, E. M., & Yang, Y. (2020). Fault Valving and Pore Pressure Evolution in Simulations of Earthquake Sequences and Aseismic Slip. 1–16.

Sibson, R. H. (1990). Conditions for fault-valve behaviour. Geological Society Special Publication, 54(January 1990), 15–28.

Sibson, R. H. (1992). Implications of fault-valve behaviour for rupture nucleation and recurrence. Tectonophysics, 211(1–4), 283–293.

Di Toro, G., Goldsby, D. L., & Tullis, T. E. (2004). Friction falls towards zero in quartz rock as slip velocity approaches seismic rates. Nature, 427(6973), 436–439.

Passelègue, F. X., Almakari, M., Dublanchet, P., Barras, F., Fortin, J., & Violay, M. (2020). Initial effective stress controls the nature of earthquakes. Nature Communications, 11(1), 1–8.

Rate-and-State frictional plasticity as a reaction-diffusion equation in a continuum model

Casper Pranger (1,2*), Patrick Sanan (2), Dave May (3), Carsten Uphoff (1), Alice Gabriel (1)
(1) LMU Munich, (2) ETH Zurich, (3) UCSD
* casper.pranger@gmail.com

Abstract

The rate- and state-dependent friction (RSF) laws (Dieterich, 1979; Ruina, 1983) have been widely successful in capturing the behavior of sliding surfaces in laboratory settings, as well as reproducing a range of natural fault slip phenomena in numerical models.

Studies of exhumed fault zones make it clear that faults consist of complex damage zones that show clear signs of multi-scale fracturing, grain diminution, hydro-thermal effects and chemical and petrological changes. Many of these observed factors have been experimentally verified, and several studies have furthered our theoretical understanding of earthquakes and other seismic phenomena as volumetric, bulk-rock processes, including Sleep (1995, 1997), Lyakhovsky and Ben-Zion et al. (2011, 2014a,b, 2016), Niemeijer and Spiers et al. (2007, 2016, 2018), Roubicek (2014), and Barbot (2019).

While the established numerical modeling approach of simulating faults as planar features undergoing friction can be a useful and powerful homogenization of small-scale volumetric processes, there are also cases where this practice falls short -- most notably when studying faults that grow and evolve in response to a changing tectonic environment. This is mainly due to the computational challenges associated with automating the construction of a fault-resolving conformal mesh.

Motivated by this issue, we formulate a continuum generalization of RSF as a reaction-diffusion equation that governs anelastic shear strain in an otherwise standard elasto-plastic medium. The resulting system of equations -- which shares important characteristics with phase field methods -- is mathematically and numerically well-behaved and recovers the original laboratory-derived interfacial Dieterich-Ruina formulation both in an integral sense and in a limit sense as the diffusion length scale tends to zero. We will discuss the advantages and disadvantages of this formulation with the aid of 1D and 2D numerical solutions.

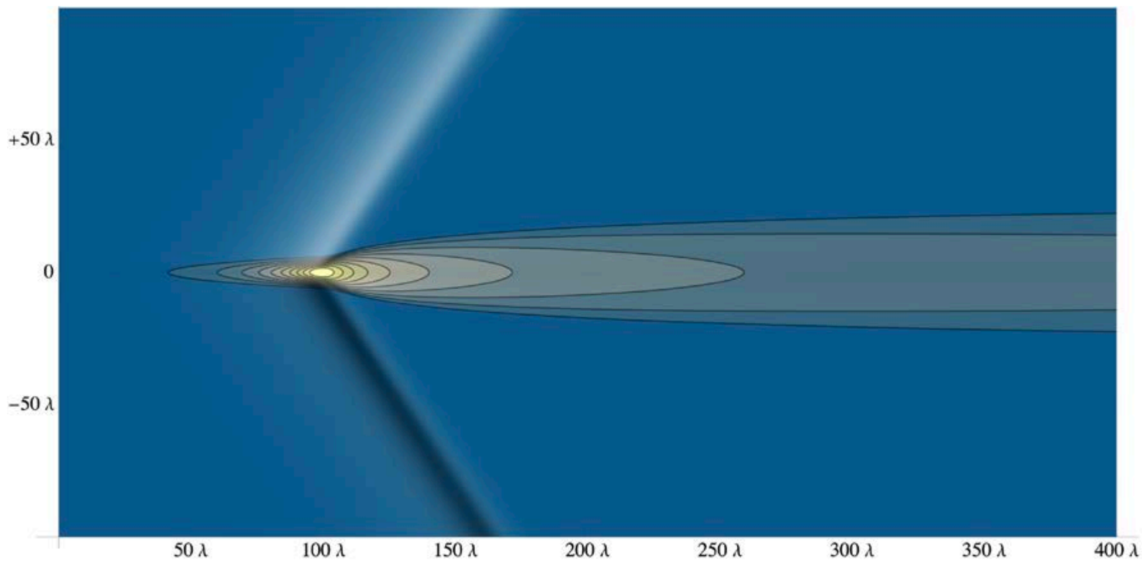

Figure 1: contours of anelastic strain rate generated using the presented model for a rupture front propagating at prescribed super-shear velocity. High strain rate is yellow, low strain rate is blue, and the contours have a linear scale. Simultaneously, the shear waves are plotted in white and black shading. No pressure waves are generated in this Mode-III out-of-plane model. Space is measured in units of λ, the controllable diffusion length scale.

References
Dieterich, J.H. (1979), J. Geophys. Res., 84 (B5), 2161.
Ruina, A. (1983), JGR: Solid Earth, 88 (B12), 10359–10370.
Sleep, N.H. (1995), JGR, 100 (B7), 13065–13080.
Sleep, N.H. (1997), JGR: Solid Earth 102 (B2), 2875–2895.
Roubíček, T. (2014), GJI 199.1, 286–295.
Lyakhovsky, Hamiel and Ben-Zion (2011), J. Mech. Phys. Solids, 59, 1752-1776.
Lyakhovsky and Ben-Zion (2014a), PAGeoph 171.11, 3099–3123.
Lyakhovsky and Ben-Zion (2014b), J. Mech. Phys. Solids 64, 184–197.
Lyakhovsky, Ben-Zion et al. (2016), GJI 206.2, 1126–1143.
Barbot (2019), Tectonophysics 765, 129–145.
Niemeijer and Spiers (2007), JGR 112, B10405,
Chen and Spiers (2016), JGR: Solid Earth 121, 8642–8665.
van den Ende, Chen et al. (2018), Tectonophysics 733, 273-295.

Analogue earthquakes, seismic cycles and seismotectonic evolution: Bridging the geodetic to geologic observation gap with experimental modelling

Matthias Rosenau (1), Ehsan Kosari (1*) *(keynote)*

(1) Helmholtz Centre Potsdam, GFZ German Research Centre for Geosciences, Potsdam, Germany.
* Contact: ehsan.kosari@gfz-potsdam.de

Abstract

Since the advent of plate tectonics an intrinsic *seismotectonic* relationship between longterm tectonic deformation on the Million year time scale and shortterm seismic or geodetic deformation manifested by earthquakes and seismic cycle deformation has been suspected. With a burst in earthquake activity, especially in subduction zones, in the past two decades and the contemporary development of space geodesy our observations on short time scales have reached an unprecedented clarity but remain limited in length. Going back into pre-instrumental to geological time, however, our observations loose systematically both resolution and completeness. Bridging this gap is essential in understanding how tectonic architecture is influenced by, and thereby reflects, its increments or vice versa. If there is a link between the time scales, we may be able to infer seismic hazard more quantitatively from tectonic structures beyond a phenomenological association between tectonically active zones and earthquakes. In this talk I will give an overview of our current understanding and strategies to study seismotectonics from an analogue modeller's perspective.

Analogue modelling enabled us to bridge the geodetic to geologic observation gap in recent years. Rock analogue materials with frictional properties akin to seismic and aseismic slip have been developed and rigorously tested. Stick-slip cycles involving locking, healing, creep, transient slip and dynamic rupture have been verified in the framework of rate-and-state friction theory to mimik the full spectrum of slip behaviors on natural faults. Viscoelastic materials with realistic relaxation behaviors were implemented as lower crustal and asthenosphere layers. Experimental monitoring by means of digital image correlation techniques advanced in terms of resolution to a degree allowing observing subtile displacements at high frequency and to setup scale models of subduction zones with a seismogenic megathrust in the lab. Importantly, seismotectonic scale models exist in a space-time continuum and can be run in 3D and for long times corresponding to Millions of years with no limitations on the spatial and temporal resolution of the process.

Those methodological advances allow us nowadays to study the feedback between short and long time scales and test Aristotle's phrase "The whole is greater than the sum of the parts" in the seismotectonic framework: Do earthquakes have an impact on the tectonic evolution or are they merely increments passing by without imprint? Or vice versa: If we ignore individual earthquakes, do we miss something? I will provide examples, mainly from subduction settings, where analogue modelling in combination with natural observations and simulation helped in answering those questions related to the feedback between short- and long-term deformation but also in understanding the spatiotemporal variability of earthquakes with the aim to better constrain seismic and tsunami hazard.

Session 5

Rheology & fluids

- Antoine Auzemery. *Role of crust-mantle decoupling for subduction initiation: application to magma-poor and magma-rich passive margins* ***(keynote)***
- Maria-Gema Llorens. *Ice-sheet flow transitions: for how long can crystallographic preferred orientations be preserved?*
- Sylvain Mayolle. *Investigating non-linear fault damage zone scaling through analog modeling*
- Maria Natale Castillo. *Modeling approach to estimate seismic attenuation from dry and wet upper crustal rock's rheology*
- Ludovic Räss. *Spontaneous flow and strain localisation arising from multi-physics coupling – forward and inverse supercomputing approaches* ***(keynote)***
- Jacqueline Reber. *Impact of semi-brittle rheology on deformation dynamics: An experimental investigation* ***(keynote)***

Role of hydration-induced serpentinization and magmatism in the formation subduction zones at passive margins

Antoine Auzemery (1), Philippe Yamato (2), Thibault Duretz (2), Ernst Willingshofer) (1), Liviu Matenco (1), Kristof Porkoláb (1) *(keynote)*. Contact: antoine.auzemery@gmail.com

(1) Utrecht University, Faculty of Geosciences, Department of Earth Sciences.
(2) Université de Rennes, CNRS, Géosciences Rennes, UMR 6118, Rennes 35000, France

Abstract

Recent numerical and analogue studies show that subduction initiation at passive margins requires the development of a shear zone at the base of the crust that subsequently propagates into the mantle lithosphere. Such findings suggest that a critical factor for subduction initiation is the degree of rheological crust-mantle coupling at continental passive margins, controlled by structures and composition inherited from rifting. Of particular interest is interaction between magmatism, deformation and hydration during passive margin formation.

Therefore, our study focuses on the unresolved question of subduction zone formation at passive continental margins and aims at identifying the role of rift-induced processes in the formation and evolution of subduction zones, for scenarios where convergence is orthogonal to the passive margin. Model results highlight that hydration-induced serpentinization and magmatic budget at passive margins are key factors that control the development of subduction faults at ocean-continent boundaries. Our modelling infers that the original reactivation of a serpentinized mantle during contraction enables the propagation of deformation toward the necking zone and the transfers of deformation to the mantle lithosphere. In contrast, passive margins intruded and underplated by magmatism favours intra-oceanic subduction initiation. This mode of subduction initiation is driven by the strong rheological coupling of the passive margin that inhibits the continent-ward propagation of deformation.

The relevance of the modelling results is demonstrated for the Alps and Dinarides-Hellenides orogenic systems, where contrasting types of continental rifted margins are observed, and different mode of subduction initiation are documented. In the western Alps, initiation of subduction is driven by a basal thrust at the base of the continental crust along a magma-poor passive margin. In contrast, along the magma-rich passive margin of the Dinarides-Hellenides, subduction was intra-oceanic.

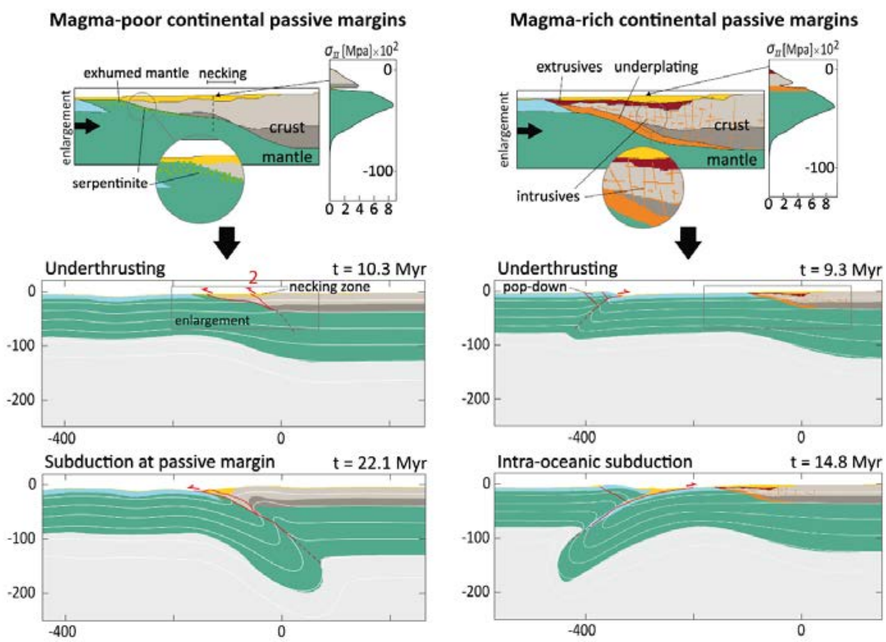

Figure 1: Subduction initiation for magma-poor and magma-rich passive margin settings.

Ice-sheet flow transitions: for how long can crystallographic preferred orientations be preserved?

Maria-Gema Llorens (1*), Albert Griera (2), Paul D. Bons (3,4), Ilka Weikusat (3,5), David Prior (6), Enrique Gomez-Rivas (7), Tamara de Riese (3), Ivone Jimenez-Munt (1), Daniel García-Castellanos (1) and Ricardo A. Lebensohn (8)

(1) Department of Structure and Dynamics of the Earth, Geosciencies Barcelona CSIC, Spain, (2) Departament de Geologia, Universitat Autònoma de Barcelona, Spain, (3) Department of Geosciences, Eberhard Karls University Tübingen, Germany (4) China University of Geosciences, Beijing, China (5) Alfred Wegener Institute Helmholtz Centre for Polar and Marine Research, Germany. (6) Department of Geology, University of Otago, New Zealand, (7) Departament de Mineralogia, Petrologia i Geologia Aplicada, Facultat de Ciències de la Terra, Universitat de Barcelona, Spain . (8) Theoretical Division, Los Alamos National Laboratory, Los Alamos, NM, USA.

* Contact: mgllorens@geo3bcn.csic.es

Abstract

Creep due to ice flow is generally thought to be the main cause for the formation of crystallographic preferred orientations (CPOs) in polycrystalline anisotropic ice. However, linking the development of CPOs to the ice flow history requires a proper understanding of the ice aggregate's microstructural response to flow transitions.
In this contribution the influence of ice deformation history on the CPO development is investigated by means of full-field numerical simulations at the microscale. We simulate the CPO evolution of polycrystalline ice under combinations of two consecutive deformation events up to high strain. Ice polycrystalline viscoplastic deformation was simulated using the Fast Fourier Transform algorithm (VPFFT), within the numerical open-source platform ELLE (http://www.elle.ws).
A volume of ice is first deformed under co-axial boundary conditions, which results in a CPO. The sample is then subjected to different boundary conditions (co-axial or non-coaxial) in order to observe how the deformation regime switch impacts on the CPO.
The model results indicate that the second flow event tends to destroy the first, inherited fabric, with a range of transitional fabrics. However, the transition is slow when crystallographic axes are critically oriented with respect to the second imposed regime. Therefore, interpretations of past deformation events from observed CPOs must be carried out with caution, particularly, in areas with complex deformation histories.

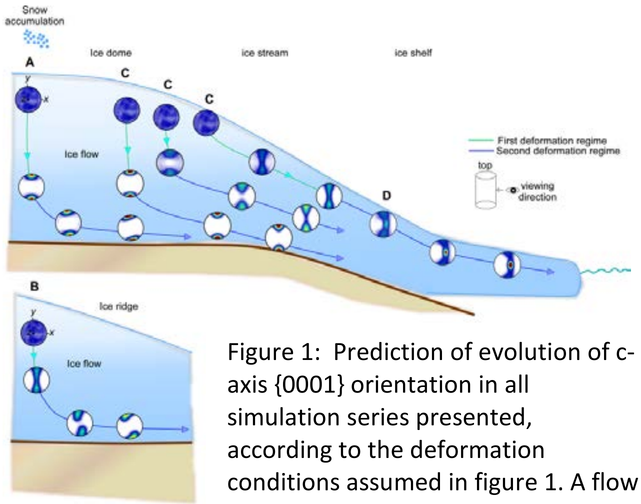

Figure 1: Prediction of evolution of c-axis {0001} orientation in all simulation series presented, according to the deformation conditions assumed in figure 1. A flow change produces an overprint of the previous CPO, with a range of transition fabrics.

References

Bons, P.D., Koehn, D., Jessell, M.W., 2008. Microdynamic Simulation. Lecture Notes in Earth Sciences 106, Springer, Berlin. 405 pp.
Lebensohn, R.A., Rollett, A.D. 2020. Spectral methods for full-field micromechanical modelling of polycrystalline materials. Computational Materials Science, 173, p.109336.
Llorens, M.G., Gomez-Rivas, E., Ganzhorn, A.C., Griera, A., Steinbach, F., Roessiger, J., Labrousse, L., Walte, N.P., Weikusat, I., Bons, P.D. 2019. The effect of dynamic recrystallisation on the rheology and microstructures of partially molten rocks. Journal of Structural Geology, 118, pp.224-235.

Investigating non-linear fault damage zone scaling through analog modeling

Sylvain Mayolle (1*), R. Soliva (1), S. Dominguez (1), C. Wibberley (2), and Y. Caniven (3)

(1) Géosciences Montpellier Laboratory, University of Montpellier, France, (2) TOTAL EP, CSTJF, France, (3) Rice University, USA
* Contact: sylvain.mayolle@umontpellier.fr

Abstract

Fault damage zones strongly influence fluid flow and seismogenic behavior of faults. Their thickness is thought to scale linearly with fault displacement until reaching a threshold value. Using analog modeling with different frictional layer thicknesses, we investigate damage zone dynamic evolution during normal fault growth. We show that experimental damage zone growth with displacement is not linear but progressively tends towards a threshold thickness, being larger in the thicker models.

This threshold thickness increases significantly at fault segment relay zones. As the thickness threshold is approached, the failure mode progressively transitions from dilational shear to isochoric shear. This process affects the whole layer thickness and develops as a consequence of fault segment linkage as inferred in nature when the fault zone matures.

These findings suggest that fault damage zone widths are limited both by different scales of mechanical unit thickness and the evolution of failure modes, ultimately controlled in nature by lithology and deformation conditions.

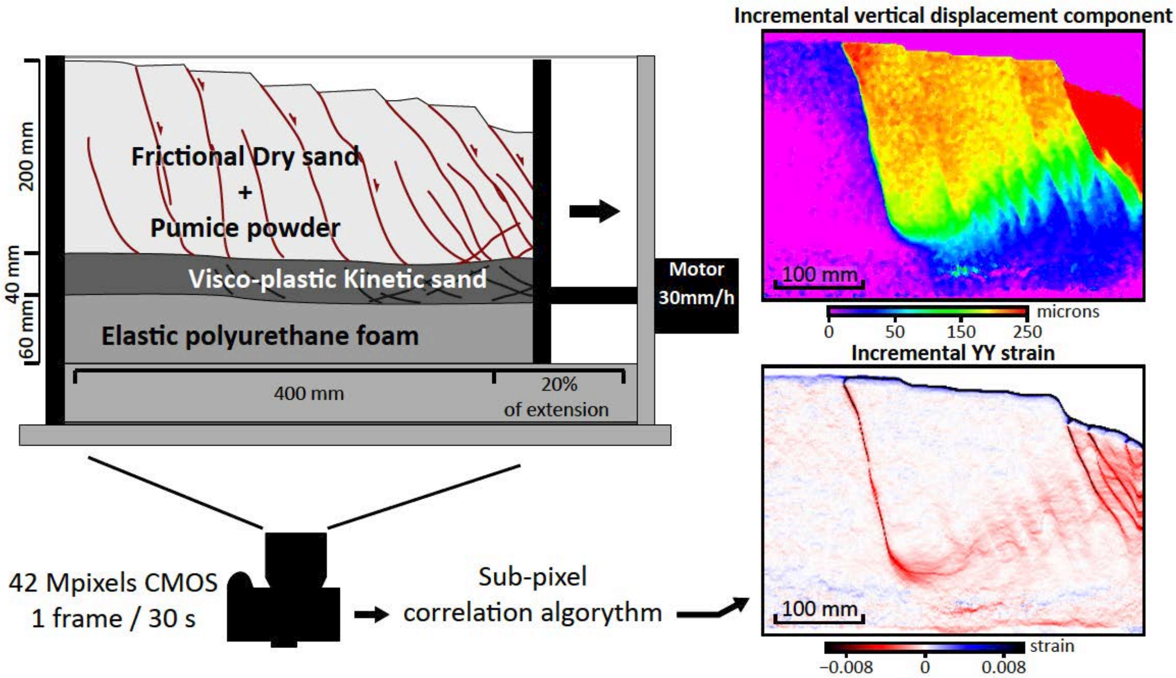

Figure 1: Experimental setup. A basal elastic foam is slowly uncompacted imposing extensional deformation in the upper visco-plastic kinetic sand and frictional layers. Vertical displacements and YY strain field derived from the sub-pixel image correlation are shown on the right.

References

Sylvain Mayolle, Roger Soliva, Stéphane Dominguez, Christopher Wibberley, Yannick Caniven; Nonlinear fault damage zone scaling revealed through analog modeling. *Geology* 2021; doi: https://doi.org/10.1130/G48760.1

Modeling approach to estimate seismic attenuation from dry and wet upper crustal rock's rheology

Maria Aurora Natale Castillo (1*), Magdala Tesauro (1,2), Mauro Cacace (3)
(1) University of Trieste, Department of Mathematics and Geosciences, Trieste, Italy, (2) Dept. of Earth Sciences, Utrecht University, Utrecht, Netherlands, (3) German Research Centre for Geosciences (GFZ) Potsdam
* Contact: mariaaurora.natalecastillo@phd.units.it.

Abstract

The elementary definition of the attenuation is referred to the damped harmonic oscillator as the fractional loss of energy per wave cycle. In some cases, it is used to describe the physical properties of the system that cause a disturbance (Stein and Wysession, 2003). For instance, the energy decay over time of some of the Earth's normal modes (directly analogous to a damped oscillator), exhibits attenuation due to the material distribution in the earth. The attenuation can be quantified in terms of the seismic quality factor Q. At given absorption bands, Q can be considered nearly constant and can be related to the superposition of different mechanisms that causes the conversion of seismic energy into internal heat. These mechanisms in turn depend on the material composition and grain size and vary with temperature and pressure, such that higher pressure decreases attenuation, whereas higher temperature promotes the opposite (Stein and Wysession, 2003). On the other hand, the viscous deformation of crustal rocks occurs through different anelastic mechanisms, including diffusion creep, numerous mechanisms of the dislocation creep, pressure solution that exhibits dependency on their structure, composition, and fluid content, as well as on their P-T conditions (e.g., Burov, 2011). Therefore, it is likely that seismic attenuation and the viscous modes of deformations of rocks can be correlated, based on their dependency on the aforementioned conditions, as expressed by an Arrhenius-type equation (Farina et al., 2019).

Despite many studies provided indications that rocks' seismic attenuation and viscous deformation are intrinsically related (considering their common dependency on composition, grain size, fluid content, and T-P conditions), their quantitative relationships have been very poorly investigated. In this study, we explore plausible relationships, implementing a modeling strategy to derive seismic attenuation from diverse rock's rheologies and to quantitatively estimate the reduction in the Q factor in correspondence to the depth of the brittle-to-ductile transition (BDT). For that, we rely on a Burgers mechanical model to derive shear wave attenuation ($1/Q_S$), for several dry and wet crustal rheology, thermal conditions, and different strain rates values. This allows us to establish geothermal and mechanical conditions at which the BDT occurs and to cross-correlate this transition to computed shear seismic wave attenuation values.

In particular, we observe a relatively significant Q_S reduction (10^{-8}) for strain rates of 10^{-13} s^{-1}, despite the assumed rock's rheology and thermal conditions. These first results confirm our hypothesis that variations in the Q_S factor can be effectively used to identify the depth to the BDT in tectonically active areas. This effect is particular relevant in the presence of fluid saturated rheology (Figure 1).

Ongoing and future works will focus on a further validation of the modelling implications by systematic analyses of observations, derived from rocks' laboratory experiments, which will be used to add constraints on the relationship between seismic attenuation and rheological flow laws to be used for geodynamic modelling.

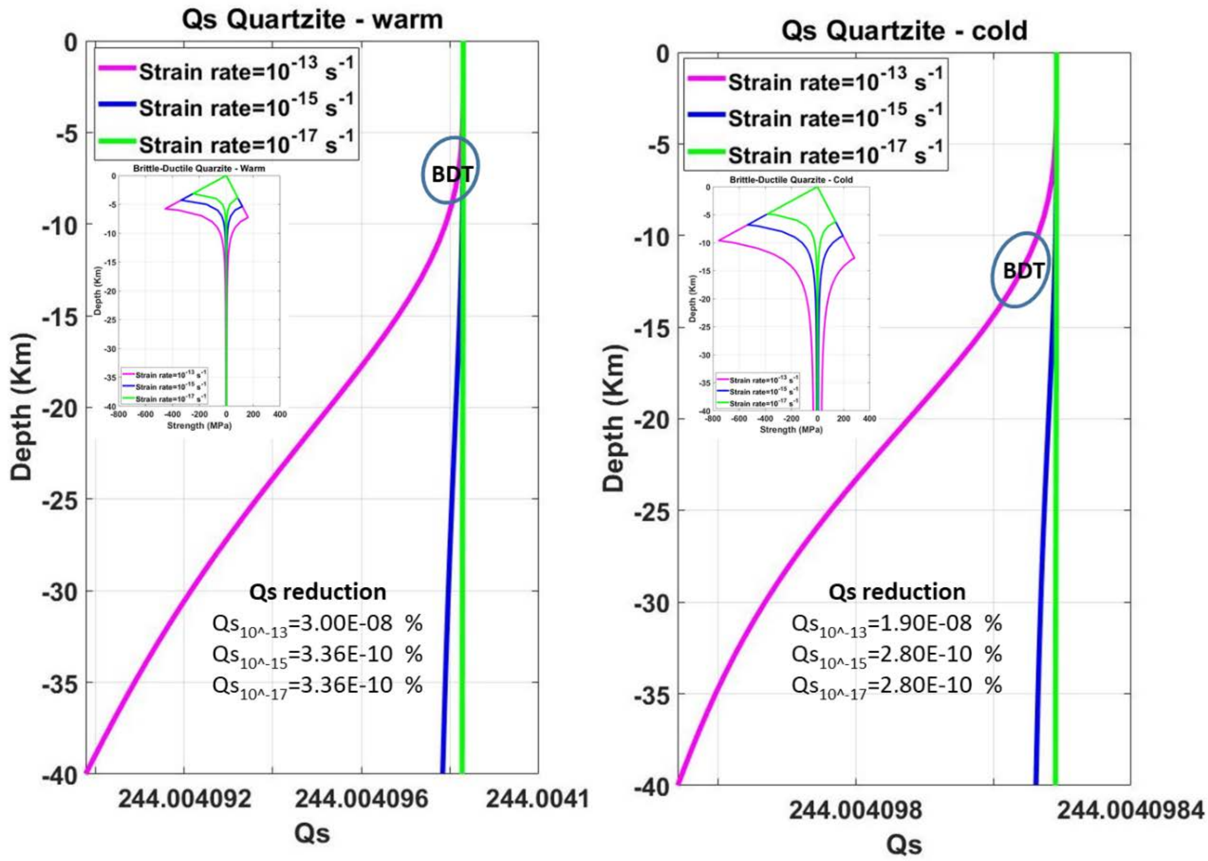

Figure 1: *Qs*-Depth distribution (Dry quartzite rheology using a warm and cold geotherm).

References

Stein, S. & Wysession, M. (2003). An Introduction to Seismology, Earthquakes, and Earth Structure. Blackwell Publishing Ltd, pp.498.

Burov, E.B. (2011). Rheology and strength of the lithosphere. Mar. Pet. Geol., 28, 1402–1443. https://doi.org/10.1016/j.marpetgeo.2011.05.008.

Farina, B., Poletto, F., Mendrinos, D., & Carcione, J.M. (2019). Seismic properties in conductive and convective hot and super-hot geothermal systems. Geothermics, 82, 16-33. https://doi.org/10.1016/j.geothermics.2019.05.005.

Spontaneous flow and strain localisation arising from multi-physics coupling – forward and inverse supercomputing approaches

Ludovic Räss (1, 2) *, Samuel Omlin (3), Stefan Schmalholz (4), Yuri Podladchikov (4) *(keynote)*
(1) Laboratory of Hydraulics, Hydrology and Glaciology (VAW), ETH Zurich, Zurich, Switzerland, (2) Swiss Federal Institute for Forest, Snow and Landscape Research (WSL), Birmensdorf, Switzerland, (3) Swiss National Supercomputing Centre - CSCS, Lugano, Switzerland, (4) Institute of Earth sciences, University of Lausanne, Lausanne, Switzerland
* Contact: luraess@ethz.ch

Abstract

The interplay among different physical processes from Earth's deeper interior towards the shallow subsurface may lead to the spontaneous localisation of flow and strain. For example, diffusive processes such as fluid and heat flow or chemical reactions may alter the petrophysical properties of subsurface environments initiating localised deformation. Because of the nonlinear feedbacks, localised deformation may develop over time creating narrow regions of intense action. Understanding spontaneous localisation arising from multi-physics coupling requires specific predictive tools capable to resolve the physical processes on various scales in space and time. From a numerical perspective, investigating multi-physics coupling requires fast solvers capable to handle high spatial and temporal resolutions. Most important, the solvers should exhibit sufficient flexibility to allow for concise and elegant implementation of new or alternative governing systems of equations.

We here discuss latest development in combining the pseudo-transient method to the emerging and widely portable Julia language. Julia permits to solve the two-language problem, combining prototyping and production application into a single, performance portable, concise code. Together with the pseudo-transient method, Julia enables teaching codes to scale on GPU-based supercomputers enabling a new era in portability. We'll demonstrate performance and scalability of multi-GPUs Julia applications on more than 1000 GPU, resolving forward and inverse hydro-mechanical problems. We recently designed a pseudo-transient adjoint-based workflow making it possible to invert for 3-D porosity fields using vertical fluid fluxes as observables. Our development relies on the `ParallelStencil.jl` and `ImplicitGobalGrid.jl` packages enabling high-performance stencil-based calculations and optimal distributed memory parallelisation. As outlook, we'll present ongoing work on resolving hydro-chemical-mechanical processes leading to the growth of veins on GPUs using the Julia framework.

Impact of semi-brittle rheology on deformation dynamics: An experimental investigation

Jacqueline E. Reber (1*) *(keynote)*
(1) Department of Geological and Atmospheric Sciences, Iowa State University, Iowa, USA
* Contact: jreber@iastate.edu

Abstract
Constraining the rheology of the lithosphere is of fundamental importance for understanding plate tectonics as well as earthquake generation. This task, however, is exceedingly difficult as a variety of deformation mechanisms contribute to the integrated strength of the lithosphere. Rocks at high-pressure and high-temperature conditions flow viscously by a number of deformation mechanisms whereas at low-pressure and low-temperature conditions rocks crack, fracture, lose cohesion and slide frictionally. At intermediate crustal depth, deformation is hence achieved by a complex spatial and temporal interplay between "viscous" and "brittle" processes. The interaction between these end-member cases where viscous flow cannot accommodate all the imposed displacement and abundant pervasive fracturing occurs leads to "semi-brittle" deformation. Semi-brittle deformation links the time scales associated with fracturing and earthquakes with the time scales associated with a flowing ductile crust leading to a mixture of stick-slip and creep. The co-occurrence of brittle and viscous deformation in rocks can be observed in the field over many length scales and in various lithologies.

Two field examples of semi-brittle deformation will serve as starting points to investigate how forces are distributed between the brittle and viscous phases, how deformation localizes, and how the two phases impact the deformation dynamics. These field observations are guiding the design of analog experiments that allow for a systematic investigation of the impact of individual phase rheology on the deformation dynamics. Using a combination of field observations and experiments has the advantages that deformation evolution can be observed and documented, length scales from micro to the macro scale can be investigated, and resulting deformation dynamics do not need to be preassigned, but can emerge from the material interactions (Figure 1). By employing various experimental materials, we can quantify the impact of the strength contrast between the brittle and viscous phases, the distribution between the phases, as well as the role of fracture formation and geometries on slip dynamics. The results show that semi-brittle rheology significantly impacts deformation dynamics, deformation localization, and the force distribution within the different material phases. All these aspects have a direct impact on the stability of fault zones and how deformation will manifest itself.

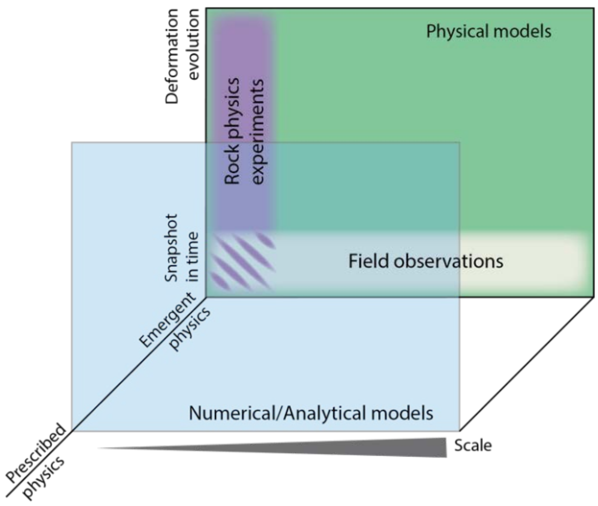

Figure 1: Schematic illustration of the different approaches in structural geology and tectonics and how they complement each other (Reber et al. 2020).

References
Reber, J. E., Cooke, M. L., and Dooley, T. P., 2020, What model material to use? A review on rock analogs for structural geology and tectonics: Earth-Science Reviews, v. 202, p. 1-21.

Session 6

Geodynamics and plate tectonics

- Kittiphon Boonma. *Geodynamic modelling of lithospheric slab tearing and its topographic response. Application to the Gibraltar Arc*
- István Bozsó. *Modelling the subduction and roll-back of narrow oceanic slabs: Formation of back-arc basins and slab detachment in the Carpathians subduction zone*
- João Duarte. *Laboratory models of subduction: interface rheology and overriding plate deformation* ***(keynote)***
- Jakub Fedorik. *Numerical validation of complex strike-slip fault system: example of Restraining Bends in Lebanon*
- Taras Gerya. *Segmentation of subducting oceanic plates in the outer rise*
- William Halter. *Numerical modelling of strain localization by anisotropy generation during viscous deformation*
- Arijit Laik. *Continental Collision in 3D buoyancy-driven whole-mantle scale numerical models*
- Laetitia Le Pourhiet. *Continental Break-up in 3D: are 2D concepts all valid?* ***(keynote)***
- Yuan Li. *Free surface models of partially molten rocks with visco-elasto-viscoplastic rheology*
- F. Maddaloni. *Effects of multi-extensional tectonics in a cratonic area: the origin of the Congo basin*
- Ana Negredo. *Continental delamination in the northern Apennines: insights from thermo-mechanical modelling*
- Jakub Pokorný. *Feedbacks between subduction dynamics and slab deformation: Combined effects of nonlinear rheology of a weak decoupling layer and phase transitions*
- Michaël Pons. *Control of subduction dynamics on shortening magnitude in the Central Andes: a thermomechanical modeling approach*
- Kristóf Porkoláb. *Extrusion of subducted crust explains the emplacement of far-travelled ophiolites*
- Lars Rüpke. *Oceanic Transform Faults revisited*
- Jonas Ruh. *Self-consistent grain size evolution controls lithospheric shear zone formation during rifting*
- Wouter Schellart. *Geodynamics of short-lived, long-lived and periodic flat slab subduction*
- Timothy Schmid. *Continental rifting in rotational systems: Unravelling rift propagation processes using spatiotemporal high resolution quantified crustal-scale analogue models*
- Guido Schreurs. *Analogue models of lithospheric-scale rifting monitored in a CT-scanner*
- Anna-Katharina Sieberer. *Internal deformation of the Dolomites Indenter, eastern Southern Alps: Insights from crustal scale analogue modelling*
- Stephan Sobolev. *Interplay of surface and deep-seated processes in initiation and evolution of plate tectonics on* ***(keynote)***
- Vincent Strak. *3D mantle flow induced by retreating and advancing slabs: insights from analogue subduction models analysed with a tomographic Particle Image Velocimetry technique*
- Kai Xue. *Overriding plate deformation and topography during slab rollback and slab rollover: insights from subduction experiments*
- Wentao Zhang. *Integrated geophysical-petrological modeling of the lithospheric mantle along the northern Apennines, Dinarides and Pannonian Basin*

Geodynamic modelling of lithospheric slab tearing and its topographic response. Application to the Gibraltar Arc

Kittiphon Boonma (1, 2), Ivone Jiménez-Munt (1*), Daniel Garcia-Castellanos (1), Taras Gerya (3)
(1) Geosciences Barcelona, Geo3BCN-CSIC, Spain, (2) Departament de Dinàmica de la Terra i de l'Oceà, Universitat de Barcelona, Spain, (3) Department of Geophysics, EDRW, ETH Zürich
* Contact: ivone@geo3bcn.csic.es

Abstract
Lithospheric slab tearing, the process by which a subducted lithospheric plate is torn apart and sinks into the Earth's mantle, has been proposed as a cause of significant surface vertical motions. Although this has been linked to the change implied in the isostatic balance in subduction zones, little is known about the mechanisms and rock properties determining the tear propagation and the uplift-subsidence rates involved. This work aims to explore the link between the tearing of subducted lithospheric slabs and the associated vertical motions.
To this purpose, we numerically simulate the process of lithospheric tearing upon continental collision, using the Betic Cordillera as a reference scenario where such tearing-uplift interaction has been proposed for this region. We used 3D thermo-mechanical numerical modelling to investigate the geodynamic parameters affecting the slab-tearing initiation and its lateral propagation, and to quantify the corresponding surface vertical motions. The Betics-inspired model suggests that the obliquity of the continental passive margin (relative to the trench axis) is a major influence on the initiation of slab tearing because it promotes a laterally diachronous continental collision which leads to slab tearing. The model illustrates an east-to-west slab tearing (tearing velocity ~ 37.6−67.6 cm/yr with the lower-mantle viscosity of up to 10^{22} Pa·s), which leads to surface uplift signature of 0.5−1.5 km across the forearc region throughout the tearing process. While the fast slab tearing (< 2 Myr over 600 km wide slab) and the lack of arcuate slab of these models limit a direct comparison with the Western Mediterranean, this approach provides a new insight into the link between slab tearing in the mantle and surface uplift. These experiments yield uplift rates of 0.23−2.16 mm/yr, as a result of slab tearing, which
is compatible with the uplift rate needed to achieve an equilibrium between seaway-uplift and seaway-erosion which could have led to the closure of marine gateways that reduced the water-flow from the Atlantic Ocean into the Mediterranean Sea during the first stage of the Messinian Salinity Crisis.

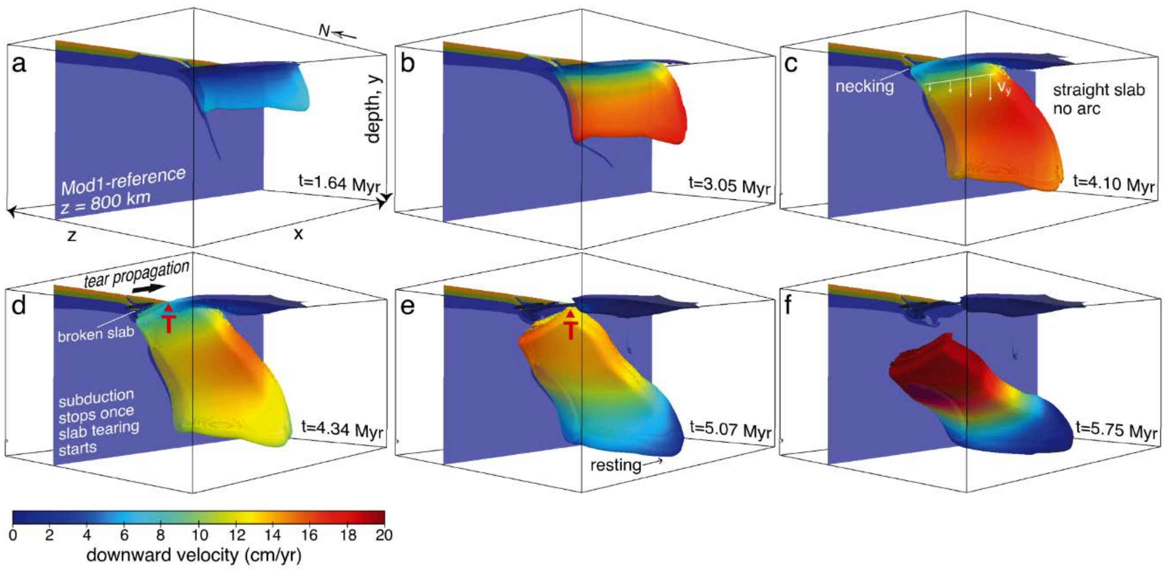

Figure 1: The evolution of the slab's downward velocity. The slab structure shown here comes from the temperature isosurface,T=1300◦C. The red 'T' illustrates the position of the slab tear. Prior necking or slab tearing, the slab subducts with little lateral velocity variation across the slab (a and b). Once the necking and the tearing has started, the higher downward velocity now shifted to side of the slab that is still attached (c and d). After the slab is completely detached (f), the slab's downward velocity regained the lateral uniformity of downward velocity

Modelling the subduction and roll-back of narrow oceanic slabs: Formation of back-arc basins and slab detachment in the Carpathians subduction zone

István Bozsó (1,2*), Ylona van Dinther (2), Attila Balázs (3), Liviu Matenco (2), István Kovács (1)
(1) Faculty of Geosciences, Utrecht University, Budapestlaan 4, 3584 CD, Utrecht, The Netherlands
(2) Geodetic and Geophysical Institute, Research Centre for Astronomy and Earth Sciences, ELKH, Sopron, Csatkai Endre utca 6.-8., Hungary
(3) Department of Earth Sciences, ETH Zürich, NO H 9.1 Sonneggstrasse 5 8092 Zürich, Switzerland

* Contact: bozso.istvan@epss.hu

Abstract

The evolution of many Mediterranean subduction systems can be explained by assuming that the formation of current geological features, such as extensional and sag back-arc basins, retreating orogenic systems and slab detachment, were mainly driven by the subduction of a narrow oceanic slab. The ongoing detachment of the Vrancea slab beneath the SE Carpathians is a noteworthy example of such subduction systems. The tectonically active Vrancea zone was formed in the Carpathians subduction system, which evolved similarly to many Mediterranean systems.

We aim to simulate the evolution of the SE Carpathians including oceanic subduction to soft collision and slab detachment by the means of fully coupled two-dimensional thermo-mechanical numerical modelling (Gerya, T. V., & Yuen, D. A., 2007). Previous similar studies assumed an up to 2-300 km wide oceanic domain, which failed to reproduce the aforementioned geological features, due to the insufficient negative buoyancy of the subducted slab. Based on our numerical experiments and geological constraints we argue that a wider oceanic slab (~550 km), slow convergence and the presence of upper plate weakness zone are required to reproduce the main geological features observed in the SE Carpathians and the extensional Pannonian Basin.

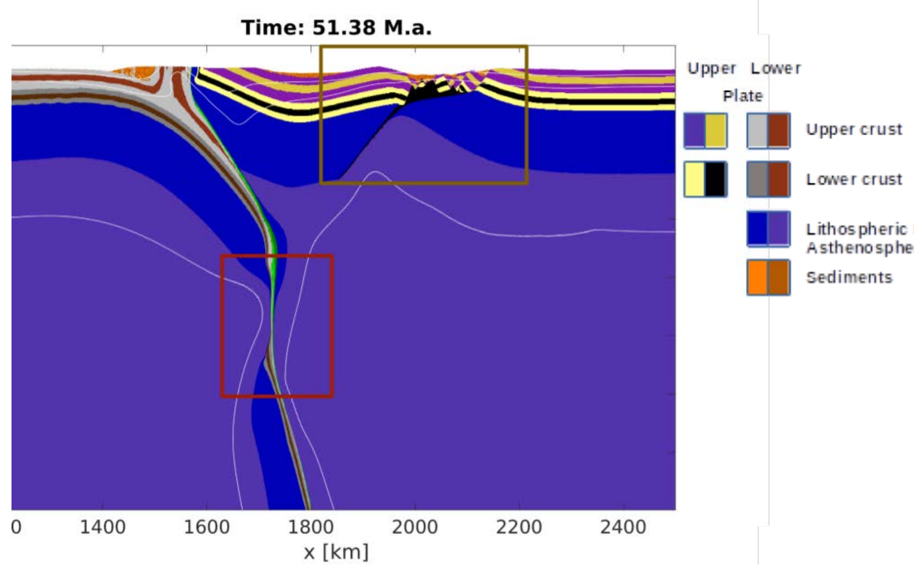

Figure 1: Composition plot of the reference model shortly after oceanic slab detachment. The two major geodynamic features are highlighted: back-arc extension (green rectangle) and detachment (red rectangle).

In this contribution we showcase the reference numerical model (Figure. 1), based on contemporary mantle structure and geodynamic reconstructions (Matenco, L., & Radivojević, D., 2012; Schmid, S. M. et al., 2020), that generates the sought geological features, and discuss its main driving forces. A parameter test has been conducted and we discuss the role of variable initial and boundary conditions that yields insights into the reconstruction of the area.

Finally, we address the limitations of our models and propose future modelling directions. An ideal continuation of our numerical approach is the implementation of seismo-thermo-mechanical modelling (Van Dinther et al., 2013) in order to explore the main drivers and sensitivity of the Recent seismic activity related to the ongoing detachment of the Vrancea slab.

References

Gerya, T. V., & Yuen, D. A. (2007). Robust characteristics method for modelling multiphase visco-elasto-plastic thermo-mechanical problems. Physics of the Earth and Planetary Interiors, 163(1-4), 83-105. https://doi.org/10.1016/j.pepi.2007.04.015

Matenco, L., & Radivojević, D. (2012). On the formation and evolution of the Pannonian Basin: Constraints derived from the structure of the junction area between the Carpathians and Dinarides. Tectonics, 31(6). https://doi.org/10.1029/2012TC003206

Schmid, S. M. et al. (2020). Tectonic units of the Alpine collision zone between Eastern Alps and western Turkey. Gondwana Research, 78, 308-374. https://doi.org/10.1016/j.gr.2019.07.005

Van Dinther, Y., Gerya, T. V., Dalguer, L. A., Corbi, F., Funiciello, F., & Mai, P. M. (2013). The seismic cycle at subduction thrusts: 2. Dynamic implications of geodynamic simulations validated with laboratory models. Journal of Geophysical Research: Solid Earth, 118(4), 1502-1525. https://doi.org/10.1029/2012JB009479

Laboratory models of subduction: interface rheology and overriding plate deformation

João Duarte (1,2*), Wouter Schellart (3), Zhihao Chen (4), Vincent Strak (3), Alexander Cruden (5) *(keynote)*
(1) Instituto Dom Luiz (IDL), Faculdade de Ciências, Universidade de Lisboa, 1749-016 Lisboa, Portugal (2) Departamento de Geologia, Faculdade de Ciências, Universidade de Lisboa, 1749-016 Lisboa, Portugal Affiliation, (3) Department of Earth Sciences, Vrije Universiteit Amsterdam, Amsterdam, Netherlands, (4) Department of Earth and Space Sciences, Southern University of Science and Technology (SUSTech), Shenzhen, China, (5) School of Earth, Atmosphere and Environment, Monash University, Melbourne, Victoria, Australia
* Contact: jdduarte@fc.ul.pt

Abstract

Laboratory models of subduction have been used for several years now. These models can usually be of two kinds: kinematically driven or internally self-consistent. In the first case, an a priori scaled velocity is imposed on the plates, while in the second case all the velocities emerge from the initial force balance. However, in self-consistent models, because the system develops on its own, it can evolve in unexpected ways or simply stall. This is usually the case if the scaling of the force balance is not properly done.

A few years ago, we decided to develop new models of subduction with both a subducting and an overriding plate in which both plates were coupled, i.e., without leaving any asthenospheric gap between the plates. We knew that the plates would stick together without a weak lubricating material in the interface. But how weak would this material have to be? If it was too weak it would flow away, if it was too strong it would glue the plates back together.

It happens that coming up with the right subduction lubricant was an enormous challenge. Even though we were extremely careful with the scaling, it took us many months of trials and errors simply because we did not know the range of strengths and viscosities over which a self-consistent subduction system would work. However, by doing this, we have learned a lot about a subduction system with an overriding plate. We learned how weak a subduction interface must be for a subduction zone to work, and we have come to understand how and why the overriding plate deforms.

In this talk, we will explore this journey, discuss some of the pitfalls in this kind of experiment, and gain new insights into the dynamics of subduction zones.

Our results suggest that subduction zone interfaces are always weak and that in narrow subduction systems the overriding plate always undergoes back-arc extension, whereas the forearc may experience extension or shortening depending on the far-field boundary conditions. We could also conclude that the main driver of back-arc extension is the sub-lithospheric mantle return flow (Duarte et al., 2013, 2015; Chen et al., 2015, 2016).

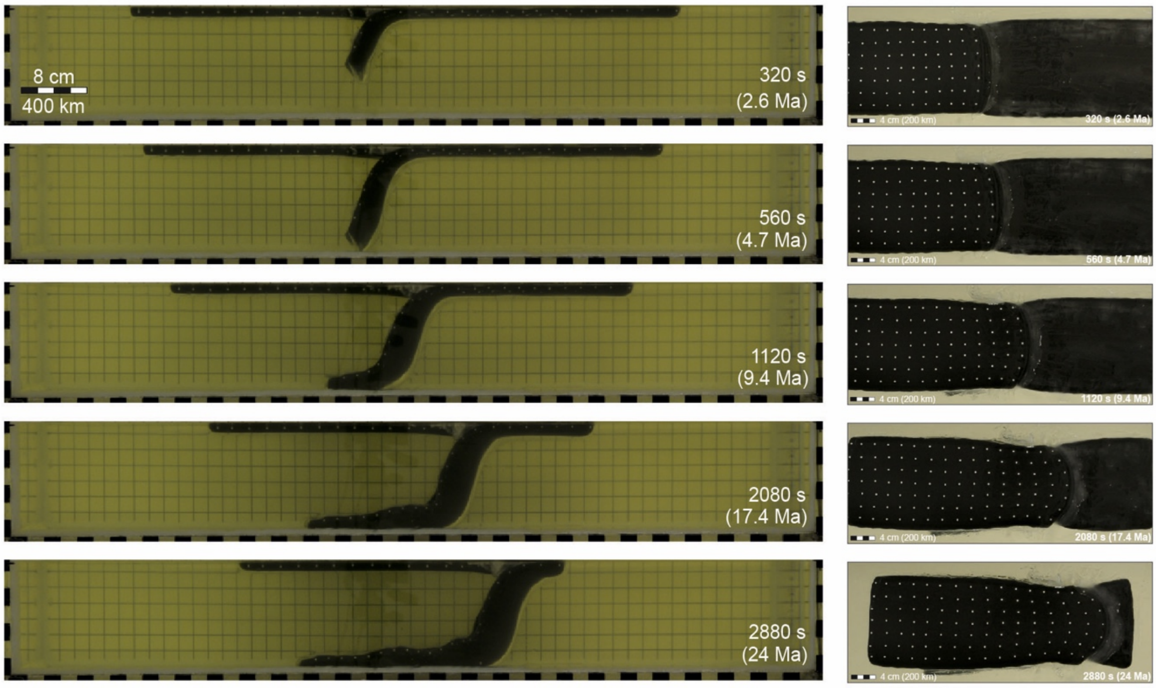

Figure 1: Subduction experiment with a subducting and an overriding plate, and an interface rheology. Side-view on the left and top-view on the right (Adapted from Duarte et al., 2013).

References

Chen, Z., Schellart, W.P., Strak, V., Duarte, J.C. (2016). Does subduction-induced mantle flow drive backarc extension? Earth and Planetary Science Letters. v 441, 200-210. https://doi.org/10.1016/j.epsl.2016.02.027

Chen, Z., Schellart, W.P., Duarte, J.C. (2015). Overriding plate deformation and variability of forearc deformation during subduction: Insight from geodynamic models and application to the Calabria subduction zone. Geochemistry, Geophysics, Geosystems. v16, 3697–3715. DOI: 10.1002/2015GC005958

Duarte, J.C., Schellart, W.P., Cruden, A.R. (2015). How weak is the subduction zone interface? Geophysical Research Letters. v41, 1-10. DOI: 10.1002/2014GL062876

Duarte, J.C., Schellart, W.P., Cruden, A.R. (2013). Three-dimensional dynamic laboratory models of subduction with an overriding plate and variable interplate rheology. Geophysical Journal International. v195, 47-66. https://doi.org/10.1093/gji/ggt257

Numerical validation of complex strike-slip fault system: example of Restraining Bends in Lebanon

Jakub Fedorik (1*), Francesco E. Maesano (2), Abdulkader Al Afifi
(1) Ali I. Al-Naimi Petroleum Engineering Research Center, King Abdullah University of Science and Technology (KAUST) (2) National Institute of Geophysics and Volcanology (INGV)
* Contact: jakub.fedorik@kaust.edu.sa

Abstract
Strike-slip structures are rarely validated because commonly used 2D restoration techniques are not applicable. The Lebanon Restraining Bend is the most prominent transpressional feature along the Dead Sea Transform (DST), and consists of two mountain ranges: Mount Lebanon on the NW, dominated by the active Yammouneh Fault, and the Anti-Lebanon Range to the SE, influenced by the Serghaya and other faults. We built a new 3D geometrical model (Fig. 1) of the fault surfaces based on structural maps onshore and offshore Lebanon, refined with an interpretation of satellite images and the DEM, and supported by analogy with experimental models of restraining bend or transpressional structures. The results of 3D numerical simulations of Restraining Bends in Lebanon, were obtained by using boundary element method of fault deformation. The model was simulated in response to the regional stress and the simulation accurately predicted the shape and magnitude of positive and negative topographic changes and fault slip directions throughout Lebanon. Furthermore, this simulation supports the hypothesis that the formation of the Anti-Lebanon Range was influenced by the intersection of the DST with the older The Syrian Arc Fold system, resulting in a failed restraining bend. In contrast, the structure of Mt. Lebanon is similar to laboratory experiments of a restraining bend with no inheritance. In addition to refined geodynamic and structural model of Restraining Bend in Lebanon, our simulation presents a new approach of how strike-slip structural models may be validated in areas where subsurface data are limited.

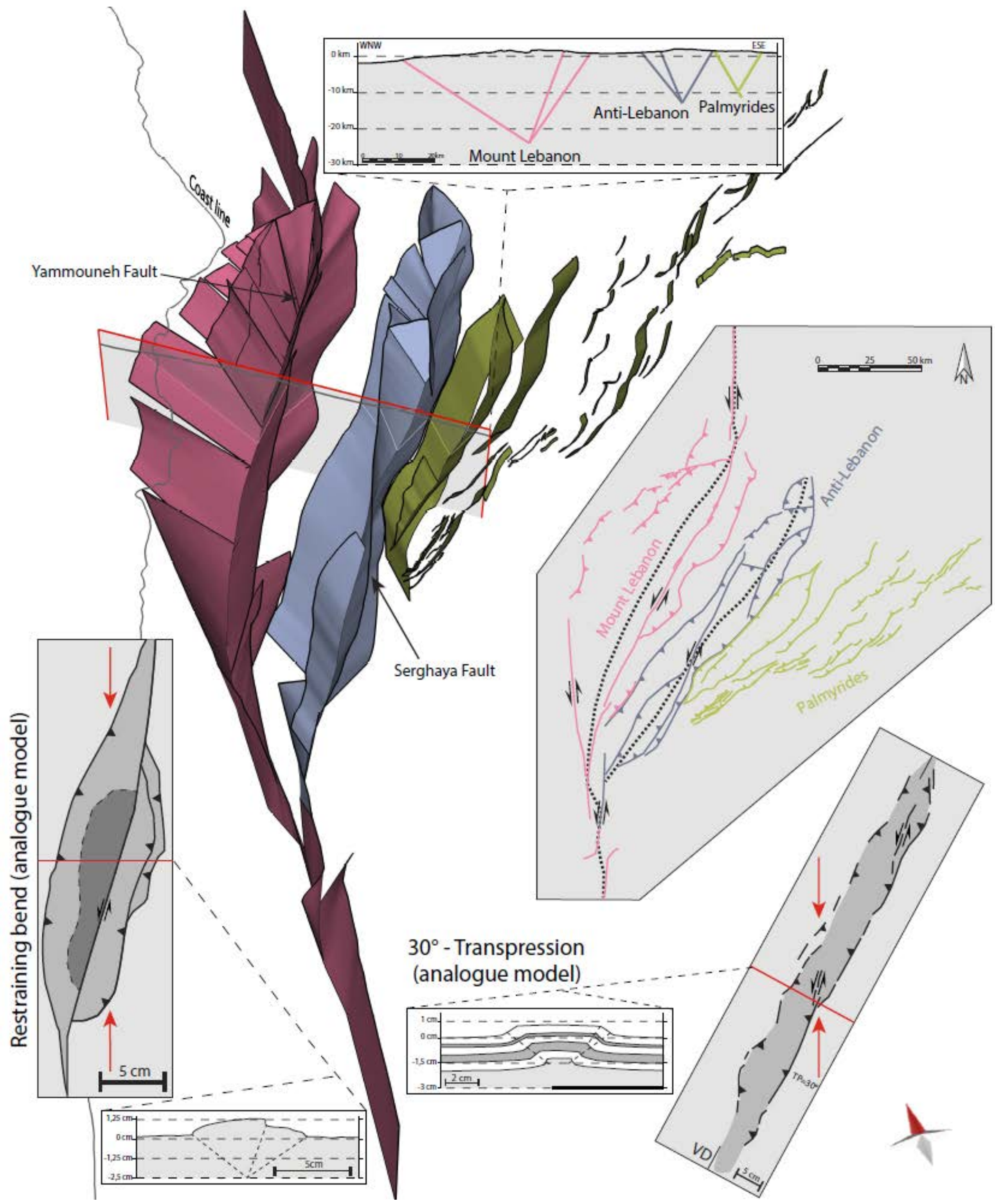

Figure 1: 3D, map and section view of Lebanon Restraing Bends. Bottom left inset: a redraw of analogue model of restraining bend (from Hatem et al., 2015); bottom right inset: a redraw of transpressional analogue model (from Casas et al., 2001).

References

Casas A.M., Gapais D., Nalpas T., Besnard K., Román-Berdiel T. (2001). Analogue models of transpressive systems. Journal of Structural Geology. v23, 733-743. https://doi.org/10.1016/S0191-8141(00)00153-X.

Hatem, A. E., Cooke M. L., and Madden E. H. (2015). Evolving efficiency of restraining bends within wet kaolin analog experiments. J. Geophys. Res. Solid Earth. v120, 1975–1992. https://doi.org/10.1002/2014JB011735

Segmentation of subducting oceanic plates in the outer rise

Taras Gerya (1*), David Bercovici (2), Thorsten Becker (3,4)
* Contact: tgerya@ethz.ch
1 ETH Zurich, Department of Earth Sciences, Zurich, Switzerland.
2 Yale University, Earth & Planetary Science, New Haven, CT, United States
3 Institute for Geophysics, Jackson School of Geosciences, The University of Texas at Austin, Austin, TX, United States
4 Department of Geological Sciences, Jackson School of Geosciences, The University of Texas at Austin, Austin, TX, United States

Abstract

Irrespective of their history, all subducting oceanic plates experience bending and normal faulting that accommodates the transition from horizontal to downward motion at the outer rise at subduction trenches. We investigated the consequences of the plate bending on the mechanical properties of subducting slabs using 2D subduction models in which both brittle and ductile deformation, as well as grain size evolution, are tracked and coupled self-consistently. Numerical results suggest that pervasive brittle-ductile slab damage and segmentation can occur at the outer rise region that strongly affects subsequent evolution of subducting slabs in the mantle. This slab-damage phenomenon explains the subduction dichotomy of strong plates and weak slabs, the development of large-offset normal faults near trenches and the occurrence of segmented seismic velocity anomalies and interfaces imaged within subducted slabs. Furthermore, brittle-viscously damaged slabs show a strong tendency for slab breakoff at elevated mantle temperatures that may have destabilized continued oceanic subduction and plate tectonics in the Precambrian.

Numerical modelling of strain localization by anisotropy generation during viscous deformation

William R. Halter (1*), Emilie Macherel (1), Thibault Duretz (1,2), Stefan M. Schmalholz (1)
(1) University of Lausanne, ISTE, Lausanne, Switzerland, (2) University of Rennes, CNRS, Rennes, France
* Contact: william.halter@unil.ch

Abstract

Localization and softening mechanisms in a deforming lithosphere are important for subduction initiation or the generation of tectonic nappes during orogeny. Many localization mechanisms have been proposed as being important during the viscous, creeping, deformation of the lithosphere, such as thermal softening, grain size reduction, reaction-induced softening or anisotropy development. However, which localization mechanism is the controlling one and under which deformation conditions is still contentious. In this contribution, we focus on strain localization in viscous material due to the generation of anisotropy, for example due to the development of a foliation. We numerically model the generation and evolution of anisotropy during two-dimensional viscous deformation in order to quantify the impact of anisotropy development on strain localization and on the effective softening. We use a pseudo-transient finite difference (PTFD) method for the numerical solution. We calculate the finite strain ellipse during viscous deformation. The aspect ratio of the finite strain ellipse serves as proxy for the magnitude of anisotropy, which determines the ratio of normal to tangential viscosity. To track the orientation of the anisotropy during deformation, we apply the so-called director method. We will present first results of our numerical simulations and discuss their application to natural shear zones.

Continental Collision in 3D buoyancy-driven whole-mantle scale numerical models

Arijit Laik (1*), Wouter P. Schellart (1) and Vincent Strak (1)
(1) Department of Earth Sciences, Vrije Universiteit Amsterdam, Amsterdam, Netherlands
* Contact: a.laik@vu.nl

Abstract

The sinking of negatively buoyant lithosphere into the Earth's mantle characteristically explains the process of subduction. In particular, free-subduction generally refers to self-consistent and dynamically evolving buoyancy-driven models of subduction in both physical and numerical modelling studies. The modelled subduction is asymmetric, single-sided, where plate kinematics and trench motions emerge from the physics in scaled laboratory models and physical approximations in numerical models.

This contribution intends to understand the driving forces of long term (~50 Ma) and sustained convergence at the India-Eurasia collisional zone within the framework of free subduction. The 3D numerical models build upon the insights from 2D numerical models where the observed modelled collisional boundary advance (migration of the boundary towards the overriding plate) rate is high, and sinking of the detached slab sustains slow convergence in the lithosphere. 3D models include two sets of modelled depths: the whole mantle (2880 km) and the upper mantle + partial lower mantle (960 km) and use the Underworld2 framework. The computationally intensive simulations have significantly large (11520 km) trench-perpendicular (in 2D and 3D) and parallel (in 3D) dimensions, which adequately scales to analogues system(s) in nature, such as the Sunda subduction zone and the India-Eurasia collision zone. Preliminary results from whole mantle models of large scale free-subduction and subsequent continent-continent collision resolve the 3D components of mantle flow and adequately estimate slab-pull exerted by subducting oceanic lithosphere. Furthermore, aid in exploring the spatio-temporal evolution and dynamics of natural collision systems.

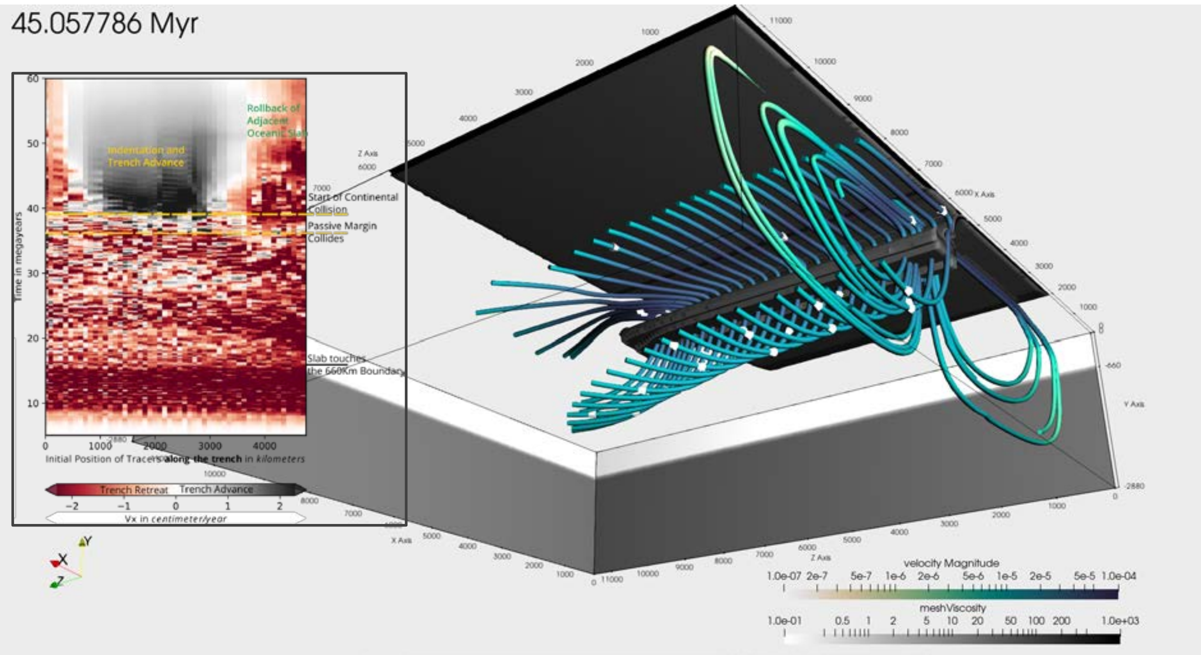

Figure 1: Streamlines and non-dimensional Viscosity Field of Model WM_mRes_1 (depth 2880 Km) at a stage before the continent enters the model's subduction zone, the velocity of the streamlines are non-dimentional. Inset shows the scaled velocity-time evolution of the tracers placed along the initial trench line of Model PM_mHRes_2 (depth 960 Km), the velocities are scaled using a reference upper-mantle viscosity of 5.0 × 10^{20} Pa s.

Continental Break-up in 3D: are 2D concepts all valid?

Laetitia Le Pourhiet (1*), Anthony Jourdon (2), Paul Perron(1), Dave May (2) *(keynote)*
(1) ISTeP, Sorbonne Université , (2) Scripps, UCSD
* Contact: Laetitia.le_pourhiet@sorbonne-universite.fr

Abstract

Since the seminal 1D dynamic classification of rifting of Buck (1991), extensive modelling work has been performed to understand how the rheological stratification of the lithosphere, the rheological laws that governs fault and shear zone weakening, the rate of stretching, melting and numerous other parameters that could be classified as tectonic inheritance influences the style of rifting and the transition to continental break-up. While 2D models capture more complexity than 1D models, the main conclusion remains. Strong, mechanically coupled lithosphere result in narrow continental margins and weak, mechanically decoupled result in wide margins dominated by differential stretching.

For the last 10 years, 3D numerical modelling has been made available, yet it remains very costly and one might ask two important questions. Is it important to run expensive 3D simulations to understand the formation of passive margins or metamorphic core complexes for which best available data set (GXT seismic profile) are rarely 3D? And as a corollari question, are the concepts based on 2D simulations always valid to analyse / interpret 3D data ? Especially in terms of initial rheological stratification of the lithosphere.

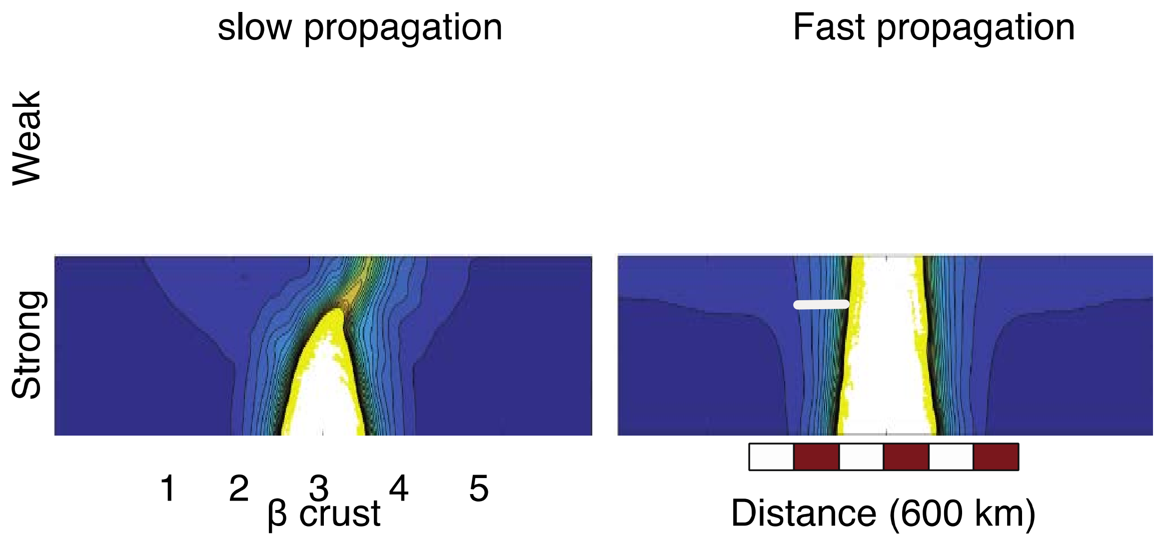

Figure 1. Map of crustal thinning (Beta factor) as a function of the initial mechanical coupling of the lithosphere and the rate of propagation of continental break up. White area represent oceanic lithosphere. (modified from Le Pourhiet et al. 2018).

I will present briefly a short synthesis of the well established 2D concepts before discussing based on 3D simulation performed in our group and published one what concepts stands and what concept need to be revisited to allow a better undertanding of extensional systems with a particular emphasis on continental break up. As a major finding in this domain is that when the rate of propagation of continental break-up in the ridge direction is faster than the rate of extension (ridge normal extension) in the simulations, the geometry of margins is much less sensitive to the rheological stratification of the lithosphere (Figure 1).

In our simulation slowing down or acceleration of continental break up propagation depends on the boundary conditions applied in the direction perpendicar to extension. Shortening results in desceleration while stretching results in acceleration. We also find that when oblique continental break up operate en echellon, all individual propagation segments put their neighbour in compression one of each other promoting slow break-up propagation. As it is very difficult to record slight component of shortening or extension in the direction of propagation, there is a large room to discussion whether fast propagation, which results in structures that are not captured by regular 2D models occurs in nature.

If narrow rifts do form within mechanically decoupled lithosphere, which is not a predicted outcome of the now well accepted 2D theory but an end-product of 3D simulations for fast break-up propagation, we expect this mode of rifting will impact the post-rift dynamics of the passive margin as sediments will be deposited on a much weaker lithosphere than predicted for a regular narrow rift. We approach this question by the mean of kinematically driven 2D simulations which permits force 2D models to follow otherwise 3D deformation paths and permit with their reduced numerical coast to simulate post rift evolution.

References

Buck, W. R. (1991). Modes of continental lithospheric extension. Journal of Geophysical Research: Solid Earth, 96(B12), 20161-20178.

Jourdon, A., Le Pourhiet, L., Mouthereau, F., & May, D. (2020). Modes of propagation of continental breakup and associated oblique rift structures. *Journal of Geophysical Research: Solid Earth*, *125*(9), e2020JB019906.

Le Pourhiet, L., Chamot-Rooke, N., Delescluse, M., May, D. A., Watremez, L., & Pubellier, M. (2018). Continental break-up of the South China Sea stalled by far-field compression. *Nature Geoscience*, *11*(8), 605-609.

Free surface models of partially molten rocks with visco-elasto-viscoplastic rheology

Yuan Li* (1), Adina E. Pusok (1), Dave A. May (2), Richard F. Katz (1)
(1) Department of Earth Sciences, University of Oxford
(2) Scripps Institution of Oceanography, University of California, San Diego
* Contact: Yuan.Li@earth.ox.ac.uk

Abstract
It is broadly accepted that magmatism plays a key dynamic role in continental and oceanic rifting. However, these dynamics remain poorly studied, largely due to the difficulty of consistently modelling liquid/solid interaction across the lithosphere. The RIFT-O-MAT project seeks to quantify the role of magma in rifting by using models that build upon the two-phase flow theory of magma/rock interaction. A key challenge is to extend the theory to account for the non-linear rheological behaviour of the host rocks, and investigate processes such as diking, faulting and their interaction. Here we present our progress in consistent numerical modelling of poro-viscoelastic-viscoplastic modelling of deformation with a free surface.

Failure of rocks (plasticity) is an essential ingredient in geodynamics models because Earth materials cannot sustain unbounded stresses. However, plasticity represents a non-trivial problem even for single-phase flow formulations with shear failure only (Spiegelman et al. 2016). What's more, in two-phase systems, tensile failure of rocks can also occur due to the overpressured magmatic flow (Keller et al., 2013). Robustly solving a discretised model that includes this physics presents severe challenges, and many questions remain as to effective solvers for these strongly nonlinear systems.

An appropriate rheological model is required to meet this challenge. The most straightforward choice is a Maxwell visco-elasto-plastic model, but this leads to grid-scale localisation and hence mesh-dependence. To obtain mesh-independent shear localisation, we employ the visco-elasto-viscoplastic model by introducing a viscous dashpot in parallel to the plasticity element (de Borst and Duretz, 2020). Whilst this formulation has shown promise in regularising shear failures in a single-phase flow model, its incorporation within two-phase systems has not been examined.

The underlying PDEs are discretised using a PETSc-based, conservative, finite-difference staggered-grid framework (FD-PDE) that supports single-/two-phase flow magma dynamics (Pusok et al., 2020). This new framework is designed to allow extensible development and rigorous code validation. Here, we present simplified model problems using the FD-PDE framework for poro-viscoelastic-viscoplastic models designed to characterise the solution quality and assess both the discretisation and solver robustness. We also present results obtained using the phase-field method (Sun and Beckermann, 2007) for representing the free surface. Verification of the phase-field approach will be shown via simplified problems previously examined in the geodynamics community (Crameri et al, 2012).

References

Spiegelman, M., May, D. A., & Wilson, C. R., (2016). On the solvability of incompressible Stokes with viscoplastic rheologies in geodynamics. Geochemistry, Geophysics, Geosystems*,* v17, 2213-2238. https://doi.org/10.1002/2015GC006228.

Keller, T., May, D. A., & Kaus, B. J. P., (2013). Numerical modelling of magma dynamics coupled to tectonic deformation of lithosphere and crust, Geophysical Journal International, v195, 1406-1442, https://doi.org/10.1093/gji/ggt306.

de Borst, R., Duretz, T., (2020). On viscoplastic regularisation of strain-softening rocks and soils. International Journal for Numerical and Analytical Methods in Geomechanics, v44, 890-903. https://doi.org/10.1002/nag.3046.

Pusok, A. E., May, D. A., & Katz, R. F., (2020). Magma dynamics using FD-PDE: a new, PETSc-based, finite-difference staggered-grid framework for solving partial differential equations, EGU General Assembly 2020, EGU2020-18690, https://doi.org/10.5194/egusphere-egu2020-18690.

Sun, Y., Beckermann, C., (2007). Sharp interface tracking using the phase-field equation, Journal of Computational Physics, v220, 626-653. https://doi.org/10.1016/j.jcp.2006.05.025.

Crameri, F., Schmeling, H., Golabek, G. J., Duretz, T., Orendt, R., Buiter, S. J. H., May, D. A., Kaus, B. J. P., Gerya, T. V., Tackley, P. J., (2012). A comparison of numerical surface topography calculations in geodynamic modelling: an evaluation of the 'sticky air' method, Geophysical Journal International, v189, 38-54. https://doi.org/10.1111/j.1365-246X.2012.05388.x.

Effects of multi-extensional tectonics in a cratonic area: the origin of the Congo basin

Maddaloni F. (1), Tesauro M. (1,2*), Gerya T. (3), Delvaux D. (4), Braitenberg C. (1)

Department of Mathematics and Geosciences, University of Trieste, Trieste, Italy, (2) Utrecht University, Earth Sciences department, (3) Institute of Geophysics, ETH Zürich, Zürich, Switzerland, (4) Royal museum of central Africa, Tervuren (BRX), Belgium
*mtesauro@units.it

Abstract

Different hypotheses attempted to explain the long-lasting subsidence of the intracratonic basins, characterized by prolonged intervals of low rate subsidence, alternating with episodic accelerations in subsidence rates. Among them, the Congo Basin (CB) occupies a large part of the Congo Craton, derived from the amalgamation of different cratonic pieces. This basin, having been repeatedly reactivated by extensional and compressional tectonic events, which determined the deposition of a thick sedimentary cover (up to ~9 km), represents a natural laboratory to study the long-term deformation of the continental interiors. The results of the interpretation of almost 3000 km of seismic reflection profiles (Delvaux et al., 2021), show that the CB started to form from a rift phase, during the late Mesoproterozoic (about 1200 Myr). This extensional phase could have been likely the effect of the action of a slow multi-divergent velocity on a cratonic lithosphere, which have induced the initial subsidence of the CB in a weaker part of the craton. We tested this hypothesis through 3D numerical models, implemented using the thermomechanical I3ELVIS code (Gerya, 2013). For this purpose, we assumed that the amalgamation of the cratonic blocks forming the Congo craton left a weak 'suture' zone in the centre, having a size of 10% or 20% of the total area and a thinner and hotter lithosphere than the surrounding cratonic areas. The results obtained showed that the tectonic structures, formed by applying a N-S and E-W uniform velocity of 2.5 mm/yr, for a maximum time lapse of 200 Myr, are principally influenced by the variation of geometry design (size and lithospheric thickness of the weak zone) and thermal boundary conditions.

The main results given by two numerical simulations, taken as reference models, consist in the formation of an almost circular subsided area in the central part of the model, as effect of the kinematic boundaries, promoting the asthenosphere upwelling. This depressed area, which can represent the first stage of formation of the Cuvette Centrale, is consequence of the replacement of part of the lithosphere with denser and stiffer mantle material. The strong lateral density variations cause the formation of a series of topographic highs and lows inside the subsided area and the significant uplift at the transition zones towards the almost undeformed cratonic parts (Figure 1). The almost circular topographic depression is intersected by two strongly subsided elongated structures, orthogonal each other, which tend to raise their surface topography in the late stages of the multi-extensional deformation (> 100 Myr). These elongated structures cross each other in the centre of the models, forming quadruple junctions, similar to those produced by the numerical models of Gerya and Burov (2018), which simulate the nucleation and evolution of the triple junctions. However, differently from their models, our quadruple junctions are apparently stable features, since they are present in almost all the time steps of the simulations (between 0.010 Myr and 200 Myr). The structures, formed during the simulated multi-extensional tectonics, well represent the first order heterogeneity characterizing the CB basement depth, taking into account that the last one has been further modified by other tectonic and climate events. In particular, the CB basement depth is characterized by a series of lows and highs, NW-SE aligned, similar to those formed in our models in the central depressed part.

References

Delvaux, D., Maddaloni, F., Tesauro, M., Braitenberg, C. (2021). The Congo Basin: Stratigraphy and subsurface structure defined by regional seismic reflection, refraction and well data. Global and Planetary Change, 198, 103407. https://doi.org/10.1016/j.gloplacha.2020.103407

Gerya, T.V. (2013). Introduction to Numerical Geodynamic Modeling. Cambridge University Press. https://doi.org/10.1017/9781316534243.

Gerya, T.V., Burov, E.T. (2018). Nucleation and evolution of ridge-ridge-ridge triple junctions: Thermomechanical model and geometrical theory. Tectonophysics, 746, 83-105. https://dx-doi.org/10.1016/j.tecto.2017.10.020.

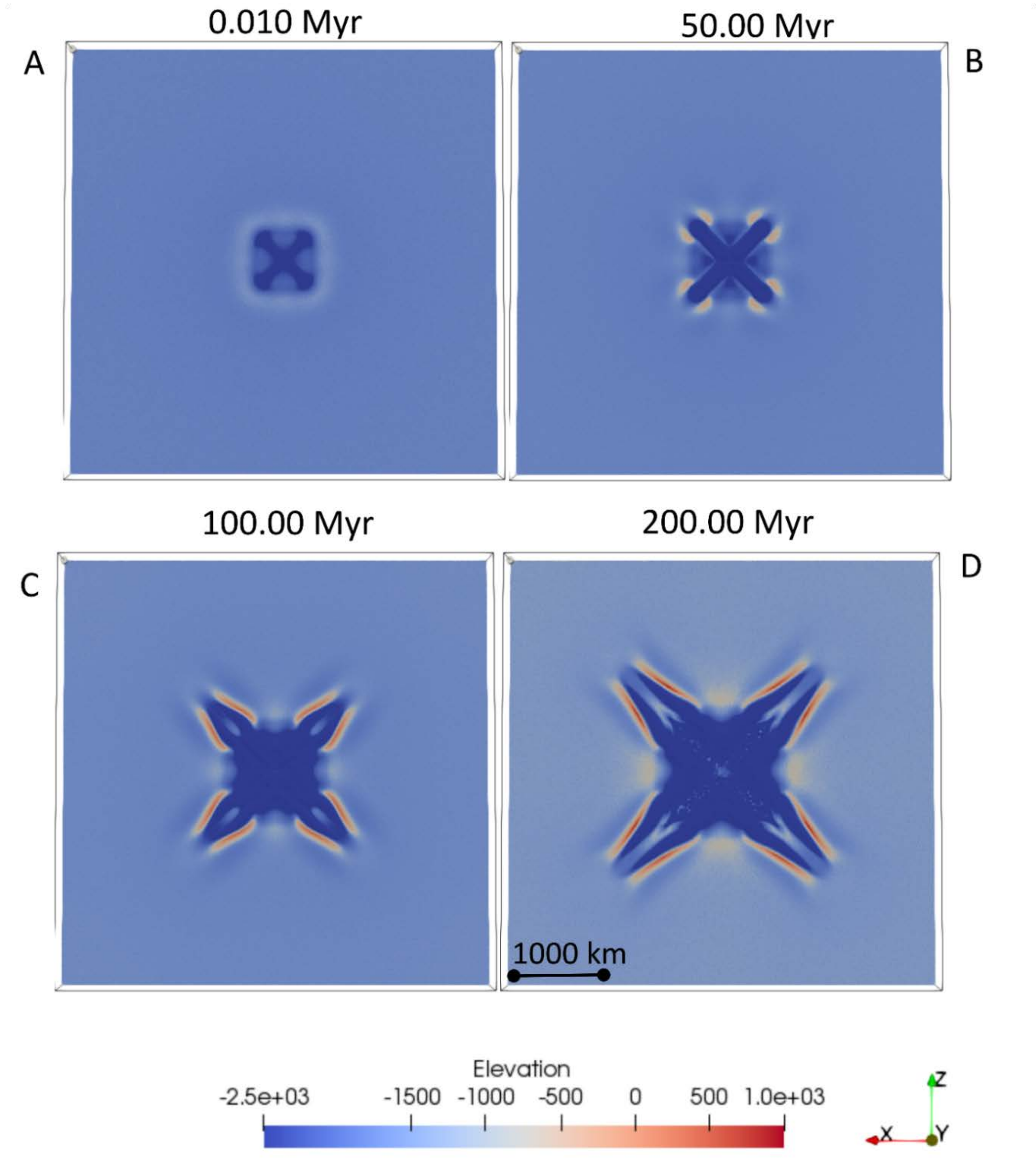

Figure 1. Example of 3D numerical simulation carried out applying a multi-divergent uniform velocity of 2.5 mm/yr for each side of the cratonic block, having a weak zone in the central part: Surface topography variations (m) at 0.010Myr (A), 50Myr (B), (C) 100 Myr, and 200Myr (D).

Continental delamination in the northern Apennines: insights from thermo-mechanical modelling.

Ana M. Negredo(1,2*), Carlos Clemente(1), Eugenio Carminati(3), Ivone Jiménez-Munt(4), Wentao Zhang(4,5), Estefania Bravo(4,5), Jaume Vergés(4), Javier Fullea(1), Montserrat Torné(4).

(1) Department of Physics of the Earth and Astrophysics, Complutense University of Madrid, Madrid, Spain,
(2) Institute of Geosciences IGEO, UCM-CSIC, Madrid, Spain
(3) Department of Earth Sciences, Università degli studi di Roma La Sapienza, Rome, Italy
(4) Group of Dynamics of the Lithosphere, Geosciences Barcelona (Geo3Bcn-CSIC), Barcelona, Spain
(5) Department of Earth and Ocean Dynamics, University of Barcelona, Barcelona, Spain

* Contact: amnegred@ucm.es

Abstract

The possibility of post-collisional continental delamination in the northern Apennines has been suggested by an increasing number of studies. We evaluate quantitatively this hypothesis by means of thermo-mechanical modelling. We use the Finite Element open source code ASPECT 2.2.0 (Bangerth et al., 2020) published under the GPL2, to solve the coupled equations of conservation of mass, momentum and energy for a 2D vertical section of an incompressible fluid. We adopt a visco-plastic rheology with a composite viscosity given by a combination of diffusion and creep dislocation viscous flow laws. The incorporation of a free surface along the top boundary allows us for properly modelling the topographic response.

The modelled cross-section strikes approximately from Corsica to the Adriatic Sea (solid blue line in Figure 1). The initial model setup simulates the scenario at ca 25 Ma, and it is characterised by compressional front being located in Corsica and the presence of some amount of continental subduction. The negative buoyancy of the slab remnant, together with the low viscosity of the dragged-down lower continental crust, promote lithospheric mantle sinking into the mantle. In turn, the low viscosity of the dragged-down lower continental crust enables asthenospheric upwelling and its lateral expansion along the lower crust.

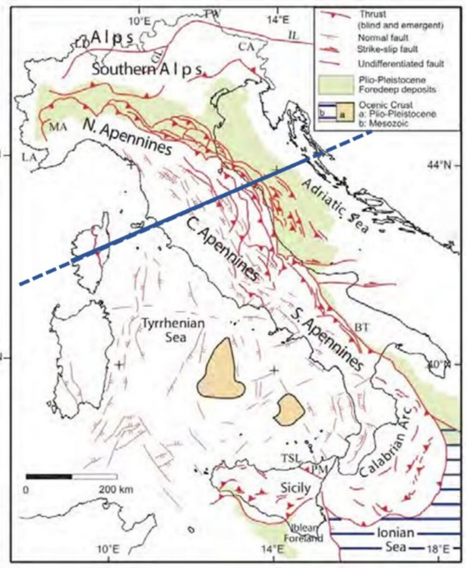

Figure 1. Trace of the modelled cross-section (dashed blue line indicates model expansion to avoid boundary effects), plotted on a simplified structural map of Italy (from Carminati et al., 2010; and references therein)

The surface response and mass distribution at two different time steps are shown in Figure 2. The horizontal velocity shows the eastward migrating pattern of extension (positive Vx horizontal gradient) and compression (negative Vx horizontal gradient). Consistent with geological data, the compressional front produced by delamination migrates about 260 km eastwards. The topographic response reflects the same eastward migrating pattern. It shows subsidence in the Tyrrhenian due to crustal thinning, then uplift in the Apennines caused by the combination of asthenospheric upwelling and crustal thickening, and subsidence at the front due to the pull exerted by the sinking lithospheric mantle. We also show that the fast asthenospheric upwelling generates partial melting, which migrates also eastwards, and high heat flow as it is observed in Tuscany.

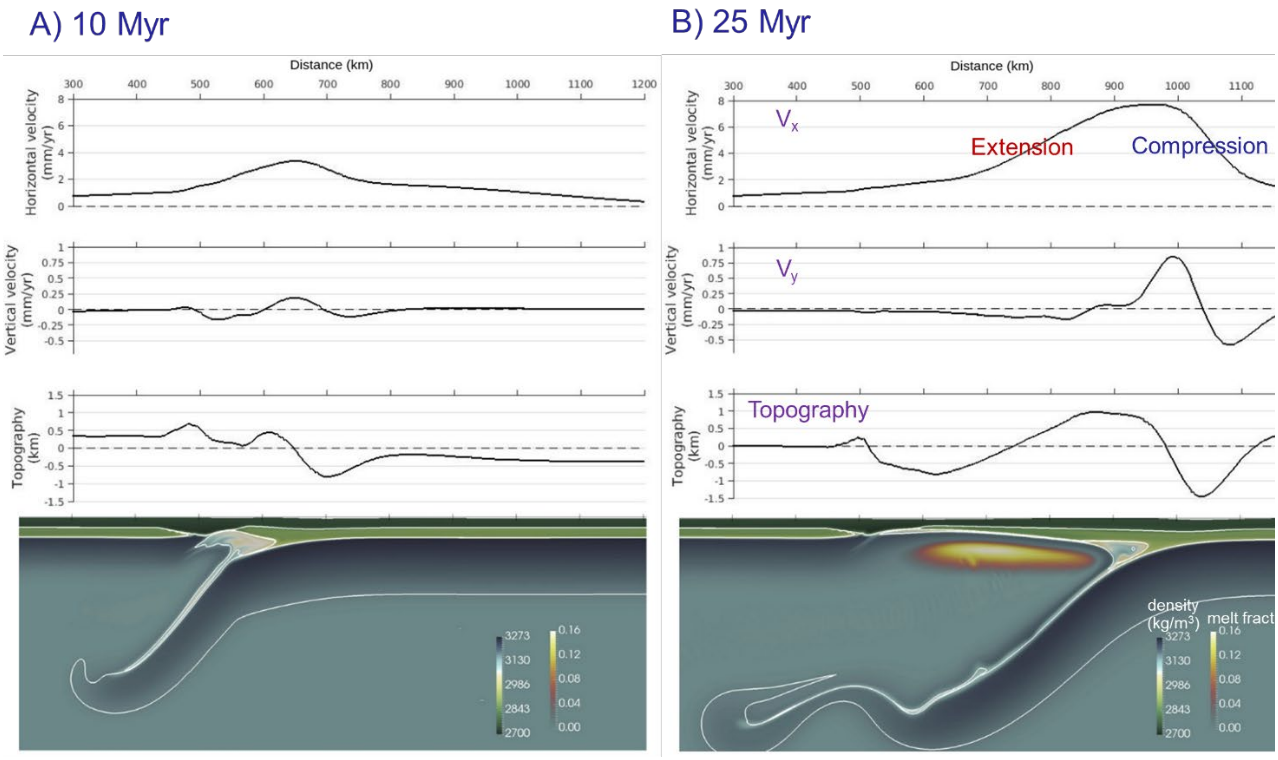

Figure 2: Distribution of density and maximum melt fraction assuming peridotite with 0.05% water content, (no vertical exaggeration). Horizontal and vertical velocities of the free surface, and topographic response.

This is a GeoCAM contribution (PGC2018-095154-B-I00)

References

Bangerth, W. Dannberg, J., Gassmoeller, R., & Heister, (2020a). ASPECT v2.2.0 (version v2.2.0). Zenodo. https://doi.org/10.5281/ZENODO.3924604. (find User Manual at https://doi.org/10.6084/m9.figshare.4865333.v7.)

Carminati, E., Lustrino, M., Cuffaro,M., & Doglioni, C. 2010. Tectonics, magmatism and geodynamics of Italy: what we know and what we imagine. ISSN 1441–8142 In: Beltrando, M., Peccerillo, A., Mattei, M., Conticelli, S., Doglioni, C. (Eds.). The Geology of Italy, Journal of the Virtual Explorer, 36. doi:10.3809/jvirtex.2010.00226. paper 8

Feedbacks between subduction dynamics and slab deformation: Combined effects of nonlinear rheology of a weak decoupling layer and phase transitions

Jakub Pokorný (1*), Hana Čížková (2), Arie van den Berg (3)
(1) Charles University Prague, Faculty of Mathematics and Physics, Department of Geophysics, Czech Republic,
(2) Charles University Prague, Faculty of Mathematics and Physics, Department of Geophysics, Czech Republic,
(3) Utrecht University, Institute of Earth Sciences, Department of Theoretical Geophysics, Netherlands
* Contact: jaakubpokorny@gmail.com

Abstract

Seismic tomography reveals a wide variety of slab deformation in the mantle transition zone and shallow lower mantle. Numerical modeling of subduction has identified several factors that control slab deformation, among them the properties of the mechanical decoupling between subducting and overriding plates was shown to have a major influence on slab velocity, rollback and deformation in the transition zone. Models with weak crust generally yield fast rollback and slab stagnation while stronger crust results in slab penetration into the lower mantle. Here we perform a detailed analysis of the effects of this weak crustal layer.

First, in models with constant crustal viscosity, we evaluate combined effects of crustal viscosity and thickness. We conclude that the dynamics of the subducting plate in the transition zone in the models with constant crustal viscosity is controlled by a frictional resistance parameter R. It is introduced as the ratio of the viscosity over the effective thickness of the weak crustal layer $R = \frac{\eta_{cr}}{d_{cr}^{eff}}$. We show that low crustal resistance associated with efficient decoupling of the plates results in slab flattening and stagnation at 660-km interface, while models with high crustal resistance exhibit less rollback and penetrating slabs. This is illustrated in Fig. 1 where we plot the resistance against the penetration depth of the slab after 150 Ma. Each model is represented by one symbol (circle, diamond or triangle). The symbols representing stagnant slabs correspond to penetration depths in the shallow lower mantle close to the 660 km boundary, while penetrating slabs are found deeper in the lower mantle. The transition between stagnant and penetrative slabs for models with constant viscosity crust is characterized by a resistance value $R_{crit} \approx 2 - 3 \times 10^{16}\ \mathrm{Pa\ s\ m^{-1}}$ represented by the dashed bar in Fig. 1. By introducing the resistance parameter we want to emphasize that the decoupling efficiency of the weak layer is not controlled by the layer viscosity alone, but rather by the combination of viscosity and thickness.

Further we apply nonlinear crustal rheology that combines dislocation creep and pseudoplastic deformation. We test the effects of varying parameterizations of the nonlinear rheological mechanisms and evaluate their effects on slab deformation. We conclude that the variations of subducting slab velocity (controlled by the buoyancy effects of the major phase transitions) induce strong time variations of the crustal viscosity that in turn enforce further acceleration or deceleration of the slab. This feedback between slab velocity and crustal viscosity strengthens transient behavior of the subducting slabs and enforces slab penetration after a transient period of stagnation. Models with nonlinear crustal rheology are represented by stars in resistance-penetration diagram in Fig. 1. Black star represents our reference model whose crustal rheological parameters are based on experiments on quartzite (Liao et al., 2017; Ranalli, 1995), green star is for model with parameters yielding weaker crust and red star for model with stronger crust. Compared to above discussed models with constant viscosity crust, here the division between the stagnant and penetrative models is shifted towards higher resistance. Apparently the time varying nature of crustal resistance in nonlinear models makes inferences about slab deformation more complicated and using one (average) resistance to characterize the models is problematic.

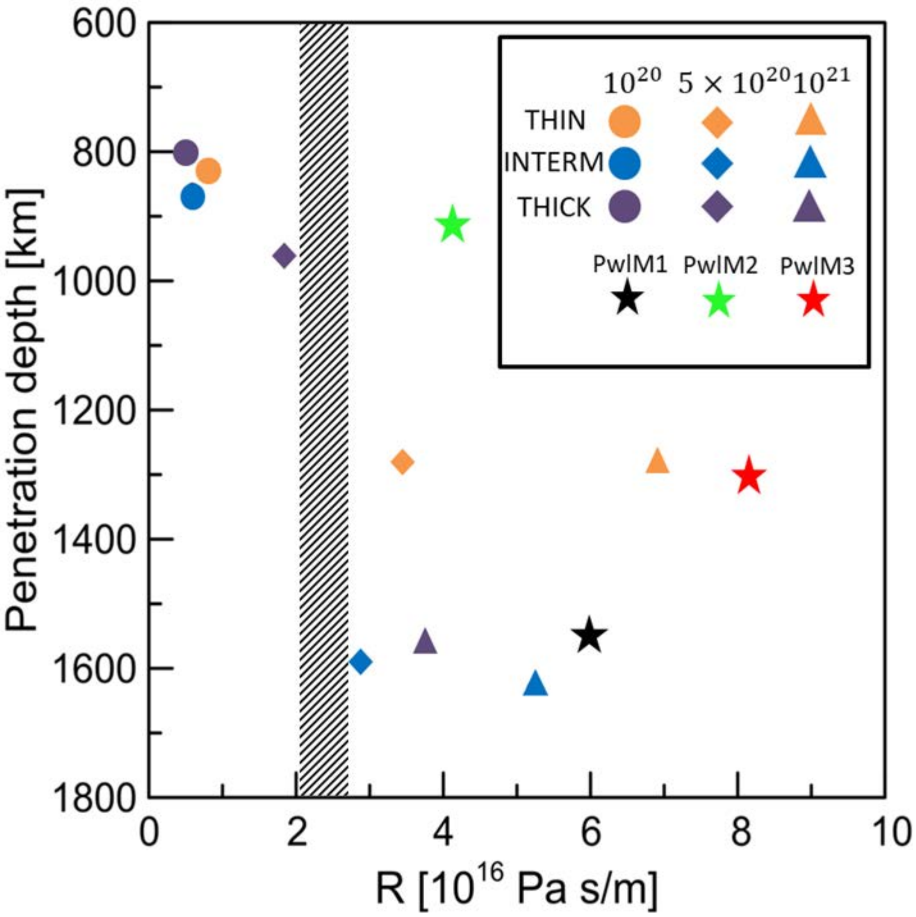

Figure 1: Penetration depth at 150 Ma as a function of crustal resistance R. R is defined as the ratio between crustal viscosity and its average thickness. Each symbol represents one of the models with constant viscosity crust (circles, diamonds and triangles) or models with nonlinear crustal rheology (stars). Black star is for model with reference crustal rheological parameters, green star for model with weaker crust and red star for model with stronger crust.

References

Liao, J., Gerya, T., Thielmann, M., Webb, A.A.G., Kufner, S.K., Yin, A., 2017. 3D geodynamic models for the development of opposing continental subduction zones: the Hindu Kush–Pamir example. Earth Planet. Sci. Lett. 480, 133–146. https://doi. org/10.1016/j.epsl.2017.10.005. ISSN 0012821X.

Ranalli, G., 1995. Rheology of the Earth. Springer Science & Business Media. ISBN 0412546701.

Control of subduction dynamics on shortening magnitude in the Central Andes: a thermomechanical modeling approach

Michaël Pons (1,2*), Stephan Sobolev (1,2)
(1) Universität Potsdam, Institut für Geowissenschaften, Germany, (2) Helmholtz-Zentrum Potsdam GFZ - Deutsches GeoForschungsZentrum, Germany

* Contact: ponsm@gfz-potsdam.de

Abstract

The subduction of the oceanic Nazca Plate under the continental South American Plate has been active since at least 180 Ma. However, the cause of the initiation of the shortening of the Andes during less than last 50 My or less, and the reasons behind the spatial and temporal variation in the magnitude of the shortening are still debated (Oncken et al., 2012).

In the case of the Central Andes, the South American plate is advancing westwards forcing the trench to retreat and the Nazca plate to roll-back. However, paleo-reconstructions of the margin position demonstrate that the trench velocity slowed down over the last ~50 My and became lower than the South American plate velocity. This difference of velocity is expressed by the shortening of the Andes. One reason for this decrease of velocity at the trench can be the anchoring of the slab in the lower mantle (Faccenna et al., 2017). Although this hypothesis provides an explanation for the initiation of shortening, it cannot explain the observed pulses of shortening (Oncken et al., 2012) as well as latitudinal variations of its magnitude (~300 km at ~18-21°S to ~100 km at 15°S latitude) .

In the central Andes, weakening mechanisms of the overriding plate (OP) such as lithospheric delamination have intensified the tectonic shortening and contributed to formation of the Altiplano-Puna plateau (Sobolev et al., 2006). Moreover, the difference in deformation style of the foreland basin, thick-skinned (e.g the Puna) and thin-skinned (e.g the Altiplano), respectively, is correlated with variations in the magnitude of shortening. Nevertheless, the influence of the strength variations in the OP on the subduction dynamics in the case of the central Andes has been poorly explored so far. Our hypothesis is that OP strength variations result in variable rates of trench roll-back. To test this hypothesis and in try to reproduce observed spatial and temporal variations of tectonic shortening in central Andes, we have built an E-W-oriented 2D geodynamic model along the Altiplano-Puna plateau which incorporated the flat subduction episode at ~35 Ma and following evolution of the lithospheric deformation. For that purpose, we used the FEM geodynamic code ASPECT. The model is semi-dynamic, which means that the oceanic plate evolves dynamically (i.e. buoyancy-driven), while the OP velocity is prescribed. Example of the model replicating deformation patterns and lithospheric structure at latitude 21 °S at present time is shown in Figure 1. We will discuss our new findings that demonstrate that not all key factors driving orogeny in central Andes have been considered in modelling studies so far.

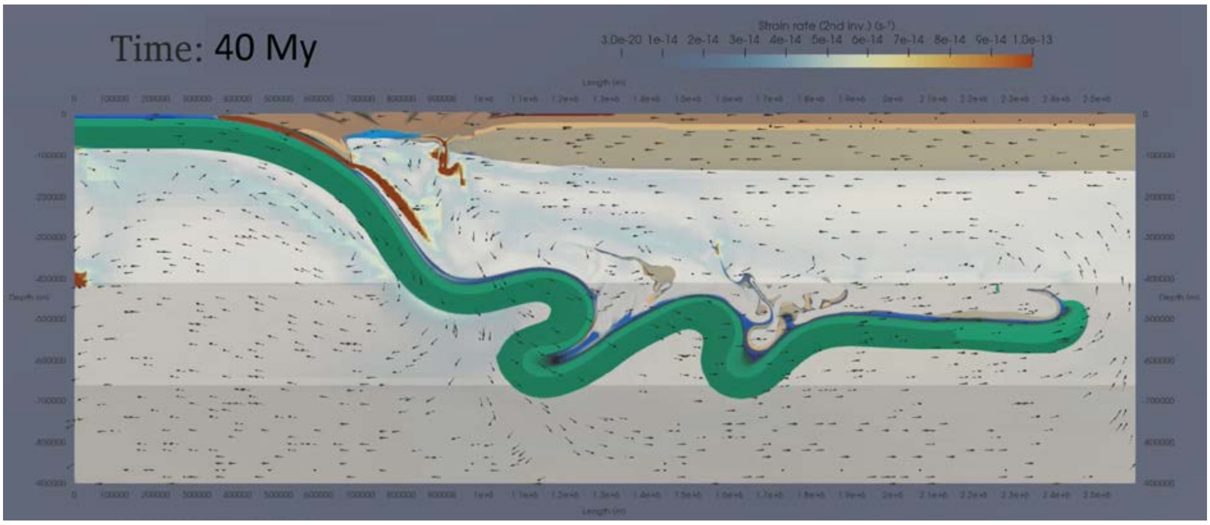

Figure 1: 2D subduction model of Central Andes at 21°S

References

Faccenna, C., Oncken, O., Holt, A. F., & Becker, T. W. (2017). Initiation of the Andean orogeny by lower mantle subduction. Earth and Planetary Science Letters, 463, 189-201.

Oncken, O., Boutelier, D., Dresen, G., & Schemmann, K. (2012). Strain accumulation controls failure of a plate boundary zone: Linking deformation of the Central Andes and lithosphere mechanics. Geochemistry, Geophysics, Geosystems, 13(12).

Sobolev, S. V., Babeyko, A. Y., Koulakov, I., & Oncken, O. (2006). Mechanism of the Andean orogeny: insight from numerical modeling. In The Andes (pp. 513-535). Springer, Berlin, Heidelberg.

Extrusion of subducted crust explains the emplacement of far-travelled ophiolites

Kristóf Porkoláb (1, 2*), Thibault Duretz (3), Philippe Yamato (3,4), Antoine Auzemery (1), Ernst Willingshofer (1)

(1) Faculty of Geosciences, Utrecht University, Utrecht, Netherlands, (2) Institute of Earth Physics and Space Science, Sopron, Hungary, (3) Univ Rennes, CNRS, Géosciences Rennes, Rennes, France, (4) Institut Universitaire de France (IUF), Paris, France
* Contact: kristof.porkolab@gmail.com

Abstract
Continental subduction below oceanic plates and associated emplacement of ophiolite sheets remain enigmatic chapters in global plate tectonics. Numerous ophiolite belts on Earth exhibit a far-travelled ophiolite sheet that is separated from its oceanic root by tectonic windows exposing continental crust, which experienced subduction-related high pressure-low temperature metamorphism during obduction. Despite these frequently observed field relations, the link between continental subduction-exhumation dynamics and far-travelled ophiolite emplacement is poorly understood. Here we combine data collected from ophiolite belts worldwide with thermo-mechanical simulations of continental subduction dynamics to show the causal link between the extrusion of subducted continental crust and the emplacement of far-travelled ophiolite sheets. Our results reveal that buoyancy-driven extrusion of subducted crust triggers necking and breaking of the overriding oceanic upper plate (Figure 1). The broken-off piece of oceanic lithosphere is then transported on top of the continent along a flat thrust segment and becomes a far-travelled ophiolite sheet separated from its root by the extruded continental crust.

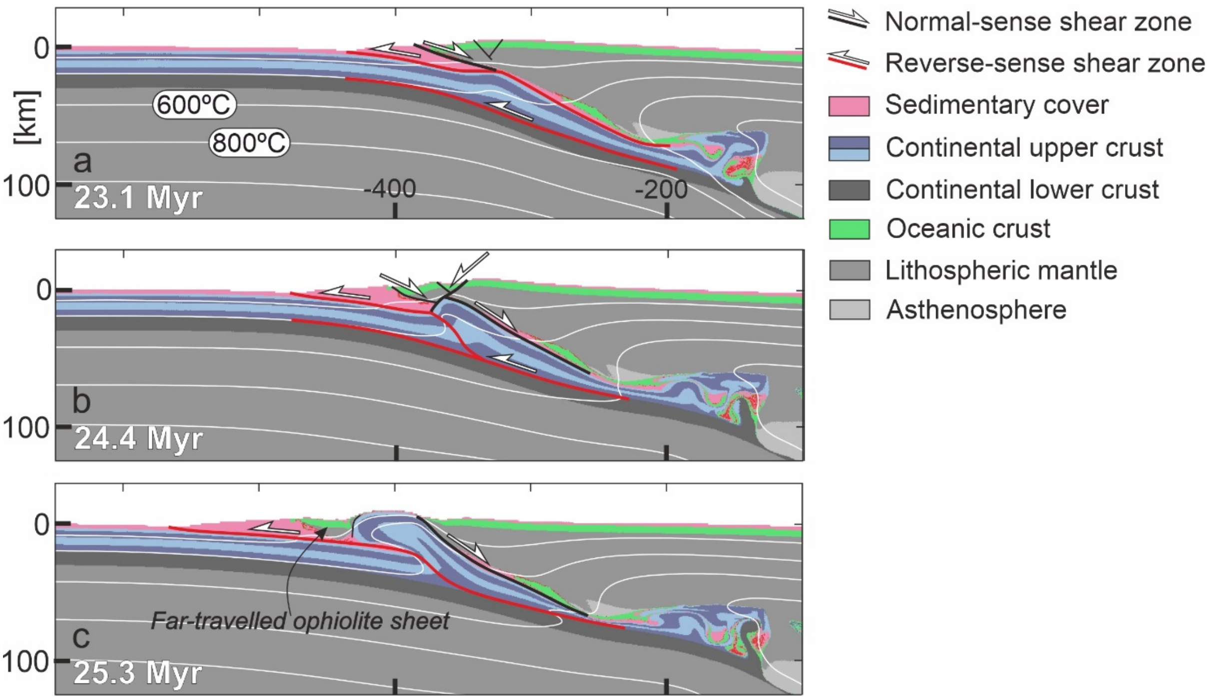

Figure 1: Compositional domains and structural interpretation of the reference model during the extrusion of the continental upper crust. Decoupling in the subducting plate and the initiation of upper plate extension (a) is followed by the initial extrusion of the continental upper crust and related necking of the oceanic upper plate (b), which eventually leads to the emplacement of a far-travelled ophiolite sheet (c).

Self-consistent grain size evolution controls lithospheric shear zone formation during rifting

Jonas B. Ruh (1*), Leif Tokle (2), Whitney M. Behr (1)
(1) Structural Geology and Tectonics Group, Geological Institute, Department of Earth Sciences, ETH Zürich, Switzerland
* Contact: jonas.ruh@erdw.ethz.ch

Abstract

In geodynamic numerical models, grain-size-independent dislocation creep often solely defines the governing crystal-plastic flow law in the upper mantle. However, grain-size-dependent diffusion creep may become the dominant deformation mechanism if grain size is sufficiently small. Previous studies implying composite diffusion-dislocation creep rheologies and fixed grain size suggest that the upper mantle is stratified with the dominant mechanism being dislocation creep at shallow depths and diffusion creep further down. Studies with variable grain size in the upper mantle depending on common grain-size evolution models demonstrate that the contrary might be the case, where diffusion creep is acting within the mantle lithosphere and dislocation creep in the asthenosphere below. Diffusion creep as a dominant mechanism has important implications for the overall strength of the lithosphere and therefore for the dynamic evolution of lithospheric-scale extension and orogeny.

Here, we present a 2D thermo-mechanical numerical model with a composite diffusion-dislocation creep flow law coupled to a self-consistent grain-size evolution model based on the paleowattmeter (Austin and Evans, 2007). Such a model allows us to estimate apparent grain size distribution and the dominant deformation mode within the upper mantle and to investigate the importance of grain size reduction for strain localization in the lithosphere during continental rifting. We test the influence of water in the mantle that is both affecting its viscosity and rate of grain growth. Furthermore, the effect of localized grain-size-dependent weakening on the long-term strength and elastic thickness of continental lithosphere is investigated and compared to pure dislocation creep and composite constant grain size experiments to test their validity.

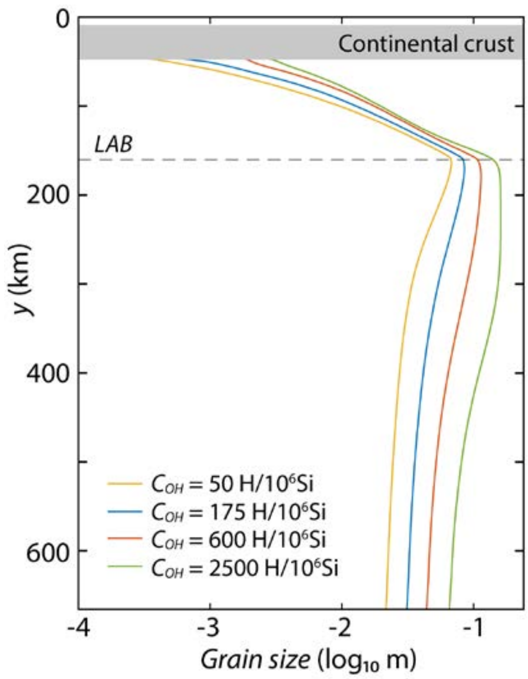

Figure 1: Olivine grain size along a vertical profile at the side of the model domain after 5 Myr of divergence. C_{OH} indicates applied fluid content affecting both viscous creep and olivine grain growth.

The numerical model employs a visco-elasto-plastic rheology and measures 1000 x 670 km with a 33-km-thick crust and a thermally-induced (1345°C) lithosphere-asthenosphere boundary (LAB) at 150 km depth. Lithospheric divergence is imposed by horizontal velocities of 5 mm/yr at both sides of the model domain. Grain size evolution of crustal and mantle material is separated into independent reduction and growth terms. Only mechanical work related to dislocation creep adds to grain size reduction which in turn enhances diffusion creep and grain growth (Evans and Austin, 2007). Therefore, if dislocation creep dominates deformation, grain size is mainly defined by dynamic recrystallization, whereas grain size during diffusion creep is determined by grain growth.

Results of upper mantle extension indicate olivine grain sizes of ~7 cm for large parts of the upper mantle below the LAB, while in the lithosphere grain size ranges from ~1 mm at the Moho to ~5 cm at the LAB (Figure 1). This grain size distribution indicates that dislocation creep dominates deformation in the entire upper mantle. However, diffusion creep activates along lithospheric-scale shear zones during rifting where intense grain size reduction occurs to local stress increase (Figure 2). We furthermore test the implications of wet and dry olivine rheology and respective crystal growth laws and interpret their effects on large-scale tectonic processes. Our results help explain strain localization during extension by strength loss related to grain size reduction and consequent diffusion creep activation.

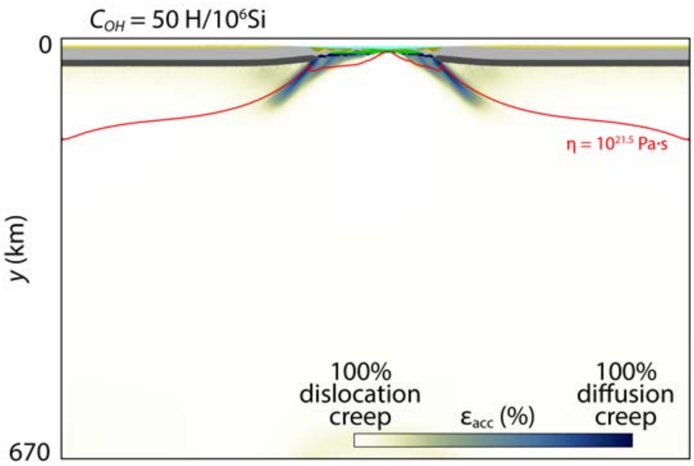

Figure 2: Fraction of accumulated viscous strain related to diffusion and dislocation creep. Blue indicates that strain accumulated by diffusion creep, while white colors denote dislocation creep related strain accumulation.

References

Austin, Nicholas J., and Brian Evans. "Paleowattmeters: A scaling relation for dynamically recrystallized grain size." *Geology* 35.4 (2007): 343-346.

Oceanic Transform Faults revisited

Lars Rüpke (1*), Ingo Grevemeyer (1), Jason P. Morgan (2), Karthik Iyer (1), Colin W. Devey (1)
(1) GEOMAR Helmholtz Centre for Ocean Research Kiel, (2) Southern University of Science and Technology, Shenzhen, China
* Contact: lruepke@geomar.de

Abstract

Oceanic Transform Faults (OTF) are fundamental to plate tectonics. At transforms, tectonic plates move horizontally past one another along small circles of plate motion, displaying strike-slip motion with lithosphere or crust being neither created nor destroyed. Oceanic fracture zones are the passive extension of the active transform faults and are visible as thousands of kilometers long scars in the ocean floor. In terms of subsidence, they should follow a simple trend given by plate cooling.

We have recently analyzed multibeam bathymetric data from 41 oceanic transform faults and their associated fracture zones and found that this assumption is incorrect (Grevemeyer et al., 2021). Rather, we find that the seafloor along transform faults is systemically deeper than at the associated fracture zones, which are therefore not simple passive continuations of their active transforms. To investigate the underlying mechanisms, we first used 3-D geodynamic models (using ASPECT) to understand what makes the pronounced transform valley. In a second step, we further analyzed the bathymetric data to find out what drives the anomalous subsidence at the ridge transform intersection (RTI). Our models show that a surface strike-slip kinematic boundary condition, will, due to the age-offset that causes an asymmetry in plate strength, turn into a slightly oblique and thereby extensional shear zone at depth. We interpret this extensional component as the process that makes the valley. This implies a progressive shift from near seafloor strike-slip tectonics to oblique shearing at depth. Detailed analyses of the bathymetric data showed that when this thinned lithosphere passes the opposite ridge-transform intersection, it appears to experience magmatic addition explaining the shallower relief of the fracture zones. This makes accretion at transform-fault systems a two-stage process, fundamentally different from accretion elsewhere along mid-ocean ridges.

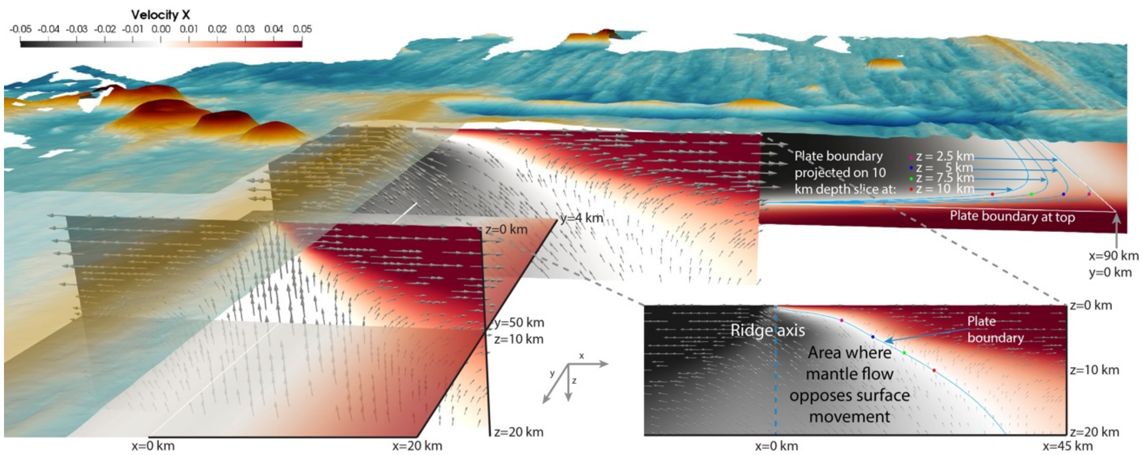

Figure 1: Figure shows the results of a 3-D viscoplastic geodynamic mantle flow model using parameters for the Clipperton Transform Fault. The solid white line on the z=10km plane marks the downward-projected location of the surface strike-slip boundary. The value of the horizontal x-velocity component is colour-coded. Beneath the spreading axis 50 km away from the Ridge-Transform-Intersection (RTI), mantle flow is symmetrical and shows the typical triangular-shaped pattern of passive mantle upwelling. Close to the RTI, mantle flow becomes highly asymmetric. This modifies the surface strike-slip motion into an oblique shear zone at depth.

References

Grevemeyer, I., Rupke, L.H., Morgan, J.P., Iyer, K., Devey, C.W., 2021. Extensional tectonics and two-stage crustal accretion at oceanic transform faults. Nature, 591(7850): 402-407.

Geodynamics of short-lived, long-lived and periodic flat slab subduction

Wouter P. Schellart (1*), Vincent Strak (1)
(1) Department of Earth Sciences, Vrije Universiteit Amsterdam, Amsterdam, Netherlands
* Contact: w.p.schellart@vu.nl

Abstract

Flat slab subduction is a peculiar type of subduction that occurs when the subducted slab lies flat below the base of the overriding plate for up to several hundred kilometers before bending into the deeper mantle (Barazangi and Isacks, 1976; Manea et al., 2017; Schellart, 2020). It is found in only a few places on Earth, most notably the Central Chile subduction segment, the Peru subduction segment and the Mexico subduction segment (Manea et al., 2017). Flat slab subduction has been ascribed to a variety of causes, including subduction of buoyant ridges/plateaus and forced trench retreat (e.g. Pilger, 1981; Gutscher et al., 2000; van Hunen et al., 2004; Manea and Gurnis, 2007; Antonijevic et al., 2015; Liu and Currie, 2016). Ridge/plateau subduction, however, shows irregular spatial correlations with flat slabs (Skinner and Clayton, 2013), while forced trench retreat has required external forcing in geodynamic subduction models, which might be insufficient or absent in nature (Schellart and Strak, 2021).

Here we present buoyancy-driven numerical geodynamic models using the code Underworld, and aim to investigate flat slab subduction in the absence of external forcing. The models are set up in a large two-dimensional domain, 10 000 km long by 2900 km deep, that includes a subducting plate, an overriding plate, the upper mantle and the entire lower mantle. Furthermore, we test the influence of a variety of subduction zone parameters, including overriding plate strength, subducting plate thickness, presence/absence of a buoyant ridge/plateau on the subducting plate and mantle viscosity stratification on flat slab formation and its evolution.

Flat slab subduction is reproduced during normal oceanic subduction in the absence of ridge/plateau subduction and without externally forced plate motion. Indeed, in our buoyancy-driven 2D environment, flat slab subduction is prevented during ridge/plateau subduction. Flat slab subduction only commences after a prolonged period of upper mantle slab dip angle reduction during lower mantle slab penetration. The flat slab is supported by mantle wedge suction, vertical compressive stresses at the base of the slab and upper mantle slab buckling stresses. Our models demonstrate three modes of flat slab subduction, namely short-lived, long-lived and periodic flat slab subduction, which occur for different model parameter combinations. Most models demonstrate slab folding at the 660 km discontinuity, which produces periodic changes in the upper mantle slab dip angle. With relatively high overriding plate strength, such folding results in periodic changes in the dip angle of the flat slab segment, which can lead to periodic flat slab subduction, providing a potential explanation for periodic arc migration. Flat slab subduction ends due to the local overriding plate shortening and thickening it produces, which forces mantle wedge opening and a reduction in mantle wedge suction. As overriding plate strength controls the shortening rate, it has a strong control on the duration of flat slab subduction, which lasts only ~6 Myr for the weakest plate and exceeds 75 Myr for the strongest plate. Progressive overriding plate shortening during flat slab subduction might explain why flat slab subduction terminated in the Eocene in western North America and in the Jurassic in South China.

References

Antonijevic, S.K., Wagner, L.S., Kumar, A., Beck, S.L., Long, M.D., Zandt, G., Tavera, H. & Condori, C. (2015). The role of ridges in the formation and longevity of flat slabs, Nature, 524, 212-215, https://doi.org/10.1038/nature14648.

Barazangi, M. & Isacks, B.L. (1976). Spatial distribution of earthquakes and subduction of the Nazca plate beneath South America, Geology, 4, 686-692.

Gutscher, M.A., Spakman, W., Bijwaard, H. & Engdahl, E.R. (2000). Geodynamics of flat subduction: Seismicity and tomographic constraints from the Andean margin, Tectonics, 19, 814-833.

Liu, S. & Currie, C.A. (2016). Farallon plate dynamics prior to the Laramide orogeny: Numerical models of flat subduction, Tectonophysics, 666, 33-47, https://doi.org/10.1016/j.tecto.2015.10.010.

Manea, V. & Gurnis, M. (2007). Subduction zone evolution and low viscosity wedges and channels, Earth and Planetary Science Letters, 264, 22-45, https://doi.org/10.1016/j.epsl.2007.08.030.

Manea, V.C., Manea, M., Ferrari, L., Orozco-Esquivel, T., Valenzuela, R.W., Husker, A. & Kostoglodov, V. (2017). A review of the geodynamic evolution of flat slab subduction in Mexico, Peru, and Chile, Tectonophysics, 695, 27-52, https://doi.org/10.1016/j.tecto.2016.11.037.
Pilger, R.H. (1981). Plate reconstructions, aseismic ridges, and low-angle subduction beneath the Andes, Geological Society of America Bulletin, 92, 448-456.
Schellart, W.P. (2020). Control of subduction zone age and size on flat slab subduction, Frontiers in Earth Science, 8, 26, https://doi.org/10.3389/feart.2020.00026.
Schellart, W.P. & Strak, V. (2021). Geodynamic models of short-lived, long-lived and periodic flat slab subduction, Geophysical Journal International, 226, 1517-1541, https://doi.org/10.1093/gji/ggab126.
Skinner, S.M. & Clayton, R.W. (2013). The lack of correlation between flat slabs and bathymetric impactors in South America, Earth and Planetary Science Letters, 371-372, 1-5, https://doi.org/10.1016/j.epsl.2013.04.013.
van Hunen, J., van den Berg, A.P. & Vlaar, N.J. (2004). Various mechanisms to induce present-day shallow flat subduction and implications for the younger Earth: a numerical parameter study, Physics of the Earth and Planetary Interiors, 146, 179-194, https://doi.org/10.1016/j.pepi.2003.07.027.

Continental rifting in rotational systems: Unravelling rift propagation processes using spatiotemporal high resolution quantified crustal-scale analogue models

Timothy C. Schmid (1*), Guido Schreurs (1), Jürgen Adam (2)
(1) Institute of Geological Sciences, University of Bern, Bern, Switzerland, (2) Earth Sciences Department, Royal Holloway University of London, Egham, United Kingdom
* timothy.schmid@geo.unibe.ch

Abstract

Here, we present new results and findings from an analogue modelling series with an extension velocity gradient to simulate continental rifting in rotational systems on a crustal scale. Our analogue model set up (Fig. 1) consists of a simplified mechanical two-layer system simulating an upper brittle and a lower ductile crust (respectively quartz sand and PDMS corundum sand mixture, Fig. 1a). A rod of ductile material ("seed"), placed on top of the viscous layer acts as a structural weakness at the base of the lower brittle layer, and ensures localized rifting. The applied extension velocity gradient causes rotational rifting and, on the other side of the rotation axis compression (Fig. 1b).

We investigate and quantify the effect of such a rift-axis parallel extension gradient on fault growth and rift propagation towards the rotation axis. For the quantitative analysis, we apply 3D Stereo Digital Image Correlation, a technique which combines 3D surface topography and respective 3D displacement fields from time-series stereo images (e.g., Adam et al., 2005). In combination with X-Ray computed tomography, we gain a comprehensive understanding of deformation evolution in analogue models of rotational rifting.

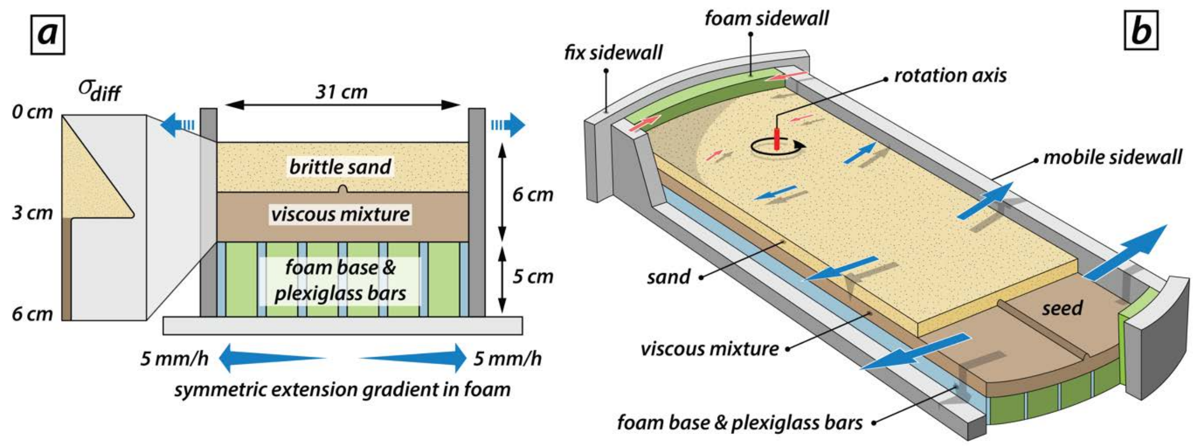

Figure 1: Model setup for conducted experiments. (a) The setup consists of a brittle sand layer on top of a PDMS/corundum sand mixture simulating a brittle upper and a viscous lower crust, respectively. The model sits on top of a foam base that extends homogeneously. (b) Cut-out view of the experimental apparatus. The box confines the model by two long movable and two short fixed curved side walls. The laundry-peg like motion defines a compressional (red arrows) and an extensional (blue arrows) domain separated by a rotation axis.

Our modelling results give insights into the 3D deformation structures of rotational rifting and reveal a rift evolution which is characterized by (1) rift propagation in two consecutive stages: A first stage showing bidirectional fault growth due to segment linkage with high rift propagation rates, and a second stage during which rift propagation occurs by unidirectional fault growth towards the rotation axis with linearly decreasing growth rates at decreasing distance to the rotation axis, (2) strain partitioning between competing conjugate normal faults with fault activity switching repeatedly from one segment of a normal fault to a segment on the oppositely dipping normal fault, and (3) active faulting migrating from the rift boundary faults inwards to intra-rift normal faults (Fig. 2). These processes occur stepwise along the rift axis as a function of bulk strain and result in a characteristic deformation pattern where different fault generations are simultaneously active.

Results from this analogue modelling study provide new findings of rotational rifting and highlight the importance of the rift-axis parallel, time dependent evolution of fault segments for the understanding of the tectonic history in rotational rift settings.

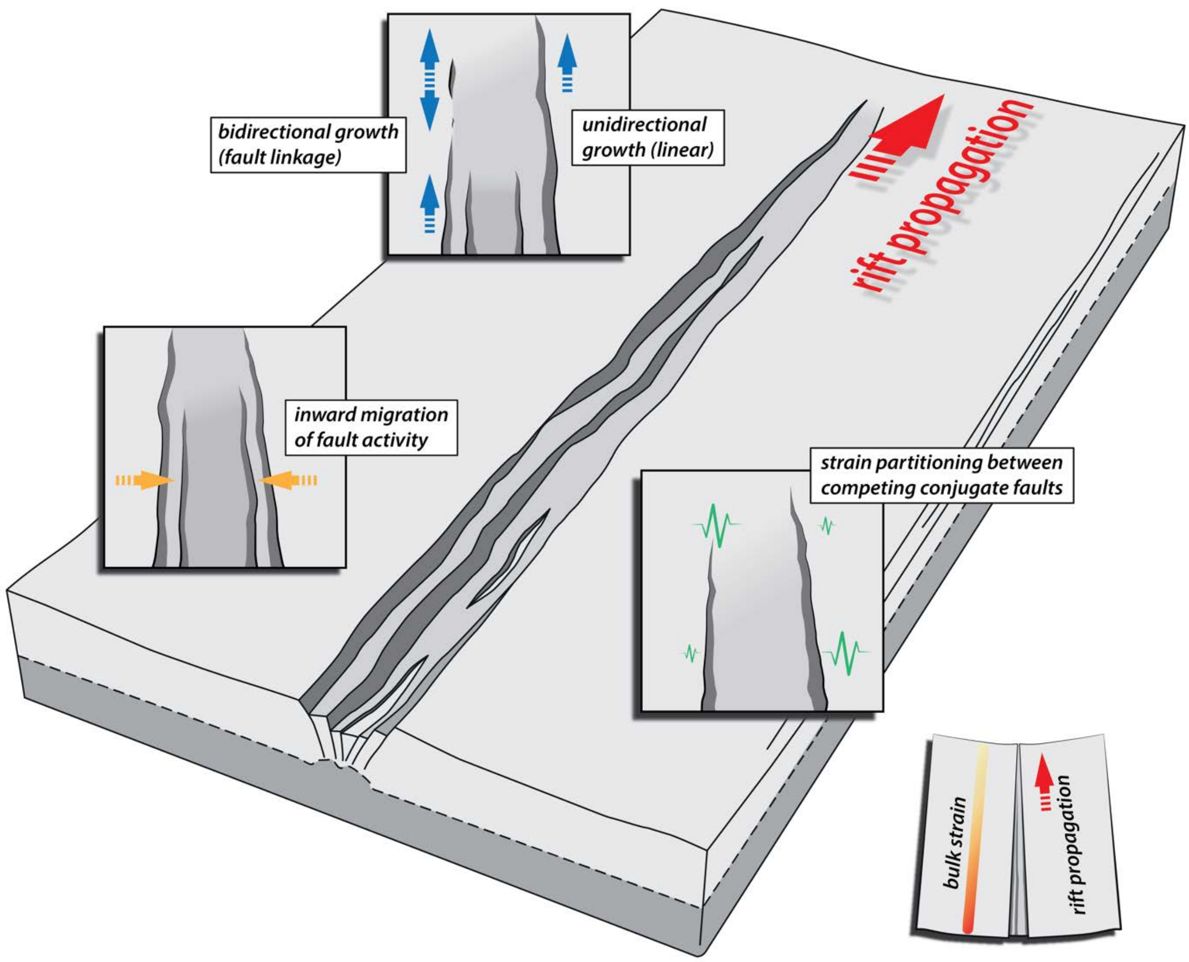

Figure 2: Sketch showing the key mechanism of rift propagation in our analogue models due to a pivoting motion around a rotation axis. Deformation processes occur stepwise as a function of increasing bulk strain with increasing distance with respect to the rotation axis (lower right corner).

References

Adam, J., Urai, J., Wieneke, B., Oncken, O., Pfeiffer, K., Kukowski, N., Lohrmann, J., Hoth, S., Van Der Zee, W., Schmatz, J. (2005). Shear localization and strain distribution during tectonic faulting - New insights from granular-flow experiments and high-resolution optical image correlation techniques. Journal of Structural Geology 27, 283–301. https://doi.org/10.1016/j.jsg.2004.08.008

Analogue models of lithospheric-scale rifting monitored in a CT-scanner

Guido Schreurs (1*), Frank Zwaan (1),
(1) University of Bern, Institute of Geological Sciences, Baltzerstrasse 1+3 Bern, Switzerland
* Contact: guido.schreurs@geo.unibe.ch

Abstract

Analogue modelling studies of rifting routinely focus on the crustal part of the lithosphere. Even though these models often contain a basal boundary condition based on an assumption regarding the underlying mantle lithosphere (Zwaan et al. 2019), the isostatic effects that a significant thinning of the lithosphere causes are ignored. Some modellers therefore involve the whole lithosphere in their models by having it float on top of a heavy fluid simulating the sub-lithospheric mantle (e.g. Brun & Beslier 1996). Such lithospheric-scale models have provided highly useful insights into rift evolution. However, the challenges of monitoring the inside of the modelled lithosphere during deformation pose a major challenge. This is especially true in models that involve a viscous lower crustal layer that decouples the upper crustal layer from the mantle layer, so that surface observations do not provide direct clues on deformation processes deep down in the model. To our knowledge, so far nobody has applied CT-scanning to monitor rifting models involving the sub-lithospheric mantle or asthenosphere.

We therefore present a new set of lithospheric-scale models, one of orthogonal and one of oblique rifting, both completed in an X-ray CT-scanner. The models, for which a novel set-up was designed, involved a typical 4-layer lithosphere, with brittle sand layers representing the competent upper crust and upper lithospheric mantel, and a viscous layer representing the ductile lower crust and lower lithospheric mantle (Fig. 1a). This 4-layer lithosphere was built up within a rectangular frame of sidewalls including an overlapping plate system on the short ends to accommodate orthogonal extension as the longitudinal sidewalls were moved apart. The short sidewalls were also equipped with a hinge system to accommodate additional lateral motion, in the case of oblique extension. The entire sidewall construction was itself placed within a basin of glucose syrup layer simulating the sub-lithospheric mantle. When moving the longitudinal sidewalls apart, the model lithosphere was stretched and this deformation was directly compensated by syrup flow from the basin into the space below the model lithosphere (Fig. 1a). In order to control the location of deformation along the central axis of the model, a weak “seed” (a ca. 1 cm high and wide ridge of viscous material) was inserted at the base of the strong mantle, i.e. the strongest layer within the (modelled) lithosphere (Fig. 1a). Model deformation was closely monitored through three high-resolution cameras providing 1-min interval time-lapse top- and oblique view pictures, whereas the CT-scanning was done at 15-min intervals.

In Model 1 (orthogonal extension), we found that the seed will early on localize deformation in the shape of normal faulting in the strong upper lithospheric mantle layer (Fig. 1a-b). This deformation was subsequently transferred into the strong upper crustal layer through low-angle shear zones within the viscous lower crustal layer, resulting in the formation of two grabens on both sides of the mantle weakness, with a general topographic depression in between (Figs. 1b, c). Of these two grabens, the left-hand one was dominant and as the model progressed, a right-lateral shear zone cutting through the whole lithosphere developed (Fig. 1d). In the meantime, the stretching and thinning (eventual necking) of the lithosphere completely separated the strong upper lithospheric mantle layers, allowing the viscous lower lithospheric mantle, and especially the syrup representing the sub-lithospheric mantle to rise up. This rise of material due to isostatic compensation brought the lower lithospheric mantle layer in contact with the lower crustal layer, and prevented complete collapse that would occur in a model with such a degree of lithospheric thinning, but without a sub-lithospheric mantle.

Model 2 reveals that 45˚ oblique extension also led to deformation in the strong upper lithospheric mantle layer, but did not cause the same localization and faulting of deformation on the surface as in Model 1 (Fig. 1a, e). Instead, only a general topographic depression developed, where upper crustal faulting only occurred at the model boundaries, even after > 3 h of extension (Fig. 1e). Hence we increased the extension velocity and thus the coupling between the upper lithospheric mantle and upper crustal layers (due to the strain-rate dependent rheology of the viscous lower crustal layer). As a result, faulting started localizing in the upper crustal layer (Fig. 1f), forming two bands of en echelon grabens on both sides of the mantle weakness (Fig. 1g).

These first model results show that both the novel modelling machine and the new set-up functions well, especially since the general results are similar to those of e.g. Brun & Beslier (1996). Yet our new CT-scans provide the first-ever direct insights into the internal deformation of a complete lithospheric-scale rifting model. Future particle image velocitmetry (PIV) analysis of these CT data will provide unique detailed quantitative insights into displacement and strain over time in such models. Furthermore, the oblique extension model suggests that oblique extension leads to less efficient localization of deformation, since higher extension rates are required to induce faulting in the upper crustal layer. This result interestingly seems to contradict the proposal by Brune et al. (2012) that oblique rifting promotes break-up.

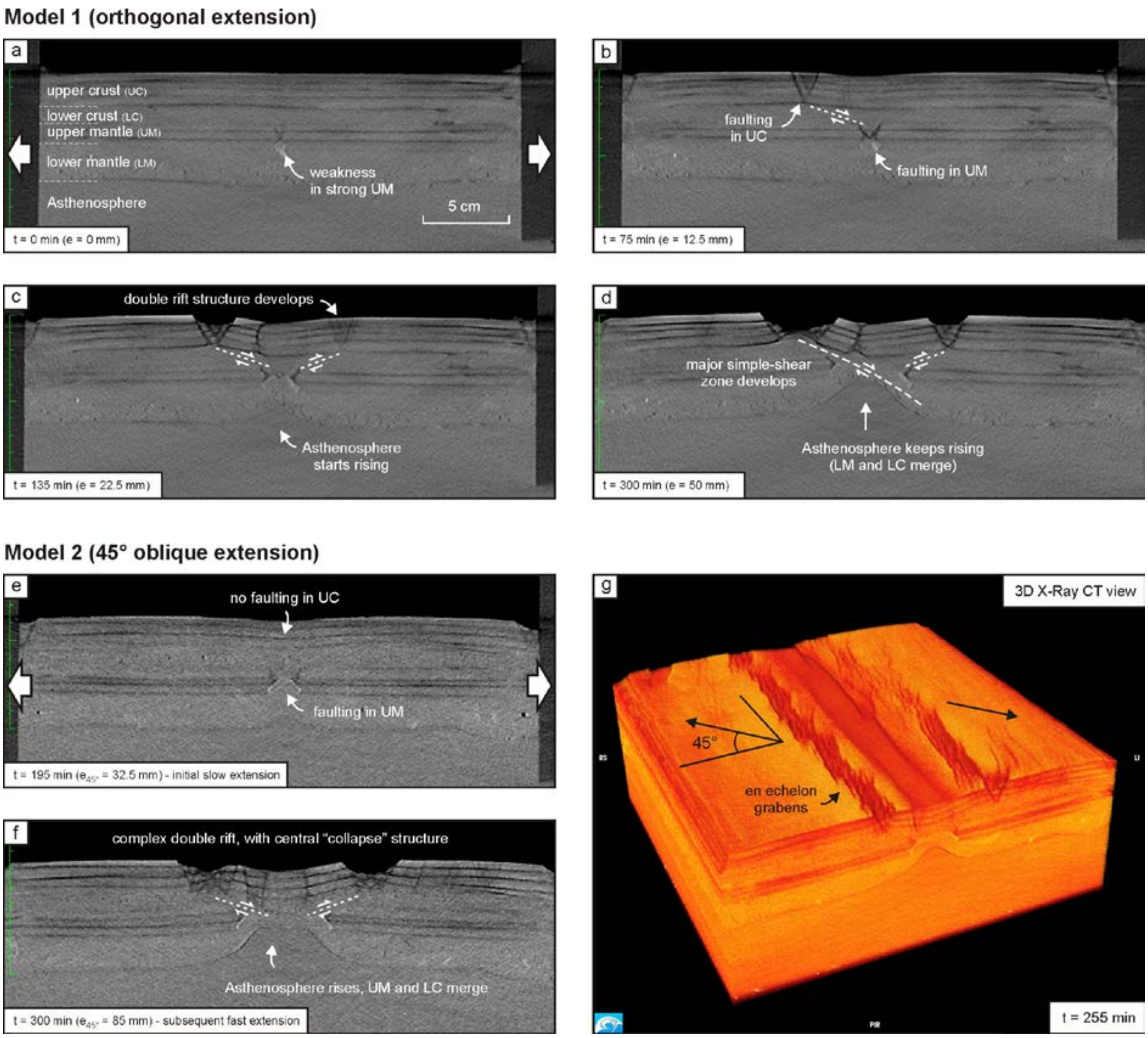

Figure 1: (a-d) CT-sections Model 1 (orthogonal extension, 10 mm/h over 5 h). (e-f) CT-sections of Model 2 (45˚ oblique extension), with a first slow extension phase and a second fast extension phase (e) end of phase 1 (10 mm/h for 195 min), (f) end of phase 2 (30 mm/h for 1:45 h). (g) 3D CT view of Model 2 at t = 255 min.

References

Brune, S., Popov, A.A., Sobolev, S.V. (2012). Modeling suggests that oblique extension facilitates rifting and continental break-up. Journal of Geophysical Research, v117. B08402. https://doi.org/10.1029/2011JB008860

Brun, J.P., Beslier, M.O. (1996). Mantle exhumation at passive margins. Earth and Planetary Science Letters. V142, 161-173. https://doi.org/10.1016/0012-821X(96)00080-5

Zwaan, F., Schreurs, G., & Buiter, S.J.H. (2019). A systematic comparison of experimental set-ups for modelling extensional tectonics. Solid Earth. v10, 1063-1097. https://doi.org/10.5194/se-10-1063-2019

Internal deformation of the Dolomites Indenter, eastern Southern Alps: Insights from crustal scale analogue modelling

Anna-Katharina Sieberer (1*), Ernst Willingshofer (2), Thomas Klotz (1), Hannah Pomella (1), Hugo Ortner (1)
(1) University of Innsbruck, Department of Geology, Innsbruck, Austria
(2) Utrecht University, Department of Earth Sciences, Utrecht, Netherlands
* Contact: anna-katharina.sieberer@uibk.ac.at

Introduction

The Dolomites Indenter (DI) represents the front of the Neogene to ongoing N(W)-directed continental indentation of Adria into Europe. Deformation of the DI is well studied along its rim, documented by important fault zones as, e.g., the Periadriatic fault system, the Giudicarie belt, and the Valsugana and Montello fault systems. The pre-shortening structure of the DI is predominantly related to Jurassic extension, which led to a platform-basin-topography controlled by NNE-SSW trending normal faults (Winterer and Bosellini, 1981). From west to east these are the Lombardian basin, Trento platform, Belluno basin, and Friuli platform (Winterer and Bosellini, 1981). This basin-platform configuration has been shortened during Alpine orogeny (Fig. 1a). Moreover, the northern Trento platform approximately coincides with the extent of the up to ~2 km thick (Avanzini et al., 2013) Permian Athesian Volcanic Group. In this contribution, we focus on the internal deformation of the DI and its eastern continuation towards the Dinarides. Through a series crustal scale analogue models, we investigate the effect of Jurassic E-W extension on the NW-SE directed deformation of the DI since Neogene times.

Experimental setup

The performed brittle and brittle-ductile analogue experiments can be grouped in two sub-series. In sub-series A, the platform-basin topography has been achieved by pre-scribing an initial strength contrast between platforms and basins followed by one stage of indentation. Additionally, rigid Permian magmatic rocks, which we assume could have led to a critical strengthening of the crust, were modelled by specifically varying the thickness and shape of the northern Trento platform. In sub-series B, graben structures were developed through an initial extensional phase, subsequently followed by compression. The evolving grabens were syn-kinematically filled up to different thicknesses depending on the material used. In both sub-series, variations in the orientation of rheological boundaries with respect to the convergence direction have been modelled. This (oblique) basin inversion allows us to test various deformational styles and wavelengths as well as timing and localisation of uplift of the DI's upper to middle crust.

The brittle upper crust of platforms was simulated with quartz sand, the brittle to ductile middle crust by either glass beads or by a mixture of polydimethylsiloxane (PDMS) silicon putty and quartz sand. The basins were filled with either quartz sand up to a platform/basin thickness ratio of 0,75 or with feldspar sand or glass beads up to the initial, non-stretched crustal thickness. Models of sub-series A were built on one fixed plastic sheet (Fig. 1b), models of sub-series B on one fixed and two mobile plastic sheets (Fig. 1c). The mobile plastic sheets were pulled from below the fixed plastic sheet in opposite directions, in order to localise extensional structures W and E of the Trento platform.

Preliminary results

Preliminary modelling results confirm the localisation of deformation in areas of lateral strength contrasts (Brun and Naplas, 1996), as transitions from platforms to basins represent (Fig. 2). The extent of strike-slip movement accompanying thrusting in those transitional areas is analysed using the strainmap code of Broerse et al. (2021). Spacing of in-sequence thrusts is larger on platforms and smaller in basins (Fig. 2b). This difference in spacing is visible in both, models of sub-series A (inversion of strength difference only) and B (inversion of strength difference and actual normal faults). The vergence of in-sequence structures varies from classic pop-up structures using putty as basal detachment for thick-skinned thrusting, to mostly foreland directed thrusting using glass beads to a combination of both using quartz sand only.

Outlook

Our findings from crustal scale analogue modelling will be combined with further kinematic field data and a comprehensive low-T thermochronology dataset of the Dolomites Indenter in order to get an integrated understanding of its 4D tectonic evolution.

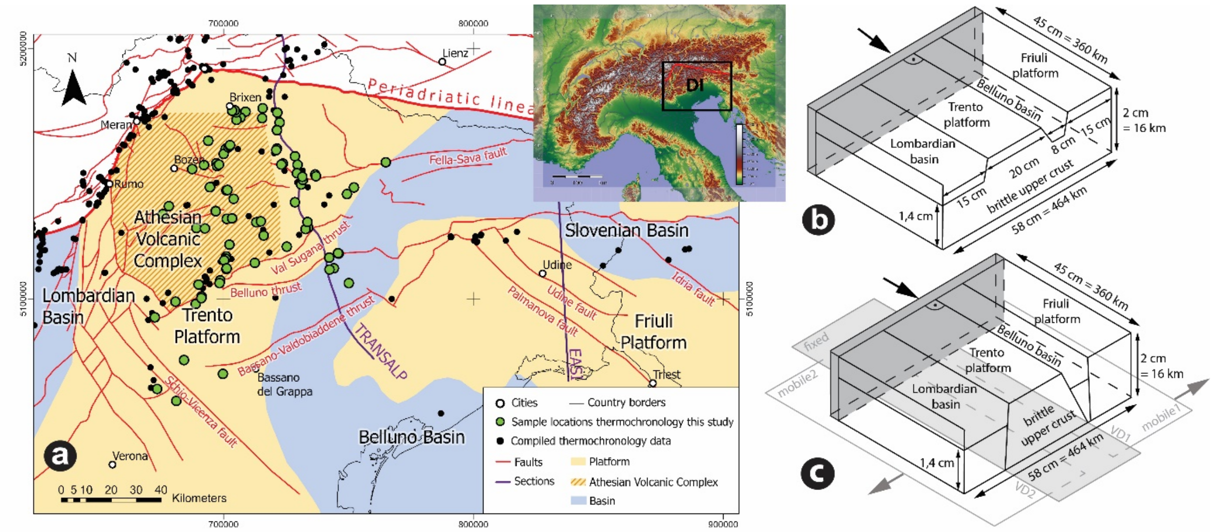

Figure 1: (a) Platform/basin configuration of the study area. (b) Experimental setup with rheological boundaries orthogonal to the backstop of sub-series A and (c) of sub-series B.

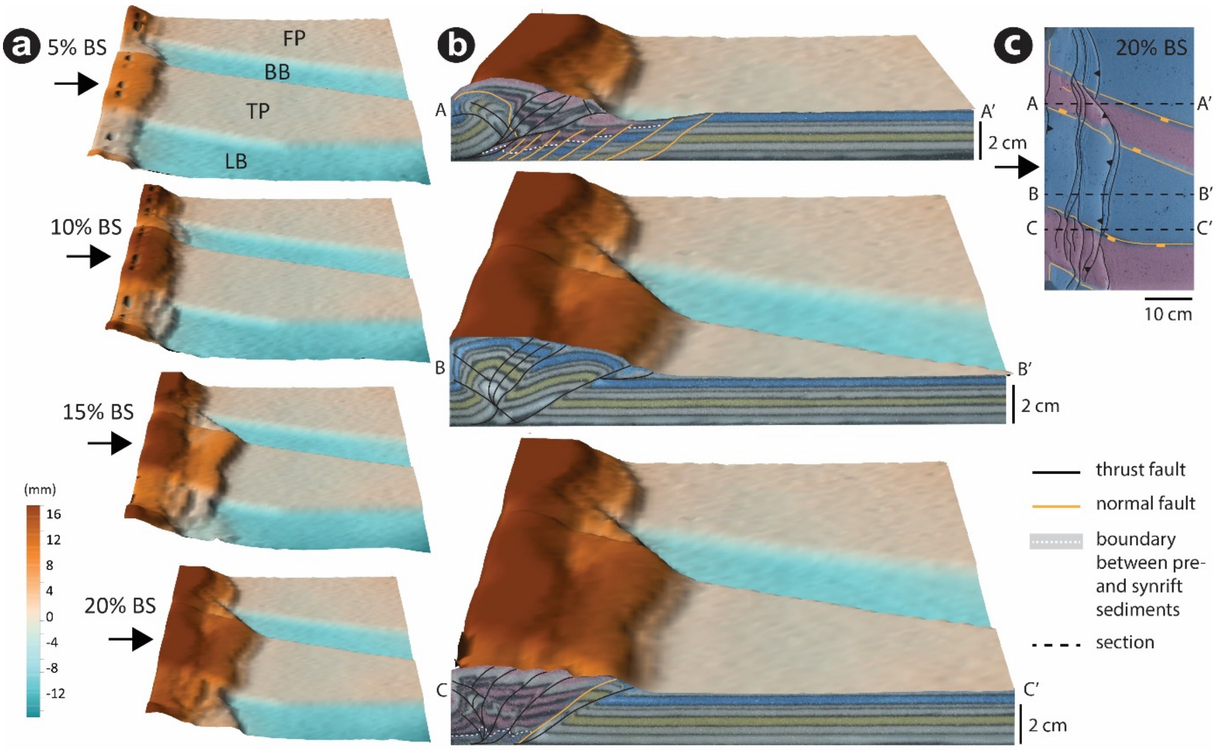

Figure 2: Experimental results of sub-series B with basin filling of quartz sand up to a platform/basin thickness ratio of 0,75 for oblique (70°) basin inversion shown through (a) surface scans (b) representative cross-sections at 20% BS, and (c) a topview picture. Abbreviations: FP = Friuli platform, BB = Belluno basin, TP = Trento platform, LB = Lombardian basin, BS = bulk shortening.

References

Avanzini, M., Bargossi, G. M., Cucato, M., Morelli, C., Prosser, G., Tomasoni, R. (2013). Note illustrative della carta geologica d'Italia alla scala 1:50.000, foglio 026 Appiano. Servizio Geologico d'Italia, APAT.

Broerse, T., Krstekanić, N., Kasbergen, C., Willingshofer, E., 2021. Mapping and classifying large deformation from digital imagery: application to analogue models of lithosphere deformation. Geophys. J. Int. v. 225, p. 984–1017.

Brun, J.-P., Nalpas, T. (1996). Graben inversion in nature and experiments. Tectonics. v. 15, no. 3, p. 677-687.

Winterer, E. L., Bosellini, A. (1981). Subsidence and Sedimentation on Jurassic Passive Continental Margin, Southern Alps, Italy. AAPG Bulletin. v. 65, no.3, 394-421.

Interplay of surface and deep-seated processes in initiation and evolution of plate tectonics on Earth

Stephan Sobolev (1,2) and MEET Modeling Group *(keynote)*
(1) Helmholtz-Zentrum Potsdam GFZ - Deutsches GeoForschungsZentrum, Germany, (2) Universität Potsdam, Institut für Geowissenschaften, Germany.
* Contact: stephan@gfz-potsdam.de

Abstract
Despite the obvious importance of plate tectonics for Earth's evolution, its origin and controlling factors remain poorly understood. Recently, by extrapolation of models of present-day plate tectonics (Figure 1a,b) to the past, it was suggested that major surface erosion events controlled the emergence and evolution of plate tectonics by providing sediments that lubricated subduction interfaces (Sobolev and Brown, 2019). Before the emergence of continents about 3Ga, the flux of sediments (lubricant) to the trenches was very limited. We suggest that subduction zones were already present at that time but were likely initiated only above hot mantle plumes, as modeled by Gerya et al. (2015). This tectonic regime of regional plume-induced retreating subduction zones (Figure 1c) was very different from the modern type of plate tectonics, but nevertheless might have been very efficient in production of early continental crust and transporting surface water and recycling of the crust into the deep Earth interiors.

After the emergence of continents, a regime of intermittent plate tectonics developed in which periods of active plate tectonics followed events of large active continental erosion and an intensive supply of sediments into the ocean. Various geological and geochemical data are consistent with the hypothesis that the two largest surface erosion and subduction lubrication events occurred after the Palaeoproterozoic Huronian global glaciations (2.45 to 2.2 billion years ago), leading to the formation of the Columbia supercontinent, and after the Neoproterozoic 'snowball' Earth glaciations (0.75 to 0.63 billion years ago) that kick-started the modern episode of active and continuous plate tectonics (Sobolev and Brown, 2019) (Figure 1c).

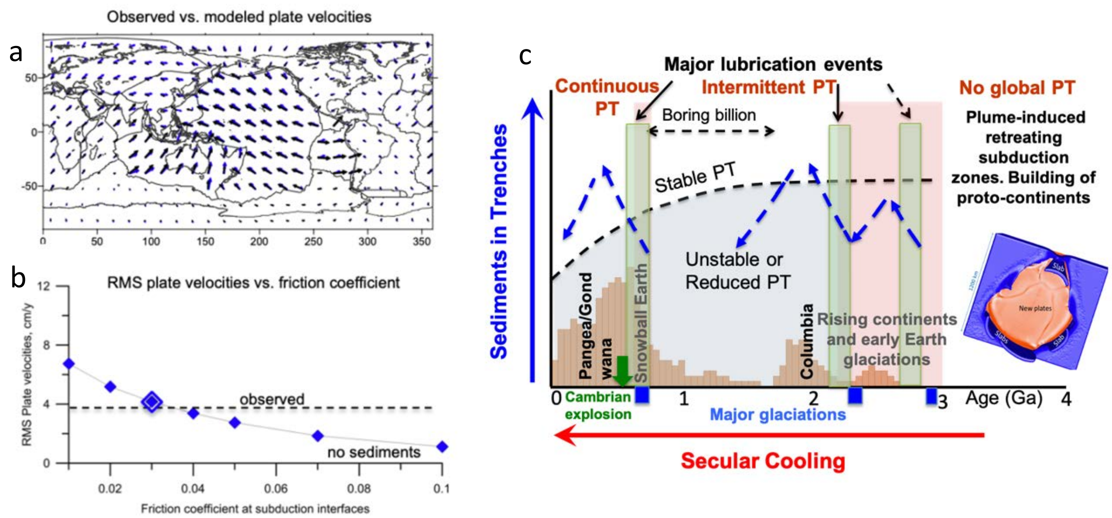

Figure 1: (a)-Global model of present-day plate tectonics (PT). (b)- The same with variable effective friction coefficient at subduction interfaces (Sobolev and Brown, 2019; see methods in Osei Tutu, et al., 2018). Large blue diamond in (b) corresponds to the best fit model of PT shown in (a). Models show that in the absence of sediments lubricating subduction interfaces, contemporary PT would be sluggish. (c)- Cartoon summarizing the factors that control the emergence and evolution of PT on Earth (modified from Sobolev and Brown, 2019). The reddish domain shows the number of passive margins (Bradley 2008), here used as a proxy for plate tectonic intensity.

We further test this hypothesis focusing at the last 1Gyr period of the Earth's history and using an updated model of Phanerozoic plate motions by Torsvik and Cocks (2016) and other published models, as well as geochemical proxies of the influence of continental sediments in seawater and in magma sources. The modeled plate velocities are relatively slow during the Neoproterozoic and then peak at about 500Ma, 100-200My after the ‘snowball Earth’ glaciations. The maximum velocity and velocity-decaying trend through most of the Phanerozoic correlates remarkably with the geochemical proxies of the influence of sediments on the composition of seawater and continental crust melt sources. This data and data on the evolution of the length of orogenic belts (Li at al., 2019) can be interpreted as the effect of a major surface erosion event during and following snowball Earth glaciations that activated plate tectonics after the so-called ´boring billion’, a period of diminished plate tectonic activity (Cawood and Hawkesworth, 2014). The snowball Earth event triggered a number of succeeded collision events that provided sediments to the trenches that lubricated subduction channels. The volume of sediments in trenches decayed with time, likely due to the decreasing length of the continental margins during assemblage of Gondwana-Pangea supercontinent. The decreasing volume of the sediments in trenches caused a reduction of plate velocities.

This is a contribution of the European Research Council (ERC) Synergy Grant Project “Monitoring Earth Evolution Through Time (MEET)”.

References

Bradley, D. C. (2008). Passive margins through earth history. Earth Sci. Rev. v91, 1–26, https://doi.org/10.1016/j.earscirev.2008.08.001

Cawood, P. A. & Hawkesworth, C. J. (2014). Earth’s middle age. Geology v42, 503–506, https://doi.org/10.1130/G35402.1

Gerya, T. V. et al. (2015). Plate tectonics on the Earth triggered by plume-induced subduction initiation. Nature v527, 221–22, https://doi.org/10.1038/nature15752

Li, Z. X. et al. (2019). Decoding Earth’s rhythms: modulation of supercontinent cycles by longer superocean episodes. Precambr. Res. v323, 1–5, https://doi.org/10.1016/j.precamres.2019.01.009

Osei Tutu, A. et al. (2018). Evaluating the influence of plate boundary friction and mantle viscosity on plate velocities. Geochem. Geophys. Geosyst. v19, 642-666.https://doi.org/10.1002/2017GC007112

Sobolev, S.V. & Brown, M. (2019). Surface erosion events controlled the evolution of plate tectonics on Earth. Nature, v570, 52-57, https://doi.org/10.1038/s41586-019-1258-4

Torsvik , T., & Cocks, L. (2016). Earth History and Palaeogeography. Cambridge: Cambridge University Press, v317 p.https://doi.org/10.1017/9781316225523

3D mantle flow induced by retreating and advancing slabs: insights from analogue subduction models analysed with a tomographic Particle Image Velocimetry technique

Vincent Strak (1*), Wouter P. Schellart (1), Kai Xue (1)
(1) Department of Earth Sciences, Vrije Universiteit Amsterdam, Amsterdam, Netherlands
* Contact: v.strak@vu.nl

Abstract

Subduction-induced mantle flow is known to have a significant geodynamic impact on Earth. The resulting quasi-toroidal circulation can produce mantle upwellings and promote associated intraplate volcanism (Jadamec and Billen, 2010; Strak and Schellart, 2014), deflect and interact with mantle plumes (Meriaux et al., 2015; Strak and Schellart, 2018), transport geochemical signatures laterally over great distances (Turner and Hawkesworth, 1998; Trua et al., 2003), deform the overriding plate (Schellart and Moresi, 2013; Sternai et al., 2014; Chen et al., 2016), and promote the generation of flat slabs due to whole-mantle circulation (Schellart and Strak, 2021). To date, modelling efforts have concentrated on characterising the 3D pattern of the mantle flow associated with slab rollback (e.g. Buttles and Olson, 1998; Kincaid and Griffiths, 2003; Schellart, 2004; Funiciello et al., 2006; Loiselet et al., 2009; Li and Ribe, 2012; Schellart and Strak, 2014; Kiraly et al., 2017), since this subduction mode is dominant on Earth (Xue et al., 2020). The mantle flow generated by advancing slabs (rollover subduction) thus remains unstudied and its geodynamic significance unclear.

Here, we conducted analogue buoyancy-driven subduction models to investigate the mantle flow generated in both retreating and advancing subduction modes. We analysed our models using a novel tomographic Particle Image Velocimetry technique, allowing us to compute the 3D velocity field in a volume of the mantle.

Our model results show that the advancing subduction mode develops a slab rollover geometry that produces a quasi-toroidal mantle flow with mantle material displaced from the mantle wedge domain to below the subducting plate, opposite to mantle flow during the retreating mode (Figure 1). This slab rollover-induced mantle flow generates an upwelling component that is laterally offset from the subducting plate and is located some ~1000 km from the trench on the subducting plate side. Such newly imaged mantle flow has implications for intraplate volcanism and the distribution of mantellic geochemical signatures associated with advancing subduction zones, such as the Makran, and continental subduction zones, such as the Himalaya.

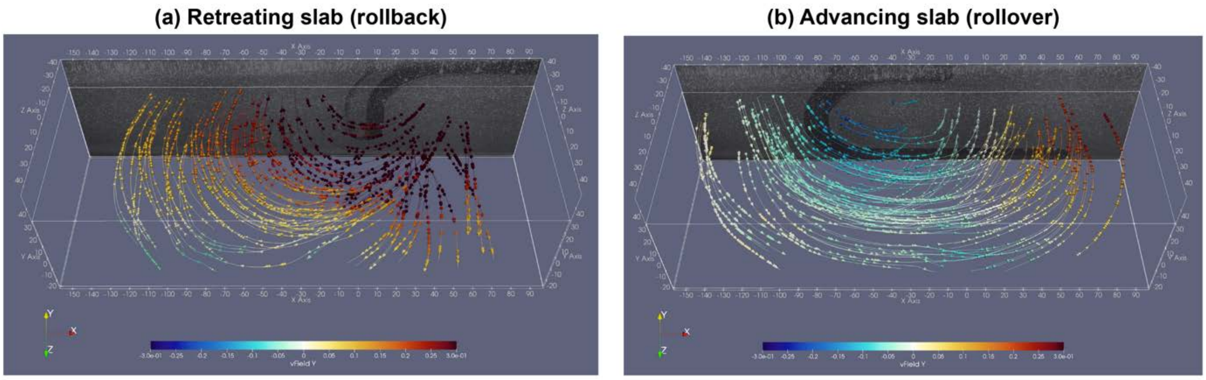

Figure 1: 3D mantle flow around lateral slab edge during (a) slab free sinking phase and (b) slab advancing phase. The direction of the flow is represented by streamlines with the colour scale indicating the magnitude of the vertical component (in mm/min).

References

Buttles, J. & Olson, P. (1998). A laboratory model of subduction zone anisotropy. Earth and Planetary Science Letters. 164, 245–262. https://doi.org/10.1016/S0012-821X(98)00211-8.

Chen, Z., Schellart, W. P., Strak, V. & Duarte, J. C. (2016). Does subduction-induced mantle flow drive backarc extension? Earth and Planetary Science Letters. 441, 200–210. https://doi.org/10.1016/j.epsl.2016.02.027.

Funiciello, F., Moroni, M., Piromallo, C., Faccenna, C., Cenedese, A. & Bui, H. A. (2006). Mapping mantle flow during retreating subduction: Laboratory models analyzed by feature tracking. Journal of Geophysical Research Solid Earth. 111, 1–16. https://doi.org/10.1029/2005JB003792.

Jadamec, M. A. & Billen, M. I. (2010). Reconciling surface plate motions with rapid three-dimensional mantle flow around a slab edge. Nature. 465, 338–341. https://doi.org/10.1038/nature09053.

Kincaid, C. & Griffiths, R. W. (2003). Laboratory models of the thermal evolution of the mantle during rollback subduction. Nature. 425, 58–62. https://doi.org/10.1038/nature01923.

Király, Á., Capitanio, F. A., Funiciello, F. & Faccenna, C. (2017). Subduction induced mantle flow: Length-scales and orientation of the toroidal cell. Earth and Planetary Science Letters. 479, 284–297. http://dx.doi.org/10.1016/j.epsl.2017.09.017.

Li, Z. H. & Ribe, N. M. (2012). Dynamics of free subduction from 3-D boundary element modeling. Journal of Geophysical Research Solid Earth. 117, 1–18. https://doi.org/10.1029/2012JB009165.

Loiselet, C., Husson, L. & Braun, J. (2009). From longitudinal slab curvature to slab rheology. Geology. 37, 747–750. https://doi.org/10.1130/G30052A.1.

Meriaux, C. A., Duarte, J. C., Schellart, W. P. & Meriaux, A .S. (2015). A two-way interaction between the Hainan plume and the Manila subduction zone. Geophysical Research Letters. 42, 5796–5802. https://doi.org/10.1002/2015GL064313.

Schellart, W. P. (2004). Kinematics of subduction and subduction-induced flow in the upper mantle. Journal of Geophysical Research Solid Earth. 109, 1–19. https://doi.org/10.1029/2004JB002970.

Schellart, W. P. & Moresi, L. (2013). A new driving mechanism for backarc extension and backarc shortening through slab sinking induced toroidal and poloidal mantle flow: Results from dynamic subduction models with an overriding plate. Journal of Geophysical Research Solid Earth. 118, 3221–3248. https://doi.org/10.1002/jgrb.50173.

Schellart, W. P. & Strak, V. (2021). Geodynamic models of short-lived, long-lived and periodic flat slab subduction. Geophysical Journal International. 226, 1517–1541. https://doi.org/10.1093/gji/ggab126.

Sternai, P., Jolivet, L., Menant, A. & Gerya, T. (2014). Driving the upper plate surface deformation by slab rollback and mantle flow. Earth and Planetary Science Letters. 405, 110–118. https://doi.org/10.1016/j.epsl.2014.08.023.

Strak, V. & Schellart, W. P. (2014). Evolution of 3-D subduction-induced mantle flow around lateral slab edges in analogue models of free subduction analysed by stereoscopic particle image velocimetry technique. Earth and Planetary Science Letters. 403, 368–379, https://doi.org/10.1016/j.epsl.2014.07.007.

Strak, V. & Schellart, W. P. (2018). A subduction and mantle plume origin for Samoan volcanism. Scientific Reports. 8, 10424. https://doi.org/10.1038/s41598-018-28267-3.

Trua, T., Serri, G. & Marani, M. P. (2003). Lateral flow of African mantle below the nearby Tyrrhenian plate: Geochemical evidence. Terra Nova. 15, 433–440. https://doi.org/10.1046/j.1365-3121.2003.00509.x.

Turner, S. & Hawkesworth, C. (1998). Using geochemistry to map mantle flow beneath the Lau Basin. Geology. 26, 1019–1022. https://doi.org/10.1130/0091-7613(1998)026<1019:UGTMMF>2.3.CO;2.

Xue, K., Schellart, W. P. & Strak, V. (2020). Effect of Plate Length on Subduction Kinematics and Slab Geometry: Insights From Buoyancy-Driven Analog Subduction Models. Journal of Geophysical Research Solid Earth. 125, 1–23. https://doi.org/10.1029/2020JB020514.

Overriding plate deformation and topography during slab rollback and slab rollover: insights from subduction experiments

Kai Xue (1*), Wouter P. Schellart (1) and Vincent Strak (1)

(1) Department of Earth Sciences, Vrije Universiteit Amsterdam, Amsterdam, Netherlands

* k.xue@vu.nl

Abstract

Overriding plate deformation (OPD) varies at different subduction zones, with some showing mainly overriding plate extension (e.g. Mariana, Tonga and Izu-Bonin subduction zones), while others show mainly shortening (e.g. Makran and South American subduction zones). Here we investigate how different subduction modes, namely trench retreat and trench advance, affect OPD and generate corresponding topography with fully dynamic analogue models of time-evolving subduction in three-dimensional space. We conduct two sets of experiments, one of which is characterized by trench retreat and slab rollback, and the other characterized by trench advance and slab rollover. We compute the mantle flow, the overriding plate strain and topography during subduction using the particle image velocimetry technique (PIV). The overriding plate in the experiments showing continuous trench retreat experiences overall extension, while in the experiments dominated by trench advance experiences overall shortening. Our experiments indicate that, except for the fore-arc region, the overall OPD is mainly driven by the horizontal mantle flow at the base of the OP inducing a viscous drag force (F_D), and is determined by the gradient of the horizontal mantle flow velocity (dv_x/dx). Furthermore, a large-scale trenchward overriding plate tilting and an overall subsidence of the overriding plate were observed in the experiments showing continuous trench retreat, while a landward tilting and an overall uplift of the overriding plate were observed during long-term trench advance. The difference in dynamic topography during the two different subduction modes can be ascribed to the large-scale trenchward and landward mantle flow, respectively. Our models showing trench advance provide a possible mechanism for OPD in the Makran subduction zone, which has experienced overall trench-normal tectonic shortening and extension only in a local region of the coastal Makran that is spatially comparable to that in our experiments. In addition, these models also present a good correlation of the dynamic topography with the long-wavelength, elevated topography in the overriding plate bordering the Makran subduction zone.

Integrated geophysical-petrological modeling of the lithospheric mantle along the northern Apennines, Dinarides and Pannonian Basin

Wentao Zhang (1, 2*), Montserrat Torne (1), Ivone Jiménez-Munt (1), Ana Negredo (3, 4), Estefania Bravo (1, 2), Jaume Vergés (1), Daniel García-Castellanos (1)

(1) Geosciences Barcelona (Geo3Bcn-CSIC), Barcelona, Spain
(2) Department of Earth and Ocean Dynamics, University of Barcelona, Barcelona, Spain
(3) Department of Physics of the Earth and Astrophysics, Complutense University of Madrid, Madrid, Spain
(4) Institute of Geosciences IGEO (CSIC-UCM), Madrid, Spain

*wzhang@geo3bcn.csic.es

Abstract
The target area of this work is located at the junction between the Central Mediterranean Sea and the Alpine-Carpathian orogenic belt (Fig. 1). The present-day crust and upper mantle structure of this area results from a complex tectonic scenario mainly driven by subduction of Tethyan oceanic domains, which results in orogenic belts (Apennines, Dinarides, and Carpathians) separated by extensional back-arc basins (Tyrrhenian and Pannonian) and the Adriatic microplate. During the last decades, this area has been surveyed by several geological and geophysical studies. However, the majority of them ignore the role of the petrophysical features, including chemical composition and phase transitions, on the physical properties in the lithospheric mantle. Here, we aim to derive the present-day crust and upper mantle structure (up to 400 km depth) along an about 1070 km long geo-transect, crossing the Northern Tyrrhenian Sea, the Northern Apennines, the Adriatic Sea, the Dinarides fold belt, and the Pannonian back-arc basin (Fig. 1).

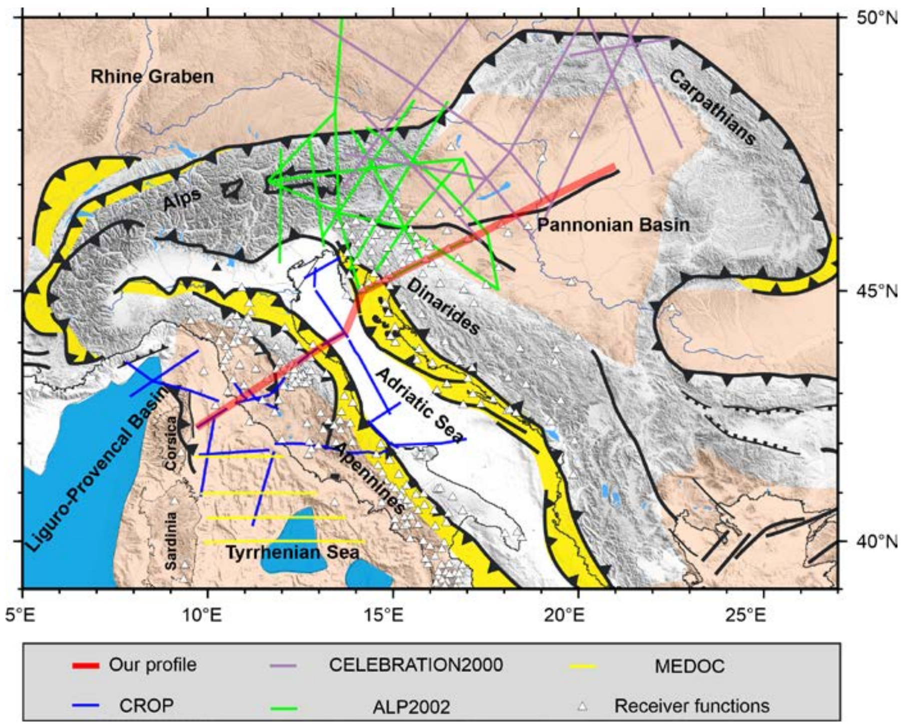

Figure 1: The tectonic setting of the study region. Thick red line shows the location of the modeled profiles. Other lines of different colors show the location of previous seismic profiles. The white triangles represent the location of the seismic stations.

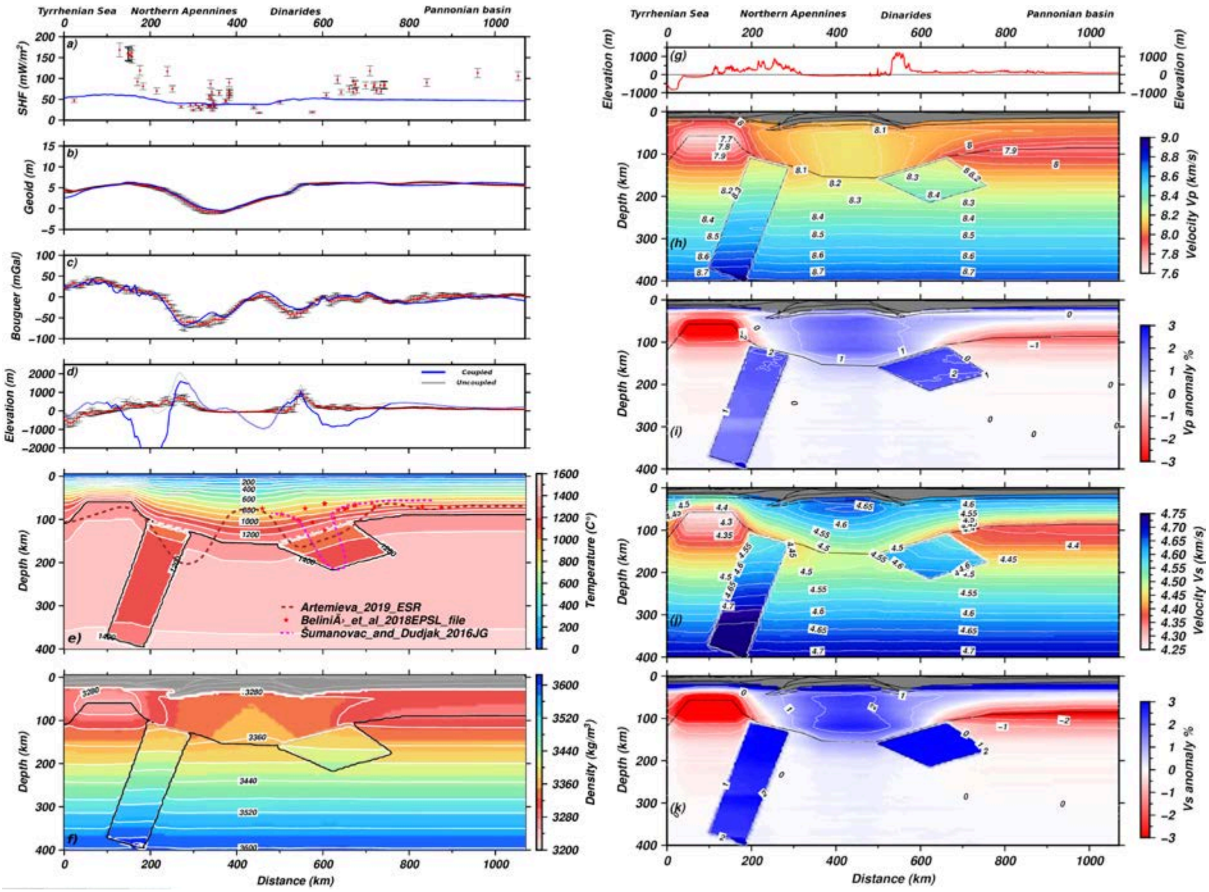

Figure 2: Modelling results. (a) Surface heat flow. (b) Geoid height. (c) Bouguer gravity anomaly. (d) Isostatic elevation ignoring the effect of slabs (blue line) and coupled elevation considering the effect of slabs (gray blue). Blue lines represent the calculated values from the model. Red dots denote measured data, and vertical bars denote the standard deviation calculated on a strip of 50-km width. (e) Temperature distribution (color pattern), lithosphere-asthenosphere boundary (thick black line). Color dashed lines are the lithosphere-asthenosphere boundary resulting from previous studies. (f) Density distribution. (g) Elevation. (h) P wave velocities. (i) P wave anomalies with respect to a reference model. (j) S wave velocities, and (k) S wave anomalies with respect to a reference model.

In our study, we apply LitMod_2.0 software (Kumar et al., 2020), an improved integrated geophysical-petrological modeling tool, which combines surface heat flow, Bouguer gravity anomaly, geoid height, elevation, mantle seismic velocities, and petrological data to study the present-day crust and upper mantle structures from a thermal, compositional, seismological and density point of view. The subducting-delaminated slabs beneath the Northern Apennines and Dinarides are incorporated into the model as thermocompositional sublithospheric anomalies with temperature anomaly of −300 °C and distinct lithospheric-mantle composition (Fig. 2). The obtained lithospheric structure shows significant lateral variations in the thermal, compositional, density, and seismological structure of the crust and upper mantle along the geotransect, which reveals the imprint of the complex geodynamic evolution of the area. This research has been funded by the GeoCAM Project (PGC2018-095154-B-I00) with the contribution of the China Scholarship Council.

References

Kumar, A., Fernàndez, M., Jiménez-Munt, I., Torne, M., Vergés, J., & Afonso, J. C. (2020). LitMod2D_2. 0: An improved integrated geophysical-petrological modeling tool for the physical interpretation of upper mantle anomalies. Geochemistry, Geophysics, Geosystems, 21(3), e2019GC008777. https://doi.org/10.1029/2019GC008777